

Exhalative Origins of Iron Formations

MICHAEL M. KIMBERLEY

Department of Marine, Earth and Atmospheric Sciences, North Carolina State University, Raleigh NC 27695-8208
(U.S.A.)

Abstract

Kimberley, M.M., 1989. Exhalative origins of iron formations. *Ore Geol. Rev.*, 5: 13-145.

Iron formations are stratigraphic units which are largely composed of iron-rich chemical sedimentary rock, here called ironstone. Most aspects of iron formations continue to be controversial and so one must read voluminous literature to appreciate either the range of iron-formation characteristics or the conflicting interpretations of those characteristics. Most protagonists in the ongoing debate may be classified into two groups, i.e. those who support a shallow weathering source for the iron (weathering of land or surficial seafloor sediment) and those who invoke deep weathering (hydration of new crust or late diagenesis of sediments) followed by exhalation of ferriferous fluids through the seafloor. The present review concludes that deep weathering has been the source of all iron formations. Cherty iron formations are attributed to hydration of new crust. Noncherty iron formations are attributed to exhalation of late-diagenetic fluids which have been driven through a continental margin by seismic pumping.

Iron-formation controversies are reviewed herein through the development of flow charts which illustrate relationships among the many controversies. Preferred routes through these flow charts are suggested for both cherty and noncherty iron formations but the reader readily may select other routes. The mode of iron supply (deep or shallow weathering) is the most fundamental among many other issues, e.g., the mechanism for long-term maintenance of abundant dissolved iron within a large water body. The iron in any extensive iron formation which is consistently thicker than 10 m is attributed to a long-lasting suboxic mass of seawater which lacked H₂S. The paucity of H₂S either has been due to a paucity of all sulfur species or to an inhibition of sulfate reduction under reducing conditions, as in the modern Orca Basin under the Gulf of Mexico. Water in the Orca Basin contains up to 20 ppm Mn²⁺ just below the oxic-suboxic interface and an average of 1.6 ppm Fe²⁺ throughout the suboxic region.

Cherty iron formations are attributed to low-temperature (<300°C) hydration of newly formed igneous crust by seawater. Peak production of cherty iron formations, e.g. during the beginning and end of the Proterozoic, is attributed to particularly rapid crustal accumulation in opening rifts, followed by abrupt failure of the rift and low-temperature hydration of the new crust. Rifts presumably opened, failed, and became sheared by transform faults more rapidly on a radioactively hotter young planet. Broad submarine transform fault zones are characterized by seismic pumping of seawater. Exhalative sedimentation of small cherty iron formations within rifts has continued into the Phanerozoic and a partial modern analog exists in the Red Sea.

Noncherty iron formations are attributed to seismic pumping of seawater through an ophiolite-bearing sedimentary pile along a continental margin. Iron-dissolving fluids are hypothesized to have been hypersaline because of pumping through evaporites or cooling plutons within the sedimentary pile. The production rate of noncherty iron formations has not changed much through Earth history. A modern analog exists in the continental margin of Venezuela where the soft-sediment equivalent of ferrous-silicate ironstone is accumulating near Cabo Mala Pascua. Ferrous-silicate (berthierine) ironstone is accumulating where exhalations rise quickly and reach the shallow ocean before precipitating iron. More slowly rising coastal and many deep-water exhalations in Venezuela precipitate glauconite just below the sediment-water interface. If all iron formations have formed by exhalation, then manganese and phosphate deposits probably also are exhalative.

Contents

Abstract.....	13
Introduction and scope.....	17
Overview of iron formations	17
Relationship of iron formations to other ore-forming environments	17
Paleoenvironmental classification.....	17
Comparison of cherty (MECS, SVOP, and DWAT) iron formations.....	18
Comparison of noncherty (SCOS, SOPS, and COSP) iron formations	20
Questions excluded from genetic flow charts	21
Introduction	21
Did iron precipitate onto the seafloor or is it a diagenetic replacement?	21
Have most iron formations accumulated in fresh water or salty water?	21
Were Precambrian oceans sufficiently alkaline for predominance of H_3SiO_4^- ?	21
Have most iron formations accumulated in shallow or deep water?.....	21
Have there been long-lasting bodies of iron-rich water?.....	39
Have iron-rich oceans been devoid of sulfur-bearing species?	39
Was an oxygen-poor atmosphere a sufficient cause of iron formations?	40
Has iron been supplied as fluvial solutes?	41
Do iron formations record irreversible events in Earth history?	42
Have iron-rich fluids exhaled directly from the mantle?	43
Major genetic flow charts	44
Introduction	44
Flow chart for iron source.....	44
Flow chart for iron solubility	46
Flow chart for iron precipitation	48
Flow chart for evolution through Earth history.....	49
Minor genetic flow charts.....	51
Introduction	51
Flow chart for stratigraphic relationships	52
Flow chart for tectonic relationships	54
Flow chart for texture	55
Flow chart for banding.....	55
Flow chart for structures (except banding) in granular-oolitic ironstone	56
Flow chart for mineralogy	56
Flow chart for chert.....	58
Flow chart for carbon isotopes.....	58
Flow chart for oxygen isotopes.....	59
Flow chart for sulfur isotopes.....	60
Flow chart for major elements	62
Flow chart for minor elements (ME) and selected trace elements.....	63
Flow chart for rare-earth elements.....	64

Factors relevant to genetic modeling	64
Proposed mechanisms of iron supply to iron formations.....	64
Deep-weathering exhalative hypothesis.....	65
Young ironstone and modern analogs of ironstone.....	66
Common features of ironstone.....	68
Iron formations through Earth history	70
Archean iron formations.....	70
Isua iron formations.....	70
Helen iron formation	71
Outerring iron formation.....	71
Soudan iron formation.....	72
Proterozoic iron formations.....	72
Relationship of Proterozoic MECS-IF to crustal growth.....	72
Rocks associated with Early Proterozoic iron formations	73
Morphology of Early Proterozoic MECS-IF platforms.....	74
Facies variation in Proterozoic iron formations.....	74
Pyrite facies in Proterozoic iron formations	75
Redox indicators in Proterozoic iron formations.....	75
Putative barrier bars in Proterozoic basins	76
Limestone, ironstone, and biota on Proterozoic platforms.....	77
Late Precambrian cherty iron formations	78
Proterozoic iron formations which cover volcanoes	79
Proterozoic glauconite	79
Proterozoic noncherty oolitic iron formations (SCOS-IF)	80
Phanerozoic iron formations	81
Phanerozoic cherty iron formations.....	81
Coeval Phanerozoic ironstone and pelletal phosphorite	82
Paleozoic noncherty oolitic iron formations (SCOS-IF)	83
Mesozoic–Cenozoic oolitic iron formations (SCOS-IF)	84
Modern ferriferous seawater and sediments	84
Glauconite off the southeastern U.S.A.	84
Ferriferous hypersaline seawater in the Orca basin.....	85
Weathering source for Fe–Mn concentrations in the Baltic Sea.....	86
Quaternary ferriferous and cherty oolite on Andros Island, Bahamas	86
Modern ferriferous sediments in Venezuela	86
Relationship of red tides to sedimentary exhalation in Venezuela	87
Glauconite sedimentation in Venezuela beyond the Margarita–Cumana area.....	88
Cedros–Soldado bank in the southern Gulf of Paria	89
Coche–Margarita area.....	91
Glauconite composition and precipitation	92
Introduction	92

Mineralogy and composition of glauconite	92
Glauconite precipitation	93
Silica source for Venezuelan glauconite	94
Exhalations and the modern equivalent of ironstone in Venezuela	94
Modern equivalent of ironstone in coastal Venezuela	94
Hydrothermal apatite in the Bertonzini quarry	95
Cariaco basin	95
Proposed process of iron concentration in northeastern Venezuela	96
Exhalation in the Margarita–Cumana area	96
Punta del Hierro (Iron Point) on Margarita island	97
Genetic classification of iron formations	98
Introduction	98
One-dimensional versus two-dimensional models	98
Volcanic-exhalative versus metamorphic-exhalative models	99
Proposed genetic classification scheme	99
Diversity of existing hypotheses	101
Genesis of iron formations	102
Lithologic associations of iron formations	102
Ironstone composition and an overview of the exhalative model	103
Relevance of Precambrian atmospheric composition	104
Carbon and phosphorus in iron formations	104
Relationship of cherty to noncherty iron formations	105
Production of ferriferous fluids	106
Are rift-related evaporites a precursor to iron formations?	107
Seismic pumping of exhalative fluids	108
Plume morphology and dispersal	109
Large and thermally equilibrated water bodies	109
Precipitation of cherty ironstone on a platform	111
Effect of the atmosphere on shallow-water iron formations	113
Noncherty microlaminated ironstone in coal measures	113
Deep-water iron formations	114
Samarium–neodymium isotopes in iron formations	115
Modern and Pliocene ferriferous ooids	115
Origin of oolitic noncherty iron formations (SCOS-IF)	116
Manganese-rich iron formations and manganese formations	118
Conclusion	119
Acknowledgements	120
References	120

Introduction and scope

Like all geologic nomenclature, the nomenclature used to describe iron formations is inherently somewhat arbitrary. Arguments for or against particular terms are necessarily semantic. The mixing of semantic with scientific arguments is potentially confusing and so discussion of nomenclature is presented in a separate paper in this issue. The following discussion assumes familiarity with the accompanying paper.

An iron formation is considered to be a stratigraphic unit which consists mostly of chemical sedimentary rock with more than 15% Fe. The rock is called ironstone (Kimberley, 1978a). A manganese formation similarly is defined to contain chemical sedimentary rock with more than 15% Mn. This paper focuses on iron formations but much of the discussion would apply to manganese formations with appropriate modification. The paper is divided into four parts. The first is an overview of iron formations. The second presents the interrelated questions about genetic processes. The third is a brief review of the evolution of iron formations through Earth history and the last part draws on the historical data and modern processes to address genetic issues. Readers who are interested in a specific aspect of iron formations may locate the relevant discussion by using the Table of Contents.

Most aspects of iron formations are controversial. Only a few of these controversies may be resolved with sufficient certainty that they may be removed from further consideration. The preferred solutions to these few are presented herein prior to discussion of remaining controversies. Resolution of any one of the remaining controversies would bear on the resolution of several others and so the initial objective of this paper is to construct flow charts which illustrate these interrelationships. Each of the basic questions about iron formations is presented with just enough information to explain why the question is controversial.

Cherty iron formations are typically banded

(laminated) and only locally oolitic whereas noncherty iron formations are typically unbande and largely oolitic. Most iron formations may be classified into six paleoenvironmental groups (Table 1). The youngest voluminous cherty iron formations are Devonian whereas one of the most voluminous noncherty iron formations is Pliocene, just five million years old (Table 2). Modern marine analogs of noncherty ironstone occur off Indonesia and Venezuela.

Overview of iron formations

Relationship of iron formations to other ore-forming environments

Most iron formations appear to have accumulated near sediment-starved coasts in the same general environment as phosphorite and manganese deposits. This environment may be contrasted with more landward and more seaward ore-forming environments. In a landward-to-seaward progression of elemental affinities, uranium ores would rank as being most continental, followed by redbed-copper and Mississippi-Valley-type lead-zinc deposits before reaching the coastal Fe-Mn-P environment (e.g., Guilbert and Park, 1986). More seaward than the typical Fe-Mn-P environment lies the polymetallic massive sulfides which presently congregate near ridge axes (Scott, 1987).

Paleoenvironmental classification

Table 1 summarizes the preferred paleoenvironmental classification scheme for iron formations. This scheme is described in an accompanying paper where essential features of each classified type are reviewed. Two of the classified types are consistently cherty, i.e., the voluminous continental-shelf (MECS) iron formations and the shallow-volcanic-platform (SVOP) iron formations. Three other shallow-water types consistently lack much chert, i.e.,

the oolitic (SCOS) iron formations, the peloidal glauconitic (SOPS) iron formations, and the coal-swamp (COSP) iron formations. Deep-water (DWAT) iron formations are quite variable, including variation in chert content.

The distribution of paleoenvironmental types of iron formations through Earth history is provided in Table 2, a table which probably contains more information about iron formations than any other single table. No one table can be comprehensive, however, and other tabulations offer additional information (e.g. James, 1983; Gross, 1983). Of all known cherty iron formations, only a small percentage is listed in Table 2 because incorporation has been restricted to iron formations for which there is both compositional and petrographic data. Noncherty iron formations are relatively better represented, partly because there are fewer of them, but even for these the restriction to chemically analyzed deposits eliminates many known occurrences. Despite its limitations, Table 2 is sufficiently detailed for thorough characterization of each environmental type of iron formation listed in Table 1, both the four types which have economic importance (MECS-IF, SVOP-IF, DWAT-IF, and SCOS-IF) and the two types which are not currently exploited for iron anywhere (SOPS-IF and COSP-IF).

Table 2 clearly illustrates the evolution and cyclicity of iron formations through Earth his-

tory. The evolution of iron formations is more obvious than that of most other types of stratigraphic units. Genetic interpretation of iron formations therefore is important to a fundamental understanding of global evolution (Holland, 1984).

Comparison of cherty (MECS, SVOP and DWAT) iron formations

The oldest iron formations are MECS-IF, SVOP-IF and DWAT-IF and so these are discussed first. SVOP-IF and DWAT-IF are the environmental types with the most continuous record throughout the geologic column. Whatever the origin of cherty iron formations may have been, deep-water precipitation has occurred more continuously than shallow-water precipitation throughout Earth history. Platformal precipitation is attributed to an increase in the volume of ferriferous subsurface water until the interface with overlying iron-poor surface water became shallower than the water depth on continental shelves. The most common platform well within an ocean basin is an eroded and subsid-ing volcano. The Earth apparently has had shallow platforms since the beginning of the rock record, at about 3.9 Ga (Bridgwater et al., 1978). Here and elsewhere in this text, Ga stands for giga annum, a billion years, whereas Ma represents a million years (mega annum).

MECS iron formations commonly are enormous, extending up to 1000 km and reaching several hundred meters in thickness (Kimberley, 1978a). These dimensions are indicative of marine sedimentation (cf., Garrels, 1987). Most, but not all, DWAT iron formations are small, commonly just a few centimeters thick. Unlike other iron formations, DWAT-IF's typically recur dozens of times through a stratigraphic interval dominated by different types of strata. SVOP iron formations are intermediate in both thickness and extent. Although generally thinner than MECS iron formations, SVOP iron formations may reach a few hundred meters in thickness and may extend for a couple

TABLE 1

Paleoenvironmental classification of iron formations

Acronym	Unabbreviated term
SVOP-IF	Shallow-volcanic-platform iron formation
MECS-IF	Metazoan-poor, extensive, chemical-sediment-rich, shelf-sea iron formation
SCOS-IF	Sandy, clayey, and oolitic, shallow island-dotted-sea iron formation
DWAT-IF	Deep-water iron formation
SOPS-IF	Sandy, oolite-poor, shallow-sea iron formation
COSP-IF	Coal-swamp iron formation

hundred kilometers. The smaller extent of SVOP-IF partly reflects the smaller area of a volcanic platform than a continental shelf. Platforms which are rifted fragments of continents may have dimensions similar to those of SVOP platforms, e.g. the Bahama Banks, and some MECS-IF's have accumulated on Bahama-type platforms (Morris and Horwitz, 1983).

Thick SVOP iron formations are remarkably deficient in pyroclastic interbeds considering that they rest on volcanoes which commonly fluctuated from accumulating one volcanic rock type to another through thicknesses of a few meters. SVOP iron formations display facies changes better than any other kind of iron formation, probably because volcanic platforms include the greatest variety of juxtaposed surficial environments across short distances, ranging from the photic zone to deep water. James (1954) proposed that the MECS-IF environment around Lake Superior had a seaward gradation from oxide to carbonate to sulfide facies. However, seaward facies changes commonly are obscure in these and most other MECS iron formations.

Many SVOP iron formations exhibit a seaward gradation in ironstone mineralogy but Egorov and Timofeieva (1973) have shown that the mineralogical change with increasing water depth commonly is the opposite of the oxide-to-carbonate gradation proposed by James (1954) and adopted by Goodwin (1973) for volcanic-associated iron formations. The predominant oxide in SVOP-IF is magnetite and this preferentially occurs in the deepest-water facies, where SVOP-IF grades to DWAT-IF. Siderite predominates in the shallowest-water SVOP-IF facies. This pattern is most obvious in the Archean Outerring SVOP-IF in northwestern Canada (Table 2).

Facies changes are sufficiently common in SVOP iron formations that individual beds generally cannot be correlated over distances as great as observed in the Brockman MECS-IF in Western Australia. Meter-thick beds in the Brockman extend over an area of 60,000 km²

(Trendall, 1983b). Meter-thick beds in the Caué MECS-IF of Brazil have a lateral extent of about 30 km (Eichler, 1976). Although meter-thick beds are extensively correlative in the Brockman, thin bands are not equally correlative, as previously claimed (Trendall, 1983b). Moreover, Lambeck (1986) recommends further study of the putative varve cycle reported by Trendall (1973) in banded ironstone of the Weeli Wolli Formation. Walker and Zahnle (1986) interpret the putative cycle to indicate a lunar distance at 2.5 Ga of 52 Earth radii instead of the present 60 radii. Several investigators have attempted unsuccessfully to find varve cycles in other iron formations and so the existence of seasonal varves is considered to be uncertain.

SVOP-IF differs from MECS-IF in that it may contain silica-poor unbanded ironstone, as in portions of the Archean Helen iron formation. However, most ironstone in the Helen and other SVOP iron formations is banded like most ironstone in MECS iron formations (Goodwin, 1962). The Helen is the ideal Algoma-type deposit of Gross (1965, 1983). Banding in MECS-IF and SVOP-IF may occur at several scales from sub-millimeter thicknesses to meter thicknesses but is typically thin in DWAT-IF. Thick bands generally contain thinner bands within them. Banding may be disrupted by primary features, e.g. local fumarolic activity and widespread storm brecciation. Storm breccia is more common than another potential indicator of shallow-water conditions, i.e. oolitic texture. Oolitic texture is more prevalent in MECS iron formations and this may indicate that MECS-IF commonly forms in shallower water than does SVOP-IF. DWAT-IF is never oolitic.

Although SVOP ironstone closely resembles MECS ironstone, there are more compositional and textural differences than suggested by Gole and Klein (1981). Compositional differences are undetectable, however, in reviews which do not subdivide cherty iron formations into those which accumulated on continental shelves and those which accumulated on volcanic plat-

forms, e.g. Davy (1983). Both SVOP and MECS ironstone are remarkably deficient in major elements other than oxygen, silicon, iron, carbon, and manganese (Kimberley, 1979b). MECS ironstone also is deficient in all trace elements but SVOP and DWAT ironstone may be enriched in any element which is concentrated in stratiform sulfide ore deposits, e.g. copper (Kirkham, 1979), lead (Graf, 1977), zinc (Richards, 1966), arsenic (Goodwin et al., 1985), boron (Harder, 1954), barium (Kalugin, 1973), and/or phosphorus (Laajoki and Saikonen, 1977). Major gold deposits also occur in volcanic-associated iron formations but gold rarely is disseminated evenly throughout the iron formation (Ferguson, 1966; Fripp, 1976).

Rare-earth elements (REE) are scarce in both SVOP and MECS ironstone relative to any mudrock, e.g. shale. Cherty ironstone typically contains about an order of magnitude less REE than does mudrock. This paucity makes interpretation of REE patterns difficult because any minor contribution from pyroclastic grains or other nonchemical sediment may overwhelm the signal from chemical precipitation. One REE, europium, resembles iron in that its solubility may be enhanced by chemical reduction from the 3+ to the 2+ state. Europium is not systematically enriched or depleted in MECS ironstone but typically is enriched in SVOP ironstone. This is most obvious in the review of Fryer (1983) in which REE patterns for Archean iron formations (mostly SVOP-IF) are plotted separately from the patterns for Proterozoic iron formations (mostly MECS-IF).

One reason that SVOP-IF and MECS-IF should not be lumped together is that the europium enrichment of SVOP-IF may become interpreted as an age-dependent feature rather than an environment-dependent feature, given the abundance of SVOP-IF in the Archean and MECS-IF in the Proterozoic (Table 2). By failing to differentiate among iron formations, Fryer (1977) interpreted the decrease in europium anomalies from the Archean to the Proterozoic to indicate an increase in the oxidation state of the

atmosphere. Graf (1978) and Kimberley (1978a) simultaneously discounted this interpretation because Paleozoic SVOP-IF displays europium anomalies like those in Archean SVOP-IF.

Comparison of noncherty (SCOS, SOPS, COSP) iron formations

As for the cherty iron formations, essential features of each of the noncherty types (SCOS, SOPS, and COSP) are reviewed in an accompanying paper. A brief comparison among these types is provided here as a preamble to basic questions about all iron formations. A significant difference between noncherty oolitic (SCOS) iron formations and peloidal glauconitic (SOPS) deposits is the much greater tendency of the latter to grade to sedimentary rocks with a progressively smaller proportion of authigenic ferriferous minerals. As a result, glauconitic ironstone constitutes a negligible proportion of all sedimentary rocks which contain glauconitic peloids. In contrast, oolitic ironstone constitutes a significant proportion of all sedimentary rocks which contain any ferriferous ooids. One explanation for this difference is that the process which produces ferriferous ooids occurs rapidly if it occurs at all. In other words, the sedimentation rate of oolitic (SCOS) iron formations is much greater than that of glauconitic SOPS iron formations.

The small coal-swamp (COSP) iron formations appear to be the easiest to model genetically because they have formed in areas where abundant organics were available to consume dissolved oxygen and because the small volume of ironstone, generally less than 1 m thick and a few km in extent, does not impose a major constraint on genetic modeling. Modelers have compared coal-swamp (COSP) iron formations to modern bog iron deposits and have invoked precipitation from groundwater which originated from subaerial mounds within the swamp (Stanton, 1972a; Boardman, 1981). However, the Carboniferous COSP iron formations of

Britain are correlative with adjacent iron-rich continental sediments (redbeds) which were enriched in iron prior to burial (Boardman, 1981; Besly and Turner, 1983). This correlation would not be expected if the iron-concentrating processes had been confined to the coal-forming swamp.

Petrographically, COSP ironstone is quite distinct from the structureless modern bog deposits. COSP ironstone generally is as well laminated (banded) as typical cherty banded ironstone in Precambrian MECS or SVOP iron formations. The lamination and siderite-dominated mineralogy appear to be a product of precipitation from a ferriferous water body rather than precipitation from effusive ground water as in bog iron deposits. Even the coal-swamp (COSP) iron formations therefore present a challenge for genetic modeling.

Questions excluded from genetic flow charts

Introduction

A series of flow charts has been constructed (Figs. 1–18) to show the interrelationships among basic questions about iron formations. These flow charts do not include all published options concerning iron-formation genesis. Some concepts have found so little support that they are not discussed. Exclusion of concepts with more widespread support is defended in this section.

Did iron precipitate onto the seafloor or is it a diagenetic replacement?

Kimberley (1979a) proposed that ironstone has formed by diagenetic replacement of aragonite. However, the evidence against this concept is now so overwhelming, as reviewed herein, that diagenetic replacement is no longer sufficiently viable to be included in genetic-process flow charts. Of all types of ironstone, glauconitic ironstone most commonly displays partial

replacement, e.g., partial glauconitization of biotite (Galliher, 1935) or smectite (Hower, 1961; Murray and Mackintosh, 1968). However, the great bulk of glauconitic grains display no partial replacement and there is no evidence that any prior grain has been replaced (Kinsley et al., 1987). Primary glauconite grains may be surrounded by interstitial diagenetic glauconite which is distinguishable by its intergrowth with alloigenic clay minerals (Bartholomew et al., 1987).

Have most iron formations accumulated in fresh water or salty water?

Hough (1958) and Garrels (1987) have argued that the voluminous cherty iron formations accumulated in fresh-water lakes but all modern water bodies of the size required to make the largest iron formations are more saline than the low chloride concentration (178 ppm) envisioned by Garrels (1987). The voluminous carbonate rocks which commonly are associated with iron formations probably record sedimentation in a saline water body (Kimberley, 1978a). More specific evidence comes from the local occurrence of a sodium-rich amphibole, crocidolite, which is an accessory authigenic mineral in some cherty iron formations (Trendall and Blockley, 1970). A high sodium activity would be required in any water which would precipitate crocidolite or its precursor silicate.

Were Precambrian oceans sufficiently alkaline for predominance of $H_3SiO_4^-$?

Although iron-formation basins apparently were saline, the proportions of the major solute ions are not known and they may have been different from the proportions in average ambient seawater. Eugster and Chou (1973) have proposed that cherty iron formations accumulated in Precambrian basins which were anomalously alkaline. Relative to seawater, modern alkaline lakes are depleted in calcium, magne-

sium, and chlorine but enriched in sodium and carbonate ions.

Kempe and Degens (1985) argue that the co-existence of chert, ferrous silicates, and siderite in iron formations records Precambrian oceans which were sufficiently alkaline that the pH generally exceeded the H_4SiO_4 - $H_3SiO^-_4$ equivalence point of about 9.5 (Stumm and Morgan, 1981, p. 540). Silica would then be extremely soluble and would readily become separated from other elements to form sodic silicate deposits upon evaporation. Mild leaching of these deposits by either seawater or fresh water would convert them to chert. An abundance of CO_3^{2-} would have kept Ca^{2+} and Mg^{2+} scarce, in equilibrium with carbonate minerals. Any fluvial supply of calcium or magnesium would have resulted in carbonate sedimentation within deltaic areas instead of open-ocean platforms. A lack of calcium also would enhance the solubility of phosphorus, given the small solubility product of apatite.

The history of seawater alkalinity is difficult to estimate thermodynamically. A thermodynamic model would predict high alkalinity if seawater was formed by evaporation of river water which had become separated from soil minerals (Sillen, 1961; Mackenzie and Garrels, 1967). Such high alkalinity commonly is observed in saline lakes (Eugster and Chou, 1973). Mackenzie and Garrels (1967) hypothesized that a recombination of cations with amorphous aluminosilicates on the seafloor had prevented excessive alkalinity in seawater. However, no evidence has been found for as much "reverse weathering" as they hypothesized and alternative alkalinity-consuming mechanisms include expulsion of late diagenetic fluids (Calvert, 1983) and convection of seawater through basalt (Holland et al., 1986).

The alkaline-ocean model is rejected herein because the gypsum which it disavows is well known from the Precambrian (Buick and Dunlop, 1987) and because Early to Middle Pre-

cambrian phosphate deposits are rare compared to younger deposits (Cook and Shergold, 1986). Open-ocean platform sedimentation of carbonate rocks commonly preceded sedimentation of an equally thick iron formation (Beukes, 1983). Moreover, high alkalinity would have been as detrimental to platform sedimentation of iron formations as to carbonate formations because the abundance of aqueous iron almost certainly depended upon saturation with respect to siderite, the ferrous carbonate (Holland, 1984, p.388). At saturation, abundant CO_3^{2-} would have depressed Fe^{2+} even more than Ca^{2+} or Mg^{2+} , given the lower solubility of siderite than Ca-Mg carbonates. Despite the improbability of high alkalinity in a ferriferous water mass, the alkalinity may well have been somewhat higher than in contemporaneous iron-poor seawater.

Have most iron formations accumulated in shallow or deep water?

Noncherty Phanerozoic iron formations commonly are richly fossiliferous with animal and/or plant fossils (Table 2). These fossil assemblages clearly record shallow-water sedimentation in most cases. Water depth locally was sufficient that the immediately overlying sediments were not likely to fill the basin and allow fresh groundwater to permeate the sediment during diagenesis (Gygi, 1981). Ferriferous ooids typically are associated with shallow-water fossils in noncherty iron formations and so the occurrence of ooids in cherty iron formations generally is interpreted to record shallow-water sedimentation (e.g., Dimroth and Chauvel, 1973). The great extent and thickness of pure chemical sedimentary rock in MECS iron formations (Table 2) probably records sedimentation on a relatively shallow offshore platform (Morris and Horwitz, 1983). The same argument may be made for voluminous volcanic-associated (SVOP) deposits.

TABLE 2

Description and classification of iron formations

Explanation of abbreviations

Column A: Paleoenvironmental types of iron formations

SVOP	Shallow-volcanic-platform iron formation
MECS	Metazoan-poor, extensive, chemical-sediment-rich, shelf-sea iron formation
SCOS	Sandy, clayey, and oolitic, shallow island-dotted-sea iron formation
DWAT	Deep-water iron formation
SOPS	Sandy, oolite-poor, shallow-sea iron formation
COSP	Coal-swamp iron formation
INT1	Intermediate SCOS-SOPS iron formation
INT2	Intermediate SCOS-MECS iron formation
INT3	Intermediate SVOP-DWAT iron formation
INT4	Intermediate SVOP-MECS iron formation

Comment: Some deposits for which there is little published information and which have been classified as intermediate types may be classifiable as a single type when more becomes known about them.

Column B: Name of iron formation

Comment: In hyphenated paired names, e.g., Kirkland-Clinton, the first name refers to an individual iron formation and the second to a spatially- and temporally-related group of iron formations, except for two normally hyphenated names, i.e., Lahn-Dill and Kutan-Bulak. An addition sign (+) between names indicates that they refer to geographically-different parts of the same iron formation.

Column C: Age of sedimentation

E	Early	Devo	Devonian
M	Middle	Silu	Silurian
L	Late	Ordo	Ordovician
Plio	Pliocene	Camb	Cambrian
Mioc	Miocene	Paleoz	Paleozoic
Olig	Oligocene	PreZ	Precambrian Z (0.80–0.57 Ga)
Eoce	Eocene	LPreY	Late Precambrian Y (1.1–0.8 Ga)
Pale	Paleocene	MPreY	Middle Precambrian Y (1.4–1.1 Ga)
Cret	Cretaceous	EPreY	Early Precambrian Y (1.7–1.4 Ga)
Jura	Jurassic	LPreX	Late Precambrian X (2.0–1.7 Ga)
Tria	Triassic	MPreX	Middle Precambrian X (2.3–2.0 Ga)
Perm	Permian	EPreX	Early Precambrian X (2.6–2.3 Ga)
Penn	Pennsylvanian	LPreW	Late Precambrian W (3.2–2.6 Ga)
Miss	Mississippian	MPreW	Middle Precambrian W (3.9–3.2 Ga)

Comment: Iron formations are listed chronologically in this table. A hyphen between two of the foregoing ranges of geologic time indicates uncertainty. An addition sign (+) indicates that sedimentation spanned parts of both time ranges.

Column D: Country

Comment: Names of countries generally are abbreviated to the first six letters. The only country name which may not be immediately obvious is Australia which is abbreviated to Austra. Two iron formations straddle international borders, i.e., the Ardenne (France–Belgium) and Urucum + Mutun (Brazil–Bolivia) deposits. Asterisks are entered for these two.

Columns E and F

Latitude and longitude, respectively, in degrees and minutes. The minutes symbol (") is omitted. For deposits which are large enough to span several minutes or even degrees, the location cited represents the thickest or best known location of the iron formation.

Column G: Maximum thickness (in m) of individual iron-rich beds

Comment: Thick iron formations generally consist of iron-rich beds (beds of ironstone) interbedded with beds of iron-poor rocks, e.g. shale or sandstone. If an iron formation consists of just one, vertically continuous bed of ironstone, the thickness listed in this column (G) equals that listed in column H. For those iron formations which contain subordinate iron-poor interbeds, the maximum thickness of the ironstone beds may be characteristic of the iron-formation type. In many cases, published information about bed thickness is vague and the corresponding thickness listed herein is either greater than x m ($>x$ m) or less than x m ($< x$ m). Any unknown thickness is given as 'Unk'.

Column H: Maximum thickness of the iron formation (in m)

Comment: This is the thickness at the latitude and longitude listed in columns E and F. Any unknown thickness is given as 'Unk'.

Column I: Rock types directly below and above the iron formation

Comment: The rock type listed before the comma underlies the iron formation whereas that which follows the comma directly overlies the iron formation. Rock types are abbreviated to a two-letter sequence, the first letter of which is capitalized. This two-letter abbreviation, e.g. "Ss" for sandstone, may be modified by an abbreviated, one-letter modifier, e.g. "a" for argillaceous. Clayey (argillaceous) sandstone therefore becomes abbreviated to "aSs". The first list given below is that of the modifiers (adjectives) whereas the second list is for the rock types themselves.

List of modifiers

a	argillaceous	Co	coal
b	brecciated by sedimentary processes (erosion or slumping)	Ds	dolostone
c	calcareous	Exp	Rock overlying the iron formation has everywhere been eroded, exposing the iron formation
d	feldspathic	Gn	gneiss
e	graded bedded	Gw	graywacke
f	ferriferous but not richly glauconitic	Ign	non-volcanic igneous basement
g	glauconitic	Ja	jasper
h	dolomitic	Ke	keratophyre
i	sideritic	Ls	limestone
j	cherty	Mn	manganese-rich sedimentary rock
k	desiccation-cracked	Mu	undifferentiated mudrock
m	stromatolitic and oolitic	Mx	mixtite
n	non-marine	Ph	phyllite
o	oolitic	Po	porphyritic volcanic rock
p	carbonaceous and/or pyritic	Qz	quartzite
q	orthoquartzitic	Rh	rhyolite
r	conglomeratic	Sc	schist
s	sandy	Sh	shale
t	tuffaceous	Sl	slate
v	volcanic or partly volcanic	Ss	sandstone
An	andesite	Tu	tuff
Ar	argillite	Ub	ultrabasic volcanic rock
Ba	basalt	Ukn	unknown rock type (not described in literature)
Br	breccia	Unc	The upper surface of the iron formation is an angular unconformity
Cg	conglomerate		
Ch	chert	Vc	volcaniclastic sedimentary rock
Cl	claystone		

Column J: Ferriferous minerals

Comment: Minerals are listed in approximate order of abundance. All minerals listed to the right of a slash mark (/) are distinctly subordinate.

Am	undifferentiated ferriferous	Hm	hematite
	amphiboles	Hy	hypersthene
An	ankerite	Il	ilmenite
Ar	arsenopyrite	Ma	martite
Bi	biotite	Mc	marcasite
Be	berthierine	Mg	magnetite
Ch	chamosite (where X-ray data is lacking, this may be berthierine)	Mh	maghemite
Cl	iron-rich chlorite (this may include chamosite)	Mn	minnesotaite
Cp	chalcopyrite	No	nontronite
Cr	crocidolite	Ph	iron-rich phosphates other than vivianite
Cu	cummingtonite	Po	pyrrhotite
Ep	epidote	Px	undifferentiated iron-rich pyroxenes
Fs	undifferentiated ferriferous silicates	Py	pyrite
Ga	iron-rich garnet	Re	riebeckite, including crocidolite
Gl	glaucocite	Sd	siderite, generally not pure FeCO_3 , alternatively called chalybite
Gn	greenalite	St	stilpnomelane
Go	goethite	Vv	vivianite
Gr	grunerite		
Hb	iron-rich hornblende		

Column K: Non-ferriferous or weakly ferriferous minerals and bitumen

Comment: Minerals are listed in approximate order of abundance. All minerals listed to the right of a slash mark (/) are distinctly subordinate.

Afe	undifferentiated authigenic feldspar	Hau	hausmannite
Apa	apatite and/or collophane	Hbl	hornblende
Ant	anthophyllite	Hyp	hypersthene
Aug	augite	Ill	illite
Bar	barite	Kao	kaolinite
Bio	biotite	Mon	montmorillonite
Bit	bitumen	Psi	psilomelane
Bra	braunite	Pyr	pyrolusite
Cal	calcite	Qtz	quartz
Cht	authigenic chert, including coarsely recrystallized chert	Rho	rhodochrosite
Cly	undifferentiated clay minerals	Rut	rutile
Cry	cryptomelane	Ser	muscovite and/or sericite
Dol	dolomite	Sph	sphalerite
Fel	undifferentiated allogenetic feldspar	Spt	serpentine
Gal	galena	Sul	sulfur
Gyp	gypsum	Tal	talc
Hal	halloysite	Var	variscite

Column L: Representative chemical composition

Comment: Most weight-percent analyses are of a single representative sample but many are averages of several samples. No indication is given herein as to the number of averaged analyses. A large proportion of the published analyses list phosphorus as P instead of P_2O_5 as used herein. These and other non-conforming analyses have been converted by using conversion factors calculated from gram-atomic weights.

—	No analysis was published for this chemical component
tr.	Trace abundance
(35 Fe)	Separate analyses are unavailable for FeO and Fe ₂ O ₃ ; the total is listed as Fe because the oxidation state is unknown, in this case 35% Fe
(20 comb)	Any combined components which lie adjacent in the table, e.g., combined SiO ₂ and Al ₂ O ₃ percentages. Only two other pairs of components occur, i.e., MgO + CaO and Na ₂ O + K ₂ O

Peculiarities of sample used for chemical analysis (if any) (Iron formations nos. 15, 21, 24, 69, 95, 115, 140, 142 in Table 2)

15, 140	Small portion of sample was removed by sieving and was not analyzed
21	Sample consisted only of separated ooids
24	Portion of sample which was insoluble in dilute HCl was not analyzed. The weight percentage of insoluble sample is listed as the first entry in column M
69, 95, 115, and 142	The sample was partially weathered

Column M: Sedimentary features

Comment: If the first entry is a number, this refers to the percentage of insoluble sample, as explained above in "Peculiarities of sample used for chemical analyses".

Aqtz	Detrital quartz sand grains which are of at least fine to medium sand size are predominantly angular to subangular
Blis	Gas blisters and/or rain imprints
Brec	Breccia of undetermined sedimentary origin. The breccia may represent slumping or erosion of penecontemporaneously lithified sediment
Colo	Colloform structures
Conc	Concretions and/or nodules occur at least locally
Desi	Desiccation cracks
Evap	Crystals and/or casts of halite and/or gypsum
Fefo	Partial to (rarely) complete replacement of skeletal fossils by ferriferous minerals
Fepl	Plant matter permineralized by ferriferous minerals
Gbed	Graded bedding occurs, at least locally
Grad	Iron-rich beds occur at or near tops of graded-bedded units of detrital rock
Gran	Granular texture, a texture of rounded to angular, sand-sized grains which are devoid of internal structure
Lban	Locally, but not predominantly banded
Lent	Lenticular bedding
Loid	Locally, but not predominantly oolitic
Mban	Predominantly banded, but with bands being relatively indistinct
Motl	Mottled color
Noid	Non-oolitic. This is only used to describe non-cherty iron formations which one might expect to be oolitic. It is omitted for cherty banded iron formations which mostly are non-oolitic. One may assume that a cherty iron formation is non-oolitic unless described otherwise herein with the abbreviation Ooid, Loid, or Roid
Oobr	Oolitic, and/or pisolithic fragments are present to very abundant, including those which occur as ooid nuclei. If this symbol occurs without an accompanying "Ooid" entry, one may assume that the 'Ooid' entry was omitted because of lack of space in the table
Ooca	Ferriferous ooids occur with calcite within the layered portions which surround ooid nuclei
Ooid	Predominantly oolitic
Phos	This represents either a basal phosphate pebble bed, basal phosphatic concretions, and/or directly underlying, phosphatic-concretion-rich limestone
Piso	Locally pisolithic or, if "Piso" is the first entry, predominantly pisolithic
Pyro	Pyroclastic grains
Ripl	Ripple-marked
Roid	Very rarely oolitic
Rpup	Ripped-up clasts of iron-rich rock or limestone, i.e., intraclastic texture
Rqtz	Sand-sized quartz grains are predominantly well rounded
Slum	Slump folds

Soid	Predominantly superficial ooids, i.e. ooids with large nuclei and only thin concentric layering
Sphe	Some spherulitic grains resemble ooids but lack regular internal structure; i.e., they have pseudo-oolitic texture
Styl	Stylolites are common
Volc	Non-pyroclastic volcanic detritus is present
Wban	Predominantly well banded with distinct iron-rich and iron-poor laminae (bands)
Xbed	Cross-bedded locally
Xrip	Cross-bedded and ripple-marked locally

Column N: Most abundant fossils

Comment: In many cases, the order of abundance among the most abundant fossils could only be surmised.

Alcy	alcyonarian spicules	Ichn	ichnofossils
Alga	non-stromatolitic algae, largely boring algae	Leaf	tree leaves
Ammo	ammonites	Moll	undifferentiated mollusks
Bele	belemnites	Nosk	no skeletal fossils reported
Bone	vertebrate animal bone	Pele	marine pelecypods
Brac	brachiopods	Radi	radiolaria
Bryo	bryozoa	Shar	shark teeth
Ceph	cephalopods	Spic	sponge spicules
Corl	corals	Spor	spores
Crin	crinoids	Stro	algal stromatolite and/or oncolites
Echi	echinoids	Tril	trilobites
Form	foraminifera	Unkn	fossil content unknown
Gast	gastropods	Unsk	undifferentiated skeletal fossils
Grap	graptolites	Wood	logs and/or tree seeds

Column O: References

Comment: Complete references are given at the end of this paper. References are enumerated herein following the first letter of the author's name, e.g. A1 for the first paper by an author whose name begins with "A". An apostrophe follows the symbol of the reference which provided the set of chemical analyses in column L. Unpublished field and/or petrographic observations by the author are noted with the symbol, "+".

References:

- A1: Adeleye (1973); A2: Alling (1947); A3: Al-shanti (1966); A4: Ayres (1972).
- B1: Bayley (1959); B2: Bayley (1963); B3: Bayley and James (1973); B4: Bayley (1904); B5: Bearce (1973); B6: Belevtsev (1973); B7: Berge (1971); B8: Berge (1974); B9: Bertram and Mellon (1975); B10: Beukes (1973); B11: Bichelonne and Angot (1939); B12: Boskovitz-Rohrlich et al. (1963); B13: Bottke (1965); B14: Bottke (1966); B15: Bottke et al. (1969); B16: Bubenicek (1971); B17: Burchard (1910); B18: Burchard and Andrews (1947); B19: Burchard and Butts (1910); B20: Bushinskii (1969); B21: Button (1976).
- C1: Camacho et al. (1969); C2: Cayeux (1909); C3: Cayeux (1911a); C4: Cayeux (1911b); C5: Cayeux (1922); C6: Chase (1963); C7: Chebotarev (1960); C8: Clifford (1969); C9: Cochrane and Edwards (1960); C10: Collins et al. (1926).
- D1: Dahlstrom (1973); D2: Davidson (1961); D3: Davies (1972); D4: Davies and Dixie (1951); D5: Deubel et al. (1942); D6: Deverin (1945); D7: Dimroth (1968); D8: Dimroth and Chauvel (1973); D9: Dorf and Fox (1957); D10: Dorr (1945); D11: Dorr (1973a); D12: Dorr (1973b); D13: Dorr and Barbosa (1963); D14: Dunbar and McCall (1971); D15: DuToit (1954).
- E1: Eckel (1938); E2: Edmonds et al. (1965); E3: Edwards (1958); E4: Egorov and Timofeiva (1973); E5: Eichler (1970); E6: Einecke (1950); E7: El Sharkawi et al. (1976); E8: Eriksson (1973).

F1: Ferguson (1966); F2: Floran and Papike (1975); F3: Foslie (1949); F4: Fryer (1971).

G1: Gair (1962); G2: Gair and Han (1975); G3: Geijer (1931); G4: Goodwin (1956); G5: Goodwin (1960); G6: Goodwin (1962); G7: Goodwin (1964); G8: Goodwin (1965); G9: Gross (1967); G10: Gross (1968); G11: Gross (1972); G12: Gross (1973); G13: Grout and Wolff (1955); G14: Gruner (1946); G15: Gruss (1968); G16: Gross and McLeod (1980).

H1: Hadding (1932); H2: Hallimond (1922); H3: Hallimond (1925); H4: Hallimond (1951); H5: Harder (1954); H6: Harms (1965); H7: Harrar (1966); H8: Hawley and Beavan (1934); H9: Hayes (1915); H10: Hemingway (1951); H11: Hoenes and Troeger (1945); H12: Huber (1959); H13: Hunter (1963); H14: Hunter (1970); H15: Hurst (1930).

I1: Ikonnikov (1975).

J1: Jackson (1960); J2: James (1951); J3: James (1958); J4: James (1966); J5: James et al. (1961); J6: Jones (1955). J7: Jones (1965).

K1: Kalugin (1973); K2: Kelly (1951); K3: Kimberley (1974); K4: Kimberley and Sorbara (1976); K5: Klein and Fink (1976); K6: Kolbe and Simon (1969); K7: Krishnan (1973).

L1: Lambert (1976); L2: Lamplugh et al. (1920); L3: Landergren (1948); L4: Latal (1952); L5: Lepp (1972); L6: Lovering (1929); L7: Laajoki and Saikonen (1977).

M1: Macgregor et al. (1920); M2: Mansfield (1922); M3: Matsuzawa (1953); M4: Mellon (1962); M5: Moore (1918); M6: Muskatt (1972).

N1: Nakhla and Shehata (1967); N2: Nassim (1950); N3: H.E. Neal (pers. commun., 1975); N4: Newland and Hartnagel (1908); N5: Nicolini (1967); N6: Novokhatsky (1973).

O1: O'Rourke (1961); O2: O'Rourke (1962); O3: Oyarzun et al. (1986).

P1: Page (1958); P2: Palmquist (1935); P3: Parak (1975); P4: Petranek (1964); P5: Petruk (1977); P6: Plaksenko et al. (1973); P7: Pomerene (1964); P8: Pride and Hagner (1972); P9: Pulfrey (1933).

Q1: Quirke (1961); Q2: Quirke et al. (1960).

R1: Rechenberg (1956); R2: Reeves (1966); R3: Richards (1966); R4: Robertson (1976); R5: Robertson and Hudson (1973); R6: Ruckmick (1963); R7: Russell (1975); R8: Rutledge (1910).

S1: Sakamoto (1950); S2: Schellmann (1969); S3: Schmidt (1963); S4: Schoen (1962); S5: Schultz (1966); S6: Schweigart (1965); S7: Sellards and Baker (1934); S8: Shegelski (1975); S9: Shegelski (1976); S10: Shklnka and McIntosh (1972); S11: Shkolnik (1973); S12: Shtsherbak et al. (1973); S13: Sims (1972); S14: Sims (1973); S15: Skocek (1963a); S16: Skocek (1963b); S17: Skocek et al. (1971); S18: Sokolova (1964); S19: Solignac (1930); S20: Sorby (1857); S21: Spencer and Percival (1952); S22: Stanton (1972); S23: Stanton (1976); S24: Stobernack (1970); S25: Strakhov (1969); S26: Svitalski (1937).

T1: Taylor (1949); T2: Taylor (1951); T3: Tegengren (1921); T4: Thwaites (1914); T5: Timofeeva (1966); T6: Timofeeva and Balashov (1972); T7: Tolbert et al. (1971); T8: Trendall (1973a); T9: Trendall (1973b); T10: Trendall and Blockley (1970); T11: Tyler and Twenhofel (1952).

U1: Urban (1966).

V1: Van Hise and Leith (1911); V2: Van Houten (1967); V3: Vorona et al. (1973).

W1: Wagner (1928); W2: Watkins (1972); W3: Weber (1973); W4: White (1954); W5: Whitehead et al. (1952); W6: Willden (1960); W7: Willden (1961); W8: Wilson and Underhill (1971).

Y1: Young (1972); Y2: F.G. Young (pers. commun., 1975); Y3: Young (1922); Y4: Young (1976); Y5: Yakontova et al. (1985).

TABLE 2

No.	A	B	C	D	E	F	G	H	I	J	K	SiO_2
1	SCOS	Kerch	E Plio	USSR	45°20N	36°24E	> 5	> 16	aLs, fMu	Be, Go, Sd/Py, Gl, Vv, Ph	Qtz, Psi, Pyr, Apa, Gyp	17.5
2	SCOS	Shumaysi	Olig	Arabia	21°35N	39°33E	2.4	14	aSs, sSh	Go/Hm, Sd	Qtz, Apa, Cly, Gyp, Cal	21.2
3	SCOS	Kutan-Bulak	M Olig	USSR	46°56N	60°43E	15	Unk	fSs, fSs	Go, Be, Sd	Qtz, Cly	—
4	SCOS	Paz de Rio	Eoce	Colomb	6°11N	72°43W	8	8	aSs, pSh	Go, Hm, Be, Sd/Py	Qtz, Apa, Cht, Kao, Bit	9.4
5	SCOS	Sabanalarga	Eoce	Colomb	4°51N	73° 1W	4	4	fSh, fSh	Go, Be, Sd	Qtz, Apa	(36 ec)
6	SCOS	Djebel Ank	Eoce	Tunisi	34°16N	8°46E	> 1	8	Mu, aLs	Go	Qtz, Kao, Mon, Gyp	5.9
7	INT1	Weches	M Eoce	USA	32°59N	94°37W	> 2	46	aSs, aSs	Be, Gl/Sd, Go, Py	Qtz, Cly, Bit, Cal	32.1
8	SOPS	Hornertown	Pale	USA	40°18N	74° 2W	> 2	9.1	fSs, cSs	Gl/Py	Qtz, Cly, Cal, Apa	50.3
9	SOPS	Navesink	LL Cret	USA	40°23N	74° 0W	> 2	12.2	gSs, fSs	Gl/Py	Qtz, Cly, Cal, Apa	—
10	SCOS	Agbaja + Batati	LL Cret	Nigeri	7°50N	6°41E	15	15	aSs, Exp	Go, Be, Sd/Mg, Py	Kao, Cly, Qtz, Apa, Gyp	6.3
11	DWAT	Perapedhi	LL Cret	Cyprus	35° 5N	32°53E	15	15	Ba, aCh	Go, Py	Cht, Cly, Gyp/Apa	15.0
12	SCOS	Bahariya	L Cret	Egypt	28°29N	29° 2E	> 1	10.6	Ss, Ss	Go, Hm	Cal, Qtz, Cly, Pyr	23.4
13	SCOS	Aswan	L Cret	Egypt	24° 6N	32°54E	1.5	11.7	fSs, fSs	Hm, Go, Be	Qtz, Cly, Apa, Cht	8.9
14	SCOS	Peace River	L Cret	Canada	56°45N	118°38W	9	9	pSh, pSh	Go, No, Sd/Py	Qtz, Cht, Cly, Fel	26.6
15	SOPS	Greensand	LE Cret	Englan	50°53N	0° 1E	1.5	1.5	fSs, Cl	Gl/Mg	Qtz, Cal	48.1
16	SOPS	Grandpre	LE Cret	France	49°21N	4°52E	3	3	fSs, sMu	Go, Gl/Sd	Qtz, Cly	11.0
17	SCOS	Ramim	LE Cret	Israel	33° 5N	35°33E	2.3	2.3	fLs, fLs	Go/Hm	Cal, Dol, Qtz, Kao, Cht	4.9
18	SCOS	Seend	LE Cret	Englan	51°21N	2° 5W	> 9	> 9	gSs, Exp	Sd, Go, Gl	Qtz, Cal, Apa	21.6
19	SCOS	Yabous + Naba Barada	E Cret	Syria	33°42N	36° 9E	> 1	10	aSs, aSs	Go, Hm	Kao, Qtz/Mon, Ill	42.8
20	DWAT	Mackenzie Delta	E Cret	Canada	68°30N	136°30W	0.7	320	Mu, Mu	Sd/Py, Ma, Cl	Qtz, Apa, Cly, Mic	15.0
21	SCOS	Claxby	ME Cret	Englan	52°54N	0°12W	Unk	Unk	gSs, sMu	Go, Be/Sd, Gl, Py	Qtz, Cal, Apa	5.5
22	SCOS	Vassy	EE Cret	France	48°30N	4°59E	2.0	2.0	fMu, fMu	Go/Sd, Be	Qtz, Cal, Cly, Gyp	20.1
23	SCOS	Marsannay-le-Bois	EL Jura	France	47° 4N	4°48E	1.0	2.2	cSh, aLs	Go, Hm, Sd, Py/Gl	Cal, Qtz, Apa, Cht	6.8
24	SCOS	Westbury	EL Jura	Englan	51°15N	2° 9W	4.9	4.9	fMu, Mu	Go, Be, Sd/Py, Gl	Cal	7.5
25	SCOS	Gifhorn	EL Jura	German	52°35N	10°38E	18	18	fLs, cSh	Go, Be, Sd/Py, Hm	Cal, Qtz, Dol, Cly, Bit	14.5
26	SCOS	Chamoson	LM Jura	Switze	46°13N	7°14E	2	2	Sh, Sh	Ch, Mg, Sd/Go, Py, St	Cal, Cht, Qtz, Apa, Afe	6.6
27	SCOS	Windgaelle	LM Jura	Switze	46°48N	8°44E	3	3	aMu, aLs	Ch, Mg, Sd/Go, Py	Dol, Cal, Cly, Cht, Afe	22.4
28	SCOS	Erzegg	LM Jura	Switze	46°47N	8°15E	2	2	Sh, Sh	Ch, Py/Sd, Go, Mg	Cal, Cht, Apa, Qtz, Afe	15.6
29	INT2	La Voulte	LM Jura	France	44°47N	4°47E	7.5	7.5	aLs, aLs	Hm/Go, Sd	Cal, Cht, Apa	15.5
30	MECS	Privas	EM/MM Jura	France	44°44N	4°36E	> 2	8.5	Ls, Ls	Hm/Fs, Py	Cht, Cal	17.5
31	SCOS	Doubs	EM Jura	France	47°18N	6°11E	4	4	oLs, oLs	Go, Hm/Sd	Cal, Qtz, Fel, Afe	13.0
32	SCOS	Murchison-Kahlenberg	LE Jura	German	48°15N	7°47E	9	9	aMu, aLs	Go/Be, Hm	Cal, Qtz, Kao, Cht	18.0
33	SCOS	Red Bed-Lorraine	LE Jura	France	49°30N	5°53E	4.9	4.9	sLs, aLs	Go/Sd	Qtz, Cal, Apa	7.5
34	SCOS	Yellow Bed-Lorraine	LE Jura	France	49°27N	6° 2E	3.5	3.5	fLs, sLs	Go, Be	Cal, Qtz, Mus, Cly, Cht	9.0
35	SCOS	Gray Bed-Lorraine	LE Jura	France	49°27N	6° 2E	5.0	5.0	oLs, fLs	Go, Be/Mg, Sd	Qtz, Cal, Cht, Mus, Apa	5.2
36	SCOS	Black Bed-Lorraine	LE Jura	France	49°28N	5°55E	3.6	3.6	fSs, oLs	Sd, Be, Go	Qtz, Cal, Cht, Apa	20.7
37	SCOS	Green Bed-Lorraine	LE Jura	France	49°27N	6° 2E	2.8	2.8	cSh, fSs	Be, Sd/Go, Py	Cal, Cht, Apa	16.3
38	SCOS	Avelas	LE Jura	France	44°20N	4° 9E	1	1	Ls, aLs	Go, Hm, Be/Sd	Qtz, Mus, Fel, Cht	11.5
39	SCOS	Northampton	LE Jura	Englan	54°14N	0°54W	4.6	11.7	aLs, oLs	Be, Go, Sd/Mg, Py, Gl	Cal, Qtz, Apa, Kao, Fel	8.1
40	SCOS	Rosedale	LE Jura	Englan	54°20N	0°53W	4.3	4.3	aSs, oLs	Be, Mg, Sd	Qtz	7.0
41	SCOS	Malka	LE Jura	USSR	43°44N	43°14E	1.5	23	oMu, sMu	Go, Be, Mg, Hm/Py, Ma, Sd	Qtz, Cht, Cal, Dol	15.4
42	SCOS	Raasy	LE Jura	Scotla	57°20N	6° 0W	2.4	2.4	cSh, pSh	Be, Sd	Cal	6.5
43	SCOS	Marlstone	ME Jura	Englan	52° 6N	1°29W	5	5	fCg, cCg	Sd, Be	Cal, Apa, Qtz, Cly, Fel	9.2
44	SCOS	Frodingham	ME Jura	Englan	54°39N	0°35W	9	9	fLs, fCl	Go, Sd, Be/Py	Cal, Qtz, Apa, Ser, Dol	3.9
45	SCOS	Cleveland	ME Jura	Englan	54°33N	1°10W	2.6	7.8	sSh, fSh	Be, Sd/Py, Gl	Qtz, Cly, Apa, Cal, Cht	8.5
46	SCOS	Oberbank-Echte	ME Jura	German	51°47N	10° 3W	7	7	cMu, oLs	Be, Hm, Sd, Go/Py	Cal, Cht	12.9
47	SCOS	Kurremoella	E Jura	Sweden	55°35N	13°50E	> 19	> 32	fSs, Ukn	Sd, Be, Go/Ill, Gl	Qtz, Cht, Cal	6.6
48	SCOS	Mazenay + Change	EE Jura	France	46°56N	4°39E	2.3	2.3	Ls, fLs	Go, Hm/Py	Cal	(12.5 c)
49	SCOS	Alpha-Friederike	EE Jura	German	51°53N	10°33E	4.8	19	aSs, cMu	Go, Be, Sd/Py	Cal, Qtz, Cly	12.0
50	SCOS	Hussainiya	EE Jura	Iraq	33° 9N	40°48E	> 1	13	sMu, sMu	Hm, Go/Py	Cly, Cal, Kao, Qtz	22.6
51	INT2	Thoste	EE Jura	France	47°30N	4°20W	1.0	1.0	Ls, aLs	Go, Hm	Cht, Cal	13.3

SiO ₂	Al ₂ O ₃	Fe ₂ O ₃	FeO	MnO	MgO	CaO	Na ₂ O	K ₂ O	H ₂ O ⁺	TiO ₂	P ₂ O ₅	CO ₂	S	L.O.I.	Column M (Texture)	Column N (Fossils)	(Refs.)
17.5	4.84	52.4	9.0	0.84	0.46	1.92	0.16	0.20	8.18	—	2.49	5.23	0.12	—	Ooid, Piso, Oobr, Conc	Pele, Wood	S18, S25, Y5*
21.2	6.00	(38.8 Fe)	—	1.28	0.99	3.75	—	—	—	1.73	0.73	—	0.50	—	Ooid, Oobr, Piso, Aqtz	Wood	A3*
—	—	(50 Fe)	—	—	—	1.1	—	—	—	—	1.6	—	—	—	Ooid, Oobr, Rrup, Lent	Npel, Wood	D2*, S25
9.4	5.30	(46.6 Fe)	—	0.26	0.96	1.35	—	—	—	—	2.09	—	—	13.2	Oobr, Aqtz, Fepl, Rrup, Phos	Ichn, Wood	K5*, V2, +
(36 comb.)	(30 Fe)	—	—	—	—	—	—	—	—	—	1.47	—	0.09	—	Ooid, Oobr, Aqtz, Conc	Ichn, Wood	C1*, +
5.9	5.44	70.1	—	0.71	0.35	1.70	—	—	—	—	2.64	—	0.57	11.9	Ooid, Fefo	Shar	N5, S19*
32.1	15.5	12.7	20.4	—	5.20	1.98	2.37	3.62	5.20	—	tr.	—	—	—	Ooid, Xbed, Conc	Wood, Gast	E1*, S7
50.3	7.53	18.4	3.0	—	3.82	0.65	0.22	7.88	8.58	—	0.34	0.15	—	—	Gran, Noid, Fefo	Brac, Unsk	D9, M2*, +
—	—	—	—	—	—	—	—	5.51	—	—	0.91	—	—	—	Gran, Noid, Fefo	Bele, Unsk	M2*
6.3	8.16	(51.2 Fe)	—	0.08	0.12	0.37	—	—	—	0.54	1.73	—	0.07	—	Oobr, Piso, Fefo, Aqtz, Rrup	Pele, Gast	A1, J6*, J7
15.0	3.8	(44.0 Fe)	—	2.1	0.8	0.5	—	0.69	—	0.22	0.60	—	—	—	Lban, Noid, Gbed, Pyro, Slum	Nosk	R4, R5*
23.4	2.15	(49.1 Fe)	—	3.92	0.48	3.12	—	—	—	0.01	0.13	—	—	4.55	Piso, Ooid, Fefo	Form, Pele	N1*
8.9	2.73	(55.4 Fe)	—	0.37	0.78	2.92	—	—	—	—	2.11	—	0.06	2.38	Ooid, Oobr, Aqtz, Ripl	Unkn	A3, N1, N2*
26.6	5.95	30.8	13.0	0.18	1.52	1.74	0.33	0.51	13.8	0.19	1.57	3.13	—	17.0	Ooid, Aqtz, Rrup, Fefo, Oobr	Form, Pele	B9, M4*, P5
48.1	9.16	19.1	3.5	—	2.36	0.76	0.22	7.08	5.28	—	—	—	—	—	Gran, Noid	Unsk	H2*
11.0	3.52	(48.0 Fe)	—	0.60	1.17	tr.	—	—	15.0	—	0.40	—	—	—	Aqtz, Noid	Unkn	C5*
4.9	3.7	38.3	—	0.13	1.5	23.5	—	—	—	0.35	0.60	—	0.55	25.0	Ooid, Fefo	Unsk	B12*
21.6	5.82	17.5	25.7	0.52	0.59	2.88	0.14	0.83	3.05	0.25	0.96	16.7	0.27	—	Ooid, Fefo	Pele, Gast	H3*, L2
42.8	10.3	34.8	0.6	0.20	0.30	0.10	0.13	0.34	—	1.22	0.26	—	—	8.10	Piso, Ooid, Oobr, Aqtz, Rrup	Wood	E7*
15.0	4.53	(27.0 Fe)	—	5.72	2.87	3.31	0.18	0.37	—	0.17	7.85	—	—	21.1	Mban, Lent, Aqtz, Noid	Unkn	N3, Y1*, Y2
5.5	4.62	69.5	0.6	0.20	0.68	0.53	0.01	0.14	12.3	0.71	0.95	0.4	0.10	—	Ooid, Oobr, Aqtz	Pele, Ammo	H3*, L2
20.1	6.16	(39.6 Fe)	—	1.10	1.17	0.80	—	—	—	—	0.61	—	0.44	12.0	Ooid, Oobr, Aqtz, Rrup	Wood, Npel	C5*
6.8	5.80	(29.8 Fe)	—	—	—	21.4	—	—	—	—	—	—	—	23.5	Ooid, Oobr, Ooca, Rrup, Aqtz	Moll, Alga	C5*
7.5	3.97	6.2	26.7	0.92	2.8	2.53	—	—	—	—	0.38	14.7	0.13	—	27.6, Ooid, Oobr	Pele	H3*
14.5	5.30	37.3	5.4	0.18	1.25	14.7	0.88	0.44	—	0.15	0.87	—	0.35	17.7	Ooid, Ooca, Aqtz, Rrup, Conc	Form, Gast	K6*
6.6	5.27	24.8	23.3	—	0.97	19.6	0.52	comb.	4.27	0.31	1.21	13.3	—	—	Ooid, Oobr, Sphe, Fefo, Xbed	Crin, Moll	D6*
22.4	14.3	12.0	37.6	0.02	3.42	0.00	0.22	0.04	9.70	0.19	—	—	—	—	Ooid, Fefo, Conc	Crin, Echi	D6*
15.6	7.92	16.2	32.8	—	0.25	2.62	—	—	7.82	1.55	6.33	8.33	0.17	—	Ooid, Fefo, Conc	Crin, Echi	D6*
15.5	6.80	(46.5 Fe)	—	—	—	3.30	—	—	—	—	—	—	—	8.40	Loid, Oobr, Fefo, Lban	Aley, Moll	C5*
17.5	4.00	(47.3 Fe)	—	—	—	4.50	—	—	—	—	0.25	—	—	6.50	Lban, Noid, BreC	Spic, Aley	C5*
13.0	4.10	48.2	—	—	—	13.0	—	—	—	tr.	—	—	0.13	21.0	Ooid, Ooca, Oobr, Sphe, Aqtz	Bryo, Form	C5*
18.0	3.6	38.9	0.4	—	0.9	15.7	—	—	—	—	—	7.0	—	18.0	Ooid, Oobr, Xrip, Aqtz, Fefo	Pele, Echi	U1*
7.5	5.09	54.9	1.3	0.22	—	10.8	—	—	—	—	1.85	—	—	17.8	Oobr, Ooca, Fefo, Aqtz, Xbed	Bone, Pele	B11, B16, C5*
9.0	5.75	33.0	5.0	0.26	1.44	20.6	—	—	—	—	0.96	—	0.05	22.7	Ooid, Oobr, Aqtz, Fefo	Moll, Alga	B11*, B16, C5*
5.2	5.78	47.5	10.0	0.49	0.92	10.8	—	—	—	—	2.23	—	tr.	17.8	Ooid, Oobr, Aqtz, Fefo, Rrup	Moll, Spic	B11, B16, C5*
20.7	9.10	32.4	9.3	0.21	—	11.6	—	—	—	—	1.24	—	—	15.3	Ooid, Oobr, Fefo	Moll, Alga	B11, C5*
16.3	6.19	28.8	16.1	0.45	2.52	4.53	—	—	—	—	1.37	—	0.87	19.8	Ooid, Oobr, Sphe, Fefo	Crin, Moll	B11*, C5
11.5	7.70	(21.9 Fe)	—	—	—	24.5	—	—	—	—	—	—	—	25.2	Ooid, Ooca, Fefo, Aqtz, Rrup	Gast, Pele	C5*
8.1	7.11	12.4	36.5	0.07	3.49	5.25	—	—	4.09	—	0.80	20.3	0.03	24.4	Ooid, Ooca, Oobr, Aqtz, Fefo	Pele, Echi	L2, T1*, T2
7.0	7.13	32.6	25.9	—	—	—	—	—	—	—	9.38	—	—	—	Ooid, Conc, Rrup	Unk	H3*, H10
15.4	7.00	58.9	1.0	0.12	3.24	2.21	—	—	6.94	0.45	0.17	1.03	—	—	Ooid, Piso, Lban, Conc, Fepl	Wood	S18*, T5, T6
6.5	5.6	2.3	30.3	0.4	2.0	17.6	—	--	—	—	1.70	28.3	0.2	29.5	Ooid, Rrup	Bele, Echi	M1*
9.2	5.61	3.5	28.5	1.84	2.32	17.1	—	—	—	—	0.45	24.1	0.10	—	Oobr, Ooca, Fefo, Xrip, Aqtz	Crin, Pele	E3, H3*, W5, +
3.9	3.34	19.4	11.3	1.58	1.3	26.3	—	—	—	—	0.77	—	0.41	29.8	Oobr, Fefo, Xbed, Aqtz, Piso	Pele, Crin	D4, H3*, W5
8.5	6.12	1.8	36.9	0.42	3.75	5.54	0.05	0.03	4.05	0.36	1.30	20.7	0.05	—	Oobr, Ooca, Rrup, Fefo, Aqtz	Pele, Ammo	H3*, L2, S20
12.9	10.5	17.3	17.1	0.11	3.12	14.6	0.96	0.39	6.32	0.35	1.69	12.4	—	—	Oobr, Fefo, Conc, Rrup, Phos	Pele, Bele	B15, S2*
6.6	6.86	9.8	37.9	0.20	1.79	4.19	0.09	0.40	1.59	0.30	0.47	27.1	0.09	—	Ooid, Oobr, Aqtz	Unk	P2*
(12.5 comb.)	(35 Fe)	—	—	0.50	17.0	—	—	—	—	—	0.60	—	0.10	19.0	Ooid, Ooca, Oobr, Fefo, Rrup	Crin, Alga	C5*
12.0	7.5	31.5	7.5	0.21	2.2	16.0	(0.85)	—	7.0	0.21	1.10	13.0	0.28	—	Ooid, Oobr, Rrup, Phos	Brac, Pele	B15*
22.6	19.1	(34.1 Fe)	—	0.01	0.28	0.36	0.28	0.29	6.87	1.53	0.13	—	—	—	Ooid, Oobr, Piso, Rrup, Conc	Stro, Nosk	S17*
13.3	11.0	(47.3 Fe)	—	1.40	—	2.23	—	—	3.82	—	—	—	—	—	Gran Lban, Loid, Fefo, Lent	Moll, Brac	C3, C4, C5*

51	INT2	Thoste	EE Jura	France	47°30N	4°20W	1.0	1.0	Ls, aLs	Go, Hm	Cht, Cal	13.3
52	MECS	Vares	E-MM Tria	Yugosl	44°10N	18°20E	95	131	aLs, hLs	Sd, Hm/Mc, Mg, Cl	Cht, Cly, Ser, Bar, Qtz	8.4
53	SCOS	Desert Basin	L Perm	Austra	17°49S	123°46E	9	9	fSs, fSs	Be	Qtz, Cal, Fel, Ser	19.1
54	COSP	Raniganj	M Perm	India	23°35N	87° 7E	0.3	Unk	Sh, Sh	Sd	Cly, Qtz	18.1
55	COSP	Prestwick	E Perm	S. Afri	28° 4S	30°17E	3.0	3.0	Sh, pSh	Sd, Be/Mg	Bit, Qtz, Cly, Cal	5.1
56	COSP	Palmyra	E Perm	S. Afri	27°58S	30°26E	1.0	1.0	Ss, aCo	Sd/Py	Bit, Cal, Dol	1.4
57	COSP	Dalmellington	Penn	Scotla	55°21N	4°26W	<1.0	1.0	pSh, pSh	Sd	Bit, Cly, Cal	11.8
58	COSP	Dalry Clayband	Miss	Scotla	55°46N	4°41W	<0.5	0.5	pSh, pSh	Sd	Cal, Cly, Bit	7.6
59	MECS	Tynagh	M Miss	Irelan	53° 8N	8°22W	6.4	47.5	aLs, tLs	Hm/Cl, St, Mn, Mg, Mh, Py	Cht, Cal, Dol, Qtz, Ser	27.4
60	SCOS	Tuyun	L Devo	China	26°16N	107°29E	Unk	3	sSh, sSh	Hm	Unk	40.1
61	SCOS	Namur	ML Devo	Belgiu	50°32N	5°14E	2.0	2.0	Sh, Sh	Hm, Be, Py, Sd/Ep	Cal, Qtz, Cht, Apa	—
62	SVOP	Constanze-Lahn-Dill	LM-EL Devo	German	50°46N	8°10E	Unk	<5	Tu, Ls	Hm/Py, Ch	Cht, Cal/Bit	46.8
63	SVOP	Konigszug-Lahn-Dill	LM-EL Devo	German	50°45N	8°20E	Unk	<5	Tu, Ls	Hm/Py, Ch	Cal, Cht/Bit	2.6
64	SVOP	Grottenberg-Bredelar	LM-EL Devo	German	51°24N	8°42E	1.5	1.5	cTu, tLs	Hm/Sd, Mg, Py, Cl	Cht, Cal, Dol, Bit	6.6
65	SCOS	Martin	Devo	USA	33°15N	110°45W	2.1	2.1	aLs, Sh	Hm, Gl	Cal, Dol, Qtz	19.6
66	SCOS	Tajmiste	E-M Devo	Yugosl	41°35N	20°49E	20	20	pPh, pPh	Ch, Sd, Mg/Py	Bit	13.1
67	SVOP	Altai	E-M Devo	USSR	50°45N	91° 0E	Unk	65	Vc, cVc	Hm/Mg, Sd	Cht, Ser, Cly	—
68	INT2	Ardenne	EM Devo	****	50° 1N	4° 3E	2.5	2.5	Gw, Gw	Hm, Sd, Ch	Cht, Cal, Qtz	18.5
69	INT2	Phulchoki	Silu	Nepal	27°23N	88°23E	>2	20	qSs, fDs	Hm/Sd	Cht, Cal, Qtz, Cly	14.0
70	SCOS	Rose Hill	EM Silu	USA	40°34N	78° 6W	0.5	0.5	Sh, Sh	Hm/Ch	Cal, Cht	2.6
71	SCOS	Kirkland-Clinton	EM Silu	USA	43° 3N	75°23W	1.7	1.7	sDs, qSs	Hm/Sd, Py, Cl	Dol, Cht, Qtz	8.7
72	SCOS	Westmoreland-Clinton	EM Silu	USA	43° 2N	75°23W	0.9	0.9	fSs, cMu	Hm, Ch/Sd, Py, Cl	Dol, Cal, Qtz, Cht, Apa	15.6
73	SCOS	Wolcott-Clinton	EM Silu	USA	43°10N	75°52W	0.6	0.6	Ls, sSh	Hm/Ch, Py, Cl	Dol, Cal, Qtz	8.6
74	SCOS	Furnaceville-Clinton	EM Silu	USA	43°13N	76°50W	0.8	0.8	aLs, aLs	Hm/Ch, Py, Cl	Dol, Cht, Cal, Qtz, Apa	11.7
75	SCOS	Red Mountain	E Silu	USA	33°30N	86°46W	9.1	33	fSs, fSs	Hm/Ch, Py	Cal, Qtz, Dol, Apa	25.0
76	SCOS	Eight Meter-Vivaldi	E Silu	Spain	42°36N	6°32W	8	8	Qz, Sh	Mg, Ch, Sd/Ma, Hm	Cal	17.0
77	INT3	Lieu-lieu	Ordo-Devo	Chile	38°15S	73°15W	15	45	fCh, fCh	Mg/Ma, Py, Cp	Cht	46.9
78	SCOS	Mayville	LL Ordo	USA	43°28N	88°24W	Unk	16.8	Sh, Ds	Go/Sd, Hm, Mg, Py	Cal, Dol, Hal, Qtz, Var	5.1
79	SCOS	Llandegai	M Ordo	Wales	53°11N	4° 6W	4.2	4.2	pMu, fMu	Hm, Ch, Sd/Cl, Mg, Py, St	Qtz, Fel, Cht, Ser, Kao	12.1
80	SVOP	Austin Brook	M Ordo	Canada	47°20N	65°48W	12	44	tSc, tSc	Mg, Cl, Hm, Sd/St, Py, Bi	Cht, Qtz, Cal/Sph, Gal	21.7
81	MECS	Hafjell	Camb-Silu	Norway	68°23N	16°50E	>1	10	cSc, eSc	Mg, Hm	Cht, Cal, Apa	—
82	MECS	Sjafjell	Camb-Silu	Norway	68°21N	16°50E	>10	25	cSc, eSc	Mg, Gr, Am/Ga	Cht	35.7
83	SCOS	May-sur-Orne	LE Ordo	France	48° 6N	1°37W	6.3	6.3	dSs, sSh	Sd, Hm, Ch/Mg	Cht	10.9
84	SCOS	Ferriere-aux-Etangs	LE Ordo	France	48°39N	0°30W	4.5	4.5	sSh, sSh	Sd, Ch, Hm/Py, Go	Cht, Cal, Apa, Qtz/Bit	15.0
85	SCOS	Upper-Thuringian	ME Ordo	German	50°36N	10°49E	>10	40	fSl, fQz	Ch, Cl, Sd, Hm/Py	Qtz, Cly, Cal, Apa, Ser	15.0
86	SCOS	Sarka	ME Ordo	Czecho	49°44N	13°35E	11	20	fSh, fSh	Hm, Ch, Sd/Py, Gl	Qtz, Ill, Cal, Apa, Kao	27.1
87	INT2	Klabava	ME Ordo	Czecho	49°46N	13°30E	8.5	Unk	Cg, tSh	Hm, Ch, Sd/Py	Qtz, Cht, Ill, Apa	51.9
88	SCOS	Upper-Wabana	E Ordo	Canada	47°38N	52°59W	0.5	7.8	sSh, pSh	Hm, Ch, Sd/Py	Qtz, Apa	8.6
89	SCOS	Scotia-Wabana	E Ordo	Canada	47°38N	53°59W	1.3	4.6	aSs, aSs	Hm, Ch, Sd/Py	Apa, Qtz, Cal/Bit, Gal	15.3
90	SCOS	Pyrite-Wabana	E Ordo	Canada	47°38N	52°59W	0.5	1.2	fSs, pSh	Py	Cht, Apa, Cal	9.9
91	SCOS	Dominion-Wabana	E Ordo	Canada	47°38N	52°59W	3.3	11	fSs, fSs	Hm, Ch/Sd, Py	Qtz, Apa, Cal, Cht	12.6
92	INT2	Anjou	EE Ordo	France	47°41N	0°51W	3.5	6.8	aSs, aSs	Mg/C, Hm, Sd, Py	Cht/Afe	21.8
93	SOPS	Oland	EE Ordo	Sweden	55°51N	16°41E	0.3	2.0	pSh, gLs	Gl/Sd, Py, Ma	Cal, Qtz/Apa	51.4
94	SCOS	Sierrite-Bliss	L Camb-E Ordo	USA	32°56N	107°14W	2.1	5.5	fSs, oLs	Hm, Ch/Gl, Sd, Go	Qtz, Cal, Apa, Cht, Fel	27.0
95	MECS	Urucum + Mutun	PreZ-Ordo	****	19°15S	57°52W	>10	300	oda, Exp	Hm/Mg	Cht/Cry	17.3
96	MECS	Maly Khingan	E Camb	USSR	42°48N	131°37E	Unk	60	rDs, pSl	Sd, Mg, Hm	Cht, Dol, Cal, Rho, Hau	44.2
97	MECS	Uda	PreY-Paleoz	USSR	53°32N	134° 5E	60	300	fCh, fCh	Hm, Mg/Sd, Ch, Go, Py	Cht, Ser, Cly	—
98	MECS	Rapitan	Pre Z	Canada	65°14N	133° 0E	>10	150	fMx, fMx	Hm	Cht/Apa	25.0
99	MECS	Huanahuua	Pre Z	China	40°43N	115° 3E	2.9	6.2	kSs, pSl	Hm	Cht, Qtz	21.6
100	MECS	Low Hakos-Damara	L PreY-PreZ	S. Afr.	22°52S	17°26E	8	16	fSc, fSc	Hm, Ma, Mg	Cht	22.0
101	SCOS	Roper River	E-M PreY	Austra	14°43S	134°17E	12	51	fSh, sSh	Hm, Sd, Mg/Ch, Gn, Py	Qtz, Cht/Bit	30.3
102	SCOS	Constance Range	E-M PreY	Austra	18°35S	138° 7E	16	21	sSh, sSh	Hm, Sd, Ch/Py	Qtz, Cht, Cly/Bit	8.0
103	SVOP	Per Geiger-Kiruna	E PreY	Sweden	67°53N	20°15E	>10	250	vKe, fSs	Mg, Hm/Ma	Apa, Cht	5.0
104	SVOP	Kiirunavaara-Kiruna	E PreY	Sweden	67°52N	20°15E	>10	75	fCg, vKe	Mg, Hm/Am, Bi	Apa, Cal, Cht	1.1
105	MECS	Serra dos Carajas	L PreX-PreZ	Brazil	6° 3N	50°11W	>10	>200	Ph, Ph	Mg, Ma/Hm, Sd	Cht	56.2

13.3	11.0	(47.3 Fe)	1.40	—	2.23	—	—	3.82	—	—	—	—	—	Gran Lban, Loid, Fefo, Lent	Moll, Brac	C3, C4, C5*	
8.4	1.20	(37.2 Fe)	4.57	0.80	0.62	—	—	—	—	0.05	—	1.20	—	Lban, Loid, Fefo, Rrup	Unsk	L4*	
19.1	12.8	(35.4 Fe)	0.50	0.30	0.16	—	—	11.7	0.15	0.41	tr.	—	—	Ooid, Aqtz, Fefo	Unsk	E3*	
18.1	—	(45.2 Fe)	2.39	—	—	—	—	—	—	1.65	—	—	—	Gran, Noid	Unk	K7*	
5.1	2.35	none	50.9	0.58	0.30	0.70	—	—	—	0.33	31.8	0.18	—	Noid, Lent	Unk	W1*	
1.4	0.29	30.4	10.1	0.61	2.52	20.9	—	—	—	0.27	—	0.14	—	Mban, Noid	Leaf, Spor	W1*	
11.8	7.4	(35.6 Fe)	1.35	—	1.32	—	—	—	—	0.44	—	0.07	40.3	Noid	Wood	M1*	
7.6	5.95	(25.7 Fe)	2.25	2.60	12.9	—	—	—	1.05	1.28	—	0.23	31.4	Noid	Wood	M1*	
27.4	1.00	57.8	3.6	0.23	0.35	3.50	—	—	—	0.06	0.11	6.3	—	Lban, Conc, Grad	Stro	R7*, S5	
40.1	4.13	(28.7 Fe)	—	1.10	4.14	—	—	—	—	1.79	—	0.06	—	Ooid	Unk	H1*	
—	—	(45. Fe)	—	—	—	—	—	—	—	—	—	—	—	Ooid, Aqtz, Fefo	Bryo, Crin	C2*	
46.8	0.25	50.8	0.40	0.01	0.02	0.80	0.05	0.04	0.27	0.05	0.12	0.06	0.07	Loid, Lban, Conc	Echi, Crin	H5*	
2.6	0.75	52.6	0.88	0.11	0.21	22.4	0.05	0.03	1.12	0.1	0.08	18.5	0.31	Loid, Lban, Conc	Echi, Crin	H5*	
6.6	0.76	(37.3 Fe)	0.19	2.82	5.77	—	—	—	0.03	0.39	—	—	—	Lban, Fefo, Pyro	Moll, Brac	B13*, B14	
19.6	6.30	49.0	0.45	0.16	2.40	7.79	0.14	1.69	2.48	0.28	1.80	6.30	0.03	—	Ooid	Unk	W6, W7*
13.1	14.9	(39.7 Fe)	0.45	1.00	2.33	—	—	—	—	1.67	—	0.28	—	Ooid, Gran, Conc, Lent	Unk	L4*, P1	
—	—	(35. Fe)	<0.1	—	—	—	—	—	—	<0.1	—	—	—	Wban, Pyro, Xrip, Desi, Evap	Wood, Ichn	K1*	
18.5	11.2	(34.9 Fe)	—	—	7.59	—	—	—	—	—	—	—	—	Gran, Fefo, Roid, Aqtz	Bryo, Brac	C2*, C3	
14.0	1.50	78.3	2.93	0.02	0.69	tr.	—	—	2.04	0.10	0.13	—	tr.	Lban, Piso	Brac, Ceph	O1*, O2	
2.6	4.80	48.1	1.7	0.17	0.56	22.1	—	0.19	—	—	1.04	18.8	none	Ooid, Conc, Fefo	Brac, Crin	H14, R8*	
8.7	3.67	(21.2 Fe)	—	7.84	20.6	—	—	—	—	0.75	24.8	0.15	—	Soid, Fefo, Lent, Motl	Crin, Brac	A2*, M6, S4	
15.6	6.96	2.2	18.3	0.56	8.83	17.6	0.01	0.02	3.38	0.18	0.80	25.0	—	Ooid	Bryo, Brac	A2*, J4, M6, +	
8.6	5.04	(31.1 Fe)	—	7.37	13.7	—	—	—	—	1.58	18.8	0.03	—	Ooid, Fefo	Unsk	N4*, S4	
11.7	0.48	(36.3 Fe)	tr.	3.76	7.34	—	—	2.76	—	1.13	21.5	0.03	—	Ooid, Fefo	Bryo, Brac	A2*, S4	
25.0	3.01	(35.3 Fe)	0.26	—	9.89	—	—	—	—	0.78	—	0.04	—	Ooid, Fefo, Xbed, Rrup	Bryo, Crin	B5, B17, B18, B19	
17.0	—	(53. Fe)	—	—	—	—	—	—	—	1.8	—	—	—	Ooid	Nosk	R1*	
46.9	3.07	(30.6 Fe)	1.44	0.46	0.70	0.55	0.19	—	0.11	0.83	—	—	—	Wban	Nosk	O3*	
5.1	3.25	72.3	0.44	—	0.61	5.98	—	—	4.90	—	3.73	3.60	—	Oobr, Fefo, Rrup, Conc, Volc	Corl, Spic	H8*, T4	
12.1	9.50	2.1	33.7	0.14	1.52	0.92	—	—	—	0.18	1.88	3.89	0.07	—	Oobr, Piso, Gran, Aqtz, Conc	Spic, Stro	H3, H4, P9*
21.7	2.22	48.7	16.4	1.48	2.12	1.01	0.22	0.16	0.81	0.05	1.97	2.94	0.03	—	Wban, Pyro, Aqtz, Noid	Nosk	D3*
—	—	(23.3 Fe)	1.68	—	—	—	—	—	—	0.80	—	—	—	Lban	Nosk	F3*	
35.7	8.26	28.7	17.0	0.40	2.05	4.53	—	—	—	0.20	2.61	—	0.07	0.40	Wban	Nosk	F3*
10.9	4.58	(54.1 Fe)	0.09	0.03	2.85	—	—	—	—	1.93	—	tr.	3.43	Ooid	Tril	C5*, H11	
15.0	2.90	41.5	9.4	0.20	1.18	2.60	—	—	—	1.71	—	—	25.0	Ooid, Oobr, Fefo, Lban	Alga	C5*, H11	
15.0	8.48	(33.0 Fe)	1.03	1.68	3.00	—	—	—	—	0.92	13.0	—	—	Ooid, Piso, Oobr	Brac	D5*, E6	
27.1	10.5	29.1	14.4	0.06	0.84	1.24	0.57	1.94	2.18	0.83	0.52	9.60	0.09	—	Oobr, Aqtz, Rrup, Fefo, Pyro	Brac	P4*, S15, S16
51.9	6.54	22.3	5.3	0.10	1.93	3.27	0.88	0.99	2.37	0.73	0.87	2.22	0.05	—	Ooid, Mban, Pyro, Aqtz, Grad	Brac	P4*
8.6	4.82	72.7	8.4	—	—	—	—	—	—	1.22	1.38	—	—	Ooid, Motl	Brac, Ichn	G9, H9*	
15.3	9.63	44.2	19.4	0.26	1.45	1.54	0.46	0.08	5.80	—	1.07	0.43	—	—	Ooid, Xbed, Conc, Fefo, Aqtz	Brac, Alga	H9*
9.9	—	(35.2 Fe)	—	—	0.54	—	—	—	—	0.35	—	34.5	—	Ooid, Lent, Fefo	Grap, Brac	G9, H9*	
12.6	5.71	(52.6 Fe)	—	0.42	1.49	—	—	—	0.27	1.63	—	0.00	2.17	Ooid, Conc, Fefo, Aqtz	Brac, Alga	G9, H9*	
21.8	2.57	(53.6 Fe)	0.06	0.1	0.47	—	—	—	—	0.33	—	—	2.59	Loid, Lban, Fefo	Bryo, Crin	C2*, H11	
51.4	9.47	16.4	4.8	—	3.17	0.63	1.22	7.34	4.85	—	0.35	—	—	Noid, Gran, Rrup, Fefo	Brac, Grap	H1*	
27.0	—	(39.2 Fe)	—	—	1.79	—	—	—	—	1.08	—	—	—	Ooid, Piso, Sphe, Aqtz	Unsk	K2*	
17.3	0.65	(56.9 Fe)	0.08	0.06	0.06	—	0.20	—	0.05	0.14	—	0.04	—	Wban, Roid	Nosk	D10*, D11, D12	
44.2	4.58	(16.8 Fe)	11.1	1.28	2.71	—	—	0.76	—	0.14	2.60	0.01	—	Wban, Noid, Pyro, Desi	Nosk	C7*, E4	
—	5.0	(43.0 Fe)	9.0	(2 comb.)	—	—	—	—	—	0.9	—	—	—	Mban	Radi, Spic	S11*	
25.0	—	(43.0 Fe)	—	—	—	—	—	—	—	0.5	—	—	—	Wban, Pyro, Piso, Desi	Nosk	D1*, G11, G12, Y4	
21.6	—	(52.1 Fe)	0.18	—	0.62	—	—	—	—	0.30	—	0.07	—	Ooid, Piso	Stro	B20, II*, M3, T3	
22.0	0.10	(45.6 Fe)	—	0.42	5.75	0.10	0.01	—	0.06	1.40	—	0.01	4.07	Wban	Nosk	B10*	
30.3	2.26	16.5	37.0	0.78	2.09	tr.	0.16	0.14	8.73	0.03	0.01	tr.	—	Ooid, Piso, Xrip, Desi, Rrup	Nosk	C9*, E3	
8.0	0.7	52.6	22.4	0.17	0.78	0.3	—	—	0.85	0.03	0.02	13.8	—	Ooid, Piso, Xrip, Desi, Rrup	Nosk	E3, H6*	
5.0	—	(44.4 Fe)	—	—	—	—	—	—	—	9.0	—	—	—	Lban	Nosk	P3*	
1.1	—	(60.6 Fe)	0.10	1.15	—	—	1.2	—	0.33	4.49	—	—	—	Lban	Nosk	G3, L3*, P3	
56.2	0.55	39.4	1.2	—	—	—	—	—	—	0.07	—	—	—	Wban	Nosk	T7*	

106	MECS	Caue	MPreX-MPreY	Brazil	19°39S	43°14W	> 10	300	* vPh, fDs	Hm/Mg, Ma, Cl, Am	Cht, Tal, Dol	45.0
107	INT2	Broken Hill	LPreX-EPreY	Austra	31°57S	141°30E	0.9	Unk	Ch, Ch	Mg, Ga/Bi, Hm, ll, Py	Cht, Apa	37.1
108	MECS	Zhuantobe	PreX-PreZ	USSR	45°35N	71° 6E	50	750	Po, Sl	Hm/Mg, Ma, St	Cht	33.8
109	MECS	Okouma + Bafoula	LPreX	Gabon	1°33S	13°14E	10	10	pMu, pMu	Sd, Gn, Py/Cl, St	Cht, Apa, Ser/Bit	35.8
110	MECS	Sokoman	LPreX	Canada	54°49N	66°53W	> 50	244	Sl, pSl	Hm, Mg, Mn, Sd/Ma, St, Gn	Cht/Bit, Rho	51.2
111	MECS	Temiscamie	L PreX	Canada	51° 6N	73° 0W	> 10	160	pMu, pGw	Sd, An, Mg, St/Hm, Mn, Py	Cht, Dol, Qtz/Bit	31.2
112	MECS	Gunflint	M-L PreX	Canada	48°17N	90° 8W	64	165	Cg, tLs	Gn, Hm, Sd/Mg, Py	Cht, Dol, Cal/Bit	56.7
113	MECS	Biwabik	M-L PreX	USA	47°22N	93° 2W	76	230	Cg, fLs	Mn, Gn, St, Mg, Sd, Hm/Py	Cht, Cal/Bit	46.4
114	MECS	Trommald	M-L PreX	USA	46°29N	94° 1W	> 10	153	sMu, tMu	Sd, Mn, St, Hm/Mg, Cl, Gr	Cht	28.8
115	MECS	Mansfield	M-L PreX	USA	46° 5N	88°13W	> 5	46	pSl, pSl	Mg, St, Sd, Gr	Cht, Cly	3.7
116	MECS	Vulcan	M-L PreX	USA	45°48N	88° 0W	> 10	198	Sc, Unc	Mg, Ma, Hm/Gr, Ga, An	Cht, Cal, Qtz	44.6
117	MECS	Ironwood	M-L PreX	USA	46°27N	90°17W	> 5	274	Qz, pSl	Sd, Mg, Hm, Mn, St/Cl, Py	Cht	32.9
118	MECS	Iron River	M-L PreX	USA	46° 4N	88°36W	> 1	91	pSl, fGw	Sd/Cl, Py	Cht, Qtz/Bit	24.3
119	MECS	Negaunee	M-L PreX	USA	46°27N	87°36W	60	1067	fGw, fCg	Sd, Mg, Hm, Ma/Mn, St, Cl	Cht, Qtz	41.6
120	MECS	Goose Lake	M-L PreX	USA	46°28N	87°33W	Unk	30	Sl, Sl	Sd, Mg, Cl, St	Cht	43.5
121	SCOS	Daspoort	M-L PreX	S. Afr.	26°34S	27°11E	2.4	2.4	Sh, rMu	Hm, Mg, Go, Ch/An, Py	Qtz, Kao, Apa, Fel	15.2
122	SCOS	Clayband-Timeball	M-L PreX	S. Afr.	25°43S	28°13E	1.2	1.2	Sh, Sh	Mg, Ch, Sd	Apa, Qtz	5.8
123	SCOS	Pisolithic-Timeball	M-L PreX	S. Afr.	25°43S	28°13E	1.8	1.8	Sh, Ss	Hm, Go, Ch, An	Qtz	20.0
124	SCOS	Magnetic-Timeball	M-L PreX	S. Afr.	25°43S	28°13E	8.2	8.2	Sh, kSh	Mg, Go, Hm, Ch	Qtz, Cal, Apa	22.2
125	MECS	Kuruman + Penge	M-L PreX	S. Afr.	29°18S	22°20E	> 10	700	mLs, bJa	Mg, Sd, Mn, Gr/Hm, Re, St	Cht, Dol, Cal/Bit	40.7
126	MECS	Hotazel	M-L PreX	S. Afr.	27°22S	23° 0E	> 10	85	An, Unc	Ma, Mg, Hm	Cht/Cry, Bra, Rho	47.0
127	MECS	Paakkö	LM PreX	Finland	64°41N	27°53E	18	36	Ph, pSc	Mg, Sd, Gr/An, Po, Py	Cht, Apa/Bit, Bio	42.5
128	MECS	Kipalu	PreX	Canada	56° 0N	79°22W	> 10	125	cQz, tSI	Hm, Mg, Gn, Sd	Cht, Cal, Qtz, Fel	47.6
129	MECS	Kursk	PreX	USSR	51°36N	37° 7E	Unk	477	pSl, pSl	Mg, Hm, Fs/Sd, Py	Cht	40.4
130	MECS	Krivoy Rog	PreX	USSR	47°55N	33°24E	260	2000	Ub, Sc	Ma, Hm, Mg, Sd/Cl, An, St	Cht	7.8
131	MECS	Bihar + Orissa	E-M PreX	India	21°55N	85°10E	> 10	1000	tPh, tPh	Hm, Ma/Mg, Sd	Cht	61.4
132	MECS	Nimba	E PreX	Liberia	7°29N	8°41W	Unk	450	Ph, Ph	Mg, Ma, Hm/Am, Sd, Py, Cl	Cht/Ant, Apa	39.7
133	MECS	Boolgeeda-Hamersley	L PreW-X	Austra	22°20S	118°14E	213	213	Tu, Sh	Hm, Mg, Sd, An/St, Re, Py	Cht	51.4
134	MECS	Brockman-Hamersley	L PreW-X	Austra	22°20S	118°14E	366	610	fSh, Sh	Hm, Mg, Sd, An/Gn, St, Py	Cht, Cal	47.9
135	MECS	Marra Mamba-Hamersley	L PreW-X	Austra	22°20S	118°14E	183	183	pSh, Ds	Hm, Mg, Sd, An/St, Re, Py	Cht	67.4
136	MECS	Anshan	PreW-PreY	China	41° 5N	122°58E	10	250	Qz, Sl	Mg, Hm/Gr, Cu, Cl, Sd	Cht	46.2
137	MECS	Contorted Bed	L PreW-PreX	S. Afr.	26°10S	28° 2E	> 5	22	aCh, fMu	Mg, Ma	Cht, Cly	40.9
138	SVOP	Subganian	L PreW-PreX	USSR	58° 5N	122°22E	> 10	200	fGn, fGn	Mg/Am, Ma, Ga, Bi	Cht/Fel	43.3
139	MECS	Beijing	PreW-EPreX	Gabon	1° 6N	13°10E	> 10	200	Sc, Sc	Ma, Hm/Mg, Am	Cht	42.7
140	MECS	West Melville	PreW-PreX	Canada	68°13N	85°30W	> 50	400	Sc, Sc	Mg, Hm/Am, Cl, Bi, Po, Py	Cht/Apa, Mus	—
141	INT4	Main-Atl.City	PreW-EPreX	USA	42°32N	108°44W	> 5	49	Sc, fSc	Mg, Am/Bi, Cl, Hy, Ga	Cht	44.1
142	MECS	Upper-Goe	L PreW	Liberi	6°15N	10°22W	> 10	150	aSc, Ch	Mg, Hm, Gr/Ga, Bi	Cht	13.6
143	DWAT	Sheba	L PreW	S. Afr.	25°55S	30°50E	< 1	Unk	pSh, aGw	Mg, Hm	Cht, Cly	60.3
144	DWAT	Santa Claus	L PreW	Austra	31° 6N	122°14E	> 3	90	eGw, eGw	Mg/Gr, Hb	Cht	—
145	MECS	Cerro Bolívar	L PreW	Venezu	7°20N	63°35W	Unk	200	Gn, Gn	Mg, Ma/Am, Px, Bi, Cl	Cht	42.0
146	INT4	Steep Rock	L PreW	Canada	48°49N	91°39W	> 10	60	jDs, pMu	Sd, Py	Cht, Cal, Cly/Bit	3.2
147	SVOP	Helen	L PreW	Canada	48° 0N	84°48W	300	300	fCh, fCh	Sd, Py/Mg, Po, An, Cl	Cht, Dol, Cal/Cly, Bit	13.9
148	SVOP	Outerring	L PreW	Canada	64°57N	107°51W	37	37	cTu, pAr	Sd, Mg, Cl, Am, Py/Bi, Po	Cht/Cal, Dol, Bit	—
149	DWAT	Savant Lake	L PreW	Canada	50°28N	90°27W	< 0.7	Unk	fSh, aGw	Mg/Py, Hm	Cht, Cly, Bit	61.3
150	MECS	Bong Range	M PreW	Liberi	6°13N	9°10W	> 10	80	Sc, Sc	Mg, Hm, Ma/Bi, Cu, Gr	Cht	41.2
151	INT3	Lake St. Joseph	PreW	Canada	51° 2N	90°28W	3	61	sPh, sPh	Mg/Hm, Bi, Cl, Am, Ga	Cht	—
152	SVOP	Pickle Crow	PreW	Canada	51°30N	90° 4W	24	24	Ba, Ba	Sd/Mg, Po, Py	Cht	32.1
153	INT4	Seminole	PreW	USA	42°14N	107° 0W	30	92	Sc, fSl	Mg/Ma, Am, Hy	Cht	47.2
154	INT4	Nova Lima	PreW	Brazil	19°58S	43°49W	50	Unk	pPh, pPh	Sd, Mg/An, Py, Po, Cl, St	Cht, Dol/Bit	38.9
155	SVOP	Soudan	M-L PreW	USA	47°47N	90°30W	> 2	> 60	Ba, Unc	Mg, Hm, Ma/Gr, Am, Py, Sd	Cht	50.8
156	MECS	Cascade-Mozaan	M-L PreW	S. Afr.	26°49S	30°43E	12	12	Sh, Sh	Mg, Cl/Sd	Cht, Cly, Qtz	42.1

45.0	0.54	50.2	3.1	0.28	—	—	—	—	—	0.05	—	0.58	—	Wban, Noid	Nosk	D11, D12, D13, R2	
37.1	8.4	(27.7 Fe)	6.15	1.18	5.4	0.50	0.40	—	0.43	3.1	—	—	—	Wban	Nosk	R2, S22, S23*	
33.8	1.02	63.1	1.0	0.05	0.12	0.38	0.16	0.11	—	—	0.36	—	0.04	0.58	Wban	Nosk	N6, S12*
35.8	0.2	(31.2 Fe)	0.18	1.8	2.0	0.06	0.07	—	0.04	0.96	—	—	13.6	Wban, Sphe	Nosk	W3*	
51.2	0.42	42.0	3.3	0.02	0.62	0.00	0.02	0.01	2.10	0.00	0.03	0.06	0.00	—	Wban, Loid, Gran, Rpup, Xrip	Nosk	D7, D8, G10*, K5
31.2	0.14	12.6	25.7	0.68	3.94	5.17	0.05	0.10	0.54	0.02	0.13	19.7	—	—	Wban, Gran, Piso, Xbed, Rpup	Nosk	F4, G16, Q1, Q2*
56.7	3.16	5.9	11.4	0.32	2.35	4.80	0.26	0.78	2.6	0.25	0.25	9.1	1.63	—	Wban, Gran, Loid, Rpup, Ripl	Nosk, Stro	F2, G4, G5, G16*
46.4	0.90	18.7	19.7	0.63	2.98	1.60	0.04	0.13	1.60	0.04	0.08	6.90	—	1.72	Wban, Gran, Loid, Rpup, Ripl	Nosk, Stro	G14, L5*, W4
28.8	2.19	3.6	32.8	8.40	2.11	1.10	0.06	0.41	1.76	0.34	0.09	18.0	—	—	Wban, Gran, Loid, Rpup	Nosk	G13, S3*
3.7	—	(64.8 Fe)	—	—	—	—	—	—	—	0.08	—	—	—	—	Wban	Nosk	B1*
44.6	0.16	(35.6 Fe)	0.92	0.21	0.53	—	—	—	—	0.71	0.06	—	0.10	—	Wban, Loid, Gran	Nosk	B4, J3, J5*
32.9	2.46	4.8	30.8	1.33	3.58	0.62	0.00	0.00	1.69	0.27	0.09	20.9	0.09	—	Wban, Gran, Loid, Rpup	Nosk	H12*, V1
24.3	1.71	0.7	35.2	2.11	3.16	1.78	0.04	0.20	0.00	0.00	0.91	27.6	—	—	Wban, Gran, Brec, Sty	Nosk	J4*, V1
41.6	1.18	23.5	20.9	0.52	1.68	1.18	—	—	—	0.09	0.25	—	0.03	6.27	Wban, Gran, Roid, Rpup, Ripl	Nosk	B3, G2*, T11
43.5	5.3	13.7	20.8	0.58	1.7	0.32	1.2	1.4	2.0	0.22	0.24	8.5	—	—	Wban, Gran, Rpup	Nosk	B3, G2*, T11
15.2	9.23	(49.5 Fe)	tr.	—	tr.	—	—	—	—	0.77	—	—	3.50	Ooid, Piso, Lban, Ripl, Rpup	Nosk, Stro	S6, W1*	
5.8	4.40	42.0	34.4	0.90	0.90	1.50	—	—	2.90	0.26	1.19	4.75	0.08	—	Ooid, Oobr	Nosk	E8, S6, W1*
20.0	6.05	64.6	0.7	—	0.56	0.40	tr.	tr.	7.45	0.15	0.45	0.10	tr.	—	Piso, Ooid	Nosk	E8, S6, W1*
22.2	5.24	36.4	23.1	0.45	1.02	2.36	—	—	—	tr.	1.02	0.18	0.56	—	Oobr, Ooca, Xrip, Rpup, Mban	Nosk, Stro	S6, W1*
40.7	2.32	21.0	20.1	0.29	3.15	2.63	1.05	0.57	0.91	0.12	0.25	6.56	—	—	Wban, Gran, Rpup, Conc	Nosk, Stro	B10*, B21, W1
47.0	0.45	48.9	0.2	>1.8	0.01	0.17	0.12	0.53	0.01	—	—	0.34	—	—	Wban, Loid, Ooca	Nosk	B10*, D15
42.5	0.85	17.9	24.7	0.8	3.53	3.75	0.16	0.18	2.32	0.10	2.73	0.04	0.78	—	Wban, Noid	Nosk	L7*
47.6	3.82	25.9	8.8	1.73	2.08	1.46	0.04	0.70	2.9	0.06	0.08	5.2	0.02	—	Wban, Gran, Aqtz	Nosk	J3, M5, Y3, G16*
40.4	0.68	39.1	11.8	0.05	1.86	1.74	—	—	—	0.15	0.15	—	0.05	—	Wban, Noid, Rpup	Nosk	P6*, S25
7.8	1.00	(63.2 Fe)	0.21	0.05	1.18	—	—	—	—	0.08	—	—	1.80	Wban, Roid	Nosk	B6, S25, S26*	
61.4	0.10	30.6	3.2	—	0.20	0.48	0.94	comb.	1.79	—	—	0.66	—	—	Wban, Noid	Nosk	K7, S21*
39.7	0.14	44.0	12.9	0.02	0.57	0.34	—	0.1	—	0.03	0.15	—	—	—	Wban	Nosk	B8*, G15
51.4	3.34	28.7	7.7	0.16	2.33	0.64	0.26	1.35	1.98	0.16	0.25	1.28	—	—	Wban, Noid, Conc	Nosk	T9, T10*
47.9	0.33	26.0	15.2	<.01	2.49	1.85	0.12	0.11	0.68	0.03	0.19	5.11	0.04	—	Wban, Noid, Conc, Sium	Nosk	A4, T8, T9, T10*
67.4	0.04	10.9	16.5	<.01	2.16	<.01	<.01	0.31	2.39	0.02	0.36	0.07	0.02	—	Wban, Noid, Conc	Nosk	T9, T10*
46.2	—	(36.0 Fe)	0.83	—	0.92	—	—	—	—	0.10	—	0.03	—	—	Wban	Nosk	I1*, S1
40.9	4.00	50.1	0.1	—	none	none	—	—	—	—	—	—	—	—	Wban, Brec, Noid, Slum	Nosk	B10*, W1
43.3	0.08	36.1	16.5	0.04	1.33	0.62	0.13	tr.	0.09	0.22	0.14	—	0.02	1.84	Wban	Nosk	V3*
42.7	0.8	(44.6 Fe)	—	—	—	—	—	—	—	0.08	—	—	0.7	Wban	Nosk	S14*	
—	—	(30.0 Fe)	—	—	—	—	—	—	0.08	0.07	—	0.02	—	—	Wban	Nosk	W2, W8*
44.1	3.85	30.8	15.5	0.09	2.80	1.31	1.22	0.36	—	—	—	—	—	—	Wban	Nosk	B2, B3, P8*
13.6	—	(57.2 Fe)	—	—	—	—	—	—	—	—	0.52	—	—	6.0	Wban	Nosk	B7*
60.3	1.53	(26.5 Fe)	0.22	0.14	0.47	0.15	—	—	0.13	0.02	—	—	—	—	Wban	Nosk	D14*
—	—	—	—	—	—	—	—	—	—	—	—	—	—	—	Wban	Nosk	C6, G15, R6*
42.0	—	(39 Fe)	—	—	—	—	—	—	—	—	—	—	—	—	Wban	Nosk	K4, S10*, +
3.2	0.29	(41.5 Fe)	1.57	2.33	3.35	—	—	—	—	0.01	—	21.1	28.0	Wban	Nosk	C10*, G6, G7, +	
13.9	3.63	3.3	28.6	1.73	5.73	4.34	0.94	0.45	1.30	0.09	0.23	27.1	3.35	—	Wban, Noid, Rpup, Conc, Pyro	Nosk	L1*, +
—	—	(20 Fe)	—	—	—	—	—	—	—	—	—	—	—	—	Wban, Rpup, Pyro, Roid, Conc	Nosk	S8*, S9, +
61.3	12.6	—	15.9	0.15	2.33	0.58	—	—	—	0.43	—	—	0.04	—	Wban, Pyro, Slum	Nosk	E5*, G15, S24
41.2	0.87	40.5	13.0	0.15	1.35	0.84	0.20	comb.	0.27	0.17	0.13	0.19	0.03	—	Wban	Nosk	B10*
—	—	(35 Fe)	—	—	—	—	—	—	—	—	—	—	—	—	Wban, Noid, Pyro	Nosk	C8*, G8
32.1	1.43	9.6	31.1	0.13	2.17	2.28	0.08	0.14	0.39	0.14	0.16	19.0	2.09	—	Wban, Noid, Brec	Nosk	F1, H15*, +
47.2	—	(33.7 Fe)	0.01	—	—	—	—	—	—	0.10	0.09	—	0.05	—	Wban	Nosk	H7*, L6
38.9	0.05	9.7	27.6	<.01	0.8	3.1	0.22	<.01	0.1	<.01	0.08	17.9	0.53	—	Wban	Nosk	D11, G1*, P7
50.8	—	(34.1 Fe)	0.13	—	—	—	—	—	—	0.16	—	—	—	—	Wban, Rpup, Pyro	Nosk	S13*, V1
42.1	4.65	22.2	17.8	3.35	2.25	1.00	—	—	0.75	0.15	0.05	4.90	0.10	—	Lban, Loid	Nosk	B10, H13, W1*

Have there been long-lasting bodies of iron-rich water?

Marine ironstone generally is attributed to precipitation from iron-rich water but there is no consensus regarding the long-term existence of a large body of iron-rich seawater. Some hydrothermal models imply that iron precipitated from transient plumes which may never have reached chemical equilibrium with any large body of water. These models generally discount any influence of the atmosphere on iron formations (e.g., Gross, 1983). Other hydrothermal models suggest that Precambrian exhalation was sufficiently potent to overwhelm continental runoff and control marine chemistry everywhere, not just within stagnant deep basins (Fryer et al., 1979).

If one accepts the concept of large, long-lasting, iron-rich water bodies during the Precambrian, one may presume that the potential for sedimentation occurred extensively, either in areas of upwelling or along the perimeter of an iron-rich water body where iron-rich water both underlay oxidizing surface water and overlay a sediment-starved platform. Individual iron formations would have resulted from temporal or spatial variation in marine currents, biota, atmospheric conditions, upwelling, or climatically induced variation in river input. If one prefers short-lived hydrothermal plumes, one could conclude that ironstone sedimentation generally occurred within a few hundred kilometers of the hydrothermal vents, typically on the closest platform reached by the ferriferous water. Between times of hydrothermal input, background seawater may have been as iron-poor as is modern seawater.

The possibility that all portions of the oceans were iron-poor between times of exhalation is rejected herein. The large volume and lateral continuity of cherty iron formations is interpreted to record long-lasting iron-rich water bodies. Ferriferous water may well have owed its existence to exhalation but the apparent persistence of abundant dissolved iron is inter-

preted to indicate that iron and silica remained soluble after any exhalative plume reached thermal equilibrium with the sea.

Have iron-rich oceans been devoid of sulfur-bearing species?

Iron solubility reaches only a few ppb within any modern seawater which contains detectable O₂ or H₂S. Some authors doubt that iron could become reduced without concomitant reduction of sulfate, hence precipitation of iron as a sulfide (e.g., Drever, 1974). It has been proposed that Early Precambrian oceans were generally iron-rich because the concentration of sulfide ions was "vanishingly low" and "the concentration of sulfate in sea water was very much lower than that of the present day" (Walker and Brindlecombe, 1985, p. 218). However, Holland (1984) has noted that this proposal is inconsistent with both the occurrence of Precambrian gypsum deposits and the ubiquity of pyritic Precambrian mudrocks. Early Archean (3.5 Ga) sulfate evaporites occur in Australia (Buick and Dunlop, 1987). Pyrite is as strongly correlative with organic carbon in Precambrian mudrocks as in Phanerozoic mudrocks (Dimroth and Kimberley, 1976). It is therefore concluded that sulfur species were generally abundant in Precambrian seawater (Ohmoto and Felder, 1987). It is quite possible, however, that restricted basins of sulfur-depleted seawater developed locally.

Holland (1973, 1984) has suggested that iron solubility could reach a few ppm in seawater at intermediate oxidation states where siderite would be stable instead of pyrite or iron oxides. Holland's model of coexisting Fe²⁺ and SO₄²⁻ has been confirmed by the discovery of the ferriferous, sulfate-rich Orca Basin (Sheu and Presley, 1986a) and by the iron abundance in sulfate-bearing pore fluids within some surficial marine sediment (Aller and Mackin, 1988).

Highly ferriferous seawater of normal to brackish salinity presently is known to exist

only as pore fluids. Within marine water bodies, a high iron content is limited to hypersaline water, either in a deep restricted environment (Sheu and Presley, 1986a) or in a shallow pool (Sonnenfeld et al., 1977). Some shallowly buried, marine pore fluid in the Amazon delta stays within the siderite field. This has been attributed to seasonal reworking to a sediment depth greater than a meter, as revealed by profiles of ^{210}Pb , NH_4^+ , and I^- (Aller and Mackin, 1988). Reworking apparently is caused largely by bioturbation but bioturbation may not be invoked during the Early to Middle Precambrian when most cherty iron formations accumulated. Comparably iron-rich marine pore water [up to 8 ppm (0.14 mM) Fe^{2+}] occurs in a climatic setting which is the opposite of the equatorial Amazon, i.e., the northern Baltic Sea (Ingri and Ponter, 1986).

The winter ice cover over the northern Baltic apparently helps the bottom water become suboxic and ferriferous (Ingri and Ponter, 1986). In the northern Baltic, surficial crusts and nodules of iron and/or manganese oxides indicate that solutes are migrating to the sediment-water interface where they precipitate (Ingri and Ponter, 1986). An effect similar to bioturbation may occur here due to the seasonal variation from wintertime reducing conditions, when the sea is ice-covered, to springtime oxidation when river input and waves affect the bottom. Pore water under the northern Baltic Sea contains 8 ppm Fe in an area which is stagnant and reducing during the winter because of ice cover but oxidized each spring due to wave action and river input (Ingri and Ponter, 1986). Brackish pore water (200 mM Cl^-) under the southern Baltic Sea contains about as much dissolved iron as calculated by Holland (1984, p. 388) for equilibrium with both siderite and calcite, i.e. 0.05 mM Fe^{2+} (Boesen and Postma, 1988).

Pore water in Amazon deltaic sediment contains up to 0.7 mM Fe^{2+} (30 ppm) within 0.5 m of the seafloor (Aller et al., 1986). The elevated dissolved iron content is partly attribut-

able to a copious supply of hydrated iron oxides in the fluvial sediment. The sediment averages about 5.8% Fe (Aller et al., 1986). Lovley (1987) has shown experimentally that bacteria prefer to reduce ferric hydroxide in the oxidation of organic matter rather than reduce seawater sulfate, as one would expect from the greater Gibbs energy gain for reduction of ferric hydroxide (Froelich et al., 1979). Iron solubility in Amazon sediment also is enhanced by mixing of the upper meter of sediment every year (Aller and Mackin, 1988). Mixing oxidizes authigenic ferrous minerals and enhances the availability of ferric minerals for bacterial reduction.

Was an oxygen-poor atmosphere a sufficient cause of iron formations?

An anoxic atmosphere clearly cannot be invoked for the many Phanerozoic iron formations, some of which are cherty (Table 2). Oxidized Precambrian paleosol records an atmosphere with about 1% O_2 at 1.8 Ga (Zbinden and Holland, 1987). However, several textbooks (e.g., Eicher and McAlester, 1980) state that the problem of cherty iron formations is simply one of insolubility of iron under oxidizing conditions. Mel'nik (1982, p. 106) concludes that marine iron solubility can reach as much as 400 ppm Fe in the absence of free oxygen but Holland (1984) notes that only about 3 ppm would be expected in seawater saturated with respect to both siderite and calcite.

The concept that an anoxic atmosphere is a sufficient cause of iron formations enjoys widespread popularity. However, iron formations require at least two other conditions, i.e., inhibition of sulfate reduction and active dissolution of iron. Iron dissolution either may be driven by shallow weathering (subaerial or subaqueous) or by deep weathering.

Inhibition of sulfate reduction may be studied by considering modern anoxic water bodies. Ignoring fjords, four large bodies of chemically reduced seawater are presently known to occur

distant from hydrothermal vents, i.e., the Black Sea (Brewer and Spencer, 1974), the Cariaco Basin on the Venezuelan shelf (Richards, 1975), the Tyco Basin in the eastern Mediterranean (Jongsma et al., 1983), and the Orca Basin in the northern Gulf of Mexico (Sheu and Presley, 1986b). All of these basins are deep, reaching from 1.4 to over 2 km in water depth. Only the Orca water is known to be ferriferous, containing 1.6 ppm Fe^{2+} (Sheu and Presley, 1986a). This is comparable to the minimum iron concentration invoked in genetic models for iron formations (Holland, 1984). In contrast, neither the Black Sea nor the Cariaco contains more than a nanomolar concentration of dissolved iron (56 ppb). Most Black Sea water contains roughly 20 ppb Fe, about an order of magnitude more than average oxidized seawater (2 ppb Fe; see Holland, 1978). Anoxic Cariaco water contains about 6 ppb Fe (De Baar et al., 1988). These sub-nanomolar concentrations are far too low to produce an iron formation.

Active precipitation of iron to produce an iron formation requires contemporaneously active dissolution of iron because voluminous iron formations contain several times more iron than could have been dissolved at any given time in the combined oceans, no matter how ferriferous they may have been. However, the most significant inputs of iron to modern seawater, i.e. hydrothermal exhalation and seismic pumping, are not occurring at a sufficient rate to account for ancient cherty iron formations, given any reasonable estimate of the efficiency of concentration and the sedimentation rate of voluminous iron formations.

Exhalative iron input produced by late diagenesis of sediment presently appears to be smaller than the exhalative input from hydrating oceanic crust (Bäcker and Lange, 1987; Scott, 1987). Neither modern flux has yet been measured accurately but it seems unlikely that even the basaltic hydrothermal flux will prove to be comparable to the sedimentation rate of iron which Holland (1984) has estimated for

the formation of the Hamersley iron formation, i.e., $3 \times 10^{10} \text{ kg a}^{-1}$. Transport of sufficient dissolved iron to the Hamersley platform would have required seawater close to saturation with respect to siderite. Hydrothermal input of additional iron to such saturated seawater may have induced some precipitation close to each vent and so marine transport to a distant iron-formation platform may not have been very efficient.

Remnant hydrothermal vents have not been found associated with most cherty iron formations. It is concluded that if exhalation has been the prime source of iron throughout Earth history, as advocated herein, the input rate at times of voluminous ironstone sedimentation must have been much greater than the rate which occurs presently and that a decrease in atmospheric oxygen pressure is not a sufficient condition for production of voluminous iron formations. A high input rate may have existed on time scales less than 10^7 years, during rapid pumping of seawater through new crust.

Has iron been supplied as fluvial solutes?

Gruner (1922) calculated that the iron in iron formations could have been supplied as fluvial solutes from a river like the Amazon. However, Gruner (1922) overestimated the aqueous iron content of the Amazon by two orders of magnitude (Kimberley, 1979a). Lepp and Goldich (1964) estimated that the dissolved iron content of Precambrian rivers may have been substantial if the ambient atmosphere had been anoxic. However, the required degree of anoxia is inconsistent with the record of oxidized Precambrian paleosols (Holland, 1984; Zbinden and Holland, 1987).

There may have been times in the Archean when the atmosphere was sufficiently reducing that rivers did carry appreciable dissolved iron but it is unlikely that one ever could deduce what the ratio of solute/particulate iron was in any fluvial source even if such a reducing atmosphere ever existed. Seawater that could keep

fluvial Fe^{2+} dissolved also could dissolve Fe^{2+} from amorphous hydroxide coatings on fluvial clays. It is concluded that the concept of fluvial supply of abundant aqueous iron is not viable for the times of Proterozoic paleosols (Holland, *in press*) and the non-fluvial mechanism which has supplied dissolved iron at those times probably also supplied the iron during potentially more reducing times during portions of the Archean.

Do iron formations record irreversible events in Earth history?

Some authors have interpreted both cherty and noncherty iron formations to record irreversible evolutionary events (e.g., Petranek, 1964). Cloud (1973) hypothesized that voluminous iron formations mostly formed about 2 Ga ago because of irreversible proliferation of photosynthetic microbiota. However, subsequent dating of iron formations has revealed a much larger age range for voluminous deposits than envisioned by Cloud (1973) and the chronological continuity of iron formations in Table 2 is inconsistent with the concept of a biologically unique event at 2 Ga.

Cameron (1982) has noted that the pyrite in South African iron formations and shale beds older than 2.35 Ga is enriched in ^{34}S whereas younger pyrite contains isotopically light sulfur, as does modern pyrite. He interpreted this data to record the initiation of sulfate-rich seawater at 2.35 Ga, a time at which sulfate reducers either evolved or proliferated. Based on data from North America, Hattori et al. (1983) support this concept but prefer a date of 2.2 Ga. The concept of an irreversible change in the sulfate-sulfide system in the Early Proterozoic appears to be inconsistent, however, with both Archean evidence of ^{34}S -depleted pyrite (Thode and Goodwin, 1983) and Phanerozoic evidence of ^{34}S -enriched pyrite (Goodfellow, 1987). Ohmoto and Felder (1987) attribute the post-Middle Precambrian increase in sulfur-isotope fractionation to a combined decrease in oceanic

temperature and increase in sulfate concentration.

Voluminous cherty iron formations clearly record major marine modifications which must have had great impact on the biota from time to time during the Precambrian. However, these modifications recurred throughout the Precambrian and even into the Phanerozoic (Table 2). None of these iron formations appears to record any irreversible biologic development. Biota associated with cherty iron formations seem to be dominated by bacteria, including cyanobacteria which previously have been called "blue-green algae" (Cloud and Licari, 1972; Stanier and Cohen-Bazire, 1977). Over 2000 types of bacteria are listed by Skerman et al. (1980), including several which deposit iron hydroxide or manganese oxide in structures outside their cells (Ghiorse, 1984). Bacterial mutations occur rapidly in response to environmental changes and so it seems unlikely that bacterial evolution would lead rather than follow any environmental modification. Tectonomagmatic cycles are interpreted to have led environmental modification through both the Precambrian and Phanerozoic. Major cycles in these tectonomagmatic-environmental conditions appear to have been imposed upon the long-term trend of planetary cooling. Variation in abundance of iron formations is attributed to these tectonomagmatic cycles rather than biologic innovations.

The most prominent evolutionary event for which there is geologic evidence was the advent of metazoan predators about 570 Ma ago (Glaessner, 1984). Nonpredatory metazoans (Ediacara fauna) had existed for over 100 million years prior to being supplanted by the modern system which includes multi-stage food chains. Only such animals as Anthozoa (soft-bodied corals) survived the demise of the passive Ediacaran life style (Jenkins, 1985). Geologists universally recognize this event and surely hope that it will not soon be reversed. This Precambrian-Cambrian boundary has been interpreted to represent the irreversible

demise of cherty iron formations (e.g., Skinner, 1969; Baur et al., 1985). This concept is inconsistent, however, with the existence of several Phanerozoic cherty iron formations (Table 2). The metazoan requirement of an oxidizing atmosphere may well have been detrimental, however, to Phanerozoic cherty iron formations.

Have iron-rich fluids exhaled directly from the mantle?

Mantle outgassing has been proposed as a source of exhalative fluids (Gold and Soter, 1980). Given minimal knowledge of the carbon content of the mantle, it is not yet possible to estimate its capacity for occasional generation of carbonaceous volatiles which might become exhaled along with iron, phosphorus, and other elements. It is conceivable that the ferriferous fluids which become cherty iron formations are generated within the mantle and that the crust acts only as a conduit for those fluids to the hydrosphere. Another possibility is that mantle-derived volatile-rich fluids dissolve iron during their ascent through the crust. There are four lines of evidence which may support these two mantle-based hypotheses, i.e.: (1) regional or global synchronicity in some iron-precipitating events; (2) global evolution of iron-formation types; (3) ratios of carbon and oxygen isotopes which differ from those in contemporaneous seawater; and (4) modern exhalation of mantle-derived fluids. Each of these is examined briefly, starting with modern exhalation.

Analysis of helium isotopic ratios has demonstrated that mantle exhalation indeed is occurring today (e.g., Poreda et al., 1986) but the volume of exhaling fluids presently is small. Helium isotopes have not yet been reported for areas of young ironstone deposits. Fortunately, three ironstone-rich areas also exhibit modern methane exhalation which would be suitable for analysis, i.e., the Margarita-Araya platform of Venezuela, the Mahakam delta of Indonesia, and the Kerch peninsula of the U.S.S.R. All three areas have accumulated enough Tertiary

sedimentary carbonaceous matter to account for the observed methane without invoking mantle exhalation.

Iron formations contain anomalously high proportions of ^{12}C and ^{16}O relative to ^{13}C and ^{18}O . Similarly light isotopic ratios occur in modern carbonates under the Norwegian Sea where they have been attributed to exhalation of methane and hydrogen from the mantle (Lawrence and Taviani, 1988). Isotopically light CO_2 and H_2O are attributed to reaction of mantle-derived methane and hydrogen with crustal sulfate and ferric iron (Lawrence and Taviani, 1988). If further investigations support this hypothesis, it may have some bearing on the production of cherty iron formations but the available data are not conclusive.

There is considerable evidence for regional synchronicity of ironstone sedimentation across large areas, e.g. the Jurassic oolitic iron formations of Europe (McGhee and Bayer, 1985). Peaks in the production of cherty iron formations apparently occurred during the Precambrian but temporal resolution of those peaks is not yet precise (James, 1983; see also Table 2). The best evidence of Tertiary peaks lies with glauconite-rich beds which commonly are associated with phosphorite. Combined phosphorite-glauconite sedimentation is remarkably time-dependent, with the most recent global peak having occurred during the Miocene (Cook and McElhinny, 1979). Internal Earth processes, presumably mantle-driven, may be controlling such sedimentary cycles (Fischer and Arthur, 1977; Keith, 1982). Sheridan (1983) proposes a cyclicity related to plumes rising from the core-mantle boundary.

There is an obvious evolution in the proportion of cherty/noncherty iron formations throughout Earth history (fig. 1 in Kimberley, 1983). Whatever the immediate cause of this variation may have been, e.g., atmospheric evolution or evolution of deep-weathering exhalation, the ultimate cause probably has been tectonomagmatic evolution which reflects evolution of the mantle. It does not follow, how-

ever, that this variation demands a mantle source for the iron-rich fluids independent of crustal processes like weathering.

A hypothetical mantle source for iron-rich fluids may seem incompatible with the typically shallow-water environment, great stratiform extent, and crustal metal ratios in iron formations. Mantle-derived fluids presumably always have reached the Earth's surface mostly within deep ocean basins, as they mostly do today (Jenkins et al., 1978). It may be argued that any mantle-fluid supply would have resembled modern convective hydrothermal supply in that precipitation close to vents would have produced poorly stratified deposits of limited extent (Bäcker and Lange, 1987). Modern deep-sea hydrothermal precipitates characteristically have lower ratios of iron to other metals than do iron formations (Kunzendorf et al., 1984). Direct precipitation from mantle fluids within deep basins presumably would have produced polymetallic deposits like those which presently are accumulating (Kunzendorf et al., 1984).

Fluids derived from any initial fractionation of the mantle would be expected to have even higher concentrations of some trace elements than do modern ridge-associated deposits (Metz et al., 1988). However, even deep-water (DWAT) iron formations are metal-poor and DWAT iron formations constitute only a small proportion of the total volume of iron formations (Table 2). Direct precipitation of mantle fluids therefore is rejected as a source of iron formations. Nonetheless, iron formations are indirectly attributed to the mantle because of its production of new crust and its dynamics which drive seismic pumping (McCaig, 1988).

Major genetic flow charts

Introduction

Interrelationships among genetic questions are illustrated in the following charts (Figs. 1–18). One purpose of these charts is to demon-

strate that it is inappropriate to attempt to reduce the iron-formation controversy to a single question, e.g., the hydrothermal versus nonhydrothermal question of Simonson (1985).

Organization of the following charts is somewhat arbitrary. Several alternative schemes would be equally viable. Each flow-chart option carries implications which are partially explained in the few paragraphs which precede each chart. A set of basic questions is addressed in the initial set of four charts, i.e., iron source, the predominant iron-solute species, predominant precipitation mechanism, and prime cause of evolutionary change in iron-formation abundance. These four questions are followed by subsidiary controversial topics, e.g., isotopic fractionation and textures. Preferred answers to most of the questions posed by these flow charts are presented later in this paper.

Flow chart for iron source

Fe source: shallow weathering, crustal hydration, or late diagenesis? (Fig. 1.)

An inherent assumption in this question is that other possible iron sources may be ignored. These excluded possibilities include groundwater flow from peripheral areas, as proposed for noncherty iron formations by James (1966). This exclusion is based on calculations by Kimberley (1979a) and Ferguson et al. (1983) which show that the maximum potential supply would be insufficient to produce observed noncherty iron formations. Cherty iron formations are clearly too voluminous for such an iron source.

Most genetic models for iron formations assume either a shallow-weathering or deep-weathering (e.g., hydrothermal) source of the iron. The predominance of these alternatives is evident in reviews of both cherty (Kimberley, 1983) and noncherty iron formations (Kimberley, 1979a). A shallow-weathering source is most commonly invoked for noncherty iron formations (e.g., Hunter, 1970) and hydrothermal input is most commonly invoked for cherty iron formations (e.g., Goodwin et al., 1985).

Shallow Weathering: Direct input of fluvial Fe-rich grains, e.g., ooids or partial dissolution of sediment within the ocean?	Crustal hydration: Hydrothermal sources dominated chemistry of large water mass or precipitation occurred from transient plumes?	Late diagenesis: Glauconitic versus oolitic precipitates due to different rate of fluid expulsion or different fluid composition?
Shallow weathering – Fluvial ooids: Ooids formed within drainage system, by precipitation of iron supplied by groundwater, or within soil.	Crustal hydration – Dominating water mass: Sulfate-rich or sulfur-poor? If sulfur-poor, was it because of precipitation of H_2S with excess Fe^{2+} or because of precipitation of anhydrite during convection through oceanic crust?	Late diagenesis – Rate: Expulsion rate could have varied gradually so why are glauconitic-versus-oolitic deposits generally not gradational?
<i>Shallow weathering – Ooids: Groundwater:</i> Why are Fe-rich ooids essentially unknown as modern fluvial grains?	Crustal hydration – Plumes: How could plumes produce the lateral continuity of bed thickness observed in some cherty iron formations?	Late diagenesis – Composition: Why would differing compositions produce differing textures (peloidal versus oolitic)?
<i>Shallow weathering – Ooids: Soil:</i> Why do ooids never display diagenetic development of oolitic layering, as in soil spherules?		
Shallow weathering – Within oceans: Dissolution within water of seawater salinity or in hypersaline water?		
<i>Shallow weathering – Within oceans: Hypersaline:</i> How could a sufficiently large portion of the ocean become hypersaline?		
<i>Shallow weathering – Within oceans: Eusaline:</i> How could enough ferriferous pore water leak upward into the water column? Given that modern eusaline anoxic water bodies are iron-poor, why are there Phanerozoic cherty iron formations?		

Fig. 1. Flow chart for iron source. Iron source was shallow weathering, crustal hydration, or late diagenesis?

However, several authors prefer a shallow-weathering source for cherty iron formations (e.g., Garrels, 1987) and a hydrothermal source for some noncherty iron formations (e.g., Schweigart, 1965).

Variations on each of the shallow- versus deep-weathering alternatives are so diverse that there may be little similarity between two models which both invoke a similar source, e.g., the shallow-weathering model for cherty iron formations by Lepp and Goldich (1964) versus that of Holland (1984). Lepp and Goldich

(1964) propose that under an anoxic Precambrian atmosphere, ferrous solutes may have been delivered by rivers directly to the ocean and precipitated there like the calcium of limestone. Holland (1984) discounts direct fluvial input and proposes that seafloor sediment (mostly of fluvial origin) could react with a small amount of organic matter to produce iron-rich bottom waters. He proposes that these fluids would be carried by upwelling currents to precipitate on shallow platforms.

Holland (1984) apparently envisions the

iron-rich bottom waters to be expelled pore fluids, given that his cited analogs of modern iron-rich water are restricted to the suboxic zone of shallowly buried marine sediment. This suboxic zone may extend downward about a meter at most (Aller et al., 1986). If Holland (1984) envisions fluid expulsion, he does not provide a mechanism for expulsion prior to burial beneath the suboxic zone. The problem of shallow pore-fluid expulsion is addressed by Berner (1980, p. 24) who notes that, "... in the presence of steady-state compaction, water flow occurs into the sediment and not out of it as is often stated in the literature".

The possible expulsion (diffusion) of shallow pore fluids is considered to be a type of shallow-weathering source as opposed to the tectonic expulsion of deep pore fluids, e.g. by seismic pumping (McCaig, 1988). Later in this paper, a modern analog of ironstone sedimentation is attributed to seismic pumping of pore fluids in northeastern Venezuela. Modern marine ironstone sedimentation is known from only one other locality, on the Mahakam delta of Indonesia where Allen et al. (1979, p. 97) attribute the oolite to erosion of organic-rich riverbank sediment which they presume to contain abundant ferrous iron in pore water. They hypothesize precipitation of the ferrous iron during a few kilometers of travel into the marine environment. Expulsion of deep fluids is advocated herein for the Mahakam oolite, given that hydrocarbon-rich fluids frequently exhale through this petroleum-rich delta.

Flow chart for iron solubility

Fe and Si solubility constrained by oceanic T and P or higher crustal T and P? (Fig. 2)

Iron is essentially insoluble in non-acidic water if there is substantial dissolved O₂ or H₂S. Iron readily precipitates as a hydroxide or sulfide. The solubility of ferric hydroxide colloids is controlled by the activity product, $a_{\text{Fe}^{3+}} \cdot a_{\text{OH}^-}^{2.35}$, which equals 10^{-31.7} (Fox, 1988). Fe³⁺ clearly is insoluble but the ratio of Fe²⁺/Fe³⁺

begins to exceed unity without much removal of dissolved oxygen (chemical reduction). The equilibrium constant for the reaction, 0.5 O₂ + 2 Fe²⁺ + 2 H⁺ = 2 Fe³⁺ + H₂O, equals 10^{15.53} (Stumm and Morgan, 1981, p. 426). At a pH of 8 and unit activity coefficients, the ratio of Fe²⁺/Fe³⁺ therefore would exceed unity at an oxygen pressure less than 0.1 atm. This is only half of the partial pressure in the modern atmosphere.

The insolubility of iron in slightly reducing water primarily is due to reaction of Fe²⁺ to form ferric hydroxide, i.e., Fe²⁺ + 3 H₂O = Fe(OH)₃ + 3 H⁺ + e, for which the oxidation potential (pE) is controlled by the following relationship, pE = 16 - log(Fe²⁺) - 3 pH (Stumm and Morgan, 1981, p. 447). To achieve a 0.1 mM solution of Fe²⁺ (5.6 ppm) at pH 8 and unit activity coefficients, pE therefore must be -4. This pE value may be converted to an equivalent partial pressure of O₂, i.e. 10⁻⁶⁷ atm, through the following relationship, log P_{O₂} = -83.1 + 4 pH + 4 pE (Stumm and Morgan, 1981, p. 427). This result shows that abundant dissolved iron generally would not be in chemical equilibrium with more than a single molecule of dissolved O₂ in an ocean basin. The permissible concentration of dissolved H₂S is not much greater. Berner (1969) has estimated that only 10⁻⁶-10⁻⁸ M H₂S is required to convert goethite to iron sulfide by the following reaction, 2 FeOOH + 3 H₂S = 2 FeS + S + 4 H₂O.

Dissolved H₂S rapidly precipitates virtually all Fe²⁺ as a sulfide mineral (Berner, 1984). The sulfide either initially or eventually becomes pyrite unless the pH is less than 5 (Murowchick and Barnes, 1986). It has been proposed that Precambrian oceans were so sulfur-deficient that deep anoxic seawater did not contain enough H₂S to inhibit iron solubility (Drever, 1974; Walker and Brimblecombe, 1985). It is unlikely, however, that sulfur deficiency was a general feature of Precambrian oceans (Holland, 1984; Ohmoto and Felder, 1987).

Sulfur deficiency is not an absolute prerequisite for iron solubility in seawater. A sulfate

Oceanic T and P: Dissolved iron mostly Fe^{2+} (ferrous ion) or $\text{Fe}_3\text{Si}_3\text{O}_8(\text{OH})^0$ (ferrous silicate ion)?

Ocean T and P – Ferrous ion: Siderite equilibrium largely due to elevated P_{CO_2} in atmosphere or largely due to balance between low atmospheric P_{O_2} and organic carbon supply to seabed? Consistent coprecipitation of silica due to evaporation, cooling, or biota?

Ocean T and P - Fe^{2+} ion: Evaporation: How could evaporation account for deep-water iron formations?

Ocean T and P - Fe^{2+} ion: Biota: Why are no siliceous fossils preserved in cherty ironstone, even in richly fossiliferous samples?

Ocean T and P – Ferrous silicate ion: High dissolved silica just due to lack of biologic precipitation or enhanced solubility (high oceanic pH or temperature)?

Ocean T and P - $\text{Fe}_3\text{Si}_3\text{O}_8(\text{OH})^0$: Unenhanced: Did destabilization of this ion cause the small range of Fe/Si ratios in cherty iron formations?

Ocean T and P - $\text{Fe}_3\text{Si}_3\text{O}_8(\text{OH})^0$: Enhanced: Why did not variation in enhancing parameters (pH, T) cause greater variation in Fe/Si ratios?

Subsurface: Iron enrichment due to high chloride content, high acidity, or intermediate oxidation state (sulfur as sulfate)?

Subsurface – Chloride: Lack of other metals in iron-precipitating fluid due to paucity in fluid or precipitation closer to seafloor vent?

Subsurface – Chloride: Metal-poor fluid: Crustal ratios of metal solutes due to small rock volume being completely leached or large rock volume leached by solution particularly soluble for iron?

Subsurface – Chloride: Metal-rich fluid: Lack of sulfide ore deposits coeval with largest iron formations due to subduction or erosion?

Subsurface – Acid: Venting in shallow water or deep venting of thermal plumes which carry colloids to shallow water?

Subsurface – Acid: Shallow: Why is there no regional mineral zonation around former hypothetical vent locations?

Subsurface – Acid: Deep vent: How could point-source thermal plumes result in a lateral extent of ironstone beds of constant thickness (ca. 1 m) for more than 100 km?

Subsurface – Sulfate: Intermediate oxidation state due to dissolution of evaporites or reaction with organic-poor sediment?

Subsurface – Sulfate: Sediment: Could the volume of either evaporites or organic-poor sediment have been adequate to produce the required volume of iron-rich fluid of intermediate oxidation state?

Fig. 2. Flow chart for iron solubility. Fe and Si solubility constrained by oceanic T and P or higher crustal T and P?

concentration which is twice that of average seawater coexists with abundant dissolved iron in the modern Orca Basin within the Gulf of Mexico (Sheu and Presley, 1986a). The Orca Basin contains 1.6 ppm Fe^{2+} along with 4500 ppm SO_4^{2-} in a volume which exceeds the sum of all hypersaline deep basins under the Red Sea.

Although the Orca Basin demonstrates that ferriferous water may be sulfate-rich, the surest way of avoiding sulfide control on iron solubility is to lack all sulfur species, as in fresh water.

The largest iron formations have no diagnostic fossils and so the prime argument against a low-salinity origin has been the sheer volume of ironstone and the common association with carbonate rocks (Kimberley, 1978a). Given the wide range of salinity variation documented for the Mediterranean through the past 6 Ma (hypersaline to brackish: Cita, 1982), the qualitative arguments for consistent salinity in iron-formation basins are not entirely convincing. However, the lowest salinity reconcilable with

basin size would be at least brackish rather than fresh water and the sulfur content of brackish water would still present a problem for modeling iron solubility.

The vast majority of researchers assume that Fe^{2+} has been the predominant iron solute species but Winter and Buckley (1986) attribute iron-enriched marine pore fluids under the Sohm Abyssal Plain to an uncharged iron-silicate ion, $\text{Fe}_3\text{Si}_3\text{O}_3(\text{OH})_8^0$. Iron-enriched pore fluids in the Amazon delta cannot be attributed to this hypothetical iron-silicate ion because there is no correlation between iron and silica-solute abundances as in the Sohm seafloor (Aller et al., 1986). Despite the fact that Fe^{2+} apparently is the prime solute here and in most other modern iron-rich waters, the possibility that the iron in cherty iron formations mostly precipitated from $\text{Fe}_3\text{Si}_3\text{O}_3(\text{OH})_8^0$ might be appealing because precipitation of this solute might explain the consistently intimate association of silica with iron in voluminous iron formations.

If dissolved iron was mostly Fe^{2+} , the iron-silica association must be explained by coincidental precipitation of Fe^{2+} with $\text{Si}(\text{OH})_4^0$, $\text{SiO}(\text{OH})_3^-$, or some multinuclear species, e.g. $\text{Si}_4\text{O}_6(\text{OH})_6^{2-}$ (Stumm and Morgan, 1981). One way to achieve abundant dissolved silica along with abundant dissolved iron is to have alkaline oceans. Kempe and Degens (1986, p. 104) claim that "... the coexistence of chert, siderite (FeCO_3), and Fe-silicates, for example in Banded Iron Formations, is possible only under alkaline conditions". In an alkaline ocean, riverine calcium should precipitate immediately upon mixing with seawater. However, the facies distribution of Precambrian carbonate and gypsum deposits seems too similar to that throughout the Phanerozoic to support the concept of Precambrian alkaline oceans.

If one rejects the possibility of a seawater pH higher than 9.5, the surest inorganic precipitation mechanism for silica is cooling (Holland and Malinin, 1979). A temperature difference of a few tens of degrees Celsius could exist be-

tween cool surface water and warm subsurface water in an ocean with hypersaline bottom water. Silica precipitation would be expected along the horizontal interface between these two water masses. An alternative inorganic cause of silica precipitation, i.e., mild evaporation during upwelling (Holland, 1984, p. 420), would not explain deep-water cherty iron formations and would not explain the observed consistency of Fe/Si ratios in cherty iron formations of all water depths (Yeo and Gross, 1987), given inevitable variations in evaporation rate both spatially and temporally.

It is tempting to invoke biological precipitation of silica in Precambrian iron formations but no siliceous skeletons have yet been found in them (Siever, 1987). This may be an artefact of preservation, given that chert interbedded with unmetamorphosed Cretaceous phosphorite generally lacks siliceous skeletons; skeletons are found only in associated porcellanite which is rare (Soudry et al., 1981). The lack of direct evidence of Precambrian siliceous skeletons is not the only problem, however, since it would be difficult for biological mechanisms to have been equally effective throughout the water column. An interface between cool surface water and warm subsurface water presumably existed anywhere from the photic zone, where oolitic cherty iron formations apparently accumulated (Hassler, 1987), down to the realm of deep-water iron formations (Larue, 1981b).

Flow chart for iron precipitation

Precipitation due to evaporation, cooling, upwelling, or mixing along interface? (Fig. 3)

Precipitation of iron may be attributed to evaporation, to mixing of two water masses, or to a change in the temperature and/or pressure of a ferriferous fluid while rising through the ocean. Upward movement of the ferriferous fluid may be attributed either to thermal convection or geostrophic upwelling. Mixing of water masses may involve upwelling into iron-poor surface water, a horizontal interface be-

Evaporation: Why would evaporation produce observed systematic facies variations in the oxidation state of iron minerals?	Cooling: How could point-source plumes produce a sufficient volume of cooling ferriferous fluid to produce meter-thick beds which extend for a few hundred km?	Upwelling: Why do meter-thick beds of some iron formations extend for a few hundred km whereas beds of other ores attributed to upwelling, e.g., phosphorite, do not display such lateral continuity?	Mixing along Interface: Horizontal interface (stratified ocean) or inclined interface (e.g., estuarine mixing).
			Interface – Horizontal: Would precipitation be due to continuous downward diffusion of oxygen, wind-induced gravity waves, photooxidation, or climatically-controlled variation in the input of fresh water? Interface – Inclined: How would the precipitated iron solutes become separated from flocculating clays?

Fig. 3. Flow chart for iron precipitation. Precipitation due to evaporation, cooling, upwelling, or mixing along interface?

tween stable oceanic water masses, or lateral mixing of river water with seawater.

Selection of any one of the foregoing mechanisms invites correlative questions. Selection of evaporation invites a question about mineralogical variability, given variation in oxidation state, carbonate content, and silicate content among facies within iron formations. Selection of marine–nonmarine mixing raises a question about the fate of terrigenous sediment which presumably accompanied any fluvial discharge. Selection of mixing across an oceanic boundary raises a question of what stabilized the boundary long enough to produce a voluminous iron formation. Selection of rising fluids requires a choice between a thermally-driven seawater plume and topographically-induced upwelling.

Flow chart for evolution through Earth history

Have biota, the atmosphere, or heat flow controlled iron-formation evolution? (Fig. 4)

The prime academic significance of iron formations derives from the fact that the distribution through Earth history of voluminous de-

position has been demonstrably uneven on a time scale of hundreds of millions of years (James, 1983). The fact that most other sedimentary rock types do not display such great temporal variation has been a mainstay for the principle of uniformitarianism. The temporal variation in iron-formation volume largely has involved variation in cherty iron formations because all iron formations which are thicker than a few tens of meters are cherty.

It has been proposed that the distribution of cherty iron formations through Earth history records the global evolution of biota, the atmosphere, or tectonomagmatic processes. The distribution of iron formations has been attributed to climatically-induced evolution of Earth's biota (Cloud, 1973), to the chemical evolution of Earth's atmosphere (Holland, 1984), or to the evolution of tectonomagmatic processes on a cooling planet (Gross, 1983). Proponents of each of these three hypotheses advocate that evolutionary change in one factor (biota, atmosphere, or tectonism) has controlled the variable production of iron formations. For example, Gross (1983, p. 184) notes

Biota: Primarily evolution of microorganisms or evolution of metazoans?

Biota – Microorganisms: Is the long and multimodal time distribution of iron formations explicable by multiple evolutionary events of microorganisms?

Biota – Metazoans: Why did iron-formation production wane in the mid Proterozoic when there were no metazoans but did not stop in the Cambrian when metazoans appeared?

Atmosphere: Primarily decreasing P_{CO_2} or decreasing P_{O_2} ?

Atmosphere – P_{CO_2} : Can peaks in iron-formation abundance be correlated to peaks in P_{CO_2} ? Did higher P_{CO_2} help cherty iron formations through increasing stability field of siderite or through stratification of oceans due to “greenhouse” increase in temperature?

Atmosphere – P_{CO_2} : Peak IF production: Why are Late Precambrian iron formations associated with a time of glaciations given that abundant CO_2 should have warmed the Earth?

Atmosphere – P_{CO_2} : Siderite: Why would increasing P_{CO_2} produce observed concentration of ^{12}C in ironstone siderite?

Atmosphere – P_{CO_2} : Stratified ocean: Does the paucity of Carboniferous cherty iron formations, despite apparent increase in P_{CO_2} , indicate that low P_{O_2} is a corequisite for voluminous sedimentation?

Atmosphere – P_{O_2} : Is a lower P_{O_2} a sufficient atmospheric change to produce iron formations? How much lower than the modern 0.2 atm?

Atmosphere – P_{O_2} : Sufficient: Why is it that anoxia is not a sufficient condition for iron enrichment in modern marine water bodies (as opposed to pore water) and yet Early Paleozoic cherty iron formations could accumulate under oxygen-rich atmospheres?

Atmosphere – P_{O_2} : Insufficient: What other atmospheric and/or hydrospheric compositions are required in addition to anoxia?

Waning heat flow: Decreasing iron exhalation linked to continuously decreasing heat flow or have there been combined peaks of heat flow and iron sedimentation?

Waning heat flow – Continuous: If heat flow has decreased continuously, why is the time distribution of iron formations multimodal?

Waning heat flow – Peaked: Why do peaks of iron formations not coincide with peaks of massive sulfide deposits which more clearly are associated with heat flow?

Fig. 4. Flow chart for evolution through Earth history. Evolution due to biota, atmospheric composition, or waning heat flow?

"I have concluded that the deposition and distribution of iron-formation has been controlled primarily by tectonic factors, and that biogenic factors and the composition of the atmosphere had a lesser, and probably limited influence on the precipitation of these chemical sediments".

The three competing hypotheses (evolution of biota, atmosphere, or tectonism) may be evaluated by examining the stratigraphic record of iron formations, including modern marine deposits. The biologic approach favors restricted times of voluminous iron sediments, coincident with times of more rapid biologic evolution, e.g., cyanobacterial evolution (Cloud, 1973). The atmospheric approach favors restriction of cherty iron formations to the Precambrian because Phanerozoic metazoan fossils record a continuously oxygen-rich Phanerozoic atmosphere which would impede iron solubility in the hydrosphere (Holland, 1984). The tectonomagmatic approach emphasizes the supply of hydrothermal fluids emanating from fractures and deep-seated faults on the flanks of tectonic ridges (Gross, 1983). The tectonomagmatic concept accepts the possibility of voluminous iron formations in any age but with decreasing probability on a cooling planet.

Voluminous SVOP-IF formed through the Devonian (Table 2), a time when the atmosphere must have been similar to the modern atmosphere to support Devonian life forms. Most SVOP-IF specialists discount the importance of atmospheric chemistry and propose that volcanism has produced ferriferous hydrothermal solutions which exhaled into seawater (e.g., Gross, 1983; Goodwin et al., 1985). However, the Devonian Lahn-Dill svop iron formations are considerably smaller than Precambrian examples (Bottke, 1965).

Voluminous MECS-IF has not formed since the Cambro-Ordovician (Table 2; James, 1983). One explanation for the inability of subsequent oceans to make voluminous MECS-IF is that they have been too well oxygenated to dissolve much iron (e.g., Holland, 1984). Most genetic mode-

lers have proposed that Precambrian atmospheres were extremely reducing, with tens of orders of magnitude less oxygen pressure than at present (e.g., Holland, 1962; Lepp and Goldich, 1964; Garrels et al., 1973; and Eugster and Chou, 1973). Others have suggested that atmospheric oxygen was not necessarily less abundant than at present (e.g., Dimroth and Kimberley, 1974; Clemmey and Badham, 1982; and Gross, 1983).

Holland (1962, 1984) has increased his estimate of Precambrian oxygen pressure to within three orders of magnitude of the present atmosphere. It will be concluded later that iron formations are poor indicators of the oxidation state of the ambient atmosphere but could be compatible with Holland's revised estimate of atmospheric conditions, at least during much of the peak times for iron formations, i.e. from 3.5 to 2.0 Ga and from 0.8 to 0.4 Ga (James, 1983). The suggestion by Dimroth and Kimberley (1974) that atmospheric oxygen pressure has not varied by more than an order of magnitude since the Archean probably is too restrictive, as noted by Holland (1984, p. 422).

Tectonomagmatic processes would not be affected significantly by changes in biota or atmospheric oxygen but both biologic and atmospheric evolution readily could be controlled by tectonomagmatic evolution. Mantle-derived processes probably have been the underlying control on atmospheric chemistry since the early advent of photosynthesizing cyanobacteria in the Archean. Moreover, biologic evolution probably has been controlled by thermal evolution of our planet (Kimberley, 1981a; Veizer, 1983).

Minor genetic flow charts

Introduction

Several investigators have emphasized specific features of both cherty and noncherty iron formations in the deduction of genetic processes, e.g. stratigraphic relationships (Table

2), granular-oolitic texture (cherty: Dimroth and Chauvel, 1973; noncherty: Kimberley, 1983b), banded (laminated) structure (cherty: Trendall and Blockley, 1970; noncherty: Boardman, 1981), cross-bedding and ripple marks (cherty: Gross, 1972; noncherty: Hayes, 1915), mineralogy (cherty: Floran and Papike, 1975; noncherty: Maynard, 1986), carbon isotopes (cherty: Walker, 1984; noncherty: Hangari et al., 1980), oxygen isotopes (cherty: Baur et al., 1985; noncherty: Timofeyeva et al., 1976), sulfur isotopes (cherty: Cameron, 1983; noncherty: no data), major-element abundances (cherty: Davy, 1983; noncherty: Kimberley, 1979b), minor-element abundances (cherty: Gross and McLeod, 1980; noncherty: Yakontova et al., 1985), rare-earth-element patterns (cherty: Fryer, 1983; noncherty: Timofeeva and Balashov, 1972), and selected trace elements, e.g. gold (cherty: Fripp, 1976) and tungsten (cherty: Harmon et al., 1978). The following flow charts reflect these various approaches (Figs. 5–18).

Flow chart for stratigraphic relationships

Global abundance correlative with maximum inundation of continents? (Fig. 5)

The proportion of the Earth's surface covered by seawater decreased markedly at the end of the Archean (Schubert and Reymer, 1985). The Early Proterozoic was the time of greatest accumulation of iron formations and so it could be argued that initial continental emergence favored iron formations. Emergence probably has not progressively increased unidirectionally through Earth history, as modeled by Schubert and Reymer (1985), given the rapid increase in emergence which has characterized just the past couple of million years (Vail and Mitchum, 1979). Within emergent-submergent cycles, it appears that continental submergence favored Proterozoic iron formations because iron sedimentation locally peaked during inundation of deeply eroded continents (Morey, 1983). This

inundation may have resulted from rifting (Morey, 1983).

Most Precambrian iron formations cannot be correlated with variation in global sea level because a lack of stratigraphic data precludes the plotting of a continuous sea-level curve throughout the Precambrian, comparable to that of Vail and Mitchum (1979) for the Phanerozoic. The Phanerozoic curve for global sea level is readily correlated, however, with the age distribution of cherty iron formations. Phanerozoic cherty iron formations apparently coincide with times of maximum inundation of the continents. Inundation persisted from the Late Cambrian through the Mississippian and during the mid to Late Cretaceous (post-Neocomian). These are the only Phanerozoic times in which significant cherty or deep-water iron formations accumulated. Typical cherty iron formations formed during the Late Cambrian to Mississippian span (Table 2) and a large deep-water deposit accumulated during the Early Cretaceous (Albian stage; Young and Robertson, 1984).

Correlation of cherty iron formations with continental inundation carries uncertain genetic implications. The Vail curve (Vail et al., 1977; Vail and Mitchum, 1979) has been attributed to a variable spreading rate of the circum-global mid-oceanic ridge (Pitman, 1978). However, the attendant variation expected for global heat flow (Turcotte and Burke, 1978) has not resulted in correlative variation in the $^{87}\text{Sr}/^{86}\text{Sr}$ of limestone (Holland, 1984). Greater hydrothermal convection through ^{87}Sr -depleted oceanic crust should decrease the $^{87}\text{Sr}/^{86}\text{Sr}$ ratio of seawater, hence the $^{87}\text{Sr}/^{86}\text{Sr}$ ratio of limestone.

Recent observations regarding the flux of carbon-coated icy comets to Earth has demonstrated that there may have been substantial extraterrestrial input of water and carbon throughout Earth history (Frank et al., 1986). Such a substantial input seems unlikely, however, because an increase in continental emergence through Earth history would have re-

Correlative: Correlative due to rift tectonics, increased input of carbon and water in comets, or decreased exposure of fresh rock?

Correlative – Rift tectonics: Correlative because of subduction-metamorphism or because abrupt termination of rifting allows coincidental inundation plus hydration of new rift floor?

Correlative-rift tectonics - Subduction: Why has not Phanerozoic subduction produced cherty iron formations?

Correlative-rift tectonics - Hydration: How close is the Red Sea to being a good modern analog?

Correlative – Rock exposure: Decreased exposure of fresh rock enhances siderite stability through atmospheric accumulation of CO₂ or enhances oxidation of fluvial detritus through increased P_{O₂}?

Correlative - Rock exposure: CO₂: Lack of concomitant increase in P_{O₂} due to retardation of photosynthesizing cyanobacteria or O₂ consumption by exhalative hydrothermal solutes?

Correlative - Rock exposure: O₂: Increased dissolution due to increased proportion of goethite in fluvial detritus (reacting to form Fe²⁺-SO₄²⁻ solution at oxic-anoxic interface) or increased precipitation of existing Fe²⁺-rich water due to increased oxidation by atmosphere?

Correlative - Rock exposure: O₂-dissolution: Why has silica consistently precipitated with iron?

Correlative - Rock exposure: O₂-precipitation: What process kept the Fe²⁺ concentration high prior to increase in atmospheric O₂?

Uncorrelative: Locally decreased sedimentation rate (stratigraphic thinning) or correlation with other peculiar chemical sedimentary rock?

Uncorrelative – Thinning: Top of coarsening-upward sequence or bottom bed in transgressive sequence?

Uncorrelative - Thinning: Top: How could shallowing result in a greater ratio of Fe²⁺/Fe³⁺ in the iron formation than in underlying clastic sedimentary rocks?

Uncorrelative - Thinning: Bottom: Iron precipitated uniformly along oxic-anoxic interface within advancing wedge of transgressing water or in exhalative mounds which become physically reworked into tabular deposits?

Uncorrelative – Chemical association: Coal or phosphorite?

Uncorrelative - Chemical rock assoc.: Coal: Precipitation along interface in water body (iron formation areally extensive and laminated) or from effusive ground water (patchy distribution and gradations to Fe-cemented sediment)?

Uncorrelative - Chemical assoc.: Phosphorite: Fe supplied fluvially (rhexistasy due to climatic or tectonic change) or by upwelling with deep marine phosphorus?

Fig. 5. Flow chart for stratigraphic relationships. Global abundance correlative with maximum inundation of continents?

quired crude coupling between two diverse processes, i.e., cometary influx and subduction of marine pore water into an increasingly hydrated mantle. Cometary influx potentially would be more sporadic than the gradual variations in continental inundation which typify the geologic column. Nonetheless, an increase in the flux of carbon-rich comets could result in a simultaneous increase in P_{CO₂} and decrease in

P_{O₂}, jointly possibly favorable to production of cherty iron formations.

Unlike cherty iron formations, noncherty iron formations are not consistently correlative with times of maximum inundation of the continents (Van Houten, 1985). This lack of correlation may be interpreted to indicate a fundamental genetic difference between cherty and noncherty iron formations. Noncherty iron for-

mations typically are just a few meters thick at most (Table 2) and Hubbard (1988) has shown that local tectonism commonly is more important at this scale than is the Vail curve. The data of Hubbard (1988) cast doubt upon the global relevance of some details (multi-order cycles) in the Vail curve. However, the Jurassic portion of the Vail curve correlates well with oolitic (SCOS) iron formations in Germany (Vail et al., 1984; McGhee and Bayer, 1985). Ferriferous oolite apparently formed preferentially along sediment-starved basin edges. Rapid transgression of a basin edge produced extensive thin SCOS iron formations whereas thicker deposits within the basin are attributed to reworking of basin-edge oolite during a regression (McGhee and Bayer, 1985). The concept of regressive reworking is questionable, however, given the improbability of ferrous berthierine surviving much transportation along the floor of an oxidizing ocean.

Flow chart for tectonic relationships

Correlation with continental breakup? (Fig. 6)

Some well-studied Proterozoic iron formations are correlative with continental breakup, e.g. the Lower Proterozoic iron formations around Lake Superior which accumulated within "a rift-like basin that increased in size with time" (Morey, 1983, p. 38). The Late Precambrian global increase in iron formations (Yeo, 1984) similarly was correlative with continental breakup (Roberts and Gale, 1978). Continental breakup typically produces narrow seaways with locally anoxic bottom water that

preferentially preserves organic carbon, hence increasing both atmospheric P_{O_2} and the oceanic ratio of $^{13}C/^{12}C$ (Knoll, 1987). If continental breakup fosters iron formations, a concomitant increased burial rate of organic carbon may cause them to accumulate during times of increasing atmospheric P_{O_2} , contrary to the popular notion of correlation with atmospheric anoxia.

Anoxia in a restricted water body generally results from the oxidation of settling organic matter. After consumption of all dissolved oxygen, additional oxidation requires the concomitant reduction of other species, generally either SO_4^{2-} or ferric hydroxide coatings on clay minerals. Ferric hydroxide coats clays so effectively that the pH at which the grain surfaces have no electric charge (zero point of charge) in a hydroxide-clay mixture is that of the ferric hydroxide rather than a value intermediate between the hydroxide and clay (Economou and Bowers, 1987). If abundant ferric hydroxide is settling with the organic matter, reduction of Fe^{3+} is favored over reduction of SO_4^{2-} , as in the Orca Basin (Sheu and Presley, 1986a). A high sedimentation rate of organic matter into an anoxic basin would make it euxinic, i.e. rich in aqueous H_2S , and therefore poor in dissolved iron.

Continental breakup commonly produces small continental blocks which become separated from large continental blocks by basins in which the sedimentation rate is extremely high. These basins commonly become filled with evaporites and redbeds. Rapid subsidence of these sediments within a broad transform-fault zone may bring them into a subsurface environment dominated by seismic pumping (McCaig,

Surficial environments: How could ancient breakups under an oxygen-poor atmosphere produce suboxic ferriferous basins when euxinic basins presently form under an oxic atmosphere?

Crustal hydration: Does exhalation from hydrating crust have to be so potent that it temporarily decreases the oxidation state of the atmosphere?

Fig. 6. Flow chart for tectonic relationships of iron formations. Continental breakup favors iron formations because of surficial environments or crustal hydration?

1988). Given enough buried sulfate, an intermediate oxidation state may be achieved and the fluid may become dominated by ferrous bicarbonate (Fe^{2+} and HCO_3^-) and calcium sulfate (Ca^{2+} and SO_4^{2-}). The relevant silicate reactions would occur at less than 300°C and so the process would be classified as late diagenesis to very low-temperature metamorphism (Frey, 1987).

Seismically exhaled fluids readily could dominate the water chemistry of a small restricted basin. Under conditions of global cyclicity in tectonic activity, an alternation between times of crustal accumulation and hydration could affect atmospheric composition. Volcanic degassing during rapid seafloor spreading would enrich the atmosphere in CO_2 and the seafloor in both carbonates and organic matter. The ratio of $\text{C}_{\text{org}}/\text{CO}_2$ which would result from the added carbon would lie between 0.1 and 0.3 (Holland, 1984, p. 361).

Flow chart for granular texture

Difference between granules and ooids (Fig. 7)

Both cherty and noncherty ironstone are texturally comparable to limestone (Beukes, 1980; Markun and Randazzo, 1980; Kimberley 1983b). The depth dependence of limestone textures is now well understood from studies of modern carbonate sediment (Bathurst, 1975; Wilson, 1975). The paucity of modern analogs of ironstone impedes an equivalent comparison

of textures and so some investigators assume *a priori* that the limestone studies may be applied directly (Dimroth, 1977a). Facies studies of textural variation within a single iron formation support this contention because granular-oolitic texture can be traced from nearshore facies to finely laminated (banded) ironstone in deep-water facies (Goodwin, 1960; Dimroth, 1976).

Textural controversies mostly involve differentiation of primary versus diagenetic origins. However, few investigators dispute a primary origin for ooids in either cherty or noncherty ironstone (Bhattacharyya and Kakimoto, 1982). The origin of peloids (traditionally called granules) in cherty ironstone is much less obvious (La Berge, 1973; Dimroth, 1976). These ooid-sized structures are devoid of concentric structure and exhibit grain outlines which range from being well rounded to being so angular that transport seems unlikely.

Flow chart for banding

Accentuation of banding during diagenesis (Fig. 8)

The most characteristic sedimentary structure of cherty ironstone is lamination which may range upward from less than a micron in thickness to whatever lower limit is arbitrarily assigned to a bed versus a lamina. Ironstone lamination traditionally has been termed banding. The continuous gradation in layer thicknesses upward into the meter range enticed

Granules diagenetic: Due only to dewatering of gel or dewatering followed by submarine erosion?

Diagenetic – Dewatering only: Why are granules in some beds so consistently well rounded?

Diagenetic – Erosion: Why did eroded granules not pick up superficial oolitic layers?

Primary difference: Less turbulent conditions than for ooids or different composition of precipitating fluid?

Primary – Less turbulent: If composition is irrelevant, why does noncherty ironstone rarely grade into granular texture whereas cherty ironstone more commonly does?

Primary – Different composition: Why does granular cherty ironstone commonly have the same composition as oolitic cherty ironstone?

Fig. 7. Flow chart for granular textures. Granules differ from ooids because diagenetic or different primary conditions?

Greatly accentuated: Segregation due to burial pressure like metamorphic differentiation or recrystallization of metastable precipitates?

Accentuated – Burial pressure: How could burial pressure be effective in deep-water ironstone where additional pressure would be a small proportion of total pressure during early diagenesis?

Accentuated – Recrystallization: Given that silica is the only phase consistently present in banded ironstone, its recrystallization presumably causes banding, so why is ordinary chert not consistently banded?

Unaccentuated: How could some oolitic beds be both banded and oolitic?

Fig. 8. Flow chart for banding. Have ironstone bands been greatly accentuated during diagenesis?

Trendall and Blockley (1970) to substitute the term “macrobands” for bed. Retention of the term, bed, seems preferable, however, because beds are defined for all other chemical sedimentary rocks, including laminated gypsum which closely resembles banded ironstone.

It has been argued that ironstone banding is a diagenetic feature (Duff et al., 1967, p. 189) and a diagenetic origin indeed can be deduced locally, e.g. in cherty ironstone which apparently has had a banded structure superimposed on an oolitic texture (Dimroth and Chauvel, 1973, their fig. 10). Elsewhere, isotopic differences between ironstone bands apparently record primary sedimentary differences (Baur et al., 1985). If banding is accentuated by partial segregation of silica from iron minerals during diagenesis, this segregation may be analogous to diagenetic accentuation of lamination during early diagenesis in other types of sediment (Duff et al., 1967). Late diagenetic effects are evident where the thickness of a set of ironstone bands laterally varies by an order of magnitude (Trendall and Blockley, 1970).

Flow chart for structures (except banding) in granular-oolitic ironstone

Shallow-water structures and sedimentation depth (Fig. 9)

Many common sedimentary structures have been reported from both noncherty iron for-

mations and granular-to-oolitic cherty iron formations. Cross-bedding and ripple marks occur in both granular-oolitic cherty ironstone (Gross, 1972; Hall and Goode, 1978) and non-cherty oolitic ironstone (Hayes, 1915; Edmonds et al., 1965). The only major researcher who has doubted that these structures record shallow-water sedimentation has been Hallimond (1925, 1951) who noted that a shallow agitated environment would not be conducive to sedimentation of chemically reduced ironstone during the oxygen-rich Phanerozoic. However, even Hallimond (1951) recognized the improbability of a deep-water origin for observed structures and textures. It is concluded herein that a range of water depths which is characteristic of continental shelves (less than 200 m) may be safely assumed if these structures collectively occur in granular-oolitic ironstone, whether cherty or not. A more precise estimate of water depth within the 0–200 m range would be controversial, however, given the susceptibility of most ironstone minerals to oxidation.

Flow chart for mineralogy

Were iron minerals chemically reduced diagenetically? (Fig. 10)

Ironstone mineralogy integrates the history of initial precipitation, early diagenesis, late

Less than 20 m: Hydrothermal plume (spread along surface of ocean because of high T), or shallow interface between oxic-anoxic water bodies (maintained within wave zone because of high salinity contrast), or rapid reworking of shallow mounds of exhalative (unoxidized) ooids?

Less than 20 m – Hydrothermal: How could marine surface currents be so consistent as to produce great lateral extent of meter-thick laminated beds in Hamersley iron formations?

Less than 20 m – Interface: Why do Phanerozoic oolitic formations commonly contain stenohaline fauna?

Less than 20 m – Mounds: Why were the ooids not completely oxidized during shallow erosion of mounds?

Range of 20–200 m: Noncherty ferriferous oolite occurs under less than 5 m of water on the Mahakam delta. Is this just an exception or is noncherty oolite inherently irrelevant to cherty oolite?

Range 20–200 m – Exception: Exception because peculiarly shallow water depth due to glacially induced variation in sea level (whereas most iron formations have accumulated in nonglacial times) or because seismic pumping may occur into any water depth on a shelf and most shelf depths lie between 20 and 200 m?

Range 20–200 m – Irrelevant to cherty oolite: Irrelevant because physical properties of siliceous gel are different from the mineral mixture in noncherty ooids or because all genetic processes generally have been different for cherty ooids?

Fig. 9. Flow chart for structures (except banding) in granular-oolitic ironstone. Shallow-water structures indicate sedimentation in <20 m or 20 to 200 m?

diagenesis, and sometimes metamorphism. The system becomes progressively more closed (less mass transfer) through this progression and so deduction of any previous mineralogical assemblage becomes progressively more straightforward. Metamorphosed ironstone generally provides the least information about primary genetic processes and so highly metamorphosed ironstone is not discussed in this paper.

The most significant mineralogical changes in ironstone probably occur during early diagenesis. However, the study of early diagenesis has

been impeded by the paucity of modern analogs of ironstone. The discovery of modern ferriferous oolite in Indonesia (Allen et al., 1979) and of laminated iron-rich sediment under the Orca Basin in the Gulf of Mexico (Sheu and Presley, 1986a) will lead to studies which help elucidate early diagenetic processes.

The clearest indication of diagenesis within ironstone itself is provided by mineral growth within ooids, given that oolitic layering undoubtedly is primary. Mineralogical alternation commonly occurs at a submicroscopic scale

Not reduced: Why is siderite enriched in ^{12}C which may have come from organic matter? If oxidation is not the prime precipitator, was it mixing with surface water or cooling?

Not reduced – Mixing: Does crocidolite record high sodium activity in relatively undiluted brine?

Not reduced – Cooling: How could laterally variable cooling result in laterally homogeneous mineralogy in extensive bands?

Diagenetically reduced: Was the initial precipitate always oxides, silica, and organic matter, or mixed with alloigenic silicates?

Diagenetically reduced – Always oxides, silica and organic matter: If resulting mineralogy depended on proportions of organics and silicates, do any remnants of those correlate with iron mineralogy and/or C-S-O isotopes?

Diagenetically reduced – Variable iron precipitates: Were there ferric silicates, e.g. ferric analog of berthierine?

Fig. 10. Flow chart for iron mineralogy. Were iron minerals chemically reduced diagenetically?

within noncherty ooids and even some Early Proterozoic cherty ooids exhibit such detail, e.g. within the Gunflint Formation (Markun and Randazzo, 1980).

Deduction of initial precipitates from bulk chemical properties is best done in cherty iron-stone because it typically consists entirely of chemically precipitated minerals whereas non-cherty ironstone more commonly contains terrigenous grains.

Flow chart for chert

What does chert record ? (Fig. 11)

The abundance of chert in Precambrian iron formations records an abundance of dissolved silica. Silica solubility would have been enhanced by elevated temperature (Holland and Malinin, 1979), e.g. in exhalative fluids, but it is not obvious that such an extraneous source of silica was required. In the absence of silica-precipitating organisms, silica solubility may have reached equilibrium with amorphous silica, at about an order of magnitude higher solubility than at equilibrium with quartz (Stumm and Morgan, 1981). Biologic precipitation in the modern ocean keeps silica solubility coincidentally close to equilibrium with quartz (Calvert, 1983). An increase in the concentration of dissolved iron would affect silica solubility through precipitation of iron silicates, e.g. greenalite, berthierine, or glauconite (Harder, 1980).

Flow chart for carbon isotopes

¹²C abundance in iron formations (Fig. 12)

The carbon in the ferrous carbonates (siderite and ankerite) of cherty iron formations is typically richer in ¹²C than is the carbon in contemporaneous limestone (Perry et al., 1973; Baur et al., 1985). This either records coincidental enrichment of ¹²C along with aqueous iron in the ferriferous water body or peculiar diagenesis of ironstone. Perry et al. (1973) hypothesize that primary hematite and ¹²C-enriched organic matter reacted diagenetically to produce magnetite and ¹²C-enriched carbon dioxide. They further hypothesize that the carbon dioxide then exchanged some ¹²C for ¹³C in nearby siderite. For this hypothesis to be valid, one would expect a correlation between C_{org} and the ratio of ¹²C/¹³C in ironstone. This correlation is not apparent. The alternative hypothesis therefore deserves consideration, i.e., that ¹²C became enriched along with iron in the ferriferous water mass which precipitated cherty ironstone. If so, the ferriferous water mass probably was restricted to a single basin rather than extending throughout all of the oceans.

Various processes may affect the ratio of ¹²C/¹³C within seawater. A decrease in the global burial rate of organic matter would increase ¹²C in the dissolved CO₂ of seawater. However, the concomitant increase in atmospheric CO₂ would tend to reverse such a trend by enhancing the production of organic matter. A local increase in ¹²C may result from a local increase in organic productivity, as in a region of persistent

Evaporation: Why is there an equal proportion of chert in both deep-water and shallow-water iron formations?

Cooling: If silica precipitation is more sensitive to cooling than iron, why is there little facies variation in proportion of chert in iron formations?

Biota: Why are there no skeletal remains of siliceous microfossils?

Fe₃Si₃O₈(OH)⁰: Why is this ion not more obvious in modern environments?

Coprecipitation: Injection of plume or mixing of overlying silica-rich body with underlying iron-rich body?

Fig. 11. Flow chart for chert. Chert records evaporation, cooling, biota, Fe₃Si₃O₈(OH)⁰, or coprecipitation?

Seawater: Global difference in oceans or just in restricted water body?

Seawater – Global: Greater seawater ^{12}C content due to decrease in proportion of bacteria caused by lower P_{CO_2} or lesser global sedimentation of organic matter caused by higher P_{O_2} ?

Seawater – Local: Greater seawater ^{12}C content due to decay of organics settling into stagnant water body or exhalation of petrogenic methane?

Organic sedimentation: Increased organics in ironstone versus contemporaneous limestone due to less oxidation in stagnant water body or greater production in upwelling zone?

Organics – Less oxidation: Why did virtually all of the carbonaceous matter eventually decay whereas silicate muds preserve it well under an anoxic water body?

Organics – Upwelling production: Why are siderite beds so extensive and uniform given that upwelling exhibits considerable lateral variability?

Fig. 12. Flow chart for carbon isotopes. ^{12}C abundance in iron formations reflects seawater or burial of organics?

upwelling. An increase in ^{12}C similarly may occur where productivity is normal but organic decay is minimized due to restricted circulation. One inconsistency with either of these local-enrichment hypotheses is the paucity of C_{org} in typical ironstone. In quite a different vein, fluids from deep crustal weathering may introduce ^{12}C -enriched volatiles along with aqueous iron.

Siderite in noncherty ironstone exhibits an enrichment in ^{12}C just as in cherty ironstone (Hangari et al., 1980). However, the fossils in Phanerozoic noncherty ironstone indicate that precipitation did not occur from a long-lasting ferriferous (anoxic) water body. Nonetheless, a diagenetic origin for the ^{12}C enrichment is unattractive because ^{12}C in noncherty ironstone lacks any obvious correlation with C_{org} , just as in cherty ironstone. If noncherty ironstone has formed exhalatively, the carbon isotopic ratios may represent mixing between ^{12}C -enriched exhalative fluids and normal seawater.

Flow chart for oxygen isotopes

Enrichment in ^{16}O (Fig. 13)

Some banded cherty ironstone not only exhibits a 3‰ difference in carbon isotopic composition between adjacent microbands but also a 3‰ difference in oxygen isotopes (Baur et al., 1985). Isotopically light (^{16}O -rich) oxygen correlates with iron, as does isotopically light car-

bon. Ironstone siderite contains the lightest known oxygen in any sedimentary carbonate (Baur et al., 1985). E.C. Perry has proposed a kinetic explanation (in Baur et al., 1985), i.e. that ^{16}O preferentially precipitated with iron from seawater which contained ^{18}O -rich bicarbonate. Alternatively, ambient bicarbonate also was enriched in ^{16}O and the oxygen isotopes in ironstone record an exhalative enrichment in ^{16}O which accompanied an enrichment in ^{12}C , aqueous iron, and silica. An exhalative enrichment in ^{16}O would result from hydration of new oceanic crust at temperatures less than 300°C (Muehlenbachs, 1986).

According to the exhalative hypothesis, the ferriferous water mass would be richer in ^{16}O than average contemporaneous seawater. According to the kinetic model of E.C. Perry, the opposite would occur because the iron-precipitating water mass would initially be normal seawater but accumulate ^{18}O as it precipitated ironstone. If the accumulation of ^{18}O were more rapid than mixing with average seawater, the ironstone will become richer in ^{18}O despite continuous fractionation. It is unlikely that an ironstone-precipitating water mass could remain ferriferous while mixing rapidly with normal marine reservoirs. The Perry model therefore would predict that the ironstone which appears to have accumulated most rapidly would show a progressive increase in the ratio

^{16}O -rich water: Fe-rich bands enriched in ^{16}O due to greater exhalation or seasonal precipitation of constantly ^{16}O -rich subsurface water?

^{16}O -rich water – Greater exhalation: How could the periodicity of exhalation be as even as that of some banding?

^{16}O -rich water – Seasonal precipitation: Seasonal effect is inorganic, e.g., wind-induced mixing, or bacterial bloom?

Kinetic effects: ^{18}O accumulates until ^{18}O -rich ironstone precipitates or ^{18}O does not accumulate due to mixing with fresh seawater?

Kinetic effects – Accumulation: Why has no ^{18}O -enriched ironstone been found?

Kinetic effects – No accumulation: How could the ironstone-precipitating water remain ferriferous if mixing rapidly with ordinary seawater?

Fig. 13. Flow chart for oxygen isotopes. Enrichments in ^{16}O due to ^{16}O -rich water or kinetic effects?

of $^{18}\text{O}/^{16}\text{O}$ stratigraphically upward. This prediction has not yet been tested.

The potential for bacterial modification of oxygen-isotope ratios must be acknowledged because ^{18}O is depleted along the bacteria-rich interface between ferriferous-nonferriferous water in the Orca Basin (Sheu et al., 1988; La Rock et al., 1979). Isotopic fractionation also could occur during early diagenetic recrystallization of ironstone precipitates. The isotopic composition of the bottom waters filling pores may well have differed from that along a shallow-water interface where precipitation was occurring.

Flow chart for sulfur isotopes

Evolutionary changes in sulfur isotopes (Fig. 14)

The ratio of $^{34}\text{S}/^{32}\text{S}$ in evaporite deposits has varied throughout the geologic record of evaporites. The two prime processes which fractionate sulfur isotopes in seawater are bacterial and hydrothermal reduction of sulfate, both of which concentrate ^{32}S in the resulting H_2S (Nakai and Jensen, 1964; Ohmoto and Lasaga, 1982). Evaporitic sulfate records the isotopic ratio of the remaining sulfate and so records any change in the rate of separation of ^{34}S -depleted sulfide from the well-mixed portion of the oceans.

Virtually all parts of the modern oceans are well-mixed. However, it has been estimated that

the rate of separation of ^{34}S -depleted sulfide was too rapid to be consistent with a well-mixed ocean just before the Cambrian, at the beginning of the Late Devonian, and at the end of the Early Triassic (Claypool et al. 1980). One would have to postulate either extremely rapid sedimentation of ^{34}S -depleted sulfides or a major increase in the proportion of anoxic H_2S -dominated water bodies. Garrels and Lerman (1984) prefer to assume extremely rapid sedimentation of ^{34}S -depleted sulfides but an assumption of variable proportions of H_2S -rich euxinic water bodies seems easier to reconcile with the geologic record (Goodfellow, 1987). Partition of sulfur between oxidizing and euxinic water bodies could result in a variable isotopic ratio in evaporites without any variation in the average isotopic ratio of seawater.

Sulfur isotopes in Archean sulfides, including pyrite within iron formations, generally are enriched in ^{34}S relative to Phanerozoic sulfides (Cameron, 1982; Strauss, 1986). This difference may be attributed either to a difference in the seawater reservoir from which fractionation occurred (Holland, 1984) or a difference in the fractionation mechanism (Ohmoto and Felder, 1987; Cameron, 1982).

Archean oceans have been envisioned as sulfate-poor and predating the evolution of sulfate-reducing bacteria (Cameron, 1982; Skyring and Donnelly, 1982). In contrast, Ohmoto and Felder (1987) propose that depletion of ^{34}S in Archean ironstone pyrite occurred relative to

Changing seawater: Why are Archean sulfates not highly enriched in ^{34}S ? Has seawater variation been due to evolution of: (a) sulfate-reducing bacteria, (b) evaporite sedimentation, (c) evaporite metamorphism, or (d) atmospheric oxidation?

Changing seawater – Bacterial evolution: Why is pyrite correlative with organic carbon in mudrocks of all ages if sulfate reducers have not consistently been present?

Changing seawater – Evaporite sedimentation: Does the increase in sulfur fractionation at about 2.35 Ga record an increase in continental shelves, hence evaporites?

Changing seawater – Evaporite metamorphism: Has production of ironstone been linked to rate of metamorphic recycling of sulfate evaporites?

Changing seawater – Atmospheric oxidation: How could the Archean atmosphere be too anoxic to support seawater sulfate while producing oxide-rich paleosol on granitic rocks?

Constant seawater: Why do kinetic processes hypothesized for nonfractionation (high T , no bioturbation) not impede fractionation during modern reduction of sulfate to sulfide?

Fig. 14. Flow chart for sulfur isotopes. Are evolutionary changes in sulfur isotopes due to changing seawater ratios?

seawater because of bacterial depletion of ^{34}S in precursor H_2S , as during modern pyrite precipitation, but with a much lesser degree of depletion. They attribute the lesser isotopic fractionation between Archean seawater sulfate and pyrite to a lack of bioturbation and a higher marine temperature.

Pyrite depleted in ^{34}S characterizes several deposits within the Archean (2.7 Ga) Abitibi belt, not just the Helen iron formation studied by Thode and Goodwin (1983) (Cameron and Hattori, 1987; Strauss, 1986). The Abitibi belt is roughly comparable in size to the two areas in which Cameron (1982) and Hattori et al. (1983) based their “evolutionary” concept and so it seems unreasonable to dismiss the Abitibi as being anomalous. Moreover, the Abitibi belt contains some of the best preserved of all Archean rocks (Moorhouse, 1970). Cameron and Hattori (1987) attribute the Abitibi ^{34}S -depleted pyrite to hydrothermal fractionation instead of bacterial fractionation but the kinetics

of inorganic fractionation would be too slow below 200°C (Ohmoto and Lasaga, 1982). The lamination (banding) and stratigraphic continuity of the Helen iron formation seem to indicate precipitation from seawater which was not more than 50°C from thermal equilibrium with the ambient atmosphere.

Holland (1984) notes that sulfate minerals concentrate ^{34}S and that a lack of Archean sulfate sedimentation, e.g. evaporites, would tend to enhance the proportion of ^{34}S in seawater. He proposes that Archean rivers supplied ^{34}S -depleted sulfur and that bacterially-mediated Archean pyrite acquired the same sulfur isotopic ratio as that of the river input. If the Archean bacterial fractionation during sulfate reduction to sulfide averaged 50‰ (Ohmoto and Felder, 1987), Archean seawater sulfate would have been correspondingly richer in ^{34}S than modern seawater.

Ohmoto and Felder (1987) reject Holland’s (1984) concept of ^{34}S -rich Archean seawater

because the few Archean bedded sulfate deposits are not as enriched in ^{34}S . However, these ancient sulfates do not necessarily record the sulfur isotopic ratio of Archean oceans because most have been hydrothermally altered to such minerals as barite (Reimer, 1980). Instead of a ^{34}S -rich Archean ocean, Ohmoto and Felder (1987) invoke minimal isotopic fractionation in a high-temperature Archean ocean which lacks bioturbation. Their model appears to be inconsistent, however, with modern analogs. High temperature is not inhibiting sulfur-isotope fractionation in Solar Lake of the Sinai (Y. Cohen, pers. commun., 1988) and a lack of bioturbation under the euxinic Cariaco basin is not inhibiting production of ^{34}S -depleted pyrite (-24 to $-37\text{\textperthousand}$ in De Miro, 1974, p. 158). The model of Holland (1984) is more compatible with modern processes, but probably should be modified to emphasize rapid metamorphic recycling of Archean evaporitic sulfate rather than nonsedimentation.

Flow chart for major elements

Flow chart for major elements in iron formations (Fig. 15)

No ironstone-precipitating fluid has yet been collected. Speculation about the nature of such a fluid includes uncertainty about whether iron has been a major or minor solute. If iron constituted just a few ppm in seawater, as in the

seafloor-weathering model of Holland (1984), it would have been surpassed by at least nine other solutes and may have been comparable to boric acid (H_3BO_3). If the iron-rich fluid originated in deeply buried reactions rather than by seafloor or continental weathering, the iron concentration may have been much higher than in siderite-saturated seawater where it is just 3 ppm Fe (Holland, 1984, p. 388).

The lack of alkaline earths (Ca,Mg,Sr) in iron formations may be attributed either to a predominance of aqueous Fe^{2+} or an enhanced solubility of the alkaline earths despite the alkaline earths being more concentrated in the ironstone-precipitating fluid than Fe^{2+} . Some iron formations overlie limestone and/or contain limestone interbeds (Table 2). Ca^{2+} apparently was abundant in these ferriferous fluids. Iron formations which are associated with limestone beds do not appear to be otherwise different from other iron formations and so the concentration of aqueous calcium does not appear to have strongly influenced ironstone sedimentation. The enhanced precipitation of iron to form ironstone has reflected either a contemporaneous enhanced input of aqueous iron into an iron-concentrating basin, making iron a predominant solute, or an enhanced output due to some process which has made iron particularly insoluble, e.g., oxidation.

Input: From shallow weathering or exhalation?

Input – Shallow weathering: Why is there no modern type of shallow weathering which concentrates only solutes of Si, Fe, and C?

Input – Exhalation: Why is modern exhalation of Fe and C (off Venezuela) poorer in Si but richer in P than cherty ironstone?

Output: Organic or inorganic precipitation?

Output – Organic: Once evolved, iron-concentrating bacteria should have persisted, so why have iron formations comprised such a variable proportion of all strata?

Output – Inorganic: Given the geochemical dissimilarity between Fe and Si, how could inorganic precipitation consistently produce iron formations with such a narrow compositional range?

Fig. 15. Flow chart for major elements in iron formations. Ironstone mostly Si, Fe, O, and C because basinal input or output enhanced?

Flow chart for minor elements (ME) and selected trace elements

Ratio of Fe/ME (Fig. 16)

Cherty iron formations are remarkably deficient in elements other than Si, Fe, C, and O. Manganese commonly exhibits a roughly crustal-average ratio with respect to iron whereas phosphorus less commonly approaches a crustal-average ratio. The ratios of Fe/Mn and Fe/P both approximate 60 within the continental lithosphere (Beus, 1979). Both cherty and noncherty iron formations appear to grade to texturally similar manganese formations but gradation to phosphorite is less apparent. Cherty iron formations characteristically contain almost an order of magnitude less phosphorus than noncherty iron formations (on the order of 0.1% versus 1% P₂O₅) but Proterozoic cherty iron formations with more than 1% P₂O₅ occur in Finland (Laajoki and Saikonen, 1977).

The characteristic difference in phosphate content between cherty and noncherty iron formations clearly records a fundamental difference between the two types of ferriferous fluids. Another clear difference is the greater abundance of aluminum in noncherty iron formations. Aluminum is so scarce in some cherty iron

Source leaching: Shallow or deep weathering source?

Source – Shallow weathering: Weathering of exposed continent, of fluviomarine sediment settling through anoxic brine, or of seafloor sediment? Why do Fe/ME ratios range so little, given recorded variation in climate and composition of weathering material?

Source – Deep weathering: Does a small range in Fe/ME ratios correspond to a narrow range of P-T conditions for generation of ferriferous fluid? How could deep-weathering fluids avoid occasional mixing with hotter metal-dissolving fluids?

Fig. 16. Flow chart for minor elements (collectively labelled ME). Ratios of Fe/ME due to leaching of source or distance from vent-or-river input?

formations that it barely qualifies as a minor element versus a trace element.

The ratio of each minor element to iron may be attributed either to differential concentration along with iron in the source fluid or to differential precipitation before or during precipitation of iron. As implied in the caption of Fig. 1, the concentration of iron-rich fluids either is a surficial (shallow weathering) or subsurface (deep weathering) process. Both fluvial (shallow weathering) and exhalative (deep weathering) input could provide ferriferous fluids which chemically evolve away from the fluid source (river mouth or exhaling fault plane) to achieve characteristic ratios of minor elements to iron. In the exhalative case, one could invoke precipitation within or close to a vent for the nonferrous metals which are scarce in iron formations. The greater abundance of aluminum in noncherty iron formations may record precipitation closer to a vent than in the case of cherty iron formations. An alternative to the differentiation-with-distance option is that the observed elemental ratios directly reflect the chemical reactions which dissolved iron.

Distance from vent: Lack of correlative massive sulfide deposits because they never accumulated or because either subduction or erosion has removed them?

Distance from vent – Subduction: Why is the variation in volume of massive sulfides through Earth history not coincident with variation in iron formations?

Distance from vent – Erosion: Given that iron formations generally accumulate in shallower water than massive sulfides, how could the latter be preferentially eroded?

- Is** the ratio of element/iron close to the crustal average?
What, if any, other types of sedimentary rocks have similar concentrations?
Is the element concentrated in adjacent nonchemical rocks, e.g., volcanic rocks?
Did particulate (clastic) sedimentation of this element coincide with chemical precipitation of iron?
Could the element be epigenetic, as commonly interpreted for gold?
Could the element have been concentrated biologically?
What is the relative absorption of the element onto fresh ferric hydroxide?

Fig. 17. Unstructured questions about trace elements.

Flow chart for rare-earth elements

Rare-earth elements and the composition of precipitating seawater (Fig. 18)

Fryer (1977) proposed that the rare-earth elements (REE) in cherty iron formations record the oxidation state of the iron-precipitating seawater and that Archean iron formations have characteristic europium-cerium anomalies. In contrast, Graf (1978) and Kimberley (1978a) interpreted europium-cerium anomalies to be more dependent upon an association with volcanic rocks than geologic age. Given the scarcity of REE in iron formations, it is not obvious that anomalies in their distribution uniquely reflect primary chemical sedimentation, hence ferriferous water composition, rather than minor pyroclastic sedimentation and/or post-burial modification.

Factors relevant to genetic modeling

Proposed mechanisms of iron supply to iron formations

Most reviews present the consensus about geologic topics. Unfortunately, a consensus does not exist about the most fundamental aspects of iron formations, i.e. rock names, classification of rock bodies, source of iron, transport of iron, or precipitation processes. The lack of consensus is particularly remarkable for iron deposits which have formed within the past few million years. Some voluminous deposits are so young that interpretations should be well constrained, but actually vary greatly (Kimberley, 1979a). The foregoing set of flow charts (Fig. 1–18) illustrates the breadth of controversy regarding iron formations. Several published options were eliminated from the flow charts at the outset because they were deemed inconsistent with available data. Progressive elimination of most charted options occurs in the remainder of this paper.

All five types of natural waters have been proposed to transport iron to form iron formations, i.e. river water, ground water, alkaline lake water, fluids which have exhaled into a water body, and some type of seawater, e.g. seawater modified by biologically induced anoxia. Exhalative water may have a deep-weathering, high-temperature metamorphic, or magmatic origin. Varieties of each of these five fluids have been invoked for both cherty and noncherty iron

Reflect seawater: Do europium and cerium anomalies record global oxidation states or local oxidation?

Reflect seawater – Global: Why did europium become enriched in volcanic-associated iron formations even in the Ordovician when atmosphere was oxygen-rich?

Reflect seawater – Local: How could cerium become depleted within an anoxic water body which could not accumulate manganese nodules?

Unlike seawater: Were REE controlled by exhalative processes or were REE weathered along with iron?

Unlike seawater – Exhalative: If all iron-precipitating fluids are exhalative, why are REE different in iron formations interbedded with volcanics?

Unlike seawater – Shallow weathering: Do REE variations record shallow weathering of different source rocks and/or direct input of volcanic ash?

Fig. 18. Flow chart for rare-earth elements. Do the rare-earth elements reflect the composition of precipitating seawater?

formations, as reviewed by Kimberley (1979a, 1983a). The diversity of genetic models is enormous and many authors, including this one, have abandoned a genetic model after further study.

Beyond the question of transporting medium, there are questions of fluid composition and rate of flow. Detailed discussion of these questions is reserved for a later section. However, it may be noted here that the rate of sedimentation of noncherty iron formations appears to have been similar to that of cherty iron formations (Kimberley, 1979a). Both types have accumulated quickly in shallow water and both therefore required a fairly concentrated ferriferous solution.

Among the five possible aqueous-transport processes for ferriferous fluids, the exhalative possibility is most readily reconciled with the requirement of a concentrated solution. Fossil assemblages rule out the alkaline-lake hypothesis for at least the Phanerozoic iron formations, both the cherty and noncherty varieties (Table 2). Kimberley (1979a) showed that other alternative processes would have been insufficiently potent to produce the voluminous Kerch iron formation which is just five million years old (Table 2). For example, it is difficult to imagine how river water could become very ferriferous or how it could become cleanly separated from fluvial detritus. Ordinary seawater is an even more improbable source because the Kerch deposit contains about eight times more iron than all the oceans combined (Kimberley, 1979a). Lateral supply of ground water would be too slow to produce a voluminous iron formation and the vertical ground-water flow proposed by Kimberley (1979a) would require a special deltaic setting which subsequent authors have shown to be inconsistent with the stratigraphic record (Gygi, 1981).

Each of the five aqueous-transport processes has subset processes. Among those who support exhalative models, most authors invoke thermal convection of seawater through submarine basalt, comparable to the modern seabed con-

vection which is producing iron-manganese mounds (Fehn, 1986; Barrett et al., 1987). Extensive hydration of newly formed crust is indeed considered herein to be the most likely source of the iron and silica in cherty iron formations whereas noncherty iron formations are attributed to seismic pumping through a continental margin which includes hydrating ultramafic bodies.

Deep-weathering exhalative hypothesis

The deep-weathering exhalative hypothesis is developed more fully later in this paper but is introduced here. In the following discussion, it is shown that peak production of cherty iron formations has followed global peaks in crustal accumulation and may be related to post-magmatic rifting. The collective volume of contemporaneous cherty iron formations is roughly proportional to the volume of immediately preceding magmatism. Iron formations which cover volcanoes have formed within a few million years of cessation of magmatism whereas Early Proterozoic continental-shelf iron formations generally formed a few hundred million years after growth of the crust on which they rest.

The magma generating new crust would exhale carbonaceous volatiles to the oceans and atmosphere. Proliferation of hot spots under the continents would produce multiple rift basins like the modern Red Sea. Incipient rifts like the Red Sea commonly accumulate voluminous evaporites which may become deeply buried with interbedded clastic sediment (Sonnenfeld, 1984). If a transform fault were to develop along the length of a rift, seismic pumping would drive CO₂-rich seawater along the fault zone. If the fault lay along a continental margin, the pore waters would migrate from one segment of the margin to another. These segments could be quite diverse, e.g., along the transform fault zone of coastal Venezuela where there are thick piles of young evaporite-bearing sediments, former island-arc blocks of metamorphic rock, and ultramafic to granite intrusions (Beets et

al., 1984). Even old granitic intrusions may heat seismically-pumped water because they concentrate heat-producing radioactive nuclides (Cathles, 1977).

Iron is ubiquitously available for dissolution along virtually any transform fault system which can produce a fluid caustic to iron. For example, mudrock like shale averages about 4.5% Fe (Blatt et al., 1980, p. 383). Compared to other ore deposits, iron formations represent a small concentration of metal relative to average rock. Whatever their deep source, it is hypothesized that ferriferous fluids which produce iron formations typically have risen rapidly along major faults, as envisioned by Gross (1983). The hypothetical upward migration of hypersaline fluids would require faults which were kept open by a combination of deep-seated tectonic activity and rising volatiles.

Fluids which have formed noncherty iron formations probably have exhaled at a lower temperature and pressure than those which formed cherty deposits. Cooler temperatures and lower pressures may have been partially caused by a slow rise through poorly consolidated sediment which did not readily support open cracks. A decrease in temperature and pressure would induce precipitation of silica prior to exhalation (Holland and Malinin, 1979). Cool fluids presently are dissolving iron from smectite as they rise around the Gulf of Mexico (Posey et al., 1986). Metalliferous oil-field brines in Mississippi commonly contain 300–500 ppm Fe^{2+} (6–9 mM Fe^{2+}) (table 5 of Carpenter et al., 1974). Hypersaline vents are directly observable under more than 3 km of water at the western base of the Florida platform (Paull and Neumann, 1987) and range from exposed land to hundreds of meters of water depth on the Venezuelan shelf and slope (Kimberley and Llano, in press).

Young ironstone and modern analogs of ironstone

Genetic modeling in this paper is partly based on field work along the northeastern coast of

Venezuela where the author has found iron silicates to be accumulating over hundreds of square kilometers of the shallow seafloor (Figs. 19, 20, 21). Most of this sediment contains less than 15% Fe but the modern equivalent of iron-stone (berthierine ooids + CaCO_3 fossils with > 15% Fe) occurs in at least one locality about 5 km offshore (Kimberley, 1988). Besides extensive iron silicates in shallow water, the Venezuelan shelf contains tens of square kilometers of highly siliceous ooze, tens of square kilometers of phosphatic sediment (De Miro, 1974), and local sulfide accumulations which may overlie vents. The modern ironstone occurs adjacent to an area which is characterized by several young (5 Ma) dacitic intrusives which are all small (< 1 km across) but associated with extensive hydrothermal alteration (Sifontes and Seijas, 1972).

The northeastern coast of Venezuela presently is a tectonically active margin which lies perpendicular to the Lesser Antilles volcanic arc (Davidson, 1983). Coastal Venezuela includes blocks of an island arc of Early Cretaceous age which collided with South America during the Late Cretaceous (Beets et al., 1984). The accreted arc may overlie a former margin which subsided during the opening of the Gulf of Mexico (Salvador, 1987). Extension and compression presently alternate along the transform-faulted Venezuelan margin. Extension is most evident in the 1.4 km deep Cariaco Basin (Fig. 19) which lies within the continental shelf (Muessig, 1984). Compression dominates the region east of the Cariaco Basin and it is here that exhalation of ferriferous fluids is most obvious (Kimberley and Llano, in press).

Earthquakes immediately east of the Cariaco Basin commonly are accompanied by volatile exhalation. Explosive exhalation of methane occurred during field work in January 1986 and has a long recorded history (Von Humboldt, 1881). Exhalation of carbon dioxide probably also occurs but is less obvious than the pyrotechnic display of methane. Exhalation unaccompanied by earthquakes has been reported

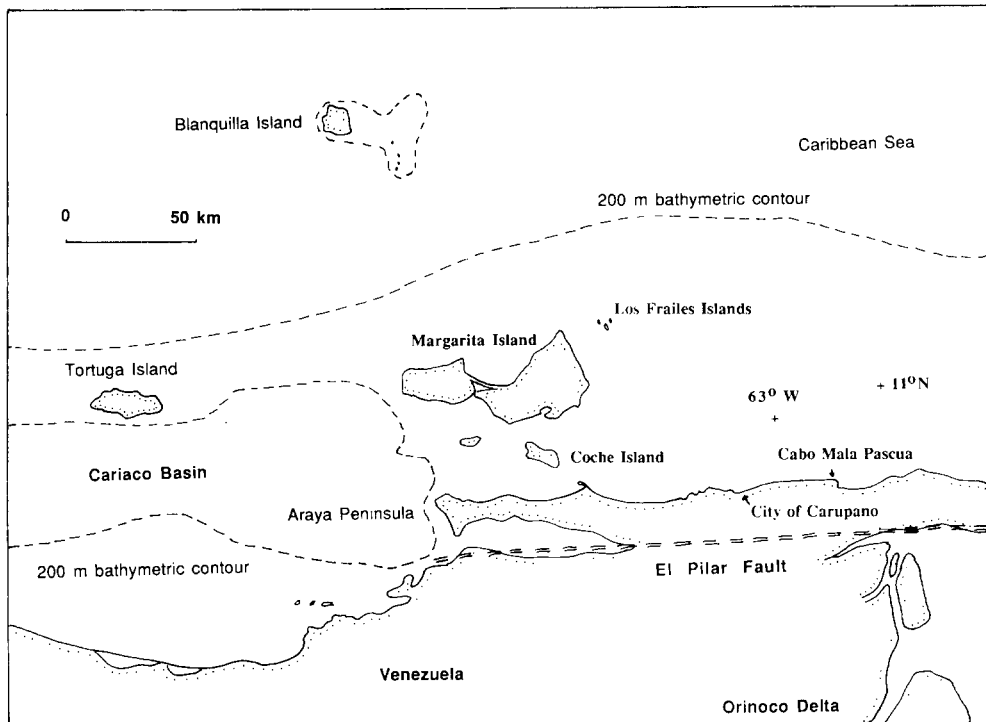


Fig. 19. Location map for northeastern South America, illustrating the eastern half of the Cariaco Basin, the Margarita-Araya platform, and the northwestern corner of the Orinoco delta. Notice that the 200 m bathymetric contour locally lies within 3 km of land. The westward extension of the El Pilar fault is not shown because its location is uncertain.

by residents of Coche island (Fig. 20). Exhalation in the El Bichar area of Coche reportedly recurs about once per decade.

Although the Venezuelan shelf locally exemplifies iron migration and concentration to produce berthierine ironstone (Kimberley, 1988), it mostly exemplifies production of peloidal (nonoolitic) glauconite like that which commonly is associated with phosphorite. Modern marine ironstone also is accumulating on the Mahakam delta of Indonesia where methane exhalation occurs as frequently as along the northern coast of Venezuela (Allen et al., 1979; Ooi Jin Bee, 1982). Methane exhalation due to heating of carbonaceous sediment is a common phenomenon elsewhere (Tissot and Welte, 1984) but most methane-rich exhalations probably are too sulfidic to transport much iron (Berner, 1981). For example, the author has observed only a thin rim of pyrite around

asphaltic diapirs which surround and feed Pitch Lake in Trinidad (Fig. 22).

A voluminous oolitic iron formation formed five million years ago in the region with greatest modern methane exhalation, the Caucasus (Shaulov, 1973). The thickest portions of this deposit lie in depressions between volatile-produced mud diapirs (Zitzmann, 1977, p. 356). Coeval Pliocene formations under the nearby Caspian Sea locally contain over 20% solutes in pore water and locally have sustained an upward displacement of gas-saturated domes greater than 1 mm per year for a few million years (Arkhipov, 1982; Didura, 1982).

All of the foregoing modern examples of ferriferous sediment are noncherty; i.e., they contain less than 5% chert. Shallow-water siliceous ooze is closely associated, however, with the modern ferriferous sediment in Venezuela. Kimberley et al. (in press) have discovered that

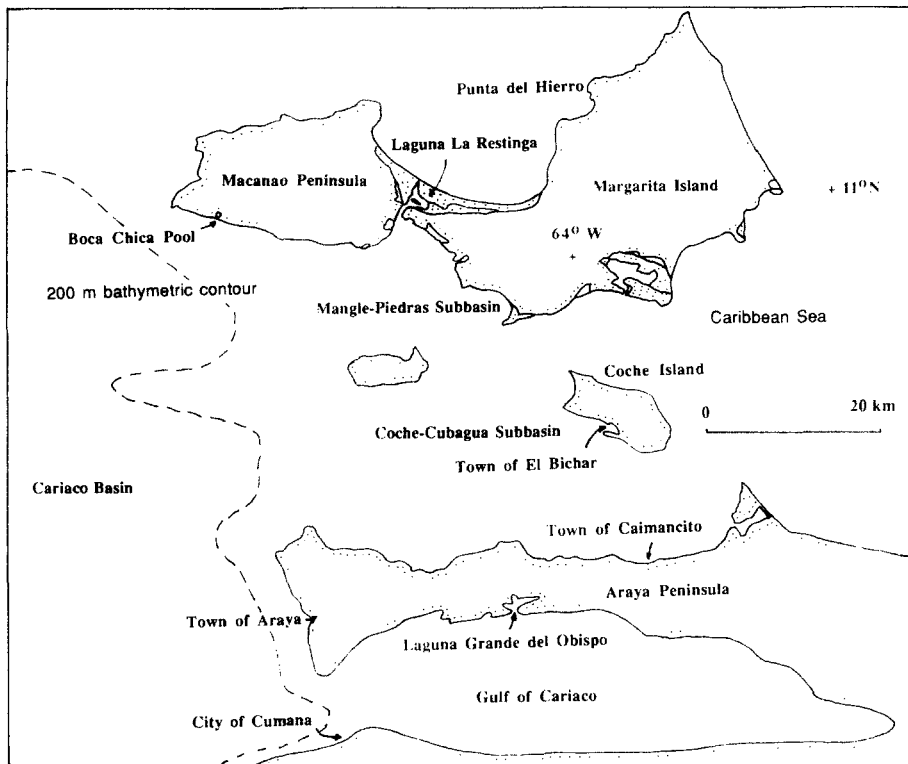


Fig. 20. Location map for the Margarita-Araya Platform, illustrating the subbasins between Margarita Island and the Araya Peninsula. Punta del Hierro lies right of the label and Laguna la Restinga occupies all of the stippled area between the Macanao Peninsula and the eastern half of Margarita Island.

fossil diatoms constitute more than 5% of the shallow (<30 m) seafloor sediment over tens of square kilometers just west of Coche Island (Fig. 20). Ferriferous sediment with intermixed silica presently is accumulating within hot vents in the Red Sea and in iron-manganese mounds near the Galapagos islands (Fehn, 1986). The hot saline fluids which are rising toward these vents are potentially corrosive to all metals (Kwak et al., 1986). Thorough leaching by these fluids would result in metal-solute ratios close to crustal abundances, as observed in most iron formations. A wide variety of other exhalative deposits may result from selective leaching by hydrothermal solutions, e.g. manganese deposits and lead-zinc sulfides (Winn and Bailes, 1987). Given that the basal beds of several iron formations are manganiferous, including the Outerring iron formation (Table 2), manganese enrichment

may have characterized the initially introduced fluids.

Common features of ironstone

A modal analysis of ironstone averaged over all iron formations of all ages would reveal a great "irony", i.e. that the most abundant mineral has not been iron-bearing. It has been quartz (recrystallized chert). Most ironstone is Precambrian and most fresh Precambrian ironstone contains over 25% recrystallized chert which is not homogeneously distributed through the rock but concentrated in chert-rich bands (Davy, 1983; Trendall, 1968).

Most cherty ironstone has been metamorphosed but the banding cannot be attributed to metamorphic differentiation - (e.g., Robin, 1979). Isotopic differences between adjacent mm-thick bands in cherty ironstone indicate

that the bands are either primary or early dia-genetic (Baur et al., 1985). Synsedimentary erosion locally has produced cross-bedded bands (Dimroth, 1977a; Simonson, 1985). Some bands have been folded by synsedimentary deformation (Dimroth and Chauvel, 1973). Lateral differences in cementation commonly have produced pinching and swelling of groups of bands (Dimroth, 1968, 1977; Trendall and Blockley, 1970).

Some banded ironstone exhibits oolitic texture which is indistinguishable from that of modern aragonitic ooids (Markun and Randazzo, 1980). This texture occurs in several cherty iron formations but oolitic ironstone is subordinate to nonoolitic ironstone in all voluminous cherty iron formations and is completely absent in most (Lougeed, 1983; Dimroth and Chauvel, 1973). Although oolitic texture characterizes a small proportion of cherty ironstone but the majority of noncherty ironstone, noncherty ironstone constitutes such a small proportion of all ironstone that the total volume of cherty oolitic ironstone may be greater than that of noncherty oolitic ironstone. For this reason, it is misleading for textbooks to distinguish between cherty and noncherty ironstone by labelling them banded and oolitic, respectively (e.g. Read and Watson, 1968).

The prime ferriferous mineral in an unweathered cherty iron formation typically is siderite, magnetite, and/or hematite. Global rank-ordering among these three is difficult because the proportions of these minerals vary greatly among iron formations and differentiation of weathered from unweathered rock locally is difficult. Some large iron formations have become metamorphosed after being deeply weathered and existing mineralogy in "fresh" metamorphosed ironstone is more oxidized than was the primary chemical sediment (Morris, 1985). Although siderite does not constitute the bulk of commercially exploited ironstone, it may well have been the most abundant primary mineral in cherty iron formations (e.g., Gar-

rels, 1987). If so, ironstone sedimentation generally cannot be attributed to oxidation of ferriferous seawater.

Ferriferous silicates are widespread in most cherty iron formations and offer the best record of metamorphic grade (Floran and Papike, 1975). Greenalite, a primary iron serpentine, occurs up to the lowest metamorphic grade and locally preserves oolitic texture in phenomenal detail (Fig. 7). Greenalite consistently is microcrystalline and commonly is transected by coarser-grained minnesotaite and stilpnomelane (Klein, 1983). Metamorphism is not necessary for production of either minnesotaite or stilpnomelane because both occur in an unmetamorphosed Carboniferous (Mississippian) cherty iron formation in Ireland (Schultz, 1966). Metamorphism typically is necessary for the crystallization of annite (a biotite mica), and various amphiboles (riebeckite and grunerite) in cherty ironstone.

Ironstone with less than 5% chert is termed noncherty (Kimberley, 1983a). Chert in noncherty ironstone generally is homogeneously distributed throughout the rock. Most Phanerozoic ironstone is noncherty and oolitic (James, 1966). Individual ooids in both cherty and noncherty ironstone closely resemble calcareous ooids in size and shape (Cayeux, 1922; Markun and Randazzo, 1980). The internal structure of ironstone ooids indicates that they have formed at the sediment-water interface rather than within marine sediment or within soil (Kimberley, 1980; Bhattacharyya and Kakimoto, 1982). An aggregation of ooids is called oolite, following Bathurst (1975). Intra-clasts of oolite occur within both cherty and noncherty ironstone (Dimroth and Chauvel, 1973; Kimberley, 1980).

The most abundant ferriferous minerals in noncherty ironstone are goethite, hematite, berthierine (an aluminous analog of greenalite and ferrous analog of serpentine), and chamosite (a ferrous variety of chlorite). It has been common for both berthierine, with 0.7 nm basal spacing, and chamosite (1.4 nm basal spacing)

to be called chamosite but differentiation would be preferable (Van Houten and Purucker, 1984). These two silicates are rarely intergrown and the predominance of chamosite in old or deeply buried iron formations indicates that it may form by replacement of berthierine (Maynard, 1986). Velde et al. (1974) describe the metamorphic conversion of 0.7 nm berthierine to 1.4 nm chamositic chlorite.

Glauconite (ferric illite) is rare in any non-cherty oolitic or cherty ironstone. Glauconite is a common accessory mineral in clastic sediments which are associated with phosphorite and is the prime mineral in the few deposits of this association which contain enough iron to qualify as ironstone (Odin and Letolle, 1980). The occurrence of glauconite is quite distinct from that of the ferrous silicates, berthierine and chamosite. Cayeux (1931, p. 259) lists the following differences. Glauconite occurs in distinct cryptocrystalline grains and almost never is a partial replacement of another authigenic iron-rich mineral. Berthierine occurs as platy crystallites which generally are intergrown with other iron-rich minerals and may partially replace them. Berthierine commonly occurs within ooids unlike glauconite. Berthierine never partially replaces siliceous fossils but commonly partially replaces echinoderm platelets. Glauconite commonly partially replaces siliceous fossils but rarely partially replaces echinoderm platelets. Berthierine generally does not occur within chambers of foraminifera but this is one of the most common sites for glauconite.

Siderite is ubiquitous in noncherty ironstone but rarely predominant. Most siderite in non-cherty ironstone has formed diagenetically whereas most siderite in cherty ironstone is primary. Magnetite is rare in noncherty ironstone unless it has been metamorphosed (Lunar and Amoros, 1979). Unmetamorphosed magnetite-rich ironstone occurs only locally (Kimberley, 1980). Pyrite is common in carbonaceous mud-rock, e.g. shale, associated with noncherty iron-

stone but less common within the ironstone itself (Kimberley, 1980).

Iron formations through Earth history

The stratigraphic record of iron formations extends from the oldest known Archean to the modern seafloor. An extensive tabulation of iron formations (Table 2) provides evidence against some common myths. For example, the end of the Precambrian did not mark the end of cherty iron sedimentation (cf. Baur et al., 1985). Phanerozoic metazoans have disturbed the lamination of iron formations but the atmospheric oxygen required for metazoan existence has not prevented the accumulation of any type of iron formation during the Phanerozoic. Although not prohibitive, abundant atmospheric oxygen may have been detrimental to Phanerozoic cherty ironstone sedimentation. Climatic change or biologic evolution within the Precambrian similarly is not correlative with iron sedimentation, as far as can be discerned. A correlation is proposed herein, however, between iron formations and tectonomagmatic cycles in the Precambrian.

Archean iron formations

Isua iron formations

All known Archean iron formations are cherty. The oldest rock sequence on Earth, the 3.75 Ga Isua Supergroup in western Greenland, contains iron formations (Hamilton et al., 1978; Appel, 1980). The Isua Supergroup is one of the earliest segregations of continental crust from the mantle, based on Sm–Nd isotopes in cherty ironstone (Miller and O’Nions, 1985). A continuous long peak in ironstone sedimentation followed and overlapped with the initial production of continental crust in the interval from 3.75 to 3.35 Ga in Greenland and South Africa (Miller and O’Nions, 1985). James (1983) sketches a broad peak in ironstone production from 3.5 Ga to 3.0 Ga.

The 2 Ga-long record of ironstone sedimentation from Isua time through the Early Proterozoic makes it unlikely that biological evolution has been the main control on sedimentation of cherty ironstone, as proposed by Cloud (1973). The paleoenvironment of the Isua Supergroup has been interpreted to be a small continent rather than a volcanic platform (Bridgwater et al., 1978; Miller and O'Nions, 1985). This is consistent with the negative europium anomaly in the cherty ironstone (Appel, 1980).

Helen iron formation

The Isua ironstone is intensely deformed and metamorphosed to amphibolite grade. Other Archean iron formations are much better preserved and have become well exposed by open-pit mining. The Archean Helen iron formation in the Algoma District of Ontario, Canada is one of the best described of all SVOP iron formations (Goodwin, 1962, 1964; Goodwin et al., 1976, 1985). SVOP (Shallow Volcanic Platform) and other iron-formation acronyms are explained in Table 1. The upper portion of the Helen SVOP-IF consists of a common variety of cherty ironstone, i.e., interlaminated (banded) siderite and recrystallized chert with roughly equal thicknesses of the two types of laminae (about 1 cm). However, the basal beds of the Helen are peculiar in consisting largely of pyrite. The beds which immediately overlie basal pyrite consist mostly of siderite with subordinate recrystallized chert.

A.M. Goodwin kindly showed two interesting features of the Helen SVOP-IF to the author, i.e. beds of extremely carbonaceous mudrock and ironstone beds which had been disrupted by rising volatiles. The carbonaceous matter probably is organic because Thode and Goodwin (1983) have demonstrated that fractionation of isotopes accompanied ironstone sedimentation (Goodwin et al., 1976). It is unlikely that the carbonaceous matter exuded as hydrocarbons, like asphaltic Pitch Lake in Trinidad. The ob-

served disruption of ironstone laminae by exhaling volatiles probably records the genetic process which produced the Helen iron formation (Goodwin et al., 1985). The exhaling volatiles must have been virtually devoid of volcanic particles, however, for a 300 m thickness of ironstone to accumulate without substantial pyroclastic interbeds (Goodwin, 1962).

Typical SVOP-IF features of the Helen iron formation include evidence of facies changes in both the ironstone and associated volcanic rocks (Morton and Nebel, 1983). Deep-water turbidite sedimentation occurred around the Helen platform and interbedded DWAT-IF is rich in magnetite. Siderite is the most abundant ferriferous phase in platform rocks. Pyrite occurs both on and off the platform. With the exception of the unique lower pyrite beds, the distribution of pyrite in this and all other cherty iron formations is more closely linked to the content of organic carbon in the rock than to the former water depth. Goodwin (1973) offers an alternative interpretation of Helen facies, one in which magnetite-rich graywacke turbidites accumulated in water shallower than that on the siderite-rich volcanic platform.

Massive sulfide deposits commonly are associated with pyritic ironstone but pyrite is remarkably subordinate to other ferriferous minerals in iron formations other than the Helen SVOP-IF. SVOP-IF's and DWAT-IF's of all ages tend to have a little more pyrite than do MECS-IF's. Given the preponderance of SVOP-IF and DWAT-IF among Archean iron formations, Archean iron formations collectively contain a greater concentration of pyrite.

Outerring iron formation

The Archean Outerring SVOP-IF, 2300 km northwest of the Helen SVOP-IF in Canada, exhibits facies relationships more clearly than the Helen because it is one of the least deformed of all Archean iron formations (Lambert, 1978). The Outerring SVOP-IF formed on top of a volcano which previously had experienced alter-

nating felsic volcanism and cauldron subsidence (Lambert, 1978). The diameter of subsidence and volcanism grew with time, producing a concentric outcrop pattern, until the entire platform subsided below sealevel immediately following ironstone sedimentation. The author has mapped the Outerring SVOP-IF along its arcuate 20 km outcrop belt and formally established lake names to record its location, e.g., Outerring, Northring and Eastring Lakes.

Continuity of the Outerring SVOP-IF over 20 km is interpreted to indicate that most volcanic activity, including cauldron subsidence, had waned prior to cherty ironstone sedimentation. The Helen SVOP-IF also accumulated upon a platform which had experienced cauldron subsidence (Sage, 1979; Morton and Nebel, 1983). It is probable that both areas experienced "intense hot-spring fumarolic (exhalative) activities" during ironstone sedimentation, as envisioned by Goodwin et al. (1985, p. 82). Goodwin (1964) has documented hydrothermal alteration of the felsic volcanics beneath the Helen SVOP-IF. Sideritic veins also transect felsic volcanics deep beneath the Outerring SVOP-IF.

Soudan iron formation

The magnetite-rich Soudan iron formation in Minnesota is distinct from the Helen and Outerring iron formations (Van Hise and Leith, 1911; Sims, 1972). The Archean Soudan was deposited on pillow lava of a mafic pile rather than a felsic pile. The water depth above the Soudan probably was greater than that above the Helen or Outerring iron formations and the Soudan is intermediate between end-member SVOP-IF and DWAT-IF. The Archean Soudan iron formation contains some of the oldest putative microfossils on Earth (Cloud and Licari, 1968; LaBerge, 1973). Like the Helen and Outerring, the Soudan contains highly carbonaceous and pyritic mudrocks (Goodwin, 1962; Cloud et al., 1965). In the Outerring SVOP-IF, pyritic and carbonaceous laminae locally alternate within

stromatolitic structures along the south shore of Outerring Lake.

Proterozoic iron formations

Relationship of Proterozoic MECS-IF to crustal growth

Most iron mining presently occurs in Proterozoic MECS deposits (Morris, 1985). The boundary between the Archean and Proterozoic is variably defined in different countries, e.g. 2.3 Ga in Australia, 2.48 Ga in Canada, 2.5 Ga in the U.S.A., and 2.6 Ga in the Soviet Union (Eicher and McAlester, 1980). The concept of an Archean-Proterozoic boundary somewhere between 2.6 and 2.3 Ga is based on a peak in production of igneous continental crust between about 3.0 and 2.7 Ga (Reymer and Schubert, 1986). Most large SVOP iron formations coincide with this Late Archean time span (Goodwin, 1973; see Table 2) and the Hamersley MECS iron formations in Australia accumulated about 0.2 Ga later (Trendall, 1983b). The Transvaal MECS iron formations in South Africa accumulated at about the same time as the Hamersley (Beukes, 1983).

MECS iron formations around the Ungava craton of eastern Canada accumulated at some time between 2.4 and 1.8 Ga (Gross and Zajac, 1983). The voluminous MECS iron formations around Lake Superior accumulated between 2.1 and 1.85 Ga (Morey, 1983). This younger time apparently coincides with another major period of global crustal growth, between 2.1 and 1.7 Ga (Reymer and Schubert, 1986; Patchett and Arndt, 1986).

Future work will refine the temporal relationship between crustal growth and iron-formation sedimentation. This is important because iron formations may have formed by exhalation coincident with rapid crustal growth or there may have been a characteristic lag time between peak crustal growth and peak ironstone sedimentation. Demonstration of a characteristic lag time would support the genetic

model advocated herein for cherty iron formations, i.e., hydration of newly accreted crust.

A peak in MECS-IF production coincided with or followed the Late Precambrian period of crustal growth, from about 0.9 to 0.6 Ga (Reymer and Schubert, 1986). Abundant cherty ironstone formed from roughly 0.7 to perhaps 0.4 Ga (Table 2; James, 1983). Mixtite accumulated between the time of peak magmatism and that of ironstone sedimentation, as during the Early Proterozoic. However, mixtite overlapped with ironstone sedimentation unlike the Early Proterozoic case. As during the Early Proterozoic, Late Precambrian MECS iron formations are sufficiently widespread and similar to represent a global cycle (Young, 1976).

Rocks associated with Early Proterozoic iron formations

In the Early Proterozoic, high relief on Archean cratons commonly became buried under thick sandstone units, some including uraniferous conglomerate (Roscoe, 1969; Kimberley, 1978b). Mixtite and other glaciogenic rocks characterize these basal Proterozoic sequences (Young, 1973). However, the glaciers had melted and continental relief had become minimal by the time MECS-IF started to accumulate. The mixtite-to-ironstone sequence occurred later in North America than most MECS-IF sedimentation in Australia. Flat unconformity surfaces beneath granular MECS-IF can be traced south of the roughly 2.5 Ga Hamersley Group along a strike of 300 km (Goode et al., 1983; Trendall, 1983b). Low relief probably was accompanied by thick weathering crusts (regolith) and efficient comminution of sediment grains before they became eroded onto a continental shelf. There is no evidence that high relief on any continent adjacent to an Early Proterozoic MECS shelf was contributing much sediment, hence much iron, to that shelf.

The rock types which directly underlie and overlie Proterozoic MECS-IF's are listed in Table 2. The lithologic variety is large but is domi-

nated by the most abundant types of sedimentary rocks, i.e., clay-bearing clastic rocks (mudrocks and graywacke) and their metamorphosed equivalents, especially in overlying strata. Thick units of feldspathic fluvial sandstone, like that which initially covered the Archean cratons, generally are not found stratigraphically adjacent to the iron formations. Within a few hundred meters of the base of Proterozoic iron formations, there commonly is quartzose marine sandstone which exhibits tidal cross-bedding (Larue, 1981b; Ojakangas, 1983). Well-sorted sandstone commonly occurs below but not above the iron formations (Simonson, 1984). Carbonate rocks and chert also are more abundant beneath than above the iron formations (Table 2).

Although the stratigraphic sequence of rock types varies globally, a common Early Proterozoic sequence is that noted by Gross (1965, p.91), i.e., "dolomite, quartzite, red and black ferruginous shale, iron-formation, black shale, and argillite, in order from bottom to top". The shale and argillite become phyllite and schist upon metamorphism and so the sequence in the Paakko MECS-IF of Finland is "dolomite, quartzite-phyllite, iron formation, black schist" (Laajoki and Saikkonen, 1977, p. 17). This stratigraphic sequence is far from universal but even its mediocre tendency for recurrence carries a genetic implication for MECS iron formations, i.e., that some regional, long-lived tectonic process has controlled the shorter-lived process of ironstone sedimentation, whatever those processes may have been. The recurring stratigraphy also justifies the incorporation of MECS-IF in a classification scheme which is based on paleoenvironment (Kimberley, 1978a) even if iron dissolution has not been an environmental (shallow weathering) product but rather related to deep weathering. The collective stratigraphic thickness of the recurring sequence generally exceeds a kilometer of shallow-water sediment and so subsidence must have accompanied sedimentation.

Morphology of Early Proterozoic MECS-IF platforms

Early Proterozoic MECS iron formations are not only voluminous collectively but also individually, e.g. those which accumulated at about 2.5 Ga within the Hamersley Group of Western Australia (Trendall, 1983b). The great extent of correlative meter-thick beds in the Hamersley records either an unprecedented lateral uniformity of sedimentary environments following cratonization in the Late Archean or an insensitivity of ironstone sedimentation to lateral variation in water depth. The water depth in these and other MECS environments was sufficiently similar over such great distances that their depositional platforms undoubtedly were convex upward because of the Earth's curvature. The Sokoman and correlative MECS iron formations in Quebec, Canada extend for over 1000 km of arc on the Earth's circumference (Gross, 1983; Gross and Zajac, 1983) and the middle would have been about 20 km higher than the edges, assuming that the Earth's radius has not changed with time (Vogt et al., 1969). As noted by Morris and Horowitz (1983), application of the term, basin, to such an environment should be explained in each paper which uses the term, e.g. Trendall (1983b).

The lack of terrigenous sediment in MECS iron formations commonly is attributed to some type of clastic trap, e.g. a minor depression between the coast and a row of offshore sand bars or barrier islands, with ironstone accumulating seaward of the quartz sand (Ojakangas, 1983). Lague and Sloss (1980) note that fault-bounded blocks characterized the MECS shelf in the Lake Superior area and so the shelf may not have been the progressively deepening margin which typically is sketched (Ojakangas, 1983). The lack of terrigenous sediment within MECS-IF could have been ensured by structural elevation of offshore blocks or erosion of deep channels between blocks, e.g. the Florida-Bahama platforms (Paull and Neumann, 1987).

It is difficult to determine if transform faulting has been active during MECS-IF sedimentation. Broad transform fault zones characteristically include deep restricted basins like the modern Cariaco Basin which extends for 200 km along the continental shelf of Venezuela (Richards, 1975). Basins like the Cariaco form as rhomb-shaped pull-aparts due to differential lateral movement along a pair of strike-slip faults which bound the basin (Muessig, 1984). Seawater in a restricted basin may become chemically distinct, even if the residence time is as short as 100 years (Richards, 1975). The aforementioned association of black shale or schist with iron formations may record development of restricted basins along former transform fault zones. As subsequently described herein, the transform-faulted, iron-accumulating margin of northeastern South America presently extends farther than the most extensive Precambrian iron formation, the 1000 km-long Sokoman iron formation (Table 2).

Facies variation in Proterozoic iron formations

Low relief on some MECS-IF shelves has resulted in negligible facies changes over great distances, e.g., in Hamersley MECS-IF of Australia (Trendall and Blockley, 1970). However, facies are mappable in some MECS-IF of the Lake Superior and Circum-Ungava (Quebec-Ontario) districts. James (1954) proposed that the facies in MECS-IF vary from shallow-water oxide ironstone through deeper-water sideritic ironstone to basinal pyritic facies. This theoretical facies scheme has been reproduced in many textbooks on ore deposits (e.g. Stanton, 1972a; Guilbert and Park, 1986).

Some workers are sufficiently convinced of the oxide-carbonate-sulfide order that they assume relative water depth from ironstone mineralogy without other evidence. This conviction is strengthened by the widespread usage of facies as a lithologic term, e.g. "carbonate facies" to signify siderite ironstone. However, some studies of MECS-IF facies disprove the uni-

versal applicability of the oxide–carbonate–sulfide order. For example, Plaksenko et al. (1973) report that mineral zonation in the Kursk MECS-IF is the opposite of James (1954), with a pyritic facies mostly nearshore, followed by a siderite–silicate facies, and the oxides in deepest water. The most highly oxidized (hematitic) ironstone in the Kursk area occurs in the deepest-water facies.

Pyrite facies in Proterozoic iron formations

The “pyrite facies” of James (1954) generally is not “iron-formation” by the definition of James (1954) or ironstone by the definition of Kimberley (1978a) because both definitions restrict these terms to chemical sedimentary rocks. The great bulk of “pyrite facies” is simply pyritic mudrock, e.g. black shale (James, 1954; Dimroth, 1976). Inappropriate reference to “pyrite-facies iron-formation” occurs in a large proportion of the papers about Proterozoic iron formations. Pyritic ironstone does exist but is largely restricted to Archean SVOP-IF and DWAT-IF, e.g. the basal Helen iron formation (Goodwin et al., 1985).

Most rocks which have been called “sulfide facies” are neither chemical sedimentary rock nor are they richer than 15% in iron. However, at least some authors have been careful to reserve the name, sulfide facies, for mudrock with more than 15% Fe (Laajoki and Saikonen, 1977). Pyritic mudrock may be fundamentally different from cherty ironstone and its inclusion in a facies scheme is questionable unless the pyrite content is noticeably greater than that of typical black shale. Even in highly pyritic mudrocks near ironstone, the pyrite content generally correlates with the organic-carbon content as in any mudrock of any age (Dimroth and Kimberley, 1976).

Pyritic mudrock in iron formations typically is interpreted to represent deep water on the assumption that pyritic mud generally accumulates in deep water. However, Dimroth (1976) cites several studies of pyritic mud and

mudrock to demonstrate that this is not a safe assumption. Much of the organic carbon in pyritic mudrock may have originated as organisms in the shallow photic zone. The preferred depositional site for this low-density organic matter would have been a low-energy environment close to the zone of production, e.g. behind a sand bar on a shallow-water shelf. This tendency for shallow-water accumulation may have been even greater in the Proterozoic than in the Phanerozoic cases cited by Dimroth (1976) if the iron-formation shelves had less oxygenated bottom water which did not oxidize the carbonaceous matter as readily.

The most carbonaceous and pyritic mudrocks in the Archean Outerring iron formation (Table 2) accumulated behind a shallow barrier of calcareous oolite. Mudrock with less organic carbon and less pyrite accumulated in deeper water, mixed with turbidites. This dichotomy of pyritic environments probably existed for many iron formations but generally has been ignored in facies models. The pyritic environment was certainly rich in dissolved hydrogen disulfide but not necessarily much poorer in dissolved oxygen than other environments which were simultaneously precipitating ferrous minerals (Berner, 1981).

Redox indicators in Proterozoic iron formations

Much of the popularity of the facies scheme of James (1954) is attributable to its seminal role in the establishment of Eh–pH diagrams in chemical sedimentology. Most workers have followed James (1954) in using Eh–pH diagrams to define chemical sedimentary environments but Berner (1981) has demonstrated that this approach is impractical. There is little variation in pH among marine environments and there is only a tiny portion of the marine realm which is gradational between being anoxic, i.e., less than one micromolar concentration of dissolved oxygen, and highly oxidized. Among the highly reduced environments, the prime variable involves the sulfurous solutes.

Berner (1981) defines three anoxic environments, one which lacks sulfur species because of sulfide precipitation, one with abundant hydrogen sulfide, and another with more sulfate than sulfide. These environments respectively are termed methanic, sulfidic, and suboxic in this paper.

An inherent assumption in the facies scheme of James (1954) is that the Proterozoic atmosphere was more oxidizing than was average Proterozoic seawater. No matter how reducing the atmosphere may have been during MECS-IF sedimentation, this remains a reasonable assumption. However, the facies evidence to support this concept is much weaker than popularly perceived, given the ubiquitous occurrence of ferrous silicates in "oxide facies" rocks, including those with high-energy textures.

The water which precipitated cherty ironstone must have been anoxic because virtually all cherty ironstone contains ferrous minerals which could not precipitate in the presence of any measurable dissolved oxygen. The ferrous silicates of the "oxide facies", e.g. greenalite, could only form in the virtual absence of dissolved oxygen (Floran and Papike, 1975). An extremely low oxidation potential is required for ferric hydroxide to be in equilibrium with either greenalite or siderite (Eugster and Chou, 1973).

All calculable oxidation potentials of precipitating fluids are much lower than Holland's (1984) estimated oxidation potential of the Early Proterozoic atmosphere, i.e., three to four orders of magnitude less than the present oxidation potential. The difference is so great that one must either conclude that iron formations formed during brief times of anoxic atmospheres or else that Dimroth (1976) underestimated water depth and they must all be subtidal (Simonson, 1985). Invoking a hydrothermal origin for MECS-IF, e.g., Simonson (1985), is not sufficient to evade this issue unless ironstone was protected from oxidation by an organic mat between incursions by iron-precipitating hydrothermal plumes. A bacterial mat probably continuously covered ferriferous

sediment below wave base but ferriferous sediment as shallow as that described by Dimroth (1976) must have been covered by an anoxic water mass. The anoxic water may have been covered by a lower-density mass of more oxidizing surface water.

The facies model of James (1954) implies that iron-precipitating oceans were chemically stratified. This concept is inherent to many genetic models, e.g., those which invoke upwelling of anoxic deep water, either suboxic seawater (Holland 1984) or methanic sulfur-depleted seawater (Drever, 1974). James (1954) and most other stratified-ocean modelers assume that the iron-precipitating oceans were progressively more anoxic with depth. However, the concept of progressive chemical reduction of seawater with depth is not essential to the genetic model advocated herein. In the following model, precipitation is attributed to chemical reaction along a horizontal interface between subsurface ferriferous water and surficial iron-poor water. Variation in precipitation along the interface would not be a simple function of water depth below the interface. Correlation of ironstone mineralogy with water-depth facies therefore carries genetic significance.

Without a good modern analog for Proterozoic MECS iron formations, it is difficult to interpret facies based on ironstone mineralogy and textures. Kimberley (1978a) proposed that the paleoenvironment of iron formations should be based on interpretations of the associated sedimentary rocks which are much better understood. Ojakangas (1983) and Larue (1981a,b) have demonstrated the viability of this approach for MECS-IF.

Putative barrier bars in Proterozoic basins

The facies model of James (1954) includes a barrier bar which separates an iron-precipitating basin from the open sea. Many subsequent interpretations of the hypothetical MECS-IF environment have included a similar restriction

to the open sea (e.g. Huber, 1959; Garrels, 1987; fig. 5 of Button, 1976). However, no facies evidence ever has been reported for a barrier near an iron formation. On the contrary, the extension of ironstone facies into deep-water turbidites is evidence against the existence of an adjacent barrier bar (Larue, 1981a,b). The theoretical justification for a barrier has been the presumed necessity of peculiar conditions to induce iron precipitation, whether the ferrous fluid has come from the landward side (Garrels, 1987) or the seaward side, e.g., the evaporative model of Button (1976). However, precipitation is not as serious a theoretical problem as is iron dissolution and transportation (Holland, 1984). Lack of a major barrier would not rule out evaporation as a precipitation mechanism in all cases because some MECS-IF environments may have resembled a Bahama-type platform where seawater slowly moves across the platform and evaporation enhances carbonate precipitation (Cloud, 1962).

The lack of evidence for a shore-parallel barrier does not prove that the MECS-IF sea was well mixed with world-average seawater. The Lake Superior and Sokoman areas may have been incipient rifts (Morey, 1983; Simonson, 1985) and the paleogeography therefore may have resembled the modern Red Sea. If so, there may have been a barrier at one end of an elongated sea rather than a shore-parallel barrier as illustrated by James (1954) and Button (1976).

Sedimentologic studies of the Nabberu (Australia), Sokoman (Quebec), and Lake Superior iron formations have shown them to be mostly shallow subtidal deposits in which coarse-grained, shallow-water ironstone typically contains various ferrous silicates, magnetite (a ferrous-ferric mineral), and/or hematite (Dimroth, 1976; Hall and Goode, 1978; Ojakangas, 1983). Associated intertidal and subaerially exposed sediment consisted of mature quartzose sand (Hall and Goode, 1978; Ojakangas, 1983; Simonson, 1984). Offshore sand bars composed of quartz or ferriferous ooids protected low-energy areas which were either landward or sea-

ward of the bars (Dimroth, 1976; Ojakangas, 1983). Siderite preferentially precipitated in these protected areas.

Limestone, ironstone, and biota on Proterozoic platforms

MECS iron formations resemble carbonate formations in their dimensions and chemical purity. Petrographic nomenclature developed for carbonate rocks is applicable to cherty ironstone with only minor modifications (Dimroth, 1968; Beukes, 1980, 1983). Some carbonate units grade upward into thick MECS-IF, e.g. the Kurnuman-Penge MECS-IF in South Africa (Button, 1976; Beukes, 1983). Textural facies across carbonate banks have direct analogs in iron-formation facies (Dimroth, 1977a). However, ironstone is not a diagenetic replacement of carbonate sediment (Kimberley, 1983). Iron and silica apparently precipitated onto the ancient seafloor to make ironstone which physically resembles limestone.

One of the similarities between Precambrian ironstone and limestone is the occurrence of stromatolites. Although stromatolites are more common in Precambrian carbonate rocks than in ironstone (Hofmann et al., 1985), the chert of ironstone has preserved the structure of Precambrian microfossils much better (Walter, 1983). Some of the best preserved microfossils in rocks of any age occur in the 2 Ga Gunflint MECS-IF in Ontario, Canada (Awramik and Barghoorn, 1977; Morey, 1983). Cell diameters generally range from 1 to 10 μm and the cells are either individual spheres or connected in long filaments (Hofmann and Schopf, 1983; Walter and Hofmann, 1983).

The wealth of microfossils in the Gunflint and other iron formations has been interpreted to indicate that biota have controlled the locations and age distribution of iron formations (e.g. Cloud, 1973, 1983; LaBerge, 1973). Microfossils in Precambrian cherty ironstone differ from those in contemporaneous iron-poor evaporites but resemble some modern micro-

biota (Knoll and Awramik, 1983). Diverse bacteria, including photosynthesizing cyanobacteria, apparently have populated the Earth since the Archean. These prokaryotes rapidly respond to changing environments but there is no evidence that their evolution has controlled environmental change. It is concluded that cherty ironstone has provided enhanced preservation of microbiota but that microbiota have not controlled the age distribution of iron formations. The chronology of iron-formation production (Table 2) is attributed to inorganic processes which have been ultimately controlled by mantle dynamics.

Although biota probably have not controlled the timing of ironstone sedimentation, they surely have responded to the introduction of ferriferous water and may have influenced both the precipitation rate and isotopic fractionation. Isotopic fractionation of carbon and oxygen of about 3 per mil has been reported by Baur et al. (1985) in successive mm-thick bands of the Hamersley iron formations. Light carbon correlates with light oxygen and with greater iron abundance. Baur et al. (1985) attribute the fractionation to biologic processes within an isotopically uniform water mass but it may represent variable precipitation (organic or inorganic) along an interface of isotopically distinct water masses. Isotopic analysis of mm-thick bands in other iron formations is eagerly awaited to clarify the fractionation processes. Phanerozoic cherty iron formations (Table 2) will be particularly informative because Phanerozoic biologic processes are better understood.

Late Precambrian cherty iron formations

The Proterozoic Era began and ended with peaks in the production of cherty iron formations on continental shelves (Table 2; James, 1983). Late Precambrian MECS-IF disproves the notion that Early Proterozoic MECS-IF represents a unique event in the evolution of our planet, the supposed increase in atmospheric

oxygen due to photosynthesis 2 Ga ago (Goldich, 1973). Late Precambrian cherty ironstone closely resembles Early Proterozoic ironstone but the associated clastic rocks differ. Unlike iron formations of any other age, Late Proterozoic cherty iron formations commonly are closely associated with mixtites of probable glaciogenic origin (Young, 1976; Yeo, 1984).

The association of mixtite with Late Precambrian iron formations is remarkable, especially since the cherty ironstone locally contains casts of evaporite minerals (Young, 1976). Mixtite-associated Late Precambrian MECS-IF occurs in northwestern Canada (Young, 1976), adjacent Alaska (Yeo, 1984), eastern California (Yeo, 1984), southwestern Brazil (Dorr, 1973b), Southwest Africa (Beukes, 1973), south-central Australia (Trendall, 1973b), and Togo (Trompette, 1981). Dropped clasts also characterize a volcanic-associated Late Precambrian cherty iron formation in eastern Egypt (Sims and James, 1984). Unlike dropped clasts in the MECS-IF examples, these clasts may be bombs but bombs are rare in volcanic-associated iron formations of other ages.

The intimate association of glaciogenic rocks with Late Precambrian cherty ironstone may indicate that the Late Precambrian atmosphere was not sufficiently rich in carbon dioxide to be an effective greenhouse. This apparent depletion of atmospheric carbon dioxide may reflect consumption of aqueous CO₂ during contemporaneous deep weathering. The Late Precambrian climate appears to have varied considerably, given the occurrence of pseudomorphs of evaporite minerals within the ironstone itself (Young, 1976). The association of cherty ironstone with glaciogenic rocks does favor a genetic role for exhalative processes, as opposed to the climatic genetic model of Cloud (1973), because exhalative processes could have been effective under any climatic conditions. Exhalation may have occurred during both the warm climate of the Early Proterozoic and the generally cold climate of the Late Proterozoic.

Like Early Proterozoic MECS-IF, Late Pre-

cambrian MECS-IF fails to exhibit the consistent europium enrichment of SVOP-IF. The voluminous Rapitan MECS-IF is markedly depleted in europium (Yeo, 1984, p. 147). Europium enrichment certainly is not a characteristic feature of all cherty iron formations, as implied by Pimentel-Klose and Jacobsen (1985). The Rapitan MECS-IF contains a slightly greater concentration of phosphorus than do typical Early Proterozoic iron formations, i.e., 0.2%–0.5% phosphate (Yeo, 1984, p. 143). However, this phosphate concentration is less than half of that in typical noncherty iron formations of Early Proterozoic or younger age (Table 2). Exceptionally phosphatic (2.5% phosphate) MECS-IF accumulated during the Early Proterozoic in Finland (Laajoki and Saikonen, 1977).

Proterozoic iron formations which cover volcanoes

Proterozoic iron formations which cover volcanoes are most notable for their scarcity (Table 2). This scarcity has been the main detraction from exhalative hypotheses for Proterozoic MECS-IF (James and Sims, 1973). However, the exhalative processes favored herein are not attributed to contemporaneous building of volcanoes and so a lack of Proterozoic volcanic-platform (SVOP) iron formations is not considered to negate all exhalative models. Shallow volcanic platforms generally are scarce in the rift-basin setting which is envisioned herein for MECS iron formations.

The tectonic style of the Proterozoic contrasts sharply with that of the Archean and the attendant contrast in iron formations surely reflects this global change (Tarling, 1978). Accretion of volcanoes to become continental blocks was much more common in the Late Archean (Schubert and Reymer, 1985). A higher proportion of volcanoes became accreted during the Early Paleozoic than during the Proterozoic and the preservation of SVOP-IF correspondingly improved with this enhanced

preservation of volcanic platforms (Kimberley, 1978a). The proposal of Gole and Klein (1981) to lump MECS-IF and SVOP-IF into a single category would impede the use of iron formations to help unravel the tectonomagmatic evolution of planet Earth.

Proterozoic glauconite

The literature on iron formations has been enlivened by dogmatic statements like the claim by Cloud (1955) that glauconite is restricted to the Phanerozoic and the claim by Baur et al. (1985) that banded cherty iron formations are restricted to the Precambrian. Both claims are patently false, although Baur et al. (1985) might justify their claim by invoking a definition of “banded iron formation” which differs from any published definition, i.e., one that specifies a minimum stratigraphic thickness greater than 65 m (Kalugin, 1973). There are no voluminous Mesozoic or Cenozoic cherty iron formations but there are several Paleozoic examples which are comparable to Proterozoic iron formations (Table 2).

There is little question about the definition of glauconite, *sensu stricto* (Van Houten and Purucker, 1984), and there is no question but that glauconite is scattered throughout the Proterozoic. Ubiquitous Early Proterozoic glauconite occurs in the 1100 m-thick Gordon Lake Formation of the Huronian Supergroup in the Elliot Lake uranium district of Canada (Chandler, 1986). This voluminous glauconitic formation accumulated prior to sedimentation of the equally voluminous cherty iron formations around Lake Superior, about 500 km west of Elliot Lake (Young, 1983). Glauconite also is abundant in the Early Proterozoic Frere and Windidda Formations of Western Australia (Hall and Goode, 1978). Thicknesses of the Frere and Windidda Formations are 1300 m and 350 m, respectively. Glauconite occurs as pellets in the Early Proterozoic of both Western Australia and the Elliot Lake area although no

pellet-forming metazoans had evolved in the Early Proterozoic.

Examples of Middle Proterozoic glauconitic sandstone are even more common than those of the Early Proterozoic, e.g. within the Belt Supergroup of Montana (Gulbransen et al., 1963) and in the Vindhyan basin of India (Singh, 1980). An example of Late Proterozoic glauconite was cited in the initial rebuttal of the claim of Precambrian nonexistence for glauconite (Schaub, 1955).

Despite the aforementioned examples of Proterozoic glauconite, it should be noted that glauconite probably formed less frequently during the Proterozoic than during the Phanerozoic, coincident with the contrast in abundances of phosphorite. Uncertainty about the original content of glauconite in the (typically metamorphosed) Precambrian rocks stems from its susceptibility to transformation to such minerals as stilpnomelane during low-temperature metamorphism (Frey, 1987). Although the most ubiquitous ironstone sedimentation during the Precambrian was nonaluminous, aluminous phases like glauconite and berthierine have predominated throughout the Phanerozoic.

Glauconite and other authigenic ferriferous silicates presently are forming on the seafloor in many areas (DeMiro, 1974; Odin, 1985; Bornhold and Giresse, 1985). Despite the relative ease of studying such an ongoing genetic process, there is not much more consensus about modern glauconite precipitation than about ancient ironstone precipitation. The similarities between Early Proterozoic and modern glauconitic sediments are interpreted to indicate similar genetic processes throughout at least the past 2.5 Ga, whatever those processes may have been.

Although glauconite has not yet been reported from the Archean, it probably will be found with more thorough study of the few weakly metamorphosed Archean rocks which accumulated in the preferred environment for modern glauconite precipitation, i.e., on the

seaward edge of a continental shelf and adjacent slope (Odin and Matter, 1981).

Proterozoic noncherty oolitic iron formations (SCOS-IF)

Noncherty iron formations, i.e. those with less than 5% chert, are exceedingly rare throughout the Precambrian (Table 2). However, the few Precambrian examples are sufficiently similar to the many Phanerozoic examples that metazoans evidently have not been necessary to produce the major features of noncherty iron formations. Precambrian iron formations include examples of typical oolitic noncherty deposits which accumulated in shallow island-dotted seas (SCOS-IF), e.g. the Early Proterozoic Timeball Hill (South Africa) iron formations which accumulated on an Early Proterozoic delta (Eriksson, 1973; Schweigart, 1965).

The general setting of the earliest known SCOS deposits is remarkably similar to the setting of a modern marine example on the Mahakam delta of Indonesia (Allen et al., 1979). Like the modern Mahakam delta, the Timeball Hill delta had several distributary channels, some of which periodically were abandoned. Winnowing during channel abandonment produced coarsening-upward sequences (Eriksson, 1973). Coarsening-upward sequences due to winnowing are a common characteristic of SCOS-IF throughout Earth history (Van Houten and Karasek, 1981; Maynard, 1983).

The texture, mineralogy, and chemical composition of the Timeball Hill SCOS iron formations are remarkably similar to typical Phanerozoic SCOS iron formations (Table 2). Most remarkable is the abundance of phosphate as in Phanerozoic SCOS-IF (Wagner, 1928). Although some of the phosphate content of Phanerozoic SCOS-IF is attributable to fossils of phosphatic metazoans (Hayes, 1915, p. 56), no metazoans had evolved to concentrate phosphorus in the Early Proterozoic. The thickness of the Timeball Hill SCOS-IF beds is similar to

Phanerozoic SCOS-IF, ranging from 1–8 m (Wagner, 1928).

Lower Proterozoic SCOS-IF occurs within the Turee Creek Formation of Western Australia (Button, 1975) and Middle Proterozoic (1.4 Ga) SCOS-IF occurs in northern Australia, i.e., the Constance Range and Roper River deposits (Trendall, 1973b; Edwards, 1958). Unlike contemporaneous cherty iron formations, these SCOS iron formations have consistently thin beds, generally less than 10 m of continuous chemical sediment. As in weakly metamorphosed Phanerozoic SCOS-IF, the 1.4 Ga ironstone in northern Australia consists of ooids which are composed of siderite, ferrous silicate, hematite, and magnetite within a slightly cherty matrix. Cochrane and Edwards (1960) note that the chert is a late-stage replacement of siderite. The ferrous silicate is a 0.7 nm (7 Å) clay which is intermediate in aluminum content between end-member berthierine and greenalite (Cochrane and Edwards, 1960). Mud cracks, ripple marks, cross-bedding, and associated conglomerate have been interpreted to record shallow sedimentation (Harms, 1965).

Phanerozoic iron formations

Phanerozoic cherty iron formations

Cherty iron formations certainly occur in Phanerozoic sequences despite ongoing claims to the contrary (e.g., Baur et al., 1985). A dozen Phanerozoic examples of MECS-IF and SVOP-IF are listed herein (Table 2) and in Kimberley (1978a), along with another half-dozen examples of deposits intermediate between MECS-IF and SCOS-IF. O'Rourke (1961) was one of the first to draw attention to cherty Phanerozoic iron formations but the Himalayan deposits which inspired his paper are really intermediate between MECS-IF and SCOS-IF (Phulchoki deposit in Table 2).

Unfortunately, some of the best examples of Phanerozoic cherty iron formations are not readily accessible. The 60 m-thick Cambrian

Maly Khingan MECS-IF occurs near Vladivostok, U.S.S.R. (Chebotarev, 1960; Egorov and Timofeieva, 1973). The 65 m-thick Devonian Altai SVOP-IF occurs near the northwestern border of Mongolia in the U.S.S.R. (Kalugin, 1973). Both of these contain moderately well banded cherty ironstone. The Altai SVOP-IF formed in shallow water, given the occurrence of mud cracks, halite casts, and gas-bubble cavities (Kalugin, 1973).

Massive-sulfide deposits are associated with an extensive Ordovician SVOP-IF in New Brunswick, Canada (Graf, 1977; Saif, 1983). The cherty ironstone is well banded and generally indistinguishable from that in magnetite-rich Archean iron formations. Anoxygenic ferriferous fluids apparently were able to flow extensively along this Ordovician seafloor. Cherty banded ironstone of probable Ordovician age also occurs in Chile (Oyarzun et al., 1986). The Chilean ironstone is more similar to Late Precambrian cherty ironstone than Middle Precambrian cherty ironstone in that it is moderately phosphatic (0.37% P). Beds up to 15 m thick are interbedded with schist (Oyarzun et al., 1986). Less well banded ironstone characterizes the Devonian Lahn-Dill SVOP iron formations in Germany (Bottke, 1965, 1966). This ironstone is hematitic and concretionary. Chemical sedimentation apparently occurred rapidly within oxygenated seawater.

The Mississippian Tynagh MECS-IF of Ireland accumulated on and near a carbonate bank (Schultz, 1966; Russell, 1975). The iron formation is associated with massive sulfides and has been attributed to exhalation along observed faults (Russell, 1975). Incipient banding was disrupted by burrowers. Banding is not much better preserved in the Triassic Vares MECS-IF of Yugoslavia (Latal, 1952). Like the hematitic Tynagh MECS-IF, the sideritic Vares iron formation is associated with limestone (Latal, 1952). Tynagh is the only MECS-IF for which the ancient plumbing system of metamorphic fluids has been deduced from the geographic distribution of isotopic ratios (Le-

Hurayet al., 1987). Exhalation of the Tynagh MECS-IF has been attributed to seismic pumping (Boastet al., 1981). The youngest known shallow-water cherty iron formation is the Jurassic Privas MECS-IF of southern France (Cayeux, 1922). Deep-water cherty iron formations have accumulated more recently, however, e.g. the Upper Upper Cretaceous Perapedhi DWAT-IF in Cyprus (Robertson, 1976). Modern accumulation of cherty ironstone is occurring in the hypersaline deeps of the Red Sea and elsewhere (Bäcker and Richter, 1973; Bäcker and Lange, 1987; Scott, 1987).

Coeval Phanerozoic ironstone and pelletal phosphorite

The Cambrian began with a global rise in sealevel which was accompanied by global sedimentation of glauconite and phosphorite (Vail and Mitchum, 1979; Brasier, 1980). Glauconite and phosphorite accumulated during the Early and Middle Cambrian in central southeastern Asia, Australia, Europe, and eastern Canada (Matthews and Cowie, 1979). Possible explanations for the combination of sealevel rise and ferriferous sedimentation range from processes as diverse as an enhanced exhalation of mantle carbon to an influx of carbonaceous comets. The rapid evolution of Cambrian metazoa is attributed herein to a rapid influx of nutrients by seismic pumping through new crust. The complexity of metazoan anatomy subsequently has not increased much relative to the rapid increase which occurred near the beginning of the Phanerozoic.

Glauconitic ironstone (SOPS-IF) commonly has accumulated at the same time as phosphorite and therefore occurs in correlative beds, if not actually interbedded with phosphorite (Odin and Letolle, 1980). Moreover, the textures of Phanerozoic phosphorite and glauconitic ironstone are similar, both being mostly pelletal. Oolitic noncherty ironstone (SCOS-IF)

is not quite as closely associated with phosphorite but the global trends of age-versus-abundance have been remarkably similar for SCOS-IF and phosphorite throughout the Phanerozoic (fig. 5 of Cook and McElhinny, 1979).

Unlike Precambrian ironstone and phosphorite, Phanerozoic ironstone and phosphorite predominantly have been granular (Cook and McElhinny, 1979). Ironstone mostly has been oolitic with subordinate pellets whereas phosphorite mostly has been pelletal with subordinate ooids. Oolite which is hybrid ironstone-phosphorite is rare (e.g. Harrison et al., 1983) but fine-grained hybrid ironstone-phosphorite formed abundantly in deep water during the late Early Cretaceous (Aptian-Albian) in northwestern Canada (Young and Robertson, 1984). About 30 trillion kg (30×10^{12} kg) of phosphatic ironstone in the upper kilometer of section averages 33% Fe_2O_3 , 14% P_2O_5 , and 5% MnO (Young and Robertson, 1984). The deposit overlies the former boundary fault of a flysch basin which accumulated 4 km of sediment in about 10 million years. Ferriferous fluids may have been introduced from this boundary fault rather than from some anoxic marine basin because the ferriferous fluids produced calcium-deficient minerals whereas anoxic seawater generally is not deficient in calcium.

Despite the Precambrian-to-Phanerozoic increase in the proportion of granular texture, neither oolitic ironstone nor phosphorite exhibits any obvious evolution through the Phanerozoic. Moreover, the few Precambrian deposits of granular ironstone or phosphorite are similar to the many Phanerozoic granular deposits. There have been some attempts to subdivide these Phanerozoic deposits, e.g., Clinton-type versus Minette-type ironstone but these subdivisions have become overemphasized to the point where they are as much of a hindrance as a help in understanding the history of iron-phosphorus sedimentation.

*Paleozoic noncherty oolitic iron formations
(SCOS-IF)*

Except for the Carboniferous through Triassic, the Phanerozoic record of noncherty oolitic iron formations is fairly continuous, starting in the Late Cambrian (Table 2). Early to Middle Cambrian granular iron sedimentation primarily was glauconitic (e.g., Berg-Madsen, 1983) but the Late Cambrian brought oolitic ironstone to northeastern China (Feng Zhiwen et al., 1984). A Late Cambrian to Early Ordovician transgression in New Mexico started with a few meters of conglomerate and sandstone before oolitic ironstone began to accumulate along with oolitic limestone (Kelly, 1951; Chafetz et al., 1986). Late Cambrian to Middle Ordovician coastal SCOS-IF in Wales became covered with carbonaceous mud, as did the majority of subsequent Phanerozoic iron formations worldwide (Hallimond, 1925, 1951; Pulfrey, 1933; Petranek et al., 1988).

During the Early Ordovician in eastern Newfoundland, several beds of oolitic ironstone accumulated with shallow-water sediment which locally exhibits rain-drop imprints (Hayes, 1915, 1929). Eastern Newfoundland may have been much closer at this time to northwestern France where Early Ordovician SCOS-IF is interbedded with metamorphosed trilobite-bearing shale (Cayeux, 1909; Hoenes and Troger, 1945). In Czechoslovakia, Early Ordovician SCOS-IF is enclosed within tuffaceous shale in a transgressive sequence onto Precambrian basement (Berg et al., 1942 a,b; Skocek, 1963 a,b; Petranek, 1964).

Ordovician-Silurian SCOS-IF in the eastern U.S.A. accumulated in epeiric seas between rising coastal mountains and interior lowlands. SCOS-IF sedimentation started during the late Late Ordovician in northwestern Georgia (Chowns and McKinney, 1980) and during the late Late Ordovician in southeastern Wisconsin (Hawley and Beavan, 1934). One of the thickest Appalachian iron formations (33 m) accumulated during the Early Silurian in Ala-

bama (Bearce, 1973). Most Appalachian deposits are less than 3 m thick. The Appalachian SCOS iron formations collectively are often named after the early Middle Silurian (Clintonian) deposits in upstate New York (Alling, 1947; Schoen, 1962; Hunter, 1970). Appalachian SCOS-IF sedimentation continued into the Early Devonian in Nova Scotia where metamorphism has produced magnetite (Wright, 1975, p. 77). All of these Appalachian deposits accumulated in shallow water, some in intertidal environments (Maynard, 1983).

Devonian SCOS-IF is found scattered around the globe. A 2 m thick bed in Arizona grades laterally to hematite-cemented sandstone and hematite-nodule-rich limestone (Willden, 1960, 1961). In Yugoslavia, metamorphosed chamosite-siderite oolite occurs in a series of beds, each 1–20 m thick, interbedded with black phyllite (Latal, 1952; Page, 1958). In central China, Devonian hematitic SCOS-IF occurs in beds up to 3 m thick (Ikonnikov, 1975). Devonian SCOS-IF in Belgium has been interpreted to be diagenetically replaced calcareous oolite (Dreesen, 1982) but it is unlikely that this or any other SCOS-IF has formed by replacement, despite previous support for such a hypothesis (Kimmerley, 1974, 1979a). Cogent arguments against a replacement origin have been made by Maynard (1986) and Gygi (1981) among others.

The area with the most continuous record of Paleozoic SCOS-IF sedimentation is western Libya. Ferriferous ooids formed during the Early, Middle, and Late Ordovician, during the Early and Late Silurian, during the Early, Middle, and Late Devonian, and during the earliest Carboniferous (Chauvel and Massa, 1981). During the Late Devonian, SCOS-IF repeatedly accumulated within a deltaic sequence which Van Houten and Karasek (1981) have compared to the modern SCOS-IF-bearing Mahakam delta of Indonesia.

Subsequent to the earliest Carboniferous in Libya, the Carboniferous through Triassic was a time of minimal SCOS-IF sedimentation worldwide (Table 2). Only one Late Permian

deposit in northern Australia is known to be a significant exception. This 9 m-thick deposit is typical compositionally and texturally, however, including the angularity of its quartz grains (Edwards, 1958). A minor Early Triassic exception occurs in northern Italy where a little barite-rich sideritic oolite has been found (Frizzo and Baccelle, 1983). The Carboniferous through Triassic time span coincided with a prolonged lowstand of sealevel (Van Houten and Bhattacharyya, 1982).

Mesozoic-Cenozoic noncherty oolitic iron formations (SCOS-IF)

The Jurassic was the heyday of SCOS-IF sedimentation, particularly in Europe (Table 2). McGhee and Bayer (1985) have shown that ferriferous ooids accumulated extensively at times when sealevel was either rising or falling at a high rate, as determined from the seismic interpretation of Vail et al. (1984). Sealevel rose and fell cyclically through the Jurassic of Europe with a periodicity of 4–6 Ma (McGhee and Bayer, 1985). The combined sealevel-ironstone periodicity is attributed herein to tectonic activity (Hubbard, 1988) rather than the global effects envisioned by Vail et al. (1984).

SCOS-IF sedimentation in the early Early Jurassic heralded the end of the Triassic in Germany, France, and Iraq (Table 2). The iron formations in Germany and Iraq are interbedded with shale through thicknesses up to 19 m (Simon, 1969; Skocek et al., 1971) whereas the meter-thick French deposit is associated with ferruginous limestone (Cayeux, 1922, p. 36). An apparent indifference to clastic versus carbonate associations became characteristic of the subsequent plethora of Jurassic deposits (Kimberley, 1981b, p. 30).

SCOS-IF sedimentation continued into the Early Cretaceous in Europe (Table 2) and also appeared on the western side of the spreading Atlantic, in the Baltimore Canyon area (Cunliffe, 1982). SCOS-IF apparently has not accumulated around the Atlantic margin since the

Early Cretaceous but glauconitic ironstone started to accumulate along this margin in the Late Cretaceous (Table 2) and continues to form today in many localities on the continental slope or at its base.

In the Middle East, Jurassic SCOS-IF was followed by Early Cretaceous SCOS-IF, both in Israel (Rohrlich et al., 1980) and in Syria (El Sharkawi et al., 1976). The locus of maximum SCOS-IF sedimentation moved southward to Egypt in the Late Cretaceous (Bhattacharyya, 1980) and to Saudi Arabia in the Oligocene (Al-Shanti, 1966). The Late Cretaceous also produced ironstone far from the Tethyan belt, e.g. the Niger delta (Adeleye, 1973) and northern Alberta (Petruk, 1977).

Tertiary SCOS-IF has preferentially formed in Arabia, the southern U.S.S.R., and northwestern South America. Eocene to Miocene SCOS-IF is scattered along the eastern cordillera of the northern Andes (James and Van Houten, 1979; Kimberley, 1980). Oligocene to Pliocene SCOS-IF is scattered from the northern shore of the Black Sea to the Aral Sea (Zitzmann, 1977). The modern marine equivalent of ironstone occurs far from all these areas, i.e. on the Mahakam delta of Indonesia (Allen et al., 1979) and near Cabo Mala Pascua, Venezuela, as described in the following section.

Modern ferriferous seawater and sediments

Glauconite off the southeastern U.S.A.

The modern equivalent of SOPS-IF (glauconitic ironstone) occurs under 260 m of water on the northern Blake Plateau off the southeastern United States. Some of the samples provided by D.J. Mallinson from 33° 8' 58" N and 77° 17' 32" W to 33° 6' 9" N and 77° 16' 4" W contain over 75% glauconite. Glauconitic sediment extends eastward over the Blake Plateau from the toe of the continental slope which bounds the plateau on the west. The author has collected somewhat less concentrated glaucon-

ite at various localities along the continental slope of North Carolina. Most of this glauconite is attributed herein to ongoing slow exhalation from great depth. In the case of the Blake Plateau, ferriferous fluids are believed to be rising slowly along the slope-plateau boundary fault.

Ferriferous hypersaline seawater in the Orca Basin

A major milestone along the path to understanding marine dissolution of iron and manganese was the discovery of a ferriferous saline water body, the Orca Basin, below 2000 m of normal seawater under the northern Gulf of Mexico (Shokes et al., 1977). Water in the Orca Basin contains up to 20 ppm (3.6 mM) Mn²⁺ just below the oxic-anoxic interface and an average of 1.6 ppm (0.29 mM) Fe²⁺ and 4500 ppm (47 mM) SO₄²⁻ throughout the anoxic region (Trefry et al., 1984; Sheu et al., 1988). The Orca Basin is a suboxic sulfate-rich water body which owes its hypersalinity to erosion of an exposed salt diapir rather than exhalation (Addy and Behrens, 1980; Sackett et al., 1979). Aqueous iron and manganese are abundant because bacteria are failing to reduce much of the available sulfate despite ambient anoxia and settling organic matter. Bacteria apparently prefer to reduce ferric hydroxide which coats settling clay minerals (Lovley, 1987).

Inhibition of sulfate reduction is attributable to both hypersalinity and to an influx of clays coated with ferric hydroxide. Hypersalinity apparently is retarding sulfate-reducing bacteria. Inorganic reduction of sulfate is too slow to be relevant at temperatures less than about 200°C (Ohmoto and Lasaga, 1982). Thermodynamic calculations and experiments both indicate that bacteria prefer ferric hydroxide to sulfate (SO₄²⁻) as an electron donor for oxidation of organic matter (Lovley, 1987).

The Orca Basin has been presented as a modern analog of iron formations (Sheu and Presley, 1986a; Rossignol-Strick, 1987a,b). The

Orca Basin is not presently making an iron formation but iron and manganese are becoming somewhat concentrated in sediments which cover a mid-basin high. This saddle-shaped high is covered with carbonaceous mud which contains about 7% Fe, mostly as laminae of hematite (Sheu and Presley, 1986a). A much higher ratio of chemical/terrigenous sedimentation would be required to produce an iron formation. Some increase would result if the oxic-anoxic interface were shallower and spread across a sediment-starved continental shelf where the chemical precipitates could accumulate.

Chemical precipitation along the Orca oxic-anoxic interface probably is aided by bacterial activity because the water 100 m above the interface contains eight times as much adenosine 5'-triphosphate as does water at a comparable depth away from the Orca Basin (LaRock et al., 1979). A similar increase characterizes the oxic-anoxic interface of the Cariaco Basin (Karl et al., 1977). Bacterial activity also is high near the bottom of the Orca Basin where laminated, organic-rich pyritic mud is accumulating (LaRock et al., 1979; Sheu and Presley, 1986b).

Despite its limitations, the Orca Basin is considered to be the best modern analog for the hypothetical ferriferous water bodies which have precipitated shallow-water cherty iron formations. Bacteria above the oxic-anoxic interface probably resemble Precambrian microbial communities which precipitated particulates that settled to become cherty ironstone. Moreover, the Orca Basin clearly indicates that removal of sulfur from seawater is not a necessary prerequisite for a high concentration of aqueous iron (cf., Drever, 1974; Walker and Brimblecombe, 1985). It is considered unlikely, however, that a voluminous iron formation could precipitate from a basin which owes its hypersalinity to erosion of a diapir. Exhalative input of hypersaline fluids is considered to be essential.

Deep hypersaline basins which resemble the Orca Basin have been found in the eastern Mediterranean but none of these have yet been

reported to be ferriferous (Jongsma et al., 1983; Erba et al., 1987). Sulfate-rich ferriferous water occurs elsewhere under just a few centimeters (where algal covered) to meters in Venezuelan hypersaline pools on Margarita island (pers. observation) and Gran Roque island (Sonnenfeld et al., 1977).

Weathering source for Fe-Mn concentrations in the Baltic Sea

Although all iron formations are attributed herein to deep weathering, shallow weathering is the apparent source of widespread Fe-Mn crusts and nodules on the floor of the Baltic Sea. The northernmost Baltic Sea (Gulf of Bothnia) exhibits iron solubility under a simulated oxygen-poor atmosphere. The simulation occurs because of organic input during spring floods and ice cover during the winter (Ingri and Ponter, 1986). Diffusion of iron and manganese upward to the sediment-water interface results in Fe-rich crusts in the more reducing deep-water sediments and Mn-rich nodules in the less reducing shallow-water seafloor (Ingri and Ponter, 1986). Spherical nodules exhibit alternating Fe-Mn layers which apparently record seasonal changes in the ambient oxidation state (Winterhalter, 1966; Winterhalter and Siivola, 1967). Fe-rich crusts on the deeper-water seafloor (60–180 m) more closely resemble cherty ironstone morphologically and chemically, given a paucity of rare-earth elements (Ingri and Ponter, 1987).

In the southern Baltic, the Bornholm deep is a suboxic water body which lacks both O₂ and H₂S (Boesen and Postma, 1988). As in the northern Baltic, low salinity inhibits the diffusive supply of sulfate into sediment. However, sulfate reduction is rapid in the presence of abundant organic matter and large amounts of metastable iron monosulfides are accumulating (Boesen and Postma, 1988). Conversion of these to pyrite is requiring more than 500 years. A similarly slow conversion of monosulfides to

pyrite may have characterized black shale associated with some iron formations.

Quaternary ferriferous and cherty oolite on Andros Island, Bahamas

One of the most remarkable occurrences of Quaternary ferriferous sediment occurs on the northern end of Andros Island, one of the Bahaman islands. At the town of Red Bay and other localities, calcitic oolite contains about 15% SiO₂ and a few percent of iron (Kimberley, 1979a). The rock is more remarkable for its texture than its composition because it resembles oolitic banded cherty ironstone from Middle Precambrian iron formations like the Sokoman and Gunflint (Table 2). For reasons unknown, the iron on Andros is neatly segregated into centimeter-thick bands (laminae) just as in typical shallow-water cherty ironstone.

Modern ferriferous sediments in Venezuela

The emphasis on modern iron-concentrating processes in this paper is partly based on field observations by the author along the north-eastern coast of Venezuela (Figs. 19, 20). The modern equivalent of berthierine ironstone occurs here near Cabo Mala Pascua (Kimberley, 1988) and glauconitic grains constitute over 5% of the surficial shelf sediment in several areas which total a few thousand square kilometers (Fig. 21). Phosphatic grains locally are concentrated with the glauconitic grains (De Miro, 1974). The glauconitic grains display all the typical features of ancient glauconite, e.g., green to black color, nonlaminated but cracked grains, infilling of foraminiferal tests, partial replacement of carbonate grains, etc. The grains display variable crystallinity, as determined by X-ray diffraction, and so the term, "glauconitic grain", is used in the broad sense of Van Houten and Purucker (1984).

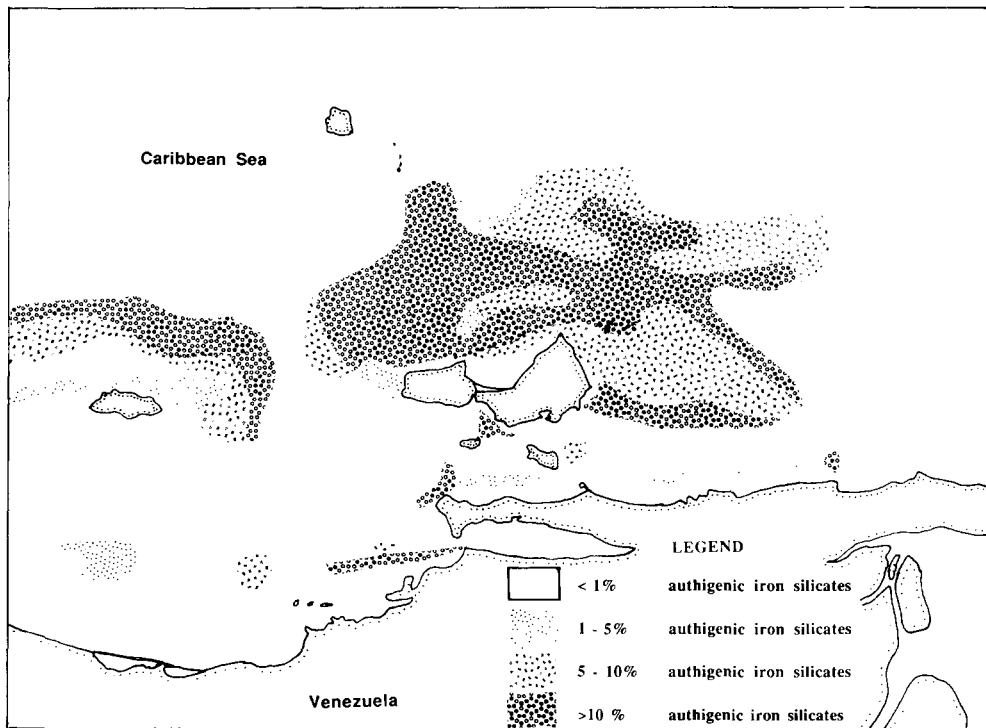


Fig. 21. Distribution of authigenic iron silicates in the fine sand fraction, modified after De Miro (1974, p. 151). Fine sand is 1-4 phi (i.e. 0.5-0.063 mm) in diameter. The authigenic iron silicates may be termed "glauconitic grains" following Van Houten and Purucker (1984) although berthierine predominates over glauconite locally. Clastic and carbonate grains of various types are partially replaced by authigenic iron silicates. Based upon a reexamination of the samples which were visually studied by De Miro (1974), the illustrated percentages include such partially glauconitic grains. The weight percent of authigenic silica in each sample is not known.

Relationship of red tides to sedimentary exhalation in Venezuela

Northeastern Venezuela is the only portion of the Caribbean which routinely experiences red tides, i.e., toxic dinoflagellate blooms (Ferraz-Reyes et al., 1985). The triggering mechanisms for these blooms are unknown and probably diverse. A plausible candidate for the nutrients which feed some of these blooms is exhalation of pore fluids driven by seismic pumping. However, red tides have not accompanied recently observed exhalations on northeastern Margarita and western Coche (Fig. 20). Immediately after an exhalation event occurred at El Bichar on Coche Island, the residents ate large quantities of exhalation-killed fish without ill effect.

Although little is known about the composi-

tion of exhaling fluids in northeastern Venezuela, it is reasonable to expect compositional variation. Some exhalations appear to be dominated by natural gas and are devoid of any metalliferous fluid. The fluids themselves probably vary compositionally. The ratio of iron/phosphorus in authigenic components of the seafloor sediment varies greatly among different portions of the platform around Margarita Island (De Miro, 1974). One may postulate that phosphate-rich exhalations induce red tides whereas phosphate-poor exhalations do not.

Several authors have suggested that red tides generally have characterized the deposition of ancient phosphorite (e.g., Brasier, 1980). Phosphatic exhalations remain an attractive explanation for the red tides in northeastern Venezuela because of the extremely high phosphorus concentrations within the dinoflagel-

late-rich waters of red tides. The dinoflagellate blooms commonly consist of over a million individuals per liter and thus have extremely high total phosphorus concentrations (Steidinger and Baden, 1984). Waning phosphate supply may be the trigger for dinoflagellates to encyst into the seabed (Anderson et al., 1985).

Red tides in northeastern Venezuela are most apparent in the shallow Gulf of Cariaco, southeast of the Cariaco Basin (Fig. 20). However, the entire Margarita-Cumana-Carupano region is characterized by occasional human deaths from eating toxin-laden seafood (Ferraz-Reyes et al., 1979; Reyes-Vasquez et al., 1979). Red tides are particularly common at the eastern end of the Gulf of Cariaco where strong earthquakes and warm springs are prevalent. Red tides occasionally are generated within Laguna Grande del Obispo, the largest lagoon off the Gulf of Cariaco (Fig. 20; Ferraz-Reyes et al., 1979). Sampling of Laguna Grande del Obispo by the author has not yet revealed any phosphatic sedimentation, however, possibly because the high relief in this tectonically active area is overwhelming the lagoon with clastic sediment. Ongoing deformation is remarkably intense around the Gulf of Cariaco. Quaternary sediments west of Laguna Grande del Obispo locally dip at more than 45°. The periodicity of major earthquakes near Laguna Grande del Obispo has averaged about 40 years since records began in 1500 (Fiedler, 1961, 1972; Lagnell, 1987).

Glauconitic sedimentation in Venezuela beyond the Margarita-Cumana area

The author has conducted limited sampling beyond the Margarita-Cumana-Carupano area but has been provided with over 800 samples which were collected on a roughly 8 km-grid spacing over most of the continental shelf of Venezuela. These gravity-corer samples have been provided by Fundacion La Salle de Ciencias Naturales and were previously examined by De Miro (1974). Glauconitic concentrations

identified in these shallow-water samples are remarkable since modern glauconite elsewhere is rare in water shallower than 50 m (Odin, 1985; Odin and Matter, 1981). The typical range for modern glauconite elsewhere is 50 to 500 m (Odin and Matter, 1981). However, a water depth of a few meters to tens of meters is closer to that interpreted from sedimentary structures in most Phanerozoic ironstone (e.g., Kimberley, 1978a, 1980, 1983).

The shallow-water glauconitic grains off northeastern Venezuela originally were interpreted to be relict (Maloney, 1971 a,b) but subsequently have been demonstrated to be modern because they cement living mollusks (De Miro, 1974). Additional evidence for modern precipitation is that tiny glauconitic grains near Caimancito are concentrated within the sheaths of recently produced fecal pellets and, within the Mangle-Piedras subbasin, glauconitic grains partially replace the shells of recently deceased mollusks (Fig. 20). Moreover, no potential glauconite supply is known from old eroding sediments.

The La Salle samples indicate that glauconitic sedimentation is a widespread phenomenon in northeastern Venezuela (De Miro, 1974). Several areas peripheral to the Margarita-Cumana platform have glauconitic concentrations which are considerably richer than those between Margarita and Cumana. One of these lies about 50 km northwest of Margarita, half way to the island of Blanquilla (Fig. 19). Glauconitic grains in the Margarita-Blanquilla area are accumulating over an area of several hundred square kilometers and in water depths which range from 50 to 2000 m. The great areal and vertical range here is comparable to that described by Bornhold and Giresse (1985) for glauconitic sediment west of Vancouver Island, Canada.

About 50 km west of Margarita Island, De Miro (1974) found that glauconitic grains are concentrated along the continental shelf which separates the Cariaco Basin from the Venezuelan Basin (Fig. 19). About 850 km west of Mar-

garita Island, glauconitic grains are plentiful in samples within and north of the Gulf of Maracaibo. Maracaibo samples contain particularly spherical and lustrous glauconitic grains. Maracaibo grains also exhibit the deep cracks which characterize many ancient glauconite grains (Triplehorn, 1966; Boyer et al., 1977). These cracks may be due to syneresis as the grain responds to the difference between the initially ferriferous chemical environment and the subsequent iron-poor seawater environment.

Glauconitic grains on the shelf east of Margarita Island locally are intermixed with pyrite as in some ancient greensands, e.g. the Cretaceous of Alberta (Ireland et al., 1983). Large pyritic concretions constitute several percent of the sediment in a few localities and may record iron exhalation into a sulfidic environment. One such locality occurs under 57 m of water near Carupano (Fig. 19), at 10°50'N and 63°10'W.

A concentration of glauconitic grains (up to 20% of the sediment) occurs about 150 km east of Carupano, a few kilometers north of the straits between the Paria Peninsula and Trinidad. These straits are called Boca del Dragon (Fig. 22). Unlike all of the aforementioned localities, this site is influenced by fluvial processes. The other areas are too arid to support large rivers (Kimberley et al., in press) but Boca del Dragon is strongly influenced by the Orinoco and San Juan rivers which supply abundant iron-rich sediment to the Gulf of Paria, which lies immediately south of the glauconitic area (Fig. 22). Satellite imagery of chlorophyll-a abundance shows an almost continuous northward flow of nutrient-rich water through the Boca del Dragon straits (Muller-Karger and McClain, 1987). These nutrients come from the Gulf of Paria (Fig. 22) which is a large estuary with an average salinity about half that of normal seawater during the rainy season (Fukouka, 1964). As in the Margarita–Blanquilla area, the water depths of glauconitic sediments in the Boca del Dragon area are greater than in most other areas of northeastern Venezuela, here about 150 m.

Cedros–Soldado bank in the southern Gulf of Paria

The fresh water in the Gulf of Paria comes from the Orinoco and San Juan rivers which also supply the estuary with abundant pedogenic goethite and kaolinite from plinthitic soils. The iron concentration below the surficial 50 cm of these soils typically is 2–5% Fe (Daugherty and Arnold, 1982). Several genetic models for Phanerozoic ironstone (Kimberley, 1979a) would predict that a sediment-starved bank within the Gulf of Paria would be an ideal location for iron concentration. Such an iron-rich platform indeed exists at 10°8'N and 61°57'W, under 7–15 m of water. This platform occurs on the Trinidadian side of the gulf near Cedros Point, across from one of the distributary mouths of the Orinoco. The Cedros–Soldado platform lies just north of a narrow (15 km) and shallow (mostly less than 4 m) channel through which an Orinoco plume enters the Gulf of Paria (Fig. 22).

The author found the water over the Cedros–Soldado platform to be less turbid and moving slower than that in the adjacent channel. The combination of greater transparency and slower currents may be enhancing organic productivity. The greater light penetration may enhance diatom growth and the slower currents may permit accumulation of low-density organic matter. Alternatively, the platform may be the site of carbonaceous exhalation comparable to that which continually feeds nearby Pitch Lake (Fig. 22). One of these two mechanisms has produced a cm-thick layer of jet black carbonaceous matter over the platform. This layer is underlain by ferriferous sediment which is pervasively tinted light olive (Munsell color 10 Y 5/4), probably because of phaeopigments (chlorophyll degradation products).

Glauconitic grains constitute a few percent of the light olive sediment on the Cedros–Soldado platform and so the iron content typically is 4–5% Fe instead of the 2–3% Fe which characterizes glauconite-poor sediment of the Gulf

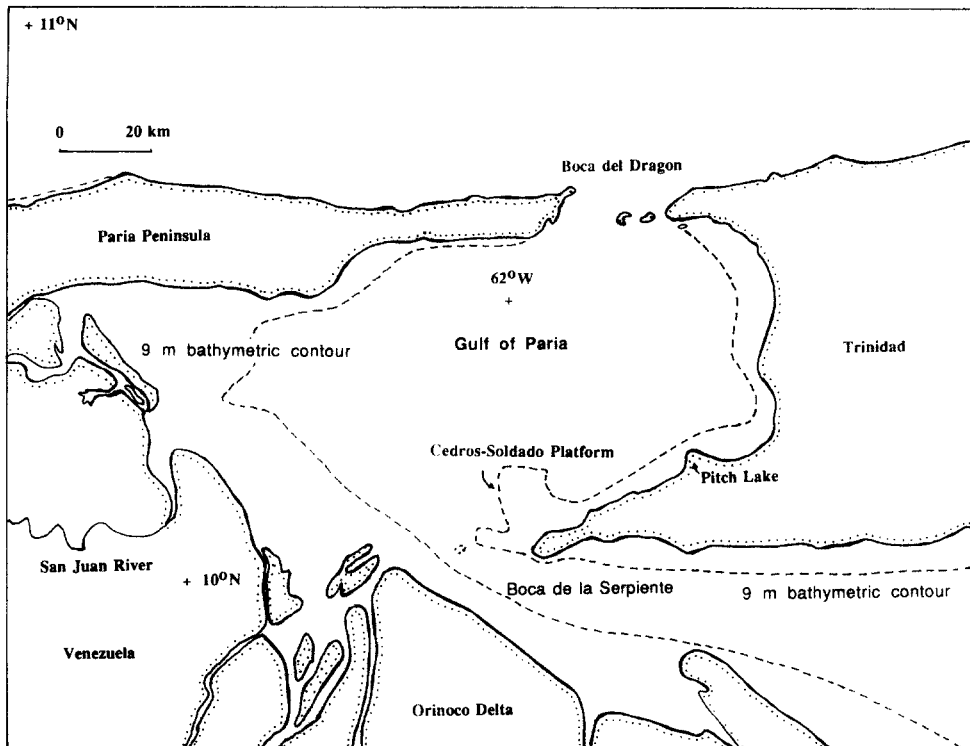


Fig. 22. Location map for the Gulf of Paria, illustrating the Cedros-Soldado platform. The 9 m bathymetric contour lies so close to shore along most of the northern coast of Trinidad and the Paria Peninsula that it cannot be shown.

of Paria (Hirst, 1962). Hirst (1962) found that iron-rich fractions of the Cedros-Soldado sediment are enriched in phosphorus by factors of 5 to 10. Glauconitic grains on the Cedros-Soldado bank apparently are forming *in situ* because the author did not find glauconitic grains in either the Orinoco sediment upstream from the bank or in the outcrops exposed on adjacent Trinidad. Outcrops at Cedros Point in southwestern Trinidad mostly are white siltstone devoid of iron-rich minerals.

The possibility of an exhalative source for the Cedros-Soldado glauconitic grains is significant despite the obvious supply of fluvial iron because exhalative diapirism characterizes the eastward extension of the underlying Los Bajos fault. Mud diapirism has characterized this fault for over a million years (Michelson, 1976). This is the western hemisphere's premier area for modern pyrite-bearing mud diapirs (Higgins and Saunders, 1967; Kerr et al., 1970). The au-

thor has observed minor pyritic mineralization around nearby Pitch Lake (Trinidad) where asphalt continually is rising to the edge of the Gulf of Paria and debouching in commercial quantities. A similarly slow and continuous rise of ferriferous fluids may be producing the observed glauconitic grains.

Aforementioned samples collected north of the northern outlet of the Gulf of Paria (Boca del Dragon) are even more glauconitic than those in the southern Gulf of Paria but this northern area lacks any immediate fluvial source and the glauconite more clearly is related to exhalation along the underlying transform fault. Water depths are an order of magnitude greater in the northern locality, 150 m versus 15 m.

If iron is being supplied by exhalation, it would be accompanied by other solutes, e.g. H_4SiO_4 . Any exhalative silica would become mixed with dissolved silica that is supplied by

the Orinoco and Amazon rivers (De Master et al., 1983). As in the case of iron, the relative importance of exhalative versus fluvial silica is unknown. Silica precipitation by diatoms is widespread in this area. The author has found that biogenic silica (diatoms) typically constitute 1–2% of the fine-grained sediments of northeastern Venezuela, with some concentrations reaching 10% SiO₂.

The hypothetical deep source for iron–phosphorus exhalation on the Venezuelan shelf is envisioned to be seismic pumping through the continental margin which lies between the westward-moving South American plate and the stationary to eastward-moving Caribbean plate. Seismic pumping is enhanced by dispersal of this transform fault zone across a shelf width on the order of 100 km (Kimberley and Llano, in press). This width is comparable to that of other major transforms (Sylvester, 1988) but several previous workers have attributed displacement in northeastern Venezuela to just the southernmost of the subparallel faults, i.e. the El Pilar (e.g., Vierbuchen, 1984).

The observed phosphate–silica–glauconite association on the Venezuelan shelf clearly is analogous to the phosphorite–chert–greensand association which repeatedly has formed globally since the Early Proterozoic, preferentially at low latitudes (Cook and McElhinny, 1979). The preference for low latitudes is consistent with Tethys–Caribbean seismic pumping.

Coche–Margarita Area

The Coche–Araya subbasin is bounded by Coche Island, Cubagua Island, and the Araya Peninsula (Fig. 20). Glauconitic grains presently are accumulating here at moderate concentrations (commonly about 5%) within sediment which contains 2–10% biogenic silica (diatoms) and up to 1% phosphate. A greater concentration of glauconitic grains (about 10%) but lesser concentration of biogenic silica (<2%) occurs in the middle of the Mangle–Piedras subbasin which lies immediately

northwest of the Coche–Cubagua subbasin (Fig. 20), 20 km northwest of Coche Island between two capes on Margarita Island, i.e. Punta Mangle and Punta de Piedras. Both the host sediment and glauconitic grains in the Mangle–Piedras subbasin differ greatly from those in the Coche–Araya subbasin. In the Mangle–Piedras subbasin, sand-sized glauconitic grains are mixed with quartzose and calcareous sand grains whereas, in the Coche–Araya subbasin, fecal pellets of silt and clay predominate. Glauconitic grains commonly fill foraminiferal tests or occur as separate sand-sized grains in the Mangle–Piedras subbasin. In the Coche–Araya subbasin, glauconitic grains typically occur as fine silt concentrated within the organic sheath of each fecal pellet. These glauconitic grains clearly are modern because they rapidly oxidize upon decay of the organic sheath.

Although texturally quite different, the Coche–Araya and Mangle–Piedras subbasins share two features which typify ancient SOPS iron formations, for which they are lean modern analogs. Both subbasins are shallow, with water depths less than 15 m, and both closely overlie an unconformity. If preserved in the ancient record, most of the Coche–Araya sediment would become a highly siliceous mudrock which could be interpreted incorrectly to have accumulated in water much deeper than 15 m.

Both the Coche–Araya and Mangle–Piedras subbasins resemble other Phanerozoic iron-concentrating basins in that they have a highly reduced thickness of Neogene sediment relative to adjacent portions of the same regional basin. The thickness of Plio–Pleistocene strata in both subbasins amounts to a few tens of meters at most but sediment thickness progressively increases seaward to reach several hundred meters within 20 km in both cases. In the case of Coche, Neogene strata dramatically increase to several kilometers of thickness within 50 km toward both the east and the west of the Cretaceous metamorphic rocks which are exposed on the island (Case and Holcombe, 1980). At the edge of both subbasins, there are

places where Quaternary sediments directly overlie Cretaceous metamorphic rocks and other places where they overlie deformed marine Tertiary sedimentary rocks.

Iron-oxide concentrations are widespread on Coche Island within shallowly buried sediment. Surficial concentrations of iron oxides occur locally along the northwestern and southwestern edges of the Margarita-Cumana platform where they lie in stark contrast against the surrounding regolith. The most spectacular concentration of iron oxides occurs along the western coast of the Araya peninsula, about 6 km south of the town of Araya (Fig. 20). A few hectares of bright red surficial sediment contrast sharply with the pale yellow regolith which characterizes the remainder of this arid coastline. Glauconitic grains are concentrated over several square kilometers of seafloor about 10 km north of this red sediment, near the northwestern corner of the Araya Peninsula. A smaller volume of ferruginous regolith occurs on Margarita island, northwest of the Araya Peninsula, where it rims the southern and eastern sides of the Boca Chica hypersaline pool (Kimberley et al., in press).

The ferruginous deposits at Boca Chica and the Araya coast respectively lie near the northeastern and southeastern corners of the Cariaco Basin. The deposits are separated by a distance of 50 km but have similar geologic settings. Both deposits overlie a narrow coastal sequence of Neogene sedimentary rocks which extends between the Cariaco Basin and an interior block of Cretaceous metamorphic rocks. The Neogene stratigraphy is similar in both sequences (Graf, 1972; Vignali, 1972). In both cases, the local deposits of ferruginous regolith are tentatively attributed to exhalation, pending ongoing study.

Glauconite composition and precipitation

Introduction

Although glauconitic ironstone constitutes less than 1% of all ancient ironstone, it consti-

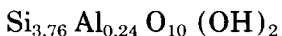
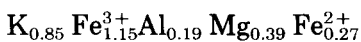
tutes a high proportion of modern marine authigenic iron mineralization and therefore deserves some attention. Study of high concentrations of modern glauconite may elucidate processes of ferriferous fluid generation deep in the Earth. Some Tertiary-Quaternary processes may resemble those of the Early to Middle Cambrian when glauconite sedimentation was particularly widespread.

Modern glauconitic precipitation occurs in several parts of the world (Odin, 1985). Marine clay-mineral precipitation is not as substantial as was previously thought (Holland et al., 1986) and so glauconitic grains are among the most voluminous aluminosilicate precipitates within shallowly buried marine sediment. One of the prime areas of modern glauconite occurs off Vancouver Island, Canada (Bornhold and Giresse, 1985). Mud diapirs are abundant in this area (Tiffin et al., 1972) and the tectonic processes which drive these mud diapirs probably also induce exhalation of the ferriferous fluids which are interpreted herein to be precipitating glauconitic grains. Exhalation of ferriferous fluids in nearby deeper water is producing polymetallic massive sulfide deposits (Scott, 1987).

Mineralogy and composition of glauconite

It has become common practice to apply the name, "glauconitic", to any authigenic, non-oolitic, green ferriferous grain within marine sediment (Van Houten and Purucker, 1984). The crystal structure of these green grains in ancient rocks is less variable than it is in modern sediment (Odin, 1985). However, the chemical composition is quite variable in both ancient and modern grains (Miki and Fukuoka, 1983), particularly as regards the ratio of ferric iron to aluminum and the ratio of ferrous iron to magnesium (Buckley et al., 1978). Buckley et al. (1978) report complete analyses for 22 grains from a variety of ancient rocks and modern sediment. An average of these anal-

yses, presented below, is used within chemical reactions in this paper.



It should be noted that all 22 samples of glauconite analyzed by Buckley et al. (1978) contain substantial ferrous iron; the average ferric/ferrous ratio in the analyzed samples is 4.3. In modern glauconitic sediment of Venezuela, reducing conditions commonly prevail because of decaying organic matter. However, occasional suspension of this sediment may cause partial oxidation of the glauconitic grains. Alternatively, bioturbation may be the dominant cause of oxidation. Oxidation has been studied in ten samples of glauconitic sediment from Venezuela and Trinidad with live indigenous fauna. The samples were placed in an aquarium where the fauna burrowed throughout the samples but reddened only the upper centimeter at most.

Glauconite precipitation

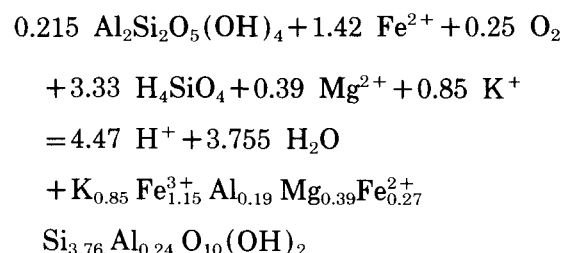
It is well known that glauconite can form by slow transformation of other seabed minerals, especially biotite (Galliher, 1935). Odin (1985) has proposed that glauconitic grains undergo a chemical evolution which may require 100,000 years of exposure to seawater. Rapid introduction of ferriferous solutions can induce rapid mineral growth, however, as demonstrated by Harder (1980) who experimentally precipitated crystalline glauconite rapidly at seawater temperatures.

Harder (1980) produced glauconite (ferric illite) at 20°C and a pH of 8.5 from a solution of 1 ppm Fe, 0.15 ppm Al, 13 ppm silica, 1000 ppm KCl, and 1000 ppm dithionite (either sodium or potassium dithionite). After only one day of ageing, an X-ray diffraction pattern of glauconite (ferric illite) was obtained with a Debye-Scherrer camera. Harder (1978) previously synthesized other "glauconitic" phases,

i.e., berthierine (aluminous ferrous iron serpentine), greenalite (nonaluminous ferrous iron serpentine), and nontronite (ferric smectite). The solutions which precipitated these phases contained 0.3–20 ppm Fe, 0–1 ppm Al, 0–1290 ppm Mg, and 13–20 ppm silica. Precipitation occurred within 3–10 days at temperatures of either 3 or 20°C and at a pH value of 7, 8 or 8.5. Reducing conditions were maintained with sodium dithionite.

The following reaction illustrates the reactants which may be required for precipitation of glauconite. It is unlikely, however, that any one chemical reaction can adequately represent formation of glauconitic minerals within shallowly buried sediment.

Reaction 1:



Given the variability of both glauconitic composition and available reactants, the precision listed for the foregoing stoichiometric coefficients should not be taken seriously. However, the relative magnitudes of these coefficients do reveal the necessity of a substantial supply of aluminum and silicon in addition to iron. In the foregoing reaction, aluminum is attributed to seabed kaolinite which reacts with rising ferriferous fluids. On the Venezuelan shelf, kaolinite is a common aluminous mineral. Micas also are present and have been shown to alter progressively to glauconitic minerals elsewhere (e.g., Odin, 1985) just as they do on the Venezuelan shelf. It is unlikely, however, that mica is the dominant source of aluminum on the Venezuelan shelf because glauconitic grains are more abundant than micas in many areas.

Most of the reactant iron, magnesium, and

potassium are attributed to a rising fluid. Dissolved oxygen is the most significant contribution attributed to seawater. The depth of precipitation within the sediment would depend upon the ratio of the upward fluid velocity to the downward movement of dissolved oxygen.

Silica source for Venezuelan glauconite

As shown in the foregoing chemical reaction (Reaction 1), neither mica nor kaolinite supplies enough silica to form glauconite and there must be an additional supply of dissolved silica. This silica either is supplied by an extraneous ferriferous fluid or by local dissolution of siliceous grains. The most reactive local siliceous grains are fossil diatoms which have precipitated from seawater. Silica is supplied to seawater by ocean-going rivers which drain areas of continental weathering (Mackenzie and Garrels, 1966). A vast quantity of dissolved silica presently is being exported from the Amazon shelf (DeMaster et al., 1983) and a significant quantity also must be exported by the Orinoco. Mixed Orinoco–Amazon waters presently influence at least part of the glauconite-rich shelf (Griffiths and Simpson, 1972; Bowles and Fleischer, 1985).

Whether of fluvial or exhalative origin, much of the silica in Venezuelan glauconite probably becomes incorporated initially into diatoms and then dissolves to form glauconite within shallowly buried sediment. If exhalative, dissolution of deeply buried diatoms would supply silica to fluids rising from great depth. High productivity of diatoms characterizes the Margarita–Araya shelf and carbon-fixation rates here are among the highest in any open-ocean water worldwide (Ballester and Margalef, 1965). The magnitude of this productivity is partly attributed herein to occasional exhalation of nutrient-rich fluids. Given abundant dissolved nutrients, silica of any source would be precipitated efficiently by diatoms. Diatoms are ubiquitous in most fine-grained shallow-

water sediment on the northeastern Venezuelan shelf.

The author has discovered that over 5% biogenic silica occurs in several tens of square kilometers of seafloor sediment under about 30 m of water between Coche and Cubagua Islands (Fig. 20). The content of organic matter in this sediment is consistently high and ranges up to 10% (Alvarez-Espejo, 1985). The day-to-day nutrient source for these diatoms appears to involve upwelling but exhalation probably has a long-term effect on nutrients, both subjacent exhalation and exhalation east of Coche Island (Kimberley and Llano, in press). A westward current of about 1 knot (50 cm s^{-1}) typically occurs throughout this region (Kimberley et al., in press). A westward plume therefore characterizes the phosphorus-rich and iron-rich seafloor sediments which appear to result from exhalation about 50 km and 80 km, respectively, east of Coche Island (Fig. 19).

Exhalations and the modern equivalent of ironstone in Venezuela

Modern equivalent of ironstone in coastal Venezuela

The only known modern equivalent of silicate ironstone occurs on the Venezuelan shelf about 80 km east of Margarita, near Cabo Mala Pascua (Fig. 19). Ferriferous ooids are accumulating here about 5 km offshore, under about 40 m of water (Kimberley, 1988). Calcareous schist at Medina Beach near Cabo Mala Pascua exhibits iron-enriched veins like those which are presumed to be conduits for iron offshore. The ironstone sediment near Cabo Mala Pascua differs somewhat from other ferriferous seafloor sediment in northeastern Venezuela both texturally and mineralogically. X-ray diffraction analysis and chemical analysis has revealed that the ferriferous ooids near Mala Pascua lack ferric illite (glauconite) and are composed entirely of berthierine, some with nuclei of quartz or calcite. This is consistent with the typical

mineralogical difference between non-glaconitic but oolitic SCOS-IF versus glauconitic but non-oolitic SOPS-IF.

Hydrothermal apatite in the Bertonzini quarry

Phosphorus is closely associated with iron in both SCOS-IF and SOPS-IF. It is therefore relevant that a plume of phosphorus-enriched sediment extends away from the Mala Pascua iron deposit along the predominant direction of marine currents (fig. 62 of De Miro, 1974). An exhalative source for the iron and phosphorus also is indicated by hydrothermal enrichments in Fe and P around young dacitic intrusives in the Mala Pascua-Carupano-Casanay area. The only young (5 Ma) igneous intrusives in north-eastern Venezuela or Trinidad are these scattered bodies which range up to 1 km across (Sifontes and Santamaria, 1972; Santamaria and Schubert, 1974; Vierbuchen, 1984).

One of the largest dacitic intrusives occurs adjacent to the Bertonzini quarry which lies 10 km south of the Carupano coast. Marble quarried at Bertonzini locally exhibits hydrothermal alteration which is attributable to the young intrusion. Local addition of iron has produced spectacular red coloration in the marble but the abundance of added iron does not appear to be as substantial as that of phosphorus, which is barely discernable by color. Bright red marble generally contains only small amounts of hematite but marble which has changed from the original bluish gray to tan locally contains more apatite than calcite.

The fluids which mineralized the Bertonzini marble are considered to be representative of fluids which are being generated presently at considerable depth beneath the Mala Pascua deposit. Igneous heating beneath Mala Pascua may be enhancing iron dissolution and fluid exhalation sufficiently that ironstone is accumulating instead of glauconitic sediment. Glauconite is ubiquitous elsewhere on the Venezuelan continental shelf within a wide range of clastic and chemical sediment (Fig. 21)

but generally enriches that sediment to less than 10% Fe.

Cariaco basin

The Venezuelan continental shelf is characterized by a regional wrench-fault system (Silver, 1975). The best known portion of this system is the Cariaco Basin (Fig. 19) which is an active pull-apart, like the Dead Sea in Israel (Richards, 1975; Garfunkel, 1981; Garfunkel et al., 1981; Sylvester, 1988). The Cariaco is one of the deepest basins within any continental shelf (1.4 km deep) and is progressively depleted in dissolved oxygen below the sill depth (50–150 m).

A group coordinated by the Woods Hole Oceanographic Institution continues to study this basin intensely (e.g., Ertel et al., 1986). Given the anoxia, it is not surprising that methane is found near the bottom (Richards, 1975). However, methane also persists in anomalous concentrations within oxygenic seawater near the top of the water column and cannot be attributed to simple upward diffusion from deep water (Ward, 1986). This methane probably is escaping along the steep faults which bound the Cariaco Basin.

Dissolved iron in the Cariaco ranges from about 200 to 300 nM (11–17 ppb Fe^{2+}) through 400 m of water depth below the oxic-anoxic interface which occurs at a depth of about 300 m (De Baar et al., 1988). Dissolved iron within the uppermost 300 m of water is typical of oxidized seawater worldwide, averaging about 50 nM (3 ppb Fe) (De Baar et al., 1988; Holland, 1978). Iron concentrations within the underlying methanic zone are maintained at about 100 nM (6 ppb Fe^{2+}) by precipitation with H_2S (De Baar et al., 1988). These low iron concentrations are consistent with the stratigraphic evidence that iron formations generally have not accumulated on the floors of euxinic seas (Kimberley, 1978a).

It is surprising that the Black Sea has been named the “type anoxic basin” by Glenn and

Arthur (1985) instead of the Cariaco Basin because the anoxic-basin shales described by Fischer and Arthur (1977) apparently formed in a truly oceanic environment like that of the Cariaco Basin instead of a land-locked environment like that of the Black Sea. The Black Sea consistently has been cited by genetic modelers of Fe-Mn deposits, e.g. Force and Cannon (1988), as the type stratified water body whereas the regional marine environment of the Cariaco more closely resembles that of typical Fe-Mn deposits.

Shallow euxinic basins are associated with many iron formations (Hallam and Bradshaw, 1979). This association is interpreted to reflect a common sedimentary response to tectonism and exhalation rather than a prerequisite restriction of marine circulation. In the case of some Fe-Mn deposits, solute concentration indeed may have occurred in restricted bottom waters prior to precipitation onto a basin rim but the modern equivalent of ironstone at Cabo Mala Pascua lies 160 km east of the Cariaco Basin and clearly did not precipitate from Cariaco water, given persistently westward currents (Kimberley et al., in press). The regional tectonic environment which produces euxinic basins apparently favors exhalation, given that the most voluminous methanic exhalations on Earth presently occur near both the Black Sea and Cariaco Basin (Gold, 1979; Gold and Soter, 1980).

Proposed process of iron concentration in northeastern Venezuela

The observed concentration of iron on both the land (ferruginous regolith) and the seafloor (glauconitic grains) in northeastern Venezuela is attributed to deep weathering reactions which are coincident with seismic pumping along the transform fault (shear zone) between the South American and Caribbean plates (McCaig, 1988; Kimberley and Llano, in press). The Neogene stratigraphic sequence which lies between Mesozoic metamorphic blocks consists of sedi-

ments which range from redbeds to highly carbonaceous mud and include substantial gypsum, as exposed on Cubagua Island (Fig. 20). Pumping of water through these rocks would result in more extensive chemical reactions than would pumping through the sediments which normally accumulate in an area of deltaic sedimentation.

It is hypothesized that dissolution of evaporite sediments at depth is enhancing the iron solubility of deep pore fluids. However, the proportion of modern authigenic iron precipitation to clastic sedimentation in northeastern Venezuela is insufficient, in comparison to ancient iron formations, to propose that the iron-concentrating processes presently are particularly efficient. They are nonetheless widespread. The author has sampled modern authigenic iron mineralization at dozens of localities from the Cariaco Basin to Trinidad, a distance of 300 km (Figs. 19, 22).

Exhalation in the Margarita-Cumana area

Ongoing sedimentary exhalation characterizes the Margarita-Cumana area of glauconitic sedimentation in northeastern Venezuela. A small earthquake during field work in January 1986 coincided with exhalation of self-igniting methane south of Margarita Island. In 1797, a major earthquake near Cumana (Fig. 20) was accompanied by major exhalation of combusting methane (Humboldt, 1881; Gold, 1979). Sedimentary exhalation also occurs without earthquakes, as during field work in May of 1987, when beaches on northeastern Margarita Island suddenly became covered with deep-water fish which had died of suffocation. Marine biologists at Fundacion La Salle found that the fish gills had become covered with organic-rich sediment, apparently blown off the seafloor.

Clear evidence of recent sedimentary exhalation in northeastern Venezuela occurs on the island of Coche, between Margarita and the mainland (Fig. 20). Most of the island consists of Quaternary fanglomerate which is remarka-

bly ferruginous (Gonzalez de Juana et al., 1980, p. 726). The fanglomerate is cut by mud diapirs and by lineaments which can be traced on aerial photographs east-west across the entire island (Kimberley and Llano, in press). Most of the lineaments have such a small ratio of displacement to lateral extent that they more closely resemble joints than high-angle faults. Both the joint surfaces and adjacent conglomerate beds have become impregnated with iron oxides, producing peculiar landforms upon erosion of uncemented sediment (plate 8 of Bermudez, 1966).

The mud diapirs on Coche exhibit drab colors, apparently due to reducing volatiles which accompanied diapir emplacement. Diapirs are surrounded by rims of iron-oxide enrichment within the adjacent fanglomerate. Similar diapirs formed near Cumana (50 km away) during the 1929 earthquake when residents observed sulfurous water and mud oozing from cracks in the ground (Fiedler, 1961). The 1929 earthquake was accompanied by a tsunami of 3–6 m wave height (Fiedler, 1961, 1972). The tsunami probably was generated by the escape through the sea surface of a large bubble of exhalative volatiles (Gold, 1979). Exhalation events have occurred twice in the past twenty years within the El Bichar bay of western Coche island (Fig. 20). On each occasion, all animal life within the bay died and all fish which entered the bay within a few days died. Little ground motion was felt by residents of El Bichar during these exhalation events but Quaternary fanglomerate is rising along a fault just north of the bay. Ongoing uplift along this fault resulted in a rockfall of the seacliff in 1987.

Although most types of iron concentration on Coche island appear to be directly exhalative in origin, at least one type apparently has involved groundwater. This type is an oxide layer of a few centimeters thickness along the base of an extensive conglomerate bed on the east-central shore, along a surface of sharp permeability contrast with an underlying bed of fine sand. Iron oxides apparently were deposited on the

surface of the gravel bed and then infiltrated downward to its base. Deposition of iron oxides on the gravel surface may have been related to pedogenic rather than exhalative processes but the clay minerals which should have occurred in any iron-rich soil are scarce within all Coche sediments.

Punta del Hierro (Iron Point) on Margarita island

The most dramatic evidence of exhalative processes on Margarita island is found at the appropriately named Punta del Hierro (Iron Point) near the town of Juan Griego (topographic map 7449-III-N0 of Venezuela). Here a block of metamorphic rock with approximate dimensions of 1.2×0.5 km has become uplifted to an elevation of almost 200 m, carrying Quaternary lagoonal sediment with it. The Quaternary sediment presently dips at about 30° seaward. The steeply dipping surface of adjacent metamorphic rock locally is covered with concretions of pure goethite, hence the name Punta del Hierro (Fig. 20). The coalescing concretions form a goethitic crust which is comparable to crusts which cover ancient seamounts (Prescott, 1988).

As elsewhere in coastal Venezuela, good exposure facilitates deduction of the iron-concentrating processes at Punta del Hierro. The Punta del Hierro block is cut by vertical veins of gypsum and potassium chabazite (a zeolite) which are several centimeters wide and which probably formed during the rapid uplift. The veins are coated with secondary crystals of apjohnite (manganese aluminum sulfate). The brine which formed these veins probably also exhaled the iron which coated the Punta del Hierro block with goethite concretions. The potassium content of the chabazite probably records a high potassium content of the brine. If so, much of the potassium in the ubiquitous glauconite of the Margarita region may have been exhaled with the iron. If potassium is exhalative, argon probably also is exhalative and

the resulting potassium-argon proportions of some modern glauconite may resemble those of ancient glauconite.

Genetic classification of iron formations

Introduction

Genetic discussions about cherty iron formations generally state at the outset that non-cherty deposits will not be considered (e.g. Trendall, 1983a; Holland, 1984). An implication of this overt restriction is that noncherty iron formations provide no relevant clues regarding the accumulation of cherty iron formations. The present review is intended to demonstrate that iron formations are best considered collectively. Cherty iron formations will be considered first, however, because they appear first in the geologic record.

There are two schools of thought regarding the genetic classification of cherty iron formations (mostly MECS and SVOP paleoenvironmental types). One school argues that they have all formed by the same basic process and should not be subdivided (Gole and Klein, 1981; Yeo and Gross, 1987). The other school prefers some type of two-fold distinction, whether based on continental versus volcanic affinities (James and Sims, 1973), large versus small tonnage (Holland, 1984), or shallow-water versus deep-water sedimentation (Dimroth, 1975).

The prime argument against subdividing cherty iron formations is that the great bulk of cherty ironstone consists of little other than oxygen, silicon, iron, carbon, and manganese (Gole and Klein, 1981; Yeo and Gross, 1987). Some small cherty iron formations grade to economic concentrations of other elements, particularly Pb, Zn, Cu, Ag, and Au, and these enriched iron formations are attributed to hydrothermal exhalation by virtually all researchers. Those who similarly attribute all other cherty iron formations to hydrothermal exhalation tend not to differentiate these metal-rich deposits from the normal iron formations

whereas the other genetic modelers are more inclined to do so.

All voluminous iron formations are remarkably poor in trace elements (Table 2). All of these continental-shelf (MECS) and volcanic-platform (SVOP) deposits probably accumulated in water shallower than the mean depth of the oceans. Iron formations which contain even moderate amounts of metals other than iron and manganese are all small. However, among small iron formations there is no apparent correlation between size and metal content and so size alone is not a definitive criterion. Few of the cherty iron formations listed in Table 2 are correlative with sulfide ore deposits. One example is the Pb-Zn-Ba-rich Tynagh iron formation which is roughly correlative with a Carboniferous ore deposit of Pb, Zn, Cu, and Ag (Russell, 1975; Boast et al., 1981; Deeny, 1987). Another is the Ordovician Austin Brook iron formation (Saif, 1983). These iron formations are slightly enriched in trace elements but are otherwise similar to normal cherty iron formations. It would be difficult to separate them convincingly into a trace-element-rich genetic category.

One-dimensional versus two-dimensional models

Many genetic models for nonvolcanic-associated iron formations, both cherty and non-cherty iron formations, are essentially one-dimensional, e.g. the groundwater models of Aldinger (1957) and James (1966), the fluvial models which have been advocated by a score of authors (listed in Kimberley, 1979a), and the marine-upwelling models of Borchert (1952, 1960, 1965), Holland (1973, 1984) and Drever (1974). Rapid changes in climatic conditions, e.g. alternating glacials and interglacials, presumably would have rapidly affected any hypothetical one-dimensional migration of iron. One-dimensional models generally invoke chemical reactions which occur at a temperature less than the highest temperature recorded

on the Earth's surface (60°C) and so may be further classified as cool or environmental models.

Volcanic-exhalative versus metamorphic-exhalative models

The most-cited alternative to one-dimensional (environmental) models is the volcanic-exhalative model (e.g. Oftedahl, 1958). However, cherty iron formations display no obvious affinity for volcanic sequences (James, 1966) and noncherty iron formations are, if anything, antipathetic to volcanic sequences. Localized heating due to volcanism actively pumps hydrothermal fluids toward the Earth's surface but regional tectonic processes presently induce a greater volume of subsurface fluid migration (Tissot and Welte, 1984). The global rate of upward migration of fluids due to a combination of compaction, regional metamorphism, and seismic pumping presently exceeds that due to processes which are creating volcanoes.

An enormous volume of seawater can become heated during seismic pumping or convection through newly formed igneous crust. The capacity of localized volcanic processes has been shown by Holland (1973) to be more limited. He noted that the required spacing of volcanoes to have produced the Hamersley MECS-IF would have been roughly one per mile around the basin perimeter. Thermal gradients around volcanoes probably have not changed dramatically through Earth history but the geothermal gradient through newly formed crust must have decreased substantially due to the decreasing concentration of radioactive nuclides (Holland, 1984).

Thermal gradients apparently were high during formation of ancient oceanic crust, as recorded by Archean komatiites (Green, 1975). Ancient rifts probably opened more rapidly than recent rifts and rift failure probably occurred more abruptly, producing a restricted basin floored by fresh crust which would simultaneously hydrate rapidly. Shearing along the mar-

gin of such a basin could result in seismic pumping which would enhance thermal convection of seawater through the hydrating crust.

Exhaling fluids from hydrating crust tend to be siliceous because virtually all primary igneous minerals lose silica upon hydration (e.g. Stumm and Morgan, 1981). Exhalative fluids may have dominated the subsurface chemistry of some ancient rift basins. Dominance of subsurface basin waters would have been essential for sedimentation of thick cherty iron formations. Dominance would have been unlikely, however, in excessively large basins or in those which opened too slowly.

Noncherty iron formations clearly are not associated with exhalation which accompanies growth of a large volcanic edifice. However, the aforementioned association of modern ironstone with young (5 Ma) plutons in northeastern Venezuela may result from ongoing seismic pumping of seawater through a cooling pluton or ophiolite body (Kimberley, 1988).

Proposed genetic classification scheme

Each voluminous cherty iron formation clearly precipitated from a water body which remained ferriferous for more than 10^5 years (Holland, 1984). A long-lasting ferriferous water body has not been a requirement, however, for most noncherty (largely oolitic) iron formations. Most debates about ferriferous water bodies have concerned removal of dissolved oxygen. The maximum concentration of aqueous O_2 is so small, however, that processes of oxygen removal are not considered herein to be as important as processes which limit the concentration of H_2S , given that sulfur solutes are over 200 times more abundant than oxygen in seawater. Modern anoxia usually results in reduction of SO_4^{2-} to H_2S and this H_2S keeps the solubility of iron about as low as does aqueous O_2 . The following genetic classification of iron formations therefore emphasizes processes which inhibit production of H_2S (Table 3).

There is no clear consensus regarding the origin of any voluminous iron formation and so the following genetic classification of iron formations (Table 3) offers many (120) classifications through combinations of modifiers. Many of these have been advocated by previous modelers but only a few are considered herein to be viable. The number of viable genetic types is comparable to the number of paleoenvironmental types (6) classified in Table 1. Classification by Table 3 immediately leads to genetic controversy whereas Table 1 facilitates discussion among researchers who choose to avoid contentious genetic arguments. For the more intrepid, Table 3 facilitates discussion of iron-concentrating processes.

Acronyms for the favored genetic types in Table 3 are essential because each complete name is an unwieldy hyphenated string. For example, the favored genetic type for shallow-water cherty iron formations on continental shelves (MECS-IF) is the Deep-weathering (continental rift)-Hypersaline (unknown exhalative fluid)-Equilibrated-Dominant type, here abbreviated to D_cH_dED. The favorite for noncherty oolitic iron formations (SCOS-IF) is Deep-weathering (sedimentary pile)-Hyper-saline (direct exhalation)-Unequilibrated-Local (D_sH_eUL) type.

The most fundamental genetic distinction in Table 3 is considered to be whether the iron dissolved by deep or shallow weathering (option A). In this simple dichotomy, "shallow weathering" includes early diagenesis in the uppermost 10 m of sediment (Berner, 1980) and "deep weathering" ranges from deeper diagenesis to low-temperature metamorphism (Frey, 1987). Given that all iron formations have accumulated in water bodies, an implication of the deep-weathering option is that the ferriferous fluids have exhaled at the Earth's surface. Four subtypes are listed for the deep-weathering option and two for the shallow-weathering option. Shallow weathering has provided aqueous iron either as fluvial input (subtype f) or through early-diagenetic weathering of sediment on the

seafloor (subtype s). Deep weathering (hydration) may have occurred in any of four environments, i.e. around an individual volcanic pile (subtype v), adjacent to a mid-oceanic ridge in a large ocean basin (subtype o), within a young rift basin (subtype r), or within a sedimentary pile which contains evaporite beds, young plutons or ophiolite (subtype s).

The option of salinity and sulfur content (option B in Table 3) is independent of the deep-versus-shallow weathering option because various compositions may be postulated for water of either source. The composition of exhalative (deep weathering) water may be unknown and variable if it exhales sporadically and then reacts with seawater to produce a long-lasting ferriferous water body which differs compositionally from the exhalative input. Any attempt to deduce the composition of the original exhalative water would be like trying to deduce the composition of average river water on the modern Earth, given only the composition of seawater. The deep-weathering option therefore has two subtypes. In one, precipitation occurs so quickly after exhalation that no long-lasting ferriferous water body is produced and so the stipulated composition applies to the exhalative fluid (subtype e). In the other, the stipulated composition applies to the deep seawater which evolves from reactions between descending surficial seawater and exhalative fluids of unknown composition (subtype u).

Like the subtype options of water chemistry, the option of thermal equilibrium (option C) applies only to the exhalative case because all shallow-weathering models imply thermal equilibrium with some water body. These two restricted applications limit the number of classifiable shallow-weathering models to 24, considering all possible combinations of the four options in Table 3 ($2 \times 4 \times 1 \times 3 = 24$).

A pair of restrictions also apply to the deep-weathering (exhalative) models in that thermal equilibration (option C) implies a sufficient supply of ferriferous fluids to dominate bottom-water chemistry (option D). The num-

TABLE 3

Genetic classification of iron formations

(A) Source of iron (depth of weathering source)

Shallow: Fe supplied by rivers, as solutes and/or reactive particulate matter

Subtypes: fluvial solutes (f) or seafloor weathering of particulates (s)

Deep: Fe supplied by hydration of either new crust or sedimentary pile

Subtypes: volcanic pile (v), new crust in large ocean (o), new crust in continental rift (r), or sediments with ophiolite, evaporites or pluton (s)

(B) Nature of iron-dissolving water

Note: Add subscript "e" if direct exhalative precipitate or "u" if unknown exhalative fluid reacted with seawater to produce Fe-rich seawater

Fresh-brackish: Basinal water contains < 1% total solutes (< 30% seawater salinity)

Sulfurous+seawater salinity: Sulfur is present mostly as sulfate and seawater has not been concentrated beyond 40 ppt

Nonsulfurous+seawater salinity: Sulfur is essentially absent because of precipitation with excess dissolved metals

Hypersaline: Salinity is > 40 ppt and may exceed that of surficial seawater. Sulfate predominates over H₂S

(C) Nature of iron-precipitating water

Equilibrated: Iron-precipitating water has equilibrated thermally with a large body of water (but this water may be hotter than world-average or overlying seawater)

Unequilibrated: Iron-precipitating water has not equilibrated thermally with any large body of water

(D) Rate of supply or production of iron-rich fluids

Dominant: Supply is sufficient to dominate bottom-water chemistry

Local: Bottom water is not continuously ferriferous but voluminous ironstone is produced close to input areas

Weak: Fe-rich grains, e.g. ooids, originally constitute a small proportion of sediment or soil but erosion and sorting produce ironstone

Note: A genetic type is defined by selecting a modifier from each category and stringing the modifiers into a hyphenated list or acronym, e.g. D_rH_eED.

ber of exhalative-equilibrated genetic types therefore is $4 \times 8 \times 1 \times 1 = 32$. A lack of thermal equilibration implies precipitation close to a vent rather than dominance of bottom-water chemistry. These precipitates may remain close to the vent (option D, subtype Local) or become subjected to erosion and sorting (option D, subtype Weak). The number of exhalative-unequilibrated types therefore is $4 \times 8 \times 1 \times 2 = 64$. The total number of all genetic types is $24 + 32 + 64 = 120$.

It is possible for thermally-equilibrated water to produce only part of an iron formation and so different portions of the iron formation may be classifiable differently. For example, the base of the Archean Helen iron formation (Goodwin et al., 1985) is interpreted herein to have precipitated from unequilibrated water whereas the remainder is attributed to thermally equilibrated water. In this case, one either may clas-

sify the iron formation by the dominant process (thermally equilibrated) or hyphenate acronyms for both classifications, e.g. the favored classification of the Helen iron formation is D_rH_eUD-D_rH_uED. In this hyphenated pair, the fluid-chemistry option (H=Hypersaline) in the first acronym applies to the exhalative fluid which is assumed to be hypersaline. This option coincidentally is hypersaline (H) in the second acronym but here it applies to a long-lasting ferriferous water body.

Diversity of existing hypotheses

A genetic classification scheme with 120 options (Table 3) is indeed diverse. Arguments are raised in this section to limit the viable options to half a dozen but it should be emphasized that the proposed focusing of discussion is not based upon any consensus among iron-

formation researchers. The genesis of iron formations continues to be one of the most controversial geologic problems. Given the substantial increase in data about iron formations during the past few decades, one would have expected a corresponding focusing of debate but the reverse has occurred. Hypotheses for SCOS-IF should be better constrained than those for other types of iron formations because there are several young SCOS iron formations (Table 2). SCOS-IF is, however, as controversial as any type. There are at least eight hypotheses for the mode of iron transportation to form SCOS-IF and thirteen hypotheses for the mode of concentration at the site of deposition (Kimberley, 1979a).

It is beyond the scope of this paper to classify all published genetic models according to the scheme of Table 3. Only a few recently published models are classified herein. Most genetic models which derive iron by shallow weathering are sufficiently detailed that they readily may be classified by the proposed scheme (Table 3). For example, Garrels (1987) has proposed a Shallow weathering-(fluvial solutes)-Fresh-Equilibrated-Dominant (S_fFED) model for microlaminated MECS iron formations. Garrels (1987) invokes fluvial input of aqueous iron to a slightly brackish basin. A model of fluvial input to an ocean would be classified as S_fSED if the iron arrives as solutes (Gruner, 1922; Lepp and Goldich, 1964) or S_sSED if iron-bearing detritus weathers on the seafloor (Holland, 1984). An oceanic model which invokes seafloor weathering under sulfur-depleted bottom water would be classified as S_sNED (Drever, 1974).

Unfortunately, several models which invoke hydrothermal supply are too vague to be classified by Table 3 (e.g. Simonson, 1985). A prime purpose of the proposed scheme is to encourage more specifics in hydrothermal models, whether the hydrothermal exhalation is attributed to local (volcanic) convection or regional hydration of new crust. Walker and Brimblecombe (1985) invoke hydration of oceanic crust by the convection of seawater. They envision such a rapid

input of hydrothermal iron to deep water that iron input overwhelms the input of sulfur by the downward mixing of sulfate-bearing surficial water into H₂S-equilibrated deep water. All H₂S is precipitated as sulfides, thus producing a sulfur-depleted ferriferous water body (type D_oN_uED). Goodwin et al. (1985) envision low-temperature exhalation into sulfate-rich seawater and immediate precipitation of cherty ironstone (type D_vS_eUD) rather than rapid cooling of hot exhalations followed by long-term maintenance of a ferriferous water body.

Genesis of iron formations

Lithologic associations of iron formations

One reason for diversity in opinion about iron formations is that they are interbedded with diverse other rocks (Table 2). Most investigators have attempted to interpret the enigmatic iron formations by studying their relationship to associated rock bodies, either sedimentary or volcanic. The interpretation of associated rocks usually is straightforward and generally influences iron-formation interpretation. As more and more iron formations have become interpreted by lithic association, one would have expected that basic similarities in sedimentary environment would have become apparent. They have not. Both SCOS-IF and MECS-IF are associated with a wide variety of clastic and chemical sedimentary rocks.

It is quite remarkable that iron formations apparently have formed in a wide variety of sedimentary environments because iron formations represent an end-member chemical sediment. End-member chemical sediments, e.g. bittern salt deposits, generally represent extreme chemical conditions which are clearly reflected in the suite of associated sedimentary rocks. Rocks associated with cherty iron formations represent the entire spectrum of climatic environments from humid tropical, e.g. most Early Proterozoic iron formations, to glacial, e.g. most Late Proterozoic iron forma-

tions. SCOS iron formations have formed in both marine and nonmarine environments, in both purely clastic and largely carbonate sequences. SCOS iron formations generally have formed in low paleolatitudes but exceptions in high paleolatitudes also occur (Van Houten, 1985).

A common stratigraphic sequence which includes cherty iron formations was noted in the foregoing discussion of Lower Proterozoic iron formations (Gross, 1965, p. 91). This sequence is not as characteristic of cherty iron formations of other ages and its recurrence in Lower Proterozoic sequences is as readily explained by deep-seated (tectonometamorphic) processes as by surficial processes. The general diversity of sedimentary environments associated with iron formations is interpreted herein to indicate that the surficial environment in which the iron accumulated was not responsible for the aqueous migration of iron. If valid, this interpretation would eliminate all hypotheses which are essentially one-dimensional, i.e. those which do not involve deep processes like deep weathering. One-dimensional models invoke iron dissolution in some surficial environment, either on the seafloor or in soil, followed by lateral transport to the site of accumulation, whether carried in a marine current, in shallow groundwater, or as fluvial load (dissolved load or suspended load).

Ironstone composition and an overview of the exhalative model

Both cherty and noncherty iron formations are sulfur-poor relative to deposits of most other metals. If they are a product of deep weathering, the paucity of reduced sulfur in the ferriferous fluids may be inherited from the original reactions occurring at depth. Noncherty iron formations may be related to deep weathering of evaporite-bearing sediments. Evaporite deposits contain little pyrite because seawater sulfate reduces to hydrogen sulfide within the water column of stratified brines. Hydrogen sulfide is weakly soluble in warm brine and so

escapes to the atmosphere (Sonnenfeld, 1984, p. 105). During deep weathering, some dissolved sulfate would become reduced and react with dissolved iron to produce pyrite but, given a sufficiently high proportion of sulfate to organic matter, substantial iron would remain in solution.

Except for abundant iron, carbonate carbon, and some manganese, the composition of cherty ironstone resembles that of contemporaneous chert. A stratigraphic unit of brecciated chert (Fleming Breccia) underlies the Sokoman iron formation in Quebec, Canada (Dimroth, 1971). The origin of this chert breccia is unknown and may have involved iron-poor exhalation which preceded ferriferous exhalation. In the Archean Outerring iron formation (Table 2), the author has observed that physical disruption locally produced abundant brecciated ironstone. The Outerring iron formation accumulated in such shallow water that any release of exhalative volatiles would have been explosive.

Isotopic studies should help resolve the origin of iron formations. Miller and O'Nions (1985) note that the rare-earth isotopes in voluminous cherty iron formations had become separated from the mantle long before these Precambrian iron formations accumulated, hence the rare earths did not come from crust which had recently differentiated from the mantle. The source of iron in cherty iron formations is interpreted herein to be recently differentiated crust and so the interpretation of Miller and O'Nions (1985) contradicts this conclusion. A possible resolution of this contradiction lies in the fact that rare earths are scarce in cherty iron formations (about 10% of crustal average) and so a significant portion of the observed rare earths may have been introduced by shallow weathering of old continental detritus on the floor of a long-lasting ferriferous water body which simultaneously was receiving ferriferous exhalations from young crust. Continental detritus may have been supplied by rivers entering the water body far from the site of cherty ironstone accumulation.

Production of iron formations clearly was more efficient on a younger and radioactively hotter planet (Table 2). Greater heat surely enhanced the rate of interaction between seawater and young crust. Greater heat would not have had much effect, however, on the rate of shallow weathering of old continents.

Relevance of Precambrian atmospheric composition

The proposed exhalative model follows the work of many others, notably Oftedahl (1958) and Gross (1980). Like Gross (1983), the present model discounts the importance of atmospheric chemistry on controlling the age distribution of iron sedimentation (cf. Holland, 1984). Atmospheric chemistry may well have been affected, however, by iron-bearing exhalations and a lower oxygen content in the atmosphere may have helped maintain long-lasting suboxia in ferriferous water bodies.

The issue of atmospheric chemistry involves the rate of sedimentation of individual beds in iron formations. These beds contain ferrous minerals which are unstable in the presence of any dissolved oxygen (Holland, 1984). Many of these beds accumulated above wave base, given extensive oolitic and intraclastic texture. If these beds had accumulated slowly, an oxygen-rich atmosphere might have supplied enough oxygen for seawater to oxidize them, despite the low solubility of oxygen in seawater (about 10 ppm at low temperatures). Precipitation is envisioned to have occurred under an interface with subsurface, high-salinity, suboxic water. In the case of oolitic cherty ironstone, wave base would have extended below this interface.

The ratio of ferrous/ferric iron is roughly equivalent between Precambrian and Phanerozoic iron formations, even in Phanerozoic iron formations which formed just a few million years ago (Table 2). This approximate equivalence apparently indicates that the sedimentation rate of individual ironstone beds generally has been fast enough to overcome potential ox-

idation, whatever the atmospheric oxygen pressure has been throughout Earth history. Unoxidized ferrous silicate (berthierine) presently is accumulating on the shallow (40 m) seafloor of Venezuela in calcareous sediment which is virtually devoid of any carbonaceous matter or other reductant (Kimberley, 1988). The ferrous mineralogy of this modern equivalent of ironstone is particularly remarkable because strong currents (> 1 knot (0.5 m s^{-1})) of oxidizing seawater commonly impinge on this seafloor. Modern and ancient iron deposits therefore appear to be imprecise indicators of the atmospheric concentration of oxygen (cf. Holland, 1984; Towe, 1983).

Iron-formation exhalation may have had a bigger effect on the atmosphere than the atmosphere has had on iron formations. Ferriferous exhalations may have introduced abundant carbon dioxide, at least during voluminous Precambrian exhalations (Kempe and Degens, 1985). Methanic exhalations probably would have been poorer in iron because of equilibrium with sulfides, whatever the source of methane (Gold, 1979; Gold and Soter, 1979, 1980, 1982; Sofer, 1985).

Carbon and phosphorus in iron formations

One of the most abundant minerals in iron formations is siderite, iron carbonate (Table 2). Iron formations therefore represent preferential burial of carbon. Voluminous cherty iron formations may record a previously voluminous input of mantle-derived carbon during rapid seafloor spreading. As in modern volcanic gases, the oxidation state of this carbon would have ranged from that of CH_4 to CO_2 (Holland, 1978). Subsequent burial would have occurred as both carbonate carbon and organic carbon. Holland (1984, p. 361) calculates that the ratio of organic carbon to carbonate carbon ($\text{C}_{\text{org}}/\text{CO}_3^{2-}$) would lie between about 0.1 and 0.3 in sediments. If the siderite of cherty iron formations represents much of the newly introduced carbonate carbon, there should have been con-

temporaneous deposition of the organic carbon as carbonaceous matter. Black shale is indeed commonly associated with both cherty and noncherty iron formations (Table 2).

Deep weathering of igneous rocks to produce siliceous exhalations may have affected climate through the consumption of carbon dioxide. The resulting atmospheric modifications would have been cyclical, however, rather than evolutionary. Precambrian oceans probably were not continuously enriched in carbon dioxide, as envisioned by Kempe and Degens (1985). Moreover, Proterozoic iron formations are not sufficiently ubiquitous to support Young's (1988) concept of continuously ferriferous Precambrian seawater. If siliceous iron-formation fluids have formed due to crustal hydration, the prime evolutionary record of cherty iron formations would be a decreasing rate of crustal production and deformation on a cooling planet. Greater deformation presumably favored seismic pumping.

Collectively, iron formations contain a large proportion of all the phosphorus in chemical sedimentary rocks, generally in the form of apatite. Most of this phosphorus is attributable to inorganic precipitation from ferriferous fluids but some apatite in noncherty iron formations occurs as well-preserved fossils (Hayes, 1915). Iron formations apparently have preserved fossils well because of high sedimentation rates (Kimberley, 1980; Hill et al., 1985). Iron formations therefore record both the biologic and tectonomagmatic evolution of Earth.

Relationship of cherty to noncherty iron formations

Phanerozoic noncherty iron formations have been attributed to a wide variety of fluvial, marine, diagenetic, and hydrothermal processes (Kimberley, 1979a). In this paper, they are attributed to hypersaline fluids which were generated by deep weathering, as were the fluids which produced cherty iron formations. Noncherty iron formations are attributed to hydra-

tion of ophiolite, evaporites and/or young plutons within a thick sedimentary pile.

It is unlikely that the fluids which have produced cherty and noncherty iron formations initially were similar, despite the potential for acquiring distinctive compositions upon ascent. Nonetheless, fluids which have produced noncherty iron formations may have become modified by ascent through young argillaceous sediment, losing silica due to cooling and extracting phosphorus. In a modern estuary, iron hydroxides absorb phosphorus until the ratio of Fe/P becomes about 14 (Lucotte and d'Anglejan, 1988). Noncherty fluids almost certainly were not exposed to seawater long enough to extract much phosphorus prior to precipitation. Siliceous ferriferous fluids apparently have formed long-lasting marine water masses but those water masses generally have not precipitated phosphatic ironstone. The ratio of Fe/P in typical noncherty ironstone is about 50 whereas in cherty ironstone the ratio commonly exceeds 500 (Table 2).

The prime argument against initial compositional similarity of cherty-noncherty fluids is that iron formations generally display no lateral or stratigraphic gradation from cherty to noncherty ironstone. One would expect that the mode of exhalation has varied with time and place during accumulation of thick iron formations. Any compositional variation related to exhalation mode should have varied correspondingly. However, there is remarkably little lateral compositional variation in most ferriferous sediment, including the modern iron-silicate-rich sediment which varies among three green silicates (glauconite, berthierine, nontronite) along 1000 km of Venezuelan coastline. A difference in exhalation rate is considered to be the prime factor controlling the compositional difference between potassium-rich glauconite and potassium-poor berthierine. Glauconite is attributed to such a slow exhalation that precipitation generally occurs within the sediment by interaction with marine pore water whereas the modern equivalent of

berthierine ironstone (Kimberley, 1988) is attributed to a sufficiently rapid exhalation that exhalative potassium escapes by mixing with bottom water.

The high aluminum content of most non-cherty ironstone may be a primary chemical feature or may be caused by physical incorporation of clays into the exhaling fluid. Ordinary clay minerals may have become mixed with the rising fluid, as during modern petroleum production in Nigeria (Lambert-Aikhionbare, 1982). Clay minerals and ferriferous fluids have been carried upward through Quaternary fan-gneiss on Coche island, Venezuela (Kimberley and Llano, in press).

Production of ferriferous fluids

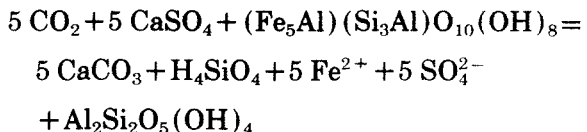
It is proposed that all iron formations are attributable to exhalation from one of two deep-weathering environments. Cherty iron formations are attributed to hydration of igneous rock in a new rift-basin floor whereas noncherty iron formations are attributed to hydration of a sedimentary pile which contains ophiolite, evaporite beds and/or cooling plutons (Table 3). All ferriferous exhalative fluids are assumed to have been hypersaline (> 40 ppt salinity or 22 ppt chlorinity). Kwak et al. (1986) propose that hot water with over 20% solutes can transport over 1% Fe. Some hypersaline (32 ppt chlorinity) exhalative fluids along the East Pacific spreading ridge contain over 650 ppm Fe (Scott, 1987). However, low-salinity exhalative fluids locally contain over 100 ppm Fe (2 mM Fe) along the mid-Atlantic ridge (Thompson et al., 1988). For an exhalative fluid to produce a voluminous iron formation, it must contain aqueous iron concentrations which are considerably higher than the 3 ppm Fe^{2+} in Holland's (1984) shallow-weathering model because deep-weathering fluid supply is inherently more limited than water movement which is driven by the hydrologic cycle.

Ferriferous fluid exhalation from sediments is attributed to seismic pumping along a trans-

form fault (McCaig, 1988). Seismic pumping also may have been essential for sufficient exhalation from young igneous crust despite the potential for convective pumping due to differential heating. Both types of exhalative fluids probably have been hypersaline but the origin of hypersalinity in exhalations from new crust is uncertain. Hypersalinity in the Salton Sea geothermal system of California is attributable to ongoing metamorphism of Plio-Pleistocene evaporites (McKibben et al., 1988). Hypersalinity of Red Sea brines long has been attributed to dissolution of deeply buried evaporites but hypersalinity also occurs in mid-oceanic ridge environments where evaporite dissolution seems unlikely (Scott, 1987). Evidence of hypersalinity in mechanically-driven exhalations exists in the aforementioned gypsiferous veins which appear to have been conduits for some of the iron exhalation from sediment in northeastern Venezuela.

Any discussion of potential hydration reactions to produce ancient ferriferous exhalations from cooling igneous crust will remain speculative until the origin of hypersalinity in modern exhalative fluids is resolved (Scott, 1987). Under an exhaling sedimentary margin like northeastern Venezuela, the following reaction (Reaction 2) may serve as a heuristic example of iron dissolution by weathering of evaporites and associated silicates.

Reaction 2:



The carbon dioxide which drives Reaction 2 is assumed to come from the dissimilatory breakdown of organic matter to carbon dioxide and methane, followed by partial separation of these two volatiles by physical processes during seismic pumping. An iron-rich chlorite is used in Reaction 2 to represent a wide variety of iron-bearing silicates and oxides. Several other ions would be affected by the proposed weathering

reactions, notably sodium and chlorine (from dissolving halite) and magnesium. These are ignored for the sake of simplicity.

The factors which would control deep weathering would be similar to those which control shallow weathering, i.e., the rate of supply of CO₂, the rate of removal of solutes, the availability of reactive minerals, temperature, and time. Production of a voluminous noncherty iron formation would require voluminous throughput of seawater and probably requires a process more potent than compressive dewatering of pore fluids, i.e. seismic pumping. It may also require local heating to enhance reaction rates. Production of a noncherty iron formation also may require local heating to enhance reaction rates or hydration of a cooling pluton or ophiolite to provide solutes.

If Reaction 2 is relevant, it may be used to estimate the minimum volume of evaporite which must dissolve to produce a given volume of noncherty ironstone. According to this reaction, a molecule of sulfate must dissolve for each atom of iron that dissolves. The mole fractions of sulfate in anhydrite and iron in average ironstone are respectively 0.7 and about 0.3. The density of ironstone is about 1.2 times that of anhydrite. To produce a unit volume of noncherty ironstone, roughly two unit volumes of anhydrite therefore must dissolve, given that $0.7/(0.3 \times 1.2) = 2$. Silica is supplied by Reaction 2 and noncherty ironstone indeed commonly contains tens of percent of chemically precipitated silica, in the form of berthierine. If the silica which is supplied by the foregoing reaction is to reach the seafloor, the exhaling fluid may have to remain warm during its ascent.

It is unlikely that Reaction 2 has any relevance for cherty iron formations. The aggregate thickness of cherty iron formations in some sequences approximates one kilometer and so the supply of saline solutions from directly beneath such an iron formation would require dissolution of a minimum thickness of 2 km of anhydrite over an area equal to that of the iron formation. A few Phanerozoic evaporite se-

quences have exceeded this minimum required thickness (Sonnenfeld, 1984). For example, the Middle Miocene salt beds are three to four kilometers thick under the Red Sea basin (Stoffers and Kuehn, 1974). However, simultaneous dissolution of such a voluminous evaporite seems improbable.

Are rift-related evaporites a precursor to iron formations?

Although evaporite dissolution seems barely adequate for production of voluminous hypersaline ferriferous solutions, evaporite dissolution may have enhanced unknown solute-concentrating processes during contemporaneous hydration of new crust. For evaporite dissolution to contribute to deep weathering, subsidence has had to be sufficiently rapid that the evaporite could become deeply buried despite its tendency to flow upward diapirically. The burial depth of salt at the time of hypothetical dissolution would have been less than the depth at which salt becomes ductile, presently about 12 km (Sonnenfeld, 1984, p. 443).

Voluminous salt accumulation is characteristic of initial rifting, as during the opening of the Gulf of Mexico (Salvador, 1987) and the Red Sea (Degens and Ross, 1969). Dissolution of salt under the Red Sea may be producing the observed small volume of cherty ironstone and dissolution of salt under the Gulf of Mexico is maintaining the ferriferous Orca water body (Trefry et al., 1984). The abundant Jurassic SCOS iron formations of Europe (Zitzmann, 1977) and Early Cretaceous SCOS-IF in the Baltimore Canyon basin of North America (Cunliffe, 1982) may be related to seismic pumping through evaporites which accumulated shortly after the opening of the Atlantic.

Evaporites are a potential source of ferriferous solutions not only because they can provide the anions needed for a high concentration of dissolved iron (Kwak et al., 1986) but because they contain a unique combination of abundant sulfate and a high proportion of nonpyritic iron.

Most other marine sediment is characterized by the early diagenetic conversion of reactive iron minerals to pyrite (Berner, 1984). Pyrite is scarce in evaporites because stratified evaporitic lagoons are sulfidic and the solubility of hydrogen sulfide is low in warm saline water (Sonnenfeld, 1984, p. 105). Hydrogen sulfide escapes to the atmosphere, depleting the water column in sulfur and inhibiting the production of sulfides within the terrigenous component of evaporitic sediment.

Fluids generated at depth from dissolution of the terrigenous component in evaporites would be poor in H_2S , as indeed the iron-formation fluids have been, given the scarcity of pyrite in all major types of iron formations. Anhydrite certainly could contribute sulfur to these fluids, as shown by Reaction 2, but anhydrite would have to be subordinate to carbonaceous matter for its sulfur to become reduced and precipitate as iron sulfide deep within the crust.

If buried evaporites have provided some of the anions for ferriferous fluids, one would expect that iron formations mostly have accumulated at low latitudes. Paleomagnetism indicates that the majority did accumulate at low latitudes but some, e.g. the Gunflint MECS-IF and Ordovician SCOS-IF's accumulated near a pole (Purucker, 1984; Van Houten, 1985). The Gunflint pole apparently was not ice-covered, however, given the lack of glacial sedimentation and abundance of algal stromatolites in the formation (Goodwin, 1960).

The production rate for cherty iron formations apparently varied through the Precambrian (James, 1983). This variation largely involves MECS iron formations. The corresponding variation in exhalation rate may be indicative of the restriction of MECS-IF production to rifts which open particularly quickly, fail, and then experience seismic pumping due to transform faulting along the length of the basin. Evaporite sedimentation would be favored by the opening of a rift at such a high rate that clastic sedimentation could not match the subsidence.

Seismic pumping of exhalative fluids

Knowledge of fluid movement deep in the crust is increasing rapidly but remains somewhat sketchy, given the complex interrelationship between thermal and mechanical processes (e.g. Fyfe et al., 1978; England et al., 1987; Moore et al., 1988). Little is known about modern "plumbing systems" and so speculation about ancient systems should be viewed critically until more deep-sea drilling is completed.

Fluid movement under the exhalation-prone shelf of northeastern Venezuela largely is attributed to shear-induced seismic pumping (e.g., McCaig, 1988) but there also is some dewatering of highly porous sediment due to compression between blocks of metamorphic rock (e.g. Lobato et al., 1983). Vierbuchen (1984) attributes most right-lateral shearing in northeastern Venezuela to motion along the El Pilar fault (Fig. 20) but Metz (1964) found no field evidence for substantial shear along this fault. Kimberley and Llano (in press) have demonstrated that several lineaments in the continental margin parallel the El Pilar fault and that shearing probably has been distributed across much of the margin. Widespread distribution of shear would enhance seismic pumping and explain the widespread distribution of modern iron-precipitating exhalation (Fig. 21).

Shearing along the continental margin of Venezuela is induced by the westward motion of South America relative to a stationary or eastward-moving Caribbean plate (e.g. Vierbuchen, 1984). Major strike-slip faults dip steeply toward either the north or south along this transform (fig. 19 of Sylvester, 1988). The transform-fault motion produces alternating compression and extension along the Venezuelan margin. Sediments under the Margarita-Araya platform alternatively experience shortening (before rupture) and extension (after rupture). After rupture, water presumably flows down the dipping planes of the prime faults and into extensional cracks which extend from the main fault planes upward through the plat-

form. As shortening proceeds, deep water is squeezed upward through the cracks and exhales (McCaig, 1988). The frequency of exhalation presumably increases up to the time of rupture when it peaks.

The alternation between extension and compression along a shear zone is considered to be essential for voluminous pumping, as opposed to the purely compressional model of Duane and De Wit (1988) or the extensional pumping model of LeHuray et al. (1987). Purely mechanical seismic pumping and related sediment dewatering are interpreted to be driving most exhalations which are producing widespread iron mineralization around Margarita (Fig. 21).

Much of the glauconite in coastal Venezuela may be precipitating from rising fluids prior to their exhalation through the seafloor. The single known occurrence of modern ironstone sediment in Venezuela, composed of berthierine, probably involves more potent exhalation which may require a heat source in addition to seismic pumping. An igneous intrusion is suspected to occur at depth beneath this site (Cabo Mala Pascua), comparable to that which produced 5 Ma-old dacite bodies nearby (Kimberley, 1988). Berthierine-forming exhalative plumes at Mala Pascua probably have been hotter and have risen faster than the ubiquitous glauconite-forming exhalations.

Seismic pumping like that in coastal Venezuela probably has been a prerequisite for most noncherty iron formations but the tectonic settings of cherty iron formations may have been different. Thermal (convective) pumping may have been more important for cherty iron formations but it seems likely that mechanical pumping also was required to provide the rate of exhalation needed to produce the enormous volume of some cherty iron formations.

Plume morphology and dispersal

All iron formations are attributed to ferriferous exhalation, typically into an ocean. What-

ever the source of a ferriferous plume, the distance which it reaches above a seabed partly depends upon the rate of heat dissipation and the degree of volatile segregation during exhalation. These two factors depend upon the exhalation rate (Solomon and Walshe, 1979). Highly siliceous plumes may have been moderately hot and exhaled at moderately high pressure, given the pressure-temperature control on silica solubility (Holland and Malinen, 1979). Abundant carbon dioxide and high temperature may have caused siliceous plumes to reach the surface of the sea in a few cases but the envisioned moderate temperature and high salinity of most plumes typically would have prevented such vertical mixing.

At the top of a plume, ferriferous minerals and silica could precipitate as colloids and begin moving with the prevailing current. It is unlikely, however, that prevailing currents have carried much particulate iron and silica directly to an iron-formation platform. Plumes are envisioned to have had minimal effect on surface-water chemistry but a long-lasting influence on subsurface-water chemistry, despite the brief existence of each plume. Plumes are envisioned to have existed in ferriferous oceans for only a small proportion (< 1 ppm) of the time. Subsurface-water chemistry probably has not been a simple reflection of plume chemistry but a long-term evolutionary product of both the hypothetical plumes and descending surface water, much as modern seawater is an evolutionary product of river water (Holland, 1978).

Large and thermally equilibrated water bodies

Most voluminous cherty iron formations are attributed herein to precipitation from thermally equilibrated water bodies which were sufficiently large to constitute much if not most of the water mass in a medium-sized marine basin. Thermal equilibration is assumed only within the ferriferous water body, not with the atmosphere or any overlying nonferriferous water body. Occasional exhalative input of ferriferous

water would produce transient thermal disequilibrium which would characterize little of basin history.

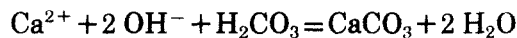
Hypothetical ferriferous water masses have been stratified in the opposite sense of modern oceans. Modern oceans are stratified such that higher temperature/higher salinity water overlies lower temperature/lower salinity water (e.g. Knauss, 1978). The bottom water in hypothetical ferriferous oceans has been hotter and more saline than surface water. Water became dense enough to sink beneath the pycnocline because of evaporation and cooling but the supply of dissolved oxygen to the ferriferous bottom water was limited because the solubility of oxygen decreases with temperature and salinity (e.g. Sonnenfeld, 1984). Modern hyper-saline water bodies may be suboxic beneath just a few meters of water depth, e.g. Boca Chica in Venezuela (Kimberley et al., in press).

Although most of the dissolved iron in the subsurface waters of ferriferous oceans is attributed to direct input by exhalation, the long-term maintenance of dissolved iron is attributed to a chemical environment like that envisioned by Holland (1984), i.e. a suboxic water body rich in SO_4^{2-} but lacking dissolved oxygen. The marine weathering reactions envisioned by Holland (1984) may have contributed some dissolved iron but clastic input near cherty iron-formation platforms clearly was minimal. Distant input may have included a potentially reactive mixture of pyroclastics, immature fluvial detritus, and iron-oxide-coated clays.

Aqueous weathering generally releases H_4SiO_4 and Fe^{2+} along with other soluble ions ($\text{Na}, \text{K}, \text{Ca}, \text{Mg}$) which are less abundant than iron or silicon in crustal rocks. A greater release of calcium and magnesium than sodium and potassium presently keeps the pH from rising into the H_3SiO_4^- field during evaporation and so silica solubility is controlled by biota. In the absence of biota, saturation would be reached with phases like opal-CT and zeolites. As previously noted, recent exhalation at Punta del Hierro, Venezuela has produced zeolite-bearing

veins just a few meters below the seafloor.

Alkalinity exerts a dominant role on the nature of weathering. There is no evidence that ferriferous water bodies have been extremely alkaline but alkalinity probably was higher than in contemporaneous nonferriferous water. Most alkaline water presently occurs where the content of aqueous CO_2 has been augmented hydrothermally and the CO_2 -charged water subsequently has reacted with silicates, particularly those of fresh volcanic or volcaniclastic rocks (Kempe and Degens, 1985). The source of iron for cherty iron formations is attributed herein to such a reaction during deep weathering. Upon evaporation or near-vent precipitation, alkaline earths ($\text{Mg}, \text{Ca}, \text{Sr}$) may precipitate as carbonates and any remaining carbonate species may become balanced by alkali elements (Na, K). Alkaline-earth ions act as a buffer against rising pH, as illustrated by the following reaction (Reaction 3):



If alkaline earths are not present to buffer rising pH, ferrous iron may assume this role.

Precipitation of siderite therefore could occur by mixing of more alkaline ferriferous seawater (richer in Fe^{2+} and OH^-) with more acidic nonferriferous seawater (richer in H_2CO_3) which would overlie the ferriferous water mass.

Development of ferriferous subsurface water probably has occurred within large but semi-enclosed basins like the Mediterranean rather than larger bodies characterized by unrestricted exchange of subsurface water with other oceans. Besides the prerequisite rapid production and new crust favored by a more radioactive planet, ferriferous water bodies probably have been favored by times with just enough continental mass to permit development of restricted basins without excessive clastic input. Local aridity may have kept clastic input low. Other favorable factors would include seismic pumping along a submerged transform fault and a partial pressure of atmospheric O_2 which

would be conducive to suboxia in a subsurface water mass.

Ferriferous subsurface water is envisioned to be suboxic (sulfate-bearing) rather than anoxic (sulfide-bearing) because of adequate mixing with oxic surface water to compensate for decay of settling organic matter. Biologic productivity in the photic zone above ferriferous water would have depended upon the frequency and composition of exhalations. It is possible that exhalation locally was slow and persistent, as appears to be the case in most glauconitic areas of the Venezuelan shelf. If so, the suprajacent photic zone may have been one of the most biologically productive non-estuarine areas on Earth. The exhalation-prone continental shelf of northeastern Venezuela shares that distinction today (Ballester and Margalef, 1965). It is difficult, however, to discern the potential contribution of exhalation to this modern productivity because the Margarita–Araya shelf may be receiving Orinoco–Amazon nutrients from the Gulf of Paria (Muller-Karger and McClain, 1987; Muller-Karger et al., 1988).

Suboxia in the hypothetical ferriferous water mass is attributed largely to oceanic stratification, occasional exhalation of methane-bearing volatiles, and organic decay rather than physical barriers which were as pronounced as in modern euxinic basins. Exhalative metals other than Fe and Mn presumably precipitated close to vents as they do today (Metz et al., 1988). Some of these metals surely escaped the immediate vicinity of vents but precipitated before reaching an iron-formation platform which typically lay hundreds of kilometers away from most vents.

Organic decay in bottom sediments could provide a little H₂S for upward diffusion from the seafloor where the H₂S could precipitate metals with lower sulfide solubility than iron or manganese, i.e. Cu, Pb, Zn, Ag, and Hg. These metals presumably were retained in deep-water shale whereas Fe and Mn migrated throughout the water mass, allowing them to precipitate along the interface with overlying surface water.

The resulting ocean would be stratified as envisioned by Borchert (1960, 1965), with H₂S-rich bottom water, suboxic intermediate-depth water, and oxic surface water (Holland, 1973; Keith, 1982). Most cherty iron formations are attributed to an extension of the suboxic–oxic interface over a shallow-water platform where precipitates did not redissolve upon settling. Although the stratified-ocean model was developed by Borchert (1952) to explain noncherty oolitic iron formations, only cherty iron formations are attributed herein to a redox-stratified ocean (Holland, 1973).

Precipitation of cherty ironstone on a platform

Precipitation of most cherty ironstone has occurred on a sediment-starved platform which probably occupied only a small part of a ferriferous basin (Morris and Horwitz, 1983). Precipitation of most shallow-water cherty ironstone is attributed to bacterially-mediated chemical reactions along an interface between iron-poor surface water and ferriferous subsurface water, comparable to that of the modern Orca Basin (La Rock et al., 1979; Sheu and Presley, 1986a).

In this model, surface water has a higher ratio of dissolved oxygen to carbon dioxide. Precipitates nucleate along the entire interface but most iron-bearing precipitates which settle away from a relatively shallow platform do not accumulate onto the seabed because of redissolution through the deep water column. A downward decrease in oxidation potential has favored dissolution of ferric precipitates and a concomitant increase in pressure has favored dissolution of siderite. Platforms therefore become a preferential sink for iron. The absolute water depth of these platforms probably has varied from a few meters to over a kilometer. A tiny amount of laminated ironstone is accumulating on a modern analog of a deep platform, the Blake Plateau off the southeastern U.S.A. (Manheim et al., 1982).

Bacterially-mediated precipitation generally

is attributed to mixing with surface water and mild cooling. Evaporation may have augmented precipitation in the shallowest environments but iron-formation platforms rarely were as shallow as the modern Bahama banks. Iron presumably has precipitated ahead of the other soluble cations partly because of oxidation and partly because its carbonate (siderite) is less soluble than the carbonates of Ca, Mg, Na, or K (Lippmann, 1973; Stumm and Morgan, 1981). Silica precipitation largely is attributed to cooling. Silica precipitation may well have been enhanced by construction of microbial tests but there is no fossil evidence in Precambrian iron formations to support this speculation. Morphological evidence exists for bacterial catalysis of iron-silica coprecipitation around modern deep-sea hydrothermal sites (Juniper and Fouquet, 1988). These bacterial forms are so delicate that they probably would not survive burial diagenesis. Preservation of siliceous microfossils is extremely rare in phosphorite-associated chert which never has been deeply buried and is less than 100 Ma old (Soudry et al., 1987). The lack of siliceous microfossils in Precambrian iron formations therefore does not rule out the possibility of ancient bacterial catalysis of iron-silica coprecipitation.

The most voluminous iron formations contain more recrystallized chert than iron minerals. Assuming a deep-weathering-exhalative origin, dissolved silica undoubtedly was introduced with hydrothermal Fe^{2+} , but the lateral extent of iron formations indicates that silica solubility cannot be attributed to temperatures vastly higher than those of contemporaneous surficial seawater. The ratio of Si/Fe is remarkably similar among all cherty iron formations, no matter how intimate their association with volcanic rocks. This lateral and temporal consistency is best explained by assuming consistent saturation with respect to mineral phases (e.g., siderite and opal-CT) at a moderate temperature. The precipitation mechanism also seems to have been consistent, probably involv-

ing bacterial mediation which resulted from minor cooling, mixing, and/or degassing. The platforms on which cherty ironstone precipitated may have included evaporitic areas which produced most of the bottom water in the hypothetical salinity-stratified oceans.

Precipitation along a deep interface would be due to diffusion but any interface shallow enough to be influenced by the wind would have internal waves travelling along the interface (Gill, 1982). These internal waves would enhance advective mixing and so the average wind velocity would control the upper boundary of the iron-rich water mass. Wind-induced upwelling is characterized by a decrease in the depth of any near-surface interface (Knauss, 1978). In the present model, wind-induced upwelling would be less effective than in the modern ocean because of the hypothetically greater increase in density with depth. Nonetheless, any coastal upwelling would preferentially induce precipitation of iron and silica (Holland, 1984).

Along modern coasts, wind commonly induces upwelling (e.g. Okuda, 1981). However, upwelling in a salinity-stratified water body could result more often from temporal variation in geothermal heating and climatic variation in the evaporative addition of hypersaline bottom water. Upwelled ferriferous water would mix with cooler surface water, promoting cooling and dilution. Turbulent mixing and iron precipitation would have characterized very shallow shelves which accumulated oolitic cherty ironstone (Dimroth and Chauvel, 1973; Hall and Goode, 1978). Oolitic cherty ironstone constitutes a higher proportion of continental-shelf (MECS) iron formations than shallow-volcanic-platform (SVOP) iron formations. The average water depth for MECS-IF apparently has been less than that of SVOP-IF because continental shelves are more commonly close to sealevel than are volcanic platforms. Isolated volcanic platforms tend to sink into oceanic lithosphere until they become guyots. Microlaminated cherty ironstone probably accumulated under a particularly deep and stable

interface between iron-poor surface water and ferriferous subsurface water.

Some microlamination in cherty ironstone may be annual (e.g. Garrels, 1987). In the exhalative model, climatically induced variation in surface water could modify its ability to cause precipitation along an interface with underlying ferriferous water. Any seasonal variation probably would be magnified by biotic response to climatic change. Photooxidative processes related to seasonal variation in solar illumination (François, 1986) are less attractive because almost all sunlight is attenuated above the probable depth of an interface which could produce microlaminated ironstone. Even though microlaminated ironstone probably was bound by a bacterial mat, bacterial binding could not have withstood very turbulent conditions and the iron-precipitating interface probably also was generally below wave base.

Microlaminae are not necessarily annual. An alternative cause of a microlamina (microband) would be an exhalative event which could recur at almost any time interval, depending on such processes as seismic pumping along an active strike-slip fault. For example, the occurrence of some exhalation somewhere in north-eastern Venezuela presently seems to be an almost annual event, based on eye-witness accounts. Microlaminated ironstone may be a product of various cyclical processes which were simultaneously active, given that lamination commonly occurs at successive scales (Trendall, 1983b; Trendall and Blockley, 1970).

Effect of the atmosphere on shallow-water iron formations

Global photosynthesis by cyanobacteria is invoked to maintain suboxic conditions in ferriferous water bodies despite occasional methaneic exhalations. Methane probably accompanied ancient exhalations as it presently does in Venezuela. There is isotopic evidence of oxygen-producing photosynthesis throughout the 3.8 Ga record of rocks on Earth (Schidlowski,

1988). Earth's atmosphere probably has been sufficiently oxidizing to precipitate ferric hydroxide and keep river water iron-depleted throughout the past 3.8 Ga (cf., Garrels, 1987). However, the Fe(II)-bearing minerals, i.e. siderite, magnetite, and the ferrous silicates, are collectively more abundant than hematite and goethite in unweathered iron formations and so oxidation has not been the sole precipitation mechanism. Precipitation of most cherty ironstone is attributed to bacterial activity along an interface across which several properties of the seawater varied, one of which was oxidation state.

Evolution of the Earth's atmosphere may have affected the development of ferriferous water bodies but variation in atmospheric oxygen has had little apparent effect on the precipitation of Phanerozoic ironstone. Phanerozoic animals record a continuously oxygen-rich atmosphere and the sedimentary structures of Phanerozoic ironstone generally record water depths shallow enough to have been affected by the atmosphere. However, the ratio of ferrous/ferric iron is no smaller in Phanerozoic ironstone than in Precambrian ironstone (Table 2).

Noncherty microlaminated ironstone in coal measures

Ironstone within coal measures traditionally has been called blackband ironstone (Stanton, 1972a). Where sufficiently thick and extensive to be mapped, a bed of blackband ironstone is classified as a coal-swamp iron formation (COSP-IF in Table 1). The prime importance of blackband ironstone is that it is the only Phanerozoic ironstone which exhibits the microlamination which characterizes a large volume of Precambrian cherty ironstone (Boardman, 1981). The small volume of young COSP-IF may help elucidate the origin of microlaminated Precambrian ironstone.

COSP-IF has been attributed to precipitation from ferriferous groundwater, analogous to bog iron deposition (Stanton, 1972a; Boardman,

1981). Ferriferous groundwater undoubtedly precipitates much of the pyrite in the marine-continental fringe around peat swamps but this process is not presently producing any extensive bed of ironstone (Andrejko et al., 1983; Harvey et al., 1983; Shimoyama, 1984). The most significant product of groundwater precipitation occurs in South Australia where water with up to 67 ppm Fe is precipitating lens-shaped goethite-hematite concretions with 30–70% Fe_2O_3 upon reaching the marine mixing zone (Ferguson et al., 1983). Ferguson et al. (1983) agree with Kimberley (1979a) that even this extreme case of groundwater supply is insufficiently potent to produce an iron formation of a few meters thickness.

Exhalation is a more promising source of iron to peat swamps, given that iron recently has accumulated at Punta del Hierro in Venezuela near the extensive Restinga peat swamp (Kimberley et al., in press). The Restinga peat lies within 12 km of another iron-concentrating area, the aforementioned iron-rich Mangle-Piedras subbasin (Fig. 20). Transgression could overlay glauconitic sand on Restinga peat with just a few meters of intervening sediment. An association of peat with overlying glauconitic sediments recurs through the Tertiary of southern Japan (Miki and Fukuoka, 1983). The peat-glaucnate association in tectonically active Japan also is attributable to seismic pumping of pore fluids.

COSP iron formations are correlative with the freshest-water facies of coal in Britain but not in Pennsylvania (Boardman, 1981). If consistently correlative with very fresh water, COSP iron formations could be attributed to a lack of sulfur under anoxic conditions, hence saturation with respect to siderite instead of pyrite. A lack of marine sulfate is not an adequate condition for iron solubility, however, because most anoxic bodies of fresh water contain either enough H_2S from decaying organic matter to precipitate iron sulfides or enough phosphate to precipitate iron as vivianite (Postma, 1981, 1982). Production of a ferriferous peat swamp

therefore requires a higher supply rate of iron than of either fluvial phosphate or organic sulfur.

A regionally high rate of iron supply apparently aided the production of coal-swamp iron formations in Britain, as evidenced by the correlation of coal-swamp iron formations with adjacent iron-rich red beds (Besley and Turner, 1983). Quaternary red beds surround the La Restinga peat swamp in Venezuela (Kimberley et al., in press). Some of this iron probably exhaled onto the surrounding coastal plain where it became mixed with fluvial sediment, as on nearby Coche Island (Kimberley and Llano, in press).

Deep-water iron formations

Most iron formations have accumulated on felsic crust which probably was not covered by deep water. Virtually all noncherty iron formations exhibit several shallow-water features, as do some cherty iron formations, e.g., the Gunflint iron formation with its stromatolite and cross-bedded oolite (Table 2). Deep-water sedimentation has produced thin beds of cherty ironstone which constitute the uppermost member of a turbidite sequence. This micro-laminated ironstone occurs more commonly in Archean than in younger sequences (Shegelski, 1978; Barrett and Fralick, 1985). The paucity of continental shelves in the Archean may have inhibited preferential precipitation on ironstone along basin edges, as hypothesized in the foregoing genetic model for shallow-water cherty iron formations. Subsurface water then would reach saturation with iron and precipitate deep-water ironstone.

Cretaceous deep-water ironstone in the Northwest Territories of Canada is particularly revealing of genetic processes. Unlike typical Phanerozoic ironstone which is restricted to a small stratigraphic interval, less than 30 m, Cretaceous ironstone along Rapid Creek occurs in thin beds which are interbedded throughout a stratigraphic range of 1 km (Young and Rob-

ertson, 1984). The ironstone is rich in both manganese (5% MnO) and phosphorus (14% P₂O₅). This ironstone is attributable to Cretaceous seismic pumping which induced migration of both petroleum and metalliferous fluids. Exhalation apparently was not sufficiently potent for long-term maintenance of a ferriferous water body and so ironstone accumulated in deep water near the hypothetical vents rather than in shallow water beneath an oxic–suboxic interface.

Samarium-neodymium isotopes in iron formations

MECS-IF, SVOP-IF, and DWAT-IF are all attributed to fluids which were moderately hot and siliceous upon exhalation. However, they differ in minor elements which presumably were leached from different rock types before or during the ascent. In the case of SVOP-IF and some DWAT-IF, the deep-weathering hypothesis would predict that much of the leached iron has come from volcanic rocks which underlay the basin (but not necessarily the iron formation).

One way to determine if the iron in a given SVOP-IF had come from leaching of an underlying volcano would be to compare isotopes of samarium and neodymium in the volcanic rocks to those in the ironstone. One would expect that the isotopic ratios for SVOP-associated volcanic rocks would indicate that differentiation of magma from the mantle occurred shortly before solidification into volcanic rock. However, all published neodymium data on iron formations indicate that differentiation from the mantle occurred long before ironstone sedimentation, indicating a sedimentary source for at least the rare-earth elements (Miller and O’Nions, 1985). Unfortunately, existing data largely represent MECS deposits and more data is needed for SVOP deposits. Moreover, additional data are required to determine if all of the sparse neodymium and samarium in cherty iron formations originated in the hypothetical deep source region for the rising ferriferous fluid

or may reflect contamination by reaction with overlying sediment. If the neodymium isotopes really do record an older source for the iron in MECS-IF, the genetic model favored herein for cherty iron formations would be untenable.

Modern and Pliocene ferriferous ooids

Why is modern marine ironstone restricted to two known localities (Mahakam Delta and Cabo Mala Pascua)? Actually, it is probable that the modern production rate of noncherty ironstone is typical of much of Earth history, given the sparse production of this rock type in most time intervals. Exhalation of carbonaceous volatiles is associated with the modern marine ferriferous oolite on the Mahakam delta of Indonesia (Allen et al., 1979; Ooi Jin Bee, 1982), with modern marine ironstone at Cabo Mala Pascua, Venezuela (Kimberley, 1988), with modern lacustrine ferriferous ooids in Lake Malawi (Muller and Forstner, 1973), and with voluminous Pliocene oolitic ironstone around the Sea of Azov, U.S.S.R. (Zitzmann, 1977; Gold and Soter, 1980). The Pliocene example is particularly graphic because the thickest ironstone accumulations (50 m) occur in basins between mud diapirs (Zitzmann, 1977). The potential for renewed ironstone sedimentation in this area probably remains high because it continues to exhibit the world’s greatest display of shallow-water volatile-induced mud diapirism (Shaulov, 1973). Moreover, some Pliocene formation fluids under the adjacent Caspian Sea contain over 20% salt (Arkhipov, 1982).

Exhalation has not previously been invoked to explain most of the modern and Pliocene ferriferous ooids. Allen et al. (1979) attribute the Mahakam ferriferous ooids to fluvial transport of iron dissolved from deltaic sediment. Lemmoalle and Dupont (1973) attribute the ferriferous ooids of Lake Chad to lacustrine leaching of iron oxides which had coated clays supplied by the Chari river. Exhalative fluids are invoked by Muller and Forstner (1973), however, to explain ferriferous ooids in Lake

Malawi. Lake Malawi apparently has accumulated a thick sequence of both evaporitic and carbonaceous sediment, as have other lakes along the African rift system (Johnson et al., 1987). Metamorphism of this sediment is a potential source of the putative exhalative fluids (Muller and Forstner, 1973).

Origin of oolitic noncherty iron formations (SCOS-IF)

SCOS iron formations are attributed to exhaled hypersaline solutions which have risen along deep faults. Hydrothermal alteration is evident near the modern SCOS deposit at Cabo Mala Pascua (Kimberley, 1988). In this modern environment, one may sample the entire ambient surface whereas only a trivial portion of the surface of subjacent rocks is observable under or around ancient iron formations. Sampling generally is limited to vertical sections. The hypothetical channelways for fluids would have occupied such small volumes of rock that the probability of observing them near ancient SCOS iron formations is minuscule.

There is no known evidence of a hydrothermal vent under an ancient SCOS iron formation. However, indirect evidence for exhalation along a coastal fault exists in the distribution and morphology of several SCOS iron formations. For example, the Ordovician Chrustenice SCOS-IF accumulated along the flank of the incipient Prague Fault in Czechoslovakia (Petránek et al., 1988). Several German SCOS deposits thicken toward one end and then terminate abruptly (Finkenwirth, 1964; Bottke et al., 1969). Direct evidence for high salinity in the iron-depositing fluids is provided by the incorporation of chlorine into berthierine in the Eocene Paz de Rio SCOS-IF (Kimberley, 1974). Similar microprobe studies of other Tertiary berthierine ooids should be conducted to determine if chlorine occurs in other young berthierine.

Modern ferriferous saline fluids occur in the subsurface around the Gulf of Mexico (Salvador, 1987; Sverjensky, 1984; Posey et al., 1986).

Fluids from this basin apparently formed both Eocene SCOS-IF in Texas (Foos, 1984) and Jurassic manganese ore in Mexico (Okita et al., 1986). Lead-zinc-rich examples of this fluid presently exhibit ratios of zinc/iron and lead/iron which approximate 1/50 (Kharaka et al., 1980). Similar ratios locally are found in SCOS-IF (Fig. 2 of Siehl and Thein, 1978). Fluid compositions which are intermediate between ferriferous ore fluids and Pb-Zn ore fluids have been documented by Blasch and Coveney (1988).

The source of SCOS-IF iron is attributed to dissolution reactions which involve hydration of ophiolite, evaporite and/or cooling plutons within a thick sedimentary pile. The resulting hypothetical saline fluids would be corrosive to several metals and could produce fluids with abundances of those metals proportionate to their crustal abundances. In particular, SCOS iron formations contain two abundant elements which commonly exhibit a roughly one-to-fifty proportion with iron just as in average continental lithosphere (Table 2). These are manganese and phosphorus, each of which constitutes about 0.1% of the continental lithosphere whereas iron constitutes 5.7% Fe (Beus, 1979).

The fluids which precipitated SCOS-IF clearly were not in chemical equilibrium with the oceanic environment in which they accumulated, given shallow-water sedimentary structures in the Fe(II)-rich ironstone (Kimberley, 1979a; Petránek et al., 1988). Despite attempts to construct thermodynamic models which suggest compatibility with slightly modified seawater (e.g. Curtis and Spears, 1968), the ferriferous fluids either were hypersaline or were devoid of sulfur, in addition to being too reducing for observed fossil life. Metazoan fossils are common in Phanerozoic SCOS-IF (Table 2) and indicate that the environment was normal except for the apparently short-lived introduction of ferriferous fluids. Calculation of the sedimentation rate for Pliocene SCOS-IF demonstrates that the fluids must have been more

ferriferous than the few ppm Fe which typically is modeled, provided that one excludes the possibility of diagenetic input of iron subsequent to sedimentation. Exclusion of this possibility is recommended herein (cf. Kimberley, 1979a).

The most consistent direct evidence of an exhalative origin for SCOS-IF is the high angularity of most quartz grains which occur in oolitic ironstone (Table 2). This angularity not only confirms a high sedimentation rate but probably records the violence of SCOS-IF exhalation. The scarcity of quartz or any other clastic grains in clastic-associated SCOS-IF is difficult to explain without invoking a process like that which Cayeux (1922, p. 40) called "rupture d'équilibre". This is especially obvious in the Paz de Rio SCOS-IF where the enclosing clastic sediments apparently were accumulating rapidly and yet much of this ironstone is pure chemical sediment (Kimberley, 1980).

Silicon consistently is depleted in SCOS ironstone relative to average continental lithosphere. This observation is somewhat misleading, however, since SCOS ironstone commonly contains as much chemically-concentrated silicon as iron. Most of this silicon occurs within an authigenic silicate (berthierine) which generally has a serpentine structure initially (Brindley, 1982; Van Houten and Purucker, 1984) but which converts to a chlorite structure (chamosite) upon deep burial (Maynard, 1986). Some ooids may have been chamosite initially given that Hardjosoesastro (1971) has found modern chamositic peloids. The source of most SCOS-IF silica is attributed to exhalation because of the apparently high sedimentation rate of SCOS-IF and its lack of admixed clastic sediment. SCOS-IF fluids probably lost several ions to ordinary seawater upon mixing, e.g. potassium and chlorine, but it is unlikely that ordinary seawater contributed much to the rapidly accumulating chemical sediment.

It is hypothesized that ooid-forming exhalations are individually more voluminous and iron-rich but of briefer duration than glauconite-forming exhalations. The ooids themselves

are believed to form rapidly upon mixing of hypersaline exhaled fluid with seawater. Violent exhalation is envisioned to break early-formed ooids and deposit fresh rims around the fragmental nuclei. This may explain why ferriferous ooids consistently display more fragmentation than do calcareous ooids (Table 2; Kimberley, 1979a, 1983b).

Exhalative fluids clearly may exhibit geographic variation in composition (e.g., Sorokin et al., 1979). However, the distribution of modern berthierine ironstone versus glauconitic sand in coastal Venezuela (Fig. 21) is more readily attributed to a difference in exhalation rate rather than a major difference in composition. Both glauconite and berthierine are accumulating in equally shallow water but only glauconite has been found under deep water. Porrenga (1967) and Berg-Madsen (1983) have proposed that water-depth control on temperature generally controls glauconite (cooler) versus berthierine (warmer) precipitation. However, there is no difference in seabed temperature between the shallow-water occurrences of glauconite versus berthierine in Venezuela or elsewhere (Rohrlich et al., 1969).

The preferential precipitation of glauconite under deep water is attributed to a slower exhalation of compositionally similar fluids under the greater weight of overlying water. Precipitation from this slowly rising water apparently occurs before reaching the seafloor and so the resulting precipitate (glauconite) is a better indicator of the exhalative (potassium-rich) fluid composition than is the shallow-water berthierine at Cabo Mala Pascua (Kimberley, 1988).

Once formed in shallow water, a mass of ferriferous ooids or glauconitic pellets would be subjected to wave and tidal transport like any marine sand, forming sand waves and barrier bars (Maynard, 1983; Teyssen, 1984). The shallowest portion of the bar would become preferentially oxidized and this portion would become the stratigraphic middle of the ironstone bed, e.g., the oxidized middle of the Paz

de Rio SCOS-IF (Kimberley, 1980). If exhalation were to occur within a protected lagoon, lagoonal ferriferous mud might grade to an oolitic bar, as in Silurian SCOS-IF of Alabama (Sheldon, 1970) and Eocene SCOS-IF of Texas (Foos, 1984).

Glaconitic pellets have accumulated in barrier islands and tidal inlets just like ooids (Chafetz, 1978). The lack of oolitic texture among glaconitic grains in such high-energy environments is interpreted to indicate that oolitic texture in SCOS-IF forms during exhalation rather than during erosion of some ferriferous precipitate. Potential differences in grain-surface microbiota are not considered to be important (cf. Dahanayake and Krumbein, 1986). Unlike ooids, the majority of glaconitic grains are attributed to slowly and persistently rising ferriferous fluids which precipitate iron just below the sediment-water interface due to reaction with suboxic porewater.

The dearth of Carboniferous SCOS-IF (Table 2) is attributed to a relative lack of contemporaneous seismic pumping. The lack of seismic pumping is attributed to a paucity of submarine transform faults along continental margins. Nonetheless, weak exhalation may have been responsible for the thin coal-swamp iron formations (COSP-IF) which characterize the Carboniferous. Exhalative fluids presumably produced ferriferous subsurface water in the small volumes of coal swamps as they had in the enormous volumes of some Precambrian rift basins. As previously noted herein, COSP-IF ironstone typically is microlaminated (banded) siderite which resembles Precambrian banded iron-stone (Boardman, 1981).

Manganese-rich iron formations and manganese formations

In iron formations with highly variable concentrations of manganese, the ratio of Mn/Fe commonly is highest either at the bottom or the top of the iron formation, e.g. the base of the Archean Outerring iron formation and the top

of the Pliocene Kerch iron formation (Table 2; Sokolova, 1964). An enrichment of exhalative manganese may be explained by the more rapid precipitation of iron upon mild oxidation (Stumm and Morgan, 1981). Although this mechanism could account for subsequent migration of aqueous manganese toward a shallow-water repository, an alternative concentration mechanism is favored herein. The preferred model invokes differential dissolution rather than differential precipitation (Postma, 1985).

To explain manganese nodules, Postma (1985) showed experimentally that a minor concentration of aqueous Fe^{2+} is sufficient for rapid reduction and mobilization of most of the available manganese encountered by a throughgoing fluid. If an exhalative system started or ended with weak concentrations of Fe^{2+} in a fluid rising through voluminous sediment (+/- pyroclastic sediment), manganese could be leached until richer than iron. If the exhalative system started and remained poor in iron but rich in volume of leached sediment, a sedimentary manganese deposit could result. Differential dissolution is preferable to differential precipitation because manganese deposits generally do not exhibit much gradation laterally in the ratio of Fe/Mn (e.g. Force and Cannon, 1988). Alternative genetic models for manganese formations based on a shallow-weathering source are considered no more viable than are shallow-weathering models for iron formations (cf. Frakes and Bolton, 1984; Bolton and Frakes, 1985; Bandopadhyay, 1988; Force and Cannon, 1988; Okita et al., 1988).

The definition of a "manganese formation" parallels that of an iron formation, i.e., a stratigraphic unit which is largely composed of a chemical sedimentary rock which contains more than 15% Mn. Manganese formations are rare in stratigraphic sequences of all ages (Force and Cannon, 1988). Only one significant manganese formation occurs in North America (Okita et al., 1988). The ratio of the total volume of manganese formations to the total volume of iron formations worldwide is less than

the ratio of these elements in average continental lithosphere, i.e. 1/60 (Beus, 1979). The single North American ore deposit occurs in Jurassic strata near Molango, Mexico (Okita et al., 1986, 1988). This deposit accumulated at a time of early rifting in the Gulf of Mexico (Salvador, 1987).

Processes similar to those invoked herein for iron formations are considered to be responsible for manganese formations. Rhodochrosite ($MnCO_3$) in manganese formations exhibits the same peculiar enrichment in ^{12}C that siderite ($FeCO_3$) exhibits in iron formations (Okita et al., 1988). This enrichment is attributed herein to an exhalative fluid because calcite and dolomite associated with rhodochrosite and siderite generally record no ^{12}C enrichment in contemporaneous seawater. Manganese mineralization at Molango, Mexico is correlative with an enrichment in ^{18}O (Okita et al., 1988) whereas iron enrichment in iron formations is correlative with a depletion in ^{18}O (Baur et al., 1985). This difference is attributed to a higher temperature of reaction during dissolution of manganese deep in the crust (Muehlenbachs, 1986).

Ferriferous ooids locally occur in both manganese and phosphate deposits (e.g. Sokolova, 1964, p. 177). Moreover, SCOS iron formations locally are phosphatic and/or manganiferous, e.g. phosphatic Ordovician SCOS-IF in Newfoundland (Hayes, 1915) and manganiferous Pliocene SCOS-IF around the Sea of Azov (Yakontova et al., 1985). However, ironstone of all types generally displays less segregation of iron from manganese than typically is achieved by modern biologic processes. The typical similarity of the Fe/Mn ratio in ironstone to that in average continental lithosphere is evidence against highly selective precipitation by biota to concentrate the iron in iron formations (Kimberley, 1983).

Conclusion

The prime issue which this paper addresses is whether shallow or deep weathering has been

the prime source of the iron in iron formations. It is concluded that all iron formations are attributable to exhalation of fluids which have become ferriferous because of deep weathering. However, modeling of iron-formation genesis by exhalation has advanced little beyond the work of Van Hise and Leith (1911) despite great advances in modeling other exhalative ores.

Gruner (1922) initiated the ongoing nonexhalative modeling of cherty iron formations, followed by James (1954, 1966), Cloud (1973), Holland (1984), and Garrels (1987), among many others (listed in Kimberley, 1983). Gruner (1922) proposed a fluvial source because he incorrectly assumed that the Amazon averages 3 ppm Fe whereas it actually contains 0.03 ppm Fe (Gibbs, 1972). Gruner eventually started the tradition of conceptual shifts by iron-formation modelers (e.g. Young, 1976, 1982) when he endorsed exhalation 24 years later. The present author also is abandoning his previous support of shallow weathering in favor of deep weathering, after 15 years (Kimberley, 1974, 1979a, 1980, 1981b, 1986).

Future understanding of iron formations probably will come most rapidly from analysis of modern ferriferous exhalations. Glauconite-forming exhalations are widespread, e.g., along the Venezuelan coast. Ooid-forming exhalations are less widespread and probably more sporadic. Future analysis should reveal both the depth and chemical reactions within the region where Fe^{2+} is dissolving. Study of the hypersaline deeps in the Red Sea already has elucidated some of the processes which form cherty iron formations.

The proposed origin of cherty iron formations differs from accepted models for most other geologic phenomena in that modern rates of the hypothetical iron-concentrating process are considered to be much smaller than the rates which have generated voluminous ancient deposits, particularly Early Proterozoic iron formations. Ancient exhalation presumably was much greater than that from such modern vents as the Ebeko volcano in the Kurile islands (Ze-

lenov, 1960; Holland, 1984, p. 386). The greater dynamics of a younger and more radioactive planet probably produced greater seismic pumping through cooling igneous rock.

At less than 300°C, newly formed hydrous minerals preferentially incorporate ^{18}O during crustal hydration and so the circulating seawater becomes enriched in ^{18}O before exhaling back into the ocean. This exhaling ferriferous fluid presumably dominates a subsurface water mass long enough to produce a cherty iron formation which is enriched in ^{18}O . Precipitation of cherty ironstone is attributed to mixing along an interface with iron-poor surface water which is cooler and less saline.

If iron formations are exhalative, it follows that most phosphorite and sedimentary manganese deposits also are exhalative but elaboration of this conclusion is beyond the scope of this paper. Iron formations, manganese deposits, and phosphorites have been attributed by previous authors to temporal variation in biota, climate, and/or atmospheric composition. It is more likely that the true relationship is the inverse of what has been proposed and that these three environmental factors have been largely controlled by global variation in the tectonomagmatic processes which have simultaneously produced iron formations.

Tectonomagmatic processes produce and consume volatiles. Atmospheric accumulation of CO_2 , for example, accompanies rapid differentiation of the mantle to produce crust whereas CO_2 becomes depleted during subsequent deep and shallow weathering. Iron formations are attributed to deep weathering aided by seismic pumping of seawater along submarine transform fault zones. An eventual understanding of iron formations will help elucidate the major tectonomagmatic cycles of planet Earth.

Acknowledgements

Like many others, the author has found the problem of iron-formation genesis to be formidable. Despite instruction from Dick Hutchin-

son at the University of Western Ontario, the importance of exhalation was not appreciated before conducting a dozen field trips to modern iron-concentrating areas in coastal Venezuela. Logistics in Venezuela have been facilitated by the Fundacion La Salle de Ciencias Naturales. Two mentors at Princeton University taught the author how to interpret aqueous geochemistry (Dick Holland) and the dependence of sedimentation on tectonics (Franklyn Van Houten). Innumerable other colleagues have made contributions, including Alan Goodwin who noted that any overview is limited by the fact that "we are all prisoners of our own experience".

References

- Addy, S.K. and Behrens, E.W., 1980. Time of accumulation of hypersaline anoxic brine in Orca Basin (Gulf of Mexico). *Mar. Geol.*, 37: 241-252.
- Adeleye, D.R., 1973. Origin of ironstones, an example from the middle Niger valley, Nigeria. *J. Sediment. Petrol.*, 43: 709-727.
- Aharon, P., Schidlowski, M., and Singh, I.B., 1987. Chronostratigraphic markers in the end-Precambrian carbon isotope record of the Lesser Himalaya. *Nature*, 327: 699-702.
- Aldinger, H., 1957. Zur Entstehung der Eisenoolithe im schwäbischen Jura. *Z. Dtsch. Geol. Ges.*, 109: 7-9.
- Alexandrov, E.A., 1979. Atlas of structures and textures of the volcanogenetic-sedimentary iron ores of Altai (A.S. Kalugin). *Econ. Geol.*, 74: 171-172.
- Allaart, J.H., 1976. The pre-3760 m.y. old supracrustal rocks of the Isua area, central west Greenland, and the associated occurrence of quartz-banded ironstone. In: B.F. Windley (Editor), *The Early History of the Earth*. Wiley-Interscience, London, pp. 177-189.
- Allen, G.P., Laurier, D. and Thouvenin, J., 1979. Etude sédimentologique du delta de la Mahakam. Cie. Fr. Pet., Notes Mem., Paris (Total), 15, 156 pp.
- Aller, R.C. and Dude, P.D., 1988. Complete oxidation of solid phase sulfides by manganese and bacteria in anoxic marine sediments. *Geochim. Cosmochim. Acta*, 52: 751-765.
- Aller, R.C. and Mackin, J.E., 1988. The dominant role of Fe-reduction in Amazon inner shelf muds. *Proc. Am. Geophys. Union, Chapman Conf. Fate of Particulate and Dissolved Components within the Amazon Dispersal System: River and Ocean*, Charleston, S. C., p. 16.
- Aller, R.C., Mackin, J.E. and Cox, R.T., Jr., 1986. Diagenesis of Fe and S in Amazon inner shelf muds: apparent

- dominance of Fe reduction and implications for the genesis of ironstones. *Cont. Shelf Res.*, 6: 263-289.
- Alling, H.L., 1947. Diagenesis of the Clinton hematite ores of New York. *Geol. Soc. Am. Bull.*, 58: 991-1018.
- Al-Shanti, A.M.S., 1966. Oolitic iron ore deposits in Wadi Fatima between Jeddah and Mecca, Saudi Arabia. *Saudi Arabia, Minist. Pet. Miner. Res., Bull.*, 2, 51 pp.
- Alvarez-Espejo, R., 1985. Dinamica sedimentaria en los canales Margarita-Coche-Araya. *Fund. Salle Cienc. Nat., Estac. Invest. Marinas de Margarita, Contrib.* 130.
- Ambrosi, J.P. and Nahon, D., 1986. Petrological and geochemical differentiation of lateritic iron crust profiles. *Chem. Geol.*, 57: 371-393.
- Anderson, D.M., Coats, D.W. and Tyler, M.A., 1985. Encystment of the dinoflagellate *Gyrodinium uncatenatum*: temperature and nutrient effects. *J. Phycol.*, 21: 200-206.
- Andrejko, M.J., Cohen, A.D. and Raymond, R. Jr., 1983. Origin of mineral matter in peat. In: R. Raymond, Jr. and M.J. Andrejko (Editors), *Mineral Matter in Peat, its Occurrence, Form, and Distribution*. Los Alamos Natl. Lab., Los Alamos, N.M., Rep. LA-9907-OBES, pp. 3-24.
- Appel, P.W.U., 1979a. Stratabound copper sulfides in a banded iron-formation and in basaltic tuffs in the Early Precambrian Isua supracrustal belt, West Greenland. *Econ. Geol.*, 74: 45-52.
- Appel, P.W.U., 1979b. Cosmic grains in an iron-formation from the Early Precambrian Isua supracrustal belt, West Greenland. *J. Geol.*, 87: 573-578.
- Appel, P.W.U., 1980. On the early Archaean Isua iron-formation, west Greenland. *Precam. Res.*, 11: 73-87.
- Apted, M.J., Waychunas, G.A. and Brown, G.E., 1985. Structure and specification of iron complexes in aqueous solutions determined by X-ray absorption spectroscopy. *Geochim. Cosmochim. Acta*, 49: 2081-2089.
- Arkipov, A.S., 1982. Hydrochemical characteristics of subsurface waters of the Pliocene sediments of the West Turkmen depression and its oil-gas potential. *Pet. Geol. (USSR)*, 20: 529-531.
- Awramik, S.M. and Barghoorn, E.S., 1977. The Gunflint microbiota. *Precam. Res.*, 5: 121-142.
- Ayres, D.E., 1972. Genesis of iron-bearing minerals in banded iron formation mesobands in the Dales Gorge Member, Hamersley Group, Western Australia. *Econ. Geol.*, 67: 1214-1233.
- Bäcker, H. and Lange, J., 1987. Recent hydrothermal metal accumulation, products and conditions of formation. In: P.G. Teleki, M.R. Dobson, J.R. Moore, and U. von Stackelberg (Editors), *Marine Minerals*. NATO Ser. C, 194. Reidel, Dordrecht, pp. 317-337.
- Bäcker, H. and Richter, H., 1973. Die rezenten hydrotherm-sedimentären Lagerstätten Atlantis-II-Tief im Roten Meer. *Geol. Rundsch.*, 62: 697-740.
- Baligh, M., Azzouz, A.S. and Martin, R.T., 1980. Core penetration tests offshore the Venezuelan coast. M.I.T. Sea Grant Rep., MITSG-80-21, 163 pp.
- Ballester, A. and Margalef, R., 1965. Producción primaria. In: *Estudios sobre el ecosistema pelágico del NE de Venezuela*. Mem. Soc. Cienc. Nat. La Salle, 25 (70, 71, and 72): 207-221.
- Bandopadhyay, P.C., 1988. Syndepositional and postdepositional features of the manganese deposits of the Proterozoic Penganga Group, Adilabad district, Andhra Pradesh, India. *Miner. Deposita*, 23: 115-122.
- Baragar, W.R.A., 1975. Miscellaneous data from volcanic belts at Yellowknife, Wolverine Lake, and James River, N.W.T. *Geol. Surv. Can., Pap.* 75-1 (A): 281-286.
- Barrett, T.J. and Jarvis, I., 1988. Rare-earth element geochemistry of metalliferous sediments from DSDP leg 92: the East Pacific Rise transect. *Chem. Geol.*, 67: 243-259.
- Barrett, T.J. and Fralick, P.W., 1985. Sediment redeposition in Archean iron formation: examples from the Beardmore-Geraldton greenstone belt, Ontario. *J. Sediment. Petrol.*, 55: 205-212.
- Barrett, T.J., Taylor, P.N. and Lugowski, J., 1987. Metalliferous sediments from D.S.D.P. leg 92: The East Pacific Rise transect. *Geochim. Cosmochim. Acta*, 51: 2241-2253.
- Bartholomew, P.R., Meyers, W.J. and Hanson, G.N., 1987. Glauconite as a geochemical indicator. *Geol. Soc. Am., Abstr. with Programs*, 19: 581.
- Barusseau, J.P. and Giresse, P., 1987. Some mineral resources of the West African continental shelves related to Holocene shorelines: phosphorite (Gabon, Congo), glauconite (Congo) and ilmenite (Senegal, Mauritania). In: P.G. Teleki, M.R. Dobson, J.R. Moore, and U. von Stackelberg (Editors), *Marine minerals*. NATO ASI Ser. C, 194. Reidel, Dordrecht, 588 pp.
- Bathurst, R.G.C., 1975. *Carbonate Sediments and their Diagenesis*, 2nd ed. Elsevier, Amsterdam, 658 pp.
- Baur, M.E., Hayes, J.M., Studley, S.A. and Walter, M.R., 1985. Millimeter-scale variations of stable isotope abundances in carbonates from banded iron-formations in the Hamersley Group of Western Australia. *Econ. Geol.*, 80: 270-282.
- Bayley, R.W., 1959. Geology of the Mary Lake quadrangle, Iron County, Michigan. *U.S. Geol. Surv., Bull.*, 1077, 112 pp.
- Bayley, R.W., 1963. A preliminary report on the Precambrian iron deposits near Atlantic City, Wyoming. *U.S. Geol. Surv., Bull.*, 1142-C, 23 pp.
- Bayley R.W. and James, H.L., 1973. Precambrian iron-formations of the United States. *Econ. Geol.*, 68: 934-959.
- Bayley, W.S., 1904. The Menominee iron-bearing district of Michigan. *U.S. Geol. Surv., Monogr.*, 46, 513 pp.
- Bearce, D.N., 1973. Origin of conglomerates in Silurian Red Mountain Formation of central Alabama; their paleogeographic and tectonic significance. *Am. Assoc. Pet. Geol., Bull.*, 57: 688-701.
- Bedarida, F. and Pedemonte, G.M., 1971. Hematite to goethite surface weathering. *Am. Mineral.*, 56: 1469-1473.

- Beets, D.J., Maresch, W.V., Klaver, G.T., Mottana, A., Bocchio, R., Beunk, F.F. and Monen, H.P., 1984. Magmatic rock series and high-pressure metamorphism as constraints on the tectonic history of the southern Caribbean. *Geol. Soc. Am., Mem.*, 162: 95-130.
- Belevtsev, Ya.N., 1954. Sopostavlenie zelezorudnix svit po-kembria SSSR (Comparison of iron ore suites in the USSR). *Dokl. Akad. Nauk Uzb. SSSR*, 97: 499-502.
- Belevtsev, Ya.N., 1973. Genesis of high-grade iron ores of Krivoyrog type. In: *Genesis of Precambrian Iron and Manganese Deposits*. Proc. Kiev Symp. (1970), UNESCO, Paris, 9: 167-180.
- Berg, G., Dahlgrun, F. and Martini, H.J., 1942a. Die Erze des bohemischen Untersilurs. In: B. Brockamp (Editor), *Zur Entstehung deutscher Eisenerzlagerstaetten*. Arch. Lagerstaettenforsch., 75: 150-155.
- Berg, G., Seitz, O. and Teichmuller, R., 1942b. Die Eisenherze im Korallenoolith von Braunschweig. In: B. Brockamp (Editor), *Zur Entstehung deutscher Eisenerzlagerstaetten*. Arch. Lagerstaettenforsch., 75: 71-78.
- Berge, J.W., 1971. Iron formation and supergene iron ores of the Goe range area, Liberia. *Econ. Geol.*, 66: 947-960.
- Berge, J.W., 1974. Geology, geochemistry and origin of the Nimba itabirite and associated rocks, Nimba County, Liberia. *Econ. Geol.*, 68: 80-92.
- Berg-Madsen, V., 1983. High-alumina glaucony from the Middle Cambrian of Oland and Bornholm, southern Baltoscandia. *J. Sediment. Petrol.*, 53: 875-893.
- Bermudez, P.J., 1966. Consideraciones sobre los sedimentos del Miocene medio al Reciente de las costas central y oriental de Venezuela. Primera parte: Ministerio de Minas e Hidrocarburos, Venezuela. *Bol. Geol.*, 7: 333-411.
- Bernard, A.J., Dagallier, G. and Soler, E., 1982. The exhalative sediments linked to the volcanic exhalative massive sulphide deposits: A case study of European occurrences. In: G.C. Amstutz et al. (Editors), *Ore Genesis, the State of the Art*. Soc. Geol. Appl. Miner. Dep., Spec. Publ., 2, Springer, Berlin, pp. 553-564.
- Berner, R.A., 1969. Migration of iron and sulfur within anaerobic sediments during early diagenesis. *Am. J. Sci.*, 267: 19-42.
- Berner, R.A., 1980. Early Diagenesis, a Theoretical Approach. Princeton Univ. Press, Princeton, N.J., 241 pp.
- Berner, R.A., 1981. A new geochemical classification of sedimentary environments. *J. Sediment. Petrol.*, 51: 359-365.
- Berner, R.A., 1984. Sedimentary pyrite formation: an update. *Geochim. Cosmochim. Acta*, 48: 605-615.
- Berner, R.A. and Landis, G.P., 1987. Chemical analysis of gaseous bubble inclusions in amber: the composition of ancient air? *Geol. Soc. Am., Abstr. Progr.*, 19: 587.
- Bertram, E.F. and Mellon, G.B., 1975. Peace River iron deposits. Alberta Res. Counc. Inf. Ser., 75, 53 pp.
- Besly, B.M. and Turner, P., 1983. Origin of red beds in a moist tropical climate (Etruria Formation, Upper Carboniferous, UK). In: R.C.L. Wilson (Editor), *Residual Deposits; Surface Related Weathering Processes and Materials*. Geol. Soc. London, Spec. Publ., 11: 131-147.
- Beukes, N.J., 1973. Precambrian iron formations of southern Africa. *Econ. Geol.*, 68: 960-1004.
- Beukes, N.J., 1980. Suggestions towards a classification of and nomenclature for iron-formation. *Trans. Geol. Soc. S. Afr.*, 83: 285-290.
- Beukes, N.J., 1983. Paleoenvironmental setting of iron-formations in the depositional basin of the Transvaal Supergroup, South Africa. In: A.F. Trendall and R.C. Morris (Editors), *Iron-formation: Facts and Problems*. Elsevier, Amsterdam, pp. 131-209.
- Beus, A.A., 1979. The chemical composition and origin of the primeval continental crust. In: L.H. Ahrens (Editors), *Origin and Distribution of the Elements*. Pergamon, Oxford, pp. 519-525.
- Bhattacharyya, D., 1980. Sedimentology of the Late Cretaceous Nubia Formation of Aswan, southeast Egypt, and the origin of the associated ironstones. Ph.D. thesis, Princeton Univ., Princeton, N.J., 122 pp.
- Bhattacharyya, D.P. and Kakimoto, P.K., 1982. Origin of ferriferous ooids; an SEM study of ironstone ooids and bauxite pisoids. *J. Sediment. Petrol.*, 52: 849-857.
- Bichelonne, J. and Angot, P., 1939. Le bassin ferrifere de Lorraine: Nancy-Strasbourg. Berger-Levrault, 438 pp.
- Blasch, S.R. and Coveney, R.M., Jr., 1988. Goethite-bearing brine inclusions, petroleum inclusions, and the geochemical conditions of ore deposition at the Jumbo mine, Kansas. *Geochim. Cosmochim. Acta*, 52: 1007-1017.
- Blatt, H., Middleton, G., and Murray, R., 1980. *Origin of Sedimentary Rocks*, 2nd ed. Prentice-Hall, Englewood Cliffs, N.J., 782 pp.
- Bloch, S., 1978. Phosphorus distribution in smectite-bearing basal metalliferous sediments. *Chem. Geol.*, 22: 353-359.
- Boardman, E.L., 1981. The genesis of Coal Measure blackband ironstones. Ph.D. dissertation, Aston Univ., Birmingham, 149 pp.
- Boast, A.M., Coleman, M.L. and Halls, C., 1981. Textural and stable isotopic evidence for the genesis of the Tynagh base metal deposit, Ireland. *Econ. Geol.*, 76: 27-55.
- Boesen, C. and Postma, D., 1988. Pyrite formation in anoxic environments of the Baltic. *Am. J. Sci.*, 288: 575-603.
- Bogashova, L.G., 1987. The role of evaporite basins in producing stratiform mineralization. *Int. Geol. Rev.*, 29: 481-490.
- Bolton, B.R. and Frakes, L.A., 1985. Geology and genesis of manganese oolite, Chiatura, Georgia, U.S.S.R. *Geol. Soc. Am. Bull.*, 96: 1398-1406.
- Bonte, P., Lalou, C. and Latouche, C., 1980. Ferromanganese deposits in cores from the Kane and Atlantis fracture areas: possible relationships with hydrothermalism. *J. Geol. Soc. London*, 137: 373-377.
- Borchert, H., 1952. Die Bildungsbedingungen mariner Ei-

- senerzlagerstaetten: Chem. Erde, 60: 49–73.
- Borchert, H., 1960. Genesis of marine sedimentary iron ores. Inst. Min. Metall. Trans., 69: 261–279.
- Borchert, H., 1965. Formation of marine sedimentary iron ores. In: J.P. Riley and G. Skirrow (Editors), Chemical Oceanography. 2: Academic Press, New York, N.Y., pp. 159–204.
- Bornhold, B.D. and Giresse, P., 1985. Glauconitic sediments on the continental shelf off Vancouver Island, British Columbia, Canada. J. Sediment. Petrol., 55: 653–664.
- Boskovitz-Rohrlich, V., Mitzmayer, A., and Mizrahi, Y., 1963. Structure and beneficiation of a low grade iron ore. Min. Mag., 108: 325–331.
- Bottke, H., 1965. Die exhalativ-sedimentaren Devonischen Roteisensteinlagerstatten des Ostsauerlandes. Beih. Geol. Jahrb., 63, 147 pp.
- Bottke, H., 1966. Die faziesgebundene Tektonik vulkanischer Schwellen im ostrheinischen Schiefergebirge. Geol. Rundsch., 55: 666–698.
- Bottke, H., Dengler, H., Finkenwirth, A., Gruss, H., Hoffman, K., Kolbe, H., Simon, P. and Thienhaus, R., 1969. Sammelwerk Deutsche Eisenerzlagerstatten, II.1. Die marin-sedimentaren Eisenerze des Jura in Nordwestdeutschland. Beih. Geol. Jahrb., 79: 391 pp.
- Bowles, F.A. and Fleischer, P., 1985. Orinoco and Amazon River sediment input to the eastern Caribbean basin. Mar. Geol., 68: 53–72.
- Boyer, P.S., Guinness, E.A., Lynch-Blosse, M.A. and Stolzman, R.A., 1977. Greensand fecal pellets from New Jersey. J. Sediment. Petrol., 47: 267–280.
- Brandt, R.T., Dorr, J.V.N.II, Gross, G.A., Gruss, H. and Semenenko, N.P., 1973. Problems of nomenclature for banded ferruginous-cherty sedimentary rocks and their metamorphic equivalents. In: Genesis of Precambrian iron and manganese deposits. Proc. Kiev Symp. (1970), UNESCO, Paris, 9: 377–380.
- Brasier, M.D., 1980. The Lower Cambrian transgression and glauconite-phosphate facies in western Europe. J. Geol. Soc. London, 137: 695–703.
- Braterman, P.S., Cairns-Smith, A.G. and Sloper, R.W., 1983. Photo-oxidation of hydrated Fe^{2+} – Significance for banded iron formations. Nature, 303: 163–164.
- Brewer, P.G. and Spencer, D.W., 1974. Distribution of some trace elements in Black Sea and their flux between dissolved and particulate phases. In: E.T. Degens and D.A. Ross (Editors), The Black Sea – Geology, Chemistry, and Biology. Am. Assoc. Pet. Geol. Mem., 20: 137–143.
- Bridgwater, D., Collerson, K.D. and Myers, J.S., 1978. The development of the Archaean gneiss complex of the North Atlantic region. In: D.H. Tarling (Editor), Evolution of the Earth's Crust. Academic Press, London, pp. 19–69.
- Brindley, G.W., 1982. Chemical compositions of berthierines – A review. Clays Clay Miner., 30: 153–155.
- Brockamp, B. (Editor), 1942. Zur Entstehung deutscher Eisenerzlagerstatten. Arch. Lagerstättforsch., 75, 186 pp.
- Bronner, G. and Chauvel, J.J., 1979. Precambrian banded iron-formations of the Ijil Group (Kediat Ijil, Reguibat shield, Mauritania). Econ. Geol., 74: 77–94.
- Bubenicek, L., 1971. Géologie du gisement de fer de Lorraine. Bull. Cent. Rech. Pau, Soc. Nat. Pet. Aquitaine, 5: 223–320.
- Buckley, H.A., Bevan, J.C., Brown, K.M., Johnson, L.R. and Farmer, V.C., 1978. Glauconite and celadonite: two separate mineral species. Mineral. Mag., 42: 373–382.
- Buick, R. and Dunlop, J.S.R., 1987. Early Archean evaporitic sediments from the Warrawoona Group, North Pole, Western Australia. Geol. Soc. Am., Abstr. Programs, 19: 604.
- Burchard, E.F., 1910. The Clinton iron-ore deposits in Alabama. Am. Inst. Min. Eng., Trans., 40: 75–133.
- Burchard, E.F. and Andrews, T.G., 1947. Iron ore outcrops of the Red Mountain Formation. Ala. Geol. Surv., Spec. Rep., 19, 375 pp.
- Burchard, E.F. and Butts, C., 1910. Iron ores, fuels and fluxes, Birmingham District, Alabama. U.S. Geol. Surv. Bull., 400, 204 pp.
- Bushinskii, G.I., 1969. Old phosphorites of Asia and their genesis. Israel Prog. Sci. Transl., Jerusalem, 266 pp.
- Button, A., 1975. The Gondwanaland Precambrian project. Univ. Witwatersrand, Econ. Geol. Res. Unit, Annu. Rep., 16: 37–54.
- Button, A., 1976. Iron-formation as an end member in carbonate sedimentary cycles in the Transvaal Supergroup. Econ. Geol., 71: 193–201.
- Cailliére, S. and Al-Maleh, A.K., 1975. Les minerais de fer de la base du Crétacé du Nord-Ouest syrien (Kurd Dagh). C. R. Acad. Sci. Paris, Sér. D, 280: 526–528.
- Cairns-Smith, A.G., 1978. Precambrian solution photochemistry, inverse segregation, and banded iron formations. Nature, 276: 807–808.
- Calvert, S.E., 1983. Sedimentary geochemistry of silicon. In: S.R. Aston (Editor), Silicon Geochemistry and Biogeochemistry. Academic Press, London, pp. 143–186.
- Camacho, R., Ulloa, C. and Pacheco, A., 1969. Yacimiento de hierro oolítico de Sabanalarga (Boyaca). Inst. Nac. Invest. Geol.-Miner., Colombia, Tech. Pap., 15, 23 pp.
- Cameron, E.M., 1982. Sulphate and sulphate reduction in early Precambrian oceans. Nature, 296: 145–148.
- Cameron, E.M., 1983. Genesis of Proterozoic iron formation: sulfur isotope evidence. Geochim. Cosmochim. Acta, 47: 1069–1074.
- Cameron, E.M. and Hattori, K., 1987. Archean sulfur cycle: evidence from sulphate minerals and isotopically fractionated sulphides in Superior Province, Canada. Chem. Geol. (Isotope Geosci. Sect.), 65: 341–358.
- Campbell, A.C., Gieskes, J.M., Lupton, J.E. and Lonsdale, P.F., 1988. Manganese geochemistry in the Guayamas Basin, Gulf of California. Geochim. Cosmochim. Acta, 52: 345–357.

- Canfield, D.E. and Berner, R.A., 1987. Dissolution and pyritization of magnetite in anoxic marine sediments. *Geochim. Cosmochim. Acta*, 51: 645-659.
- Cannon, W.F., Powers, S.L. and Wright, N.A., 1978. Computer-aided estimates of concentrating-grade iron resources in the Negaunee iron-formation, Marquette District, Michigan. U.S. Geol. Surv., Prof. Pap., 1045: 1-21.
- Carpenter, A.B., Trout, M.L. and Pickett, E.E., 1974. Preliminary report on the origin and chemical evolution of lead- and zinc-rich oil field brines in central Mississippi. *Econ. Geol.*, 69: 1191-1206.
- Case, J.E. and Holcombe, T.L., 1980. Geologic-tectonic map of the Caribbean region. U.S. Geol. Surv., Misc. Invest. Ser., Map 1-1100, 3 sheets.
- Cathles, L.M., 1977. An analysis of the cooling of intrusives by ground-water convection which includes boiling. *Econ. Geol.*, 72: 804-826.
- Cayeux, M.L., 1909. Les mineraux de fer oolithique de France. 1, Mineraux de fer primaires: Etudes des gites mineraux de la France. Serv. Carte Geol., Imprimerie Nationale, Paris, 344 pp.
- Cayeux, M.L., 1911a. Existence de restes organiques dans les roches ferrugineuses associes aux mineraux de fer huroniens des Etats-Unis. C. R. Acad. Sci., Paris, 153: 910-912.
- Cayeux, M.L., 1911b. Comparaison entre les mineraux de fer huroniens des Etats-Unis et les mineraux de fer oolithique de France. C. R. Acad. Sci., Paris, 153: 1188-1190.
- Cayeux, M.L., 1922. Les mineraux de fer oolithique de France. 2, Mineraux de fer secondaires: Etudes de gites mineraux de la France. Serv. Carte Geol., Imprimerie Nationale, Paris, 1052 pp.
- Cayeux, M.L., 1931. Introduction a l'etude petrographique des roches sedimentaires. Minist. Travaux Publics, Mem., l'explication carte geologique detaillee de la France, 524 pp.
- Chafetz, H.S., 1978. A trough cross-stratified glaucarenite: A Cambrian tidal inlet accumulation. *Sedimentology*, 25: 545-559.
- Chafetz, H.S., Meredith, J.C. and Kocurek, G., 1986. The Cambro-Ordovician Bliss Formation, southwestern New Mexico, U.S.A. - progradational sequences on a mixed siliciclastic and carbonate shelf. *Sediment. Geol.*, 49: 201-221.
- Champetier, Y., Hamdadou, E. and Hamdadou, M., 1987. Examples of biogenic support of mineralization in two oolitic ores - Lorraine (France) and Gara Djebilet (Algeria). *Sediment. Geol.*, 51: 249-255.
- Chandler, F.W., 1986. Sedimentology and paleoclimatology of the Huronian (Early Aphebian) Lorrain and Gordon Lake Formations and their bearing on models for sedimentary copper mineralization. *Geol. Surv. Can., Pap. 86-1A, Current Res., Part A*: 121-132.
- Chase, R.L., 1963. The Imataca Complex, the Panamo am-
- phibolite and the Guri trondhjemite: Precambrian rocks of the Adjuntas-Panamo quadrangle, State of Bolivar, Venezuela. Unpubl. Ph.D thesis, Princeton Univ., Princeton, N.J., 197 pp.
- Chauvel, A., Pedro, G. and Tessier, D., 1976. Role du fer dans l'organisation des materiaux kaoliniques. *Assoc. Fr. Etud. Sols*, 2: 101-113.
- Chauvel, J.-J., 1974. Les mineraux de fer de l'Ordovicien inférieur du bassin de Bretagne-Anjou, France. *Sedimentology*, 21: 127-147.
- Chauvel, J.-J. and Dimroth, E., 1974. Facies types and depositional environments of the Sokoman Iron Formation, Central Labrador Trough, Quebec, Canada. *J. Sediment. Petrol.*, 44: 299-327.
- Chauvel, J.-J. and Massa, D., 1981. Paleozoique de Libya occidentale constantes geologiques et petrographiques signification de niveaux ferrugineux oolithiques. *Cie. Fr. Pet., Notes Mem.*, 16: 25-66.
- Chebotarev, M.V., 1960. Geological structures of the South Khingan manganese deposit and essential composition of its ores. *Int. Geol. Rev.*, 2: 851-866.
- Chowns, T.M. and McKinney, F.K., 1980. Depositional facies in Middle-Upper Ordovician and Silurian rocks of Alabama and Georgia. In: *Geol. Soc. Am., Atlanta Annu. Conv., Field Trip Guide Book*, 16: 323-348.
- Cimbalkova, A., 1971. Chemical variability and structural heterogeneity of glauconites. *Am. Miner.*, 56: 1385-1398.
- Cisne, J.L., 1984. A basin model for massive banded iron-formations and its geophysical applications. *J. Geol.*, 92: 471-488.
- Cissarz, A., 1924. Mineralogisch-mikroskopische Untersuchungen der Erze und Nebengesteine des Roteisensteinlagers der Grube Maria bei Braufels an der Lahn. Mitt. Kaiser-Wilhelm-Inst. Eisenforsch. Dusseldorf, 5: 109-126.
- Cita, M.B., 1982. The Messinian salinity crisis in the Mediterranean: a review. In: H. Verckhemer and K. Hsu (Editors), *Alpine-Mediterranean Geodynamics*: Am. Geophys. Union., *Geodynamics Ser.*, 7: 113-140.
- Claypool, G.E., Holser, W.T., Kaplan, I.R. and Zak, I., 1980. The age curves of sulfur and oxygen isotopes in marine sulfate and their mutual interpretation. *Chem. Geol.*, 28: 199-260.
- Clemmey, H. and Badham, N., 1982. Oxygen in the Precambrian atmosphere: An evaluation of the geological evidence. *Geology*, 10: 141-146.
- Clifford, P.M., 1969. Geology of the western Lake St. Joseph area. Ont. Dep. Mines, *Geol. Rep.*, 70, 61 pp.
- Cloud, P.E., 1955. Physical limits of glauconite formation. *Am. Assoc. Pet. Geol., Bull.*, 39: 484-492.
- Cloud, P.E., 1962. Environments of calcium carbonate deposition west of Andros Island, Bahamas. U.S. Geol. Surv., Prof. Pap., 350, 138 pp.
- Cloud, P.E., 1973. Paleoecological significance of the banded iron-formation. *Econ. Geol.*, 68: 1135-1143.

- Cloud, P.E., 1983. Banded iron-formation - a gradualist's dilemma. In: A.F. Trendall and R.C. Morris (Editors), Iron-formation: Facts and Problems: Elsevier, Amsterdam: 401-416.
- Cloud, P.E., Gruner, J.W. and Hagen, H., 1965. Carbonaceous rocks of the Soudan iron formation (Early Precambrian). *Science*, 148: 1713-1716.
- Cloud, P.E. and Licari, G.R., 1968. Microbiotas of the banded iron formations. *Proc. Natl. Acad. Sci., U.S.A.*, 61: 779-786.
- Cochrane, G.W. and Edwards, A.B., 1960. The Roper River oolitic ironstone formations. *Mineragraph. Invest., Tech. Pap.*, 1, C.S.I.R.O., Melbourne, 28 pp.
- Collins, W.H., Quirke, T.T. and Thomson, E., 1926. Michipicoten iron ranges. *Geol. Surv. Can., Mem.*, 147, 175 pp.
- Cook, P.J. and Shergold, J.H., (Editors), 1986. Phosphate deposits of the world. 1, Proterozoic and Cambrian phosphorites. Cambridge Univ. Press, Cambridge, 386 pp.
- Cunliffe, J.E., 1982. Origin of oolitic chamosite in Baltimore Canyon basin. *Annu. Meet. Oklahoma Acad. Sci.*, (abstract).
- Cook, P.J. and McElhinny, M.W., 1979. A reevaluation of the spatial and temporal distribution of sedimentary phosphate deposits in light of plate tectonics. *Econ. Geol.*, 74: 315-330.
- Crerar, D.A., Knox, G.W. and Means, J.L., 1979. Biogeochemistry of bog iron in the New Jersey pine barrens. *Chem. Geol.*, 24: 111-133.
- Curtis, C.D. and Spears, D.A., 1968. The formation of sedimentary iron minerals. *Econ. Geol.*, 63: 257-270.
- Dahanayake, K. and Krumbein, W.E., 1986. Microbial structures in oolitic iron formations. *Miner. Deposita*, 21: 85-94.
- Dahlstrom, C., 1973. The geology of the Snake River iron deposit. *Geol. Assoc. Can., Cordilleran Sect.*, Annu. Meet., Abstr, p. 7.
- Daugherty, L.A. and Arnold, R.W., 1982. Mineralogy and iron characterization of plinthitic soils on alluvial landforms in Venezuela. *Soil Sci. Soc. Am. J.*, 46: 1244-1251.
- Davidson, C.F., 1961. Oolitic ironstones of fresh-water origin. *Min. Mag.*, 104: 158-159.
- Davidson, J.P., 1983. Lesser Antilles isotopic evidence of the role of subducted sediment in island arc magma genesis. *Nature*, 306: 253-255.
- Davies, J.L., 1972. The geology and geochemistry of the Austin Brook area, Gloucester County, New Brunswick, with special emphasis on the Austin Brook iron formation. Unpubl. Ph.D. thesis, Carleton Univ., Ottawa, Ont., 254 pp.
- Davies, W. and Dixie, R.J.M., 1951. Recent work on the Frodingham ironstone. *Yorkshire Geol. Soc. Proc.*, 28: 85-96.
- Davison, W., 1979. Soluble inorganic ferrous complexes in natural waters. *Geochim. Cosmochim. Acta*, 43: 1693-1696.
- Davy, R., 1983. A contribution on the chemical composition of Precambrian iron-formations. In: A.F. Trendall and R.C. Morris (Editors), Iron-formation: Facts and Problems, Elsevier, Amsterdam, pp. 325-343.
- Dean, W.E., Arthur, M.A. and Claypool, G.E., 1986. Depletion of ^{13}C in Cretaceous marine organic matter: source, diagenetic, or environmental signal? *Mar. Geol.*, 70: 119-157.
- De Baar, H.J.W., German, C.R., Elderfield, H. and Van Gaans, P., 1988. Rare earth element distributions in anoxic waters of the Cariaco Trench. *Geochimica et Cosmochimica Acta*, 52: 1203-1219.
- Deeney, D.E., 1987. Central Irish geology/metallogeny: A Lower Carboniferous rifting-related exhalative catastrophe? *Mineral. Deposita*, 22: 116-123.
- Degens, E.T. and Ross, D.A. (Editors), 1969. Hot Brines and Recent Heavy Mineral Deposits in the Red Sea. Springer, New York, N.Y., 600 pp.
- De Lange, G.J. and Rispens, F.B., 1986. Indication of a diagenetically induced precipitate of an Fe-Si mineral from the Nares abyssal plain, western North Atlantic. *Mar. Geol.*, 73: 85-97.
- DeMaster, D.J., Knapp, G.B. and Nittrouer, C.A., 1983. Biological uptake and accumulation of silica on the Amazon continental shelf. *Geochim. Cosmochim. Acta*, 47: 1713-1723.
- De Miro O.M. 1974. Morfología submarina y sedimentos marinos recientes del margen continental del Noroeste de Venezuela. Third U.N. Law of the Sea Conf., Caracas, Cuadernos Azules, 14, 230 pp.
- Deubel, F., Berg, G. and Gaertner, H.R.V., 1942. Die Erze des thuringischen Untersilurs. In: B. Brockamp (Editor), Zur Entstehung Deutscher Eisenerzlagerstätten, Arch. Lagerstättforsch., 75: 140-150.
- Deverin, L., 1945. Etude petrographique des minéraux de fer oolithiques du Dogger des Alpes suisses. *Beitr. Geol. Schweiz, Geotechn. Ser.*, 13 (2), 115 pp.
- Dickinson, K.A., 1988. Paleolimnology of Lake Tubutulik, an iron-meromictic Eocene lake, eastern Seward peninsula, Alaska. *Sediment. Geol.*, 54: 303-320.
- Didura, V.I., 1982. Effect of rate of growth of anticlinal structures on scale of accumulation of hydrocarbons in southwest Turkmenia. *Pet. Geol. (U.S.S.R.)*, 20: 512-514.
- Dimroth, E., 1968. Sedimentary textures, diagenesis, and sedimentary environment of certain Precambrian iron-stones. *Neues Jahrb. Geol. Palaeontol., Abh.*, 130: 247-274.
- Dimroth, E., 1971. The Attikamagan-Ferriman transition in part of the central Labrador trough. *Can. J. Earth Sci.*, 8: 1432-1454.
- Dimroth, E., 1975. Paleo-environment of iron-rich sedimentary rocks. *Geol. Rundsch.*, 64: 751-767.
- Dimroth, E., 1976. Aspects of the sedimentary petrology of cherty iron-formation. In: K.H. Wolf (Editor), Handbook of Strata-bound and Stratiform Ore Deposits, 7. Elsevier, Amsterdam, pp. 203-254.

- Dimroth, E., 1977a. Models of physical sedimentation of iron formations. *Geosci. Canada*, 4: 23-30.
- Dimroth, E., 1977b. Diagenetic facies of iron formation. *Geosci. Canada*, 4: 83-88.
- Dimroth, E. and Chauvel, J.-J., 1973. Petrography of the Sokoman iron formation in part of the central Labrador Trough, Quebec, Canada. *Geol. Soc. Am., Bull.*, 84: 111-134.
- Dimroth, E. and Kimberley, M.M., 1976. Precambrian atmospheric oxygen: evidence in the sedimentary distributions of carbon, sulfur, uranium, and iron. *Can. J. Earth Sci.*, 13: 1161-1185.
- Dodge, J.D., 1985. *Atlas of dinoflagellates*. Farrand Press, London, 119 pp.
- Dorf, E. and Fox, S.K., 1957. Cretaceous and Cenozoic of the New Jersey coastal plain. *Geol. Soc. Am., Guidebook Annu. Meet.*, Atlantic City, N.J., pp. 1-8.
- Dorr, J.V.N., II., 1945. Manganese and iron deposits of Morro do Urucum, Mato Grosso, Brazil. *U.S. Geol. Surv., Bull.*, 94-A, 47 pp.
- Dorr, J.V.N., II., 1973a. Iron-formation and associated manganese in Brazil. In : *Genesis of Precambrian Iron and Manganese Deposits*. UNESCO, *Earth Sci.*, 9: 105-113.
- Dorr, J.V.N. II., 1973b. Iron-formation in South America: *Econ. Geol.*, 68: 1005-1022.
- Dorr, J.V.N. II. and Barbosa, A.L. de M., 1963. Geology and ore deposits of the Itabira district, Minas Gerais, Brazil. *U.S. Geol. Surv., Prof. Pap.*, 341-C, 110 pp.
- Dreesen, R.J.M., 1982. Storm-generated oolitic ironstones of the Famennian (Falg-Fa2a) in the Vesdre and Dinant synclinoria (Upper Devonian, Belgium). *Ann. Soc. Geol. Belg.*, 105: 105-129.
- Dressen, R.J.M., 1987. Oolitic ironstones as event-stratigraphical marker beds within the Upper Devonian of the Belgian Ardenne shelf. *Abstr. Progr. Conf. Phanerozoic Ironstones*, Univ. Sheffield, Sheffield.
- Drever, J.I., 1974. Geochemical model for the origin of Precambrian banded iron formations. *Geol. Soc. Am., Bull.*, 85: 1099-1106.
- Duane, M.J. and De Witt, M.J., 1988. Pb-Zn ore deposits of the northern Caledonides: Products of continental-scale fluid mixing and tectonic expulsion during continental collision. *Geology*, 16: 999-1002.
- Duff, P.M.D., Hallam, A. and Walton, E.K., 1967. Cyclic sedimentation. In *Developments in Sedimentology*, 10, Elsevier, Amsterdam, 280 pp.
- Dunbar, G.J. and McCall, G.J.H., 1971. Archean turbidites and banded ironstone of the Mt. Belches area (Western Australia). *Sediment. Geol.*, 5: 92-133.
- Duncan, R.A. and Hargraves, R.B., 1984. Plate tectonic evolution of the Caribbean region in the mantle reference frame. In: W.E. Bonini, R.B. Hargraves, and R. Shagam (Editors), *The Caribbean-South American Plate Boundary and Regional Tectonics*. *Geol. Soc. Am., Mem.*, 162: 81-93.
- Du Toit, A.L., 1954. In: S.H. Haughton (Editor), *Geology of South Africa*, 3rd ed. Hafner, New York, N.Y., 611 pp.
- Eckel, E.B., 1938. The brown iron ores of eastern Texas. *U.S. Geol. Surv., Bull.*, 902, 157 pp.
- Economou, T. and Bowers, A.R., 1987. Interaction of Fe³⁺ with clay minerals. *Geol. Soc. Am., Abstr. Program*, 19: 651.
- Edmonds, E.A., Poole, E.G. and Wilson, V., 1965. Geology of the country around Banbury and Edge Hill. *G. B. Geol. Surv., Mem.*, 137 pp.
- Edwards, A.B. and Baker, G., 1951. Some occurrences of supergene iron sulphides in relation to their environments of deposition. *J. Sediment. Petrol.*, 21: 34-46.
- Edwards, A.G., 1958. Oolitic iron formation in northern Australia. *Geol. Rundsch.*, 47: 668-682.
- Egorov, E.V. and Timofeieva, N.W., 1973. Effusive iron-silica formations and iron deposits of the Maly Khingan. In: *Genesis of Precambrian iron and manganese deposits*, U.N.E.S.C.O. *Earth Sci.*, 9: 181-185.
- Eicher, D.L. and McAlester, A.L., 1980. History of the Earth. Prentice-Hall, Englewood Cliffs, N.J., 413 pp.
- Eichler, J., 1970. Die geologische Position der prakambischen Quarzbanderze (Itabirite) und die Problematik ihrer Genese. *Clausthaler Hefte Lagerstättenkd. Geochem. Miner. Rohst.*, 9: 6-26.
- Eichler, J., 1976. Origin of the Precambrian banded iron-formations. In: K.H. Wolf (Editor), *Handbook of Stratabound and Stratiform Ore Deposits*, v. 7: Elsevier, Amsterdam, pp. 157-201.
- Einecke, G., 1950. Die Eisenerzvorräte der Welt und der Anteil der Verbrauches- und Lieferländer an deren Verwertung. Verlag Stahleisen M.B.H., Dusseldorf (2 vols).
- Eisbacher, G.H., 1978. Re-definition and subdivision of Rapitan Group, Mackenzie Mountains. *Geol. Surv. Can., Pap.*, 77-35: 1-21.
- El Sharkawi, M.A., Mahfouz, S. and El Dallal, M.M.N., 1976. The pisolithic ironstones of Gdeidet Yabous and Naba Barada localities, Zebdani District, Syria. *Chem. Erde*, 35: 241-250.
- Emelyanov, Ye.M., Trimonis, G.S. and Shimkus, K.M., 1976. Amounts and distribution of Fe, Al, Ti, and Mn in Black Sea suspensates. *Geochem. Int.*, 13: 57-72.
- England, W.A., Mackenzie, A.S., Mann, D.M. and Quigley, T.M., 1987. The movement and entrapment of petroleum fluids in the subsurface. *J. Geol. Soc., London*, 144: 327-347.
- Erba, E., Rodondi, G., Parish, E., Ten Haven, H.L., Nip, M. and De Leeuw, J.W., 1987. Gelatinous pellicles in deep anoxic hypersaline basins from the eastern Mediterranean. *Mar. Geol.*, 75: 165-183.
- Eriksson, K.A., 1973. The Timeball Hill formation - a fossil delta. *J. Sediment. Petrol.*, 43: 1046-1053.
- Eriksson, K.A. and Truswell, J.F., 1974. Tidal flat associations from a lower Proterozoic carbonate sequence in South Africa. *Sedimentology*, 21: 243-309.

- Ertel, J.R., Wakeham, S.G. and Gagosian, R.B., 1986. Early diagenesis of carotenoids and lipids in Cariaco trench sediments (abstr.). EOS Trans., Am. Geophys. Union, 67: 1067.
- Eugster, H.P., 1985. Oil shales, evaporites and ore deposits. *Geoch. Cosmochim. Acta*, 49: 619–635.
- Eugster, H.P. and Chou, I.-M., 1973. The depositional environments of Precambrian banded iron-formations. *Econ. Geol.*, 68: 1144–1168.
- Ewers, W.E., 1980. Chemical conditions for the precipitation of banded iron-formations. In: P.A. Trudinger, M.R. Walter and B.J. Ralph (Editors), *Biogeochemistry of Ancient and Modern Environments*. Springer, New York, N.Y., pp. 83–92.
- Ewers, W.E., 1983. Chemical factors in the deposition and diagenesis of banded iron-formation. In: A.F. Trendall and R.C. Morris (Editors), *Iron-formation: Facts and Problems*. Elsevier, Amsterdam, pp. 491–512.
- Ewers, W.E. and Morris, R.C., 1981. Studies on the Dales Gorge member of the Brockman iron formation. *Econ. Geol.*, 76: 1929–1953.
- Fehn, U., 1986. The evolution of low-temperature convection cells near spreading centers: A mechanism for the formation of the Galapagos mounds and similar manganese deposits. *Econ. Geol.*, 81: 1396–1407.
- Feng Zhiwen, Wang Siyuan, Huang, Yongke, Yu Heng-weng, and Hu Huyan, 1984. Lithofacies features and mechanism of formation of "Zihe-type" time- and strata-bound iron ore deposits in central Shandong Province. *Geochemistry (Ti Chou Hua Hshueh, Beijing, China)*, 3: 384–395.
- Ferguson, J., Burne, R.V. and Chambers, L.A., 1983. Iron mineralization of peritidal carbonate sediments by continental groundwaters, Fisherman Bay, South Australia. *Sediment. Geol.*, 34: 41–57.
- Ferguson, S.A. 1966. Geology of Pickle Crow Gold Mines Ltd. and Central Patricia Gold Mines Ltd. No. 2 Operation. Ont. Dep. Mines, Misc. Pap., 4, 97 pp.
- Ferraz-Reyes, E., Reyes-Vasquez, G. and Bruzual, I.B., 1979. Dinoflagellate blooms in the Gulf of Cariaco, Venezuela. In: D.L. Taylor and H.H. Seliger (Editors), *Toxic Dinoflagellate Blooms*. Elsevier, New York, N.Y., pp. 155–160.
- Ferraz-Reyes, E., Reyes-Vasquez, G. and De Oliveros, A.L., 1985. Dinoflagellates of the genera the Gulf of Cariaco, Venezuela. In: D.M. Anderson, A.W. White and D.G. Baden (Editors), *Toxic Dinoflagellates*. Elsevier, New York, N.Y., pp. 69–72.
- Fiedler B.G., 1961. Areas afectadas por terremotos en Venezuela. Mem. III Congreso Geológico Venezolano, Bol. Geol., Minist. Minas Hidrocarburos, Venezuela, Publ. Espec., 3, (4): 1791–1814.
- Fiedler B.G., 1972. La liberación de energía sísmica en Venezuela, volúmenes sísmicos y mapa de isosistemas. Mem. IV Congreso Geológico Venezolano, Bol. Geol., Minist. Minas Hidrocarburos, Venezuela, Publ. Espec., 5 (4): 2441–2462.
- Finkenwirth, A., 1964. Das Eisenerz des Lias gamma am Kahlberg bei Echte und der Weissjura in Sud-Hannover. *Beih. Geol. Jahrb.*, 56, 131 pp.
- Fischer, A.G. and Arthur, M.A., 1977. Secular variations in the pelagic realm. *Soc. Econ. Paleontol. Mineral., Spec. Publ.* 25: 19–50.
- Fleet, A.J. and Robertson, A.H.F., 1980. Ocean-ridge metalliferous and pelagic sediments of the Semail nappe, Oman. *J. Geol. Soc. London*, 137: 403–422.
- Floran, R.J. and Papike, J.J., 1975. Petrology of the low-grade rocks of the Gunflint iron-formation, Ontario-Minnesota. *Geol. Soc. Am. Bull.*, 86: 1169–1190.
- Fominikh, V.G. and Skopina, N.A., 1976. Distribution of the iron-group elements in the South Ural Malyy Kuzbas iron ores. *Geochem. Int.*, 9: 88–91.
- Foos, A.M., 1984. The mineralogy, petrography, and geochemistry of the Eocene Lone Star iron ores, East Texas and the Ordovician Hooker ironstone, Northwest Georgia. Ph.D. dissertation, Univ. Texas, Dallas, Tex., 260 pp.
- Force, E.R. and Cannon, W.F., 1988. Depositional model for shallow-marine manganese deposits around black shale basins. *Econ. Geol.*, 83: 93–117.
- Foslie, S., 1949. Hafjellsmulden i ofoten og dens sedimentære jern-manganmalmer. *Nor. Geol. Unders.*, 174, 129 pp.
- Fox, L.E., 1988. The solubility of colloidal ferric hydroxide and its relevance to iron concentrations in river water. *Geochim. Cosmochim. Acta*, 52: 771–777.
- Frakes, L.A., 1979. Climates throughout geologic time. Elsevier, New York, N.Y.
- Frakes, L.A. and Bolton, B.R., 1984. Origin of manganese giants: Sea level change and anoxic-oxic history. *Geology*, 12: 83–86.
- Francois, L.M., 1986. Extensive deposition of banded iron formations was possible without photosynthesis. *Nature*, 320: 352–354.
- Francois, L.M. and Gerard, J.-C., 1986. Reducing power of ferrous iron in the Archean ocean. I, Contribution of photosynthetic oxygen. *Paleoceanography*, 1: 355–368.
- Frank, L.A., Sigwarth, J.B. and Craven, J.D., 1986. On the influx of small comets into the Earth's upper atmosphere. II, Interpretation (abstr.). *Am. Geophys. Union, Trans., EOS*, 67: 299.
- Frey, M., 1987. Very low-grade metamorphism of clastic sedimentary rocks. In: M. Frey, M. (Editor), *Low Temperature Metamorphism*. Chapman and Hall, New York, N.Y., pp. 9–58.
- Fripp, E.P., 1976. Stratabound gold deposits in Archaean banded iron-formation, Rhodesia. *Econ. Geol.*, 71: 58–75.
- Frizzo, P. and Baccelle, L.S., 1983. Rapporti strutturali e tessitura fra mineralizzazione a siderite e litotipi carbonatici nel servino (Scitico) delle Valle Lombarde. *Mem. Sci. Geol.*, 36: 195–210.
- Froelich, P.N., Klinkhammer, G.P., Bender, M.L., Luedtke,

- N.A., Heath, G.R., Cullen, D., Dauphin, P., Hammond, D., Hartman, B. and Maynard, V., 1979. Early oxidation of organic matter in pelagic sediments of the eastern equatorial Atlantic: suboxic diagenesis. *Geochim. Cosmochim. Acta*, 43: 1075-1090.
- Frost, B.R., 1978. Some aspects of the sedimentary and dia-genetic environment of Proterozoic banded iron formations: a discussion. *Econ. Geol.*, 73: 1368-1371.
- Frost, B.R., 1979a. Metamorphism of iron-formation: Paragenesis in the system Fe-Si-C-O-H. *Econ. Geol.*, 74: 775-785.
- Frost, B.R., 1979b. Mineral equilibria involving mixed volatiles in a C-O-H fluid phase: the stabilities of graphite and siderite. *Am. J. Sci.*, 279: 1033-1059.
- Fryer, B.J., 1971. Age determinations and correlations in the Circum-Ungava geosyncline. In: *Variations in Isotopic Abundances of Institute of Technology*, 19th Ann. Rep., pp. 76-85.
- Fryer, B.J., 1977. Rare earth evidence in iron-formations for changing Precambrian oxidation states. *Geochim. Cosmochim. Acta*, 41: 361-367.
- Fryer, B.J., 1983. Rare earth elements in iron-formation. In: A.F. Trendall and R.C. Morris (Editors), *Iron-formation: Facts and Problems*. Elsevier, Amsterdam, pp. 345-358.
- Fryer, B.J., Fyfe, W.S. and Kerrich, R., 1979. Archean volcanogenic oceans. *Chem. Geol.*, 24: 25-33.
- Fukuoka, J., 1964. Observaciones oceanograficas cerca de la isla de Trinidad y en las afueras de la desembocadura del rio Orinoco. *Soc. Ci. Nat. La Salle, Venezuela, Mem.*, 24: 91-97.
- Fyfe, W.S., Price, N.J. and Thompson, A.B., 1978. Fluids in the Earth's Crust. Elsevier, Amsterdam, 383 pp.
- Fyon, J.A., Crockett, J.H. and Schwarcz, H.P., 1983. The Carshaw and Malgo iron-formation-hosted gold deposits of Timmins area. In: A.C. Colvine (Editor), *The Geology of Gold in Ontario*. Ont. Geol. Surv., Misc. Pap., 110: 98-110.
- Gair, J.E., 1962. Geology and ore deposits of the Nova Lima and Rio acima quadrangles, Minas Gerais, Brazil. U.S. Geol. Surv., Prof. Pap., 341-A, 65 pp.
- Gair, J.E. and Han, T.-M., 1975. Bedrock geology and ore deposits of the Palmer quadrangle, Marquette County, Michigan. U.S. Geol. Surv., Prof. Pap., 769, 159 pp.
- Galliher, E.W., 1935. Glauconite genesis. *Geol. Soc. Am. Bull.*, 46: 1351-1365.
- Garfunkel, Z., 1981. Internal structure of the Dead Sea leaky transform (rift) in relation to plate kinematics. *Tectonophysics*, 80: 81-108.
- Garfunkel, Z., Zak, I. and Freund, R., 1981. Active faulting in the Dead Sea rift. *Tectonophysics*, 80: 1-26.
- Garrels, R.M., 1987. A model for the deposition of the microbanded Precambrian iron formations. *Am. J. Sci.*, 287: 81-106.
- Garrels, R.M. and Mackenzie, F.T., 1971. Evolution of sedimentary rocks. W.W. Norton, New York, N.Y., 397 pp.
- Garrels, R.M., Perry, E.A. Jr. and Mackenzie, F.T., 1973. Genesis of Precambrian iron-formations and the development of atmospheric oxygen. *Econ. Geol.*, 68: 1173-1179.
- Geijer, P., 1931. The iron ores of the Kiruna type. *Sver. Geol. Unders., Ser. C*, 367, 39 pp.
- Gerdes, G. and Krumbein, W.E., 1987. Biolaminated deposits. Springer, Berlin, 183 pp.
- Ghiorse, W.C., 1984. Biology of iron- and manganese-depositing bacteria. *Annu. Rev. Microbiol.*, 38: 515-550.
- Gibbs, R.J., 1972. Water chemistry of the Amazon river. *Geochim. Cosmochim. Acta*, 36: 1061-1066.
- Gill, A.E., 1982. *Atmosphere-Ocean Dynamics*. Academic Press, London, 662 pp.
- Giresse, P. and Odin, G.S., 1973. Nature mineralogique et origine des glauconies du plateau continental du Gabon et du Congo. *Sediment. Geol.*, 20: 457-488.
- Glaessner, M.F., 1984. *The Dawn of Animal Life, a Biographical Study*. Cambridge University Press, Cambridge, 244 pp.
- Glenn, C.R. and Arthur, M.A., 1985. Sedimentary and geochemical indicators of productivity and oxygen contents in modern and ancient basins: the Holocene Black Sea as the "type" anoxic basin. *Chem. Geol.*, 48: 325-354.
- Gold, T., 1979. Terrestrial sources of carbon and earthquake outgassing. *J. Petroleum Geol.*, 1: 3-19.
- Gold, T. and Soter, S., 1979. Brontides: Natural explosive noises. *Science*, 204: 371-375.
- Gold, T. and Soter, S., 1980. The deep-earth-gas hypothesis. *Sci. Am.*, 242: 154-161.
- Gold, T. and Soter, S., 1982. Abiogenic methane and the origin of petroleum. *Energy Explor. Exploit.*, 1: 89-104.
- Goldich, S.S., 1973. Ages of Precambrian banded iron-formations. *Econ. Geol.*, 68: 1126-1134.
- Gole, M.J., 1980. Mineralogy and petrology of very-low-metamorphic-grade Archean iron-formations, Weld Range, Western Australia. *Am. Mineral.*, 65: 8-25.
- Gole, M.J. and Klein, C., 1981. Banded iron-formations through much of Precambrian time. *J. Geol.*, 89: 169-183.
- Gonzalez de Juana, C., Iturrealde de Arozena and J.M., Cadillat, X.P., 1980. *Geología de Venezuela y de sus cuencas petrolíferas, FONINVES*, Caracas. Vol. 1: 1-414 and Vol. 2: 415-1031.
- Goode, A.D.T., Hall, W.D.M. and Bunting, J.A., 1983. The Nabberu Basin of Western Australia. In: A.F. Trendall and R.C. Morris (Editors), *Iron-formation: Facts and Problems*. Elsevier, Amsterdam, pp. 295-323.
- Goodfellow, W.D., 1987. Anoxic stratified oceans as a source of sulphur in sediment-hosted stratiform Zn-Pb deposits (Selwyn Basin, Yukon, Canada). *Chem. Geol. (Isotope Geosci. Sect.)*, 65: 359-382.
- Goodwin, A.M., 1956. Facies relations in the Gunflint iron formation. *Econ. Geol.*, 51: 565-595.
- Goodwin, A.M., 1960. Gunflint iron formation in the Whi-

- tefish Lake area. Ont. Dep. Mines, Annu. Rep., 69, part 7: 41-63.
- Goodwin, A.M., 1961. Genetic aspects of Michipicoten iron formation. *Trans. Can. Inst. Min. Metall.*, 64: 32-36.
- Goodwin, A.M., 1962. Structure, stratigraphy, and origin of iron formation, Michipicoten area, Algoma district, Ontario, Canada. *Geol. Soc. Am. Bull.*, 73: 561-586.
- Goodwin, A.M., 1964. Geochemical studies at the Helen iron range. *Econ. Geol.*, 59: 684-718.
- Goodwin, A.M., 1965. Geology of Pashkokogan Lake - eastern Lake St. Joseph area. Ont. Dep. Mines, Geol. Rep., 42, 58 pp.
- Goodwin, A.M., 1973. Archean iron-formations and tectonic basins of the Canadian Shield. *Econ. Geol.*, 68: 915-933.
- Goodwin, A.M., Monster, J. and Thode, H.G., 1976. Carbon and sulfur isotope abundances in Archean iron-formations and Early Precambrian life. *Econ. Geol.*, 71: 870-891.
- Goodwin, A.M., Thode, H.G., Chou, C.-L. and Karkhansis, S.N., 1985. Chemostratigraphy and origin of the late Archean siderite-pyrite-rich Helen iron formation, Michipicoten belt, Canada. *Can. J. Earth Sci.*, 22: 72-84.
- Govett, G.J.S., 1966. Origin of banded iron formations. *Geol. Soc. Am. Bull.*, 77: 1191-1212.
- Graf, C.H., 1972. Sedimentos del Terciario y Cuaternario del sur de la peninsula de Macanao: 28-32 In: C. Petzall (Editor), Sixth Caribbean Geology Conference, Margarita Island, Venezuela, Mem., Trans. Vol., CROMOTIP, Caracas, 499 pp.
- Graf, J.L. Jr., 1977. Rare-earth elements as hydrothermal tracers during the formation of massive sulfide deposits in volcanic rocks. *Econ. Geol.*, 72: 527-548.
- Graf, J.L. Jr., 1978. Rare earth elements, iron formations and sea water. *Geochim. Cosmochim. Acta*, 42: 1845-1850.
- Green, D.H., 1975. Genesis of Archean peridotitic magmas and constraints of Archean geothermal gradients and tectonics. *Geology*, 3: 15-18.
- Griffiths, R.C. and Simpson, J.G., 1972. Upwelling and other oceanographic features of the coastal waters of northeastern Venezuela. Venezuela Minist. Agric. Livestock, Office of Fishing, Ser. Recursos y Explotacion Pesqueros, 2 (4), 72 pp.
- Gross, G.A., 1965. Geology of iron deposits in Canada, 1 - General geology and evaluation of iron deposits. *Geol. Surv. Can., Econ. Geol. Rep.*, 22, 181 pp.
- Gross, G.A., 1967. Iron deposits in the Appalachian and Grenville regions of Canada. *Geology of iron deposits in Canada*, Vol. 2. *Geol. Surv. Can., Econ. Geol. Rep.*, 22, 179 pp.
- Gross, G.A., 1968. Iron ranges of the Labrador geosyncline. *Geology of iron deposits in Canada*, Vol. 3. *Geol. Surv. Can., Econ. Geol. Rep.*, 22, 111 pp.
- Gross, G.A., 1972. Primary features in cherty iron-formations. *Sediment. Geol.*, 7: 241-261.
- Gross, G.A., 1973. The depositional environment of the principal types of Precambrian iron-formations. In: *Genesis of Precambrian Iron and Manganese Deposits*. UNESCO Earth Sci. 9: 15-21.
- Gross, G.A., 1980. A classification of iron formations based on depositional environments. *Can. Mineral.*, 18: 215-222.
- Gross, G.A., 1983. Tectonic systems and the deposition of iron-formation. *Precambrian Res.*, 20: 171-187.
- Gross, G.A. and McLeod, C.R., 1980. A preliminary assessment of the chemical composition of iron formations in Canada. *Can. Mineral.*, 18: 223-229.
- Gross, G.A. and Zajac, I.S., 1983. Iron-formation in fold belts marginal to the Ungava craton. In: A.F. Trendall and R.C. Morris (Editors), *Iron-formation: Facts and Problems*. Elsevier, Amsterdam, pp. 253-294.
- Grout, F.F. and Wolff, J.F., 1955. The geology of the Cuyuna district, Minnesota, a progress report. *Minn. Geol. Surv., Bull.*, 36, 144 pp.
- Gruner, J.W., 1922. The origin of sedimentary iron formations: the Biwabik Formation of the Mesabi Range. *Econ. Geol.*, 17: 407-460.
- Gruner, J.W., 1946. Mineralogy and geology of the Mesabi Range. *Iron Range Res. Rehabil. Comm.*, St. Paul, Minn., 127 pp.
- Gruss, H., 1973. Itabirite iron ores of the Liberia and Guyana Shields. In: *Genesis of Precambrian Iron and Manganese deposits*. UNESCO Earth Sciences 9: 335-359.
- Guerrak, S., 1987a. Paleozoic oolitic ironstones of the Algerian Sahara: a review. *J. Afr. Earth Sci.*, 6: 1-8.
- Guerrak, S., 1987b. Metallogenesis of cratonic oolitic iron-stone deposits in the Bled el Mass, Azzel Matti, Ahnet and Mouydir basins, central Sahara, Algeria. *Geol. Rundsch.*, 76: 903-922.
- Guerrak, S., 1988a. Paleozoic marine sedimentation and associated oolitic iron-rich deposits, Tassilis N'Ajjer and Illizi Basin, Saharan platform, Algeria. *Eclogae Geol. Helv.*, 81: 457-485.
- Guerrak, S., 1988b. Ordovician ironstone sedimentation in Ougarta Ranges: northwestern Sahara (Algeria). *J. Afr. Earth Sci.*, 7: 657-678.
- Guerrak, S. and Chauvel, J.J., 1985. Les mineralisations ferrifères du Sahara Algérien: le gisement de fer oolithique de Mecheri Abdelaziz (bassin de Tindouf). *Mineral. Deposita*, 20: 249-259.
- Guilbert, J.M. and Park, C.F.Jr., 1986. The geology of ore deposits. Freeman, San Francisco, Calif., 985 pp.
- Gulbrandsen, R.A., Goldich, S.S. and Thomas, H.H., 1963. Glauconite from the Precambrian Belt Series, Montana. *Science*, 140: 390-391.
- Gygi, R.A., 1981. Oolitic iron formations: marine or not marine? *Eclogae Geol. Helv.*, 74: 233-254.
- Gygi, R.A. and Persoz, F., 1986. Mineralostratigraphy, litho- and biostratigraphy combined in correlation of the Oxfordian (Late Jurassic) formations of the Swiss Jura range. *Eclogae Geol. Helv.*, 79: 385-454.

- Hadding, A., 1932. The pre-Quaternary sedimentary rocks of Sweden, Part 4, Glauconite and glauconitic rocks. Lunds Universitets Arsskrift, 28, (2): 176 pp.
- Hall, W.D.M. and Goode, A.D.T., 1978. The Early Proterozoic Nabberu Basin and associated iron formations of Western Australia. *Precam. Res.*, 7: 129-184.
- Hallam, A. and Bradshaw, M.J., 1979. Bituminous shales and oolithic ironstones as indicators of transgressions and regressions. *J. Geol. Soc. London*, 136: 157-164.
- Hallam, A. and Maynard, J.B., 1987. The iron ores and associated sediments of the Chichali formation (Oxfordian to Valanginian) of the Trans-Indus Salt Range, Pakistan. *J. Geol. Soc. London*, 144: 107-114.
- Hallimond, A.F., 1922. On glauconite from the Greensand near Lewes, Sussex; the constitution of glauconite. *Mineral. Mag.*, 19: 330-333.
- Hallimond, A.F., 1925. Iron ores: bedded ores of England and Wales, petrography and chemistry. *Spec. Rep. Mineral Resources of Great Britain*, Great Britain Geol. Surv. Mem., Vol. 29, 129 pp.
- Hallimond, A.F., 1951. Problems of sedimentary iron ores. *Yorkshire Geol. Soc., Proc.*, 28: 61-66.
- Hamilton, P.J., O'Nions, R.K., Evensen, N.M., Bridgwater, D. and Allaart, J.H., 1978. Sm-Nd isotopic investigations of Isua supracrustals and implications for mantle evolution. *Nature*, 272: 41-43.
- Han, Tsu-Ming, 1978. Microstructures of magnetite as guides to its origin in some Precambrian iron-formations. *Fortschr. Miner.*, 56: 105-142.
- Hangari, K.M., Ahmad, S.N. and Perry, E.C. Jr., 1980. Carbon and oxygen isotope ratios in diagenetic siderite and magnetite from Upper Devonian ironstone, Wadi Shatti district, Libya. *Econ. Geol.*, 75: 538-545.
- Harder, H., 1954. Beitrag zur Petrographie und Genese der Hamatiterze des Lahn-Dill-Gebietes. Heidelb. *Beitr. Mineral. Petrogr.*, 4: 54-66.
- Harder, H., 1964a. On the diagenetic origin of berthierin (chamositic) iron ores. In: *Genetic Problems of Ores*. 22nd Int. Geol. Congr., New Delhi, 1964, Part 5: 193-198.
- Harder, H., 1964b. The use of trace elements in distinguishing different genetic types of marine sedimentary iron ores. In: *Genetic Problems of Ores*. 22nd Int. Geol. Congr., New Delhi 1964, Part 5: 551-556.
- Harder, H., 1978. Synthesis of iron layer silicate minerals under natural conditions. *Clays Clay Miner.*, 26: 65-72.
- Harder, H., 1980. Synthesis of glauconite at surface temperatures. *Clays Clay Miner.*, 28: 217-222.
- Hardjosoesastro, R., 1971. Note on chamosite in sediments of the Surinam shelf. *Geol. Mijnbouw*, 50: 29-33.
- Harley, D.N., 1979. A mineralized Ordovician resurgent caldera complex in the Bathurst-Newcastle mining district, New Brunswick, Canada. *Econ. Geol.*, 74: 786-796.
- Harmon, K.A., Shaw, D.M. and Crocket, J.H., 1978. Tungsten abundance in Precambrian iron-formations and other sedimentary rocks. *Econ. Geol.*, 73: 1167-1170.
- Harms, J.E., 1965. Iron ore deposits of Constance Range. In: *Geology of Australian Ore Deposits*, vol. 1. Australas. Inst. Min. Metall., pp. 264-269.
- Harrar, C.M., 1966. Wyoming iron-ore deposits. U.S. Bur. Mines, Inf. Circular 8315, 114 pp.
- Harrison, R.K., Howarth, M.K., Styles, M.T. and Young, B.R., 1983. Ooids with goyazite-crandallite rims from the top of the Marlstone Rock Bed (Toarcian, Lower Jurassic) near Harston, Leicestershire, U.K. *Inst. Geol. Sci., Short Commun.*, 83-1: 16-23.
- Harvey, R.D., Cahill, R.A., Chou, C.-L. and Steele, J.D., 1983. Mineral matter and trace elements in the Herrin and Springfield coals, Illinois Basin coal field. Ill. State Geol. Surv., Contr. Rep., 1983-4, 162 pp.
- Hassler, S.W., 1987. Paleoenvironments of the 2 Ga-old Gunflint iron formation in the Rossport-Schreiber area, Ontario, Canada. *Geol. Soc. Am., Abstr. Progr.*, 19: 570.
- Hattori, K., Krouse, H.R. and Campbell, F.A., 1983. The start of sulfur oxidation in continental environments about 2.2×10^9 years ago. *Science*, 221: 549-551.
- Hawley, J.E. and Beavan, A.P., 1934. Mineralogy and genesis of the Mayville iron ore of Wisconsin. *Am. Mineral.*, 19: 493-514.
- Hayes, A.O., 1915. Wabana iron ore of Newfoundland. *Geol. Surv. Can., Mem.*, 78, 162 pp.
- Hayes, A.O., 1929. Further studies of the origin of the Wabana iron ore of Newfoundland. *Econ. Geol.*, 24: 687-690.
- Hedberg, H.D., Moody, J.D. and Hedberg, R.M., 1979. Petroleum prospects of the deep offshore. *Am. Assoc. Pet. Geol., Bull.*, 63: 286-300.
- Hemingway, J.E., 1951. Cyclic sedimentation and the deposition of ironstone in the Yorkshire Lias. *Yorkshire Geol. Soc., Proc.*, 28: 67-74.
- Henriquez, F.J., 1974. Iron formation-massive sulphide relationships at Heath Steele, Brunswick no. 6 (N.B.) and Matagami Lake, Bell Allard (Quebec). Unpubl. M.S. thesis, McGill Univ., Montreal, Que.
- Higgins, G.E. and Saunders, J.B., 1967. Report on 1964 Chatham mud island, Erin bay, Trinidad, West Indies. *Am. Assoc. Pet. Geol., Bull.*, 51: 55-64.
- Hildebrand, R.S., 1986. Kiruna-type deposits: their origin and relationship to intermediate subvolcanic plutons in the Great Bear magmatic zone, Northwest Canada. *Econ. Geol.*, 81: 640-659.
- Hill, C.R., Moore, D.T., Greensmith, J.T. and Williams, R., 1985. Palaeobotany and petrology of a Middle Jurassic ironstone bed at Wrack Hills, North Yorkshire. *Proc. Yorkshire Geol. Soc.*, 45: 277-292.
- Hirst, D.M., 1962. The geochemistry of modern sediments from the Gulf of Paria - I The relationship between the mineralogy and the distribution of major elements. *Geochim. Cosmochim. Acta*, 26: 309-334.
- Hoefs, J., Mueller, G., Schuster, K.A. and Walde, D., 1987. The Fe-Mn ore deposits of Urucum, Brazil: An oxygen isotope study. *Chem. Geol.*, 65: 311-319.

- Hoenes, D. and Troger, E., 1945. Lagerstaetten oolithischer Eisenerze in Nordwestfrankreich. *Neues Jahrb. Mineral., Geol. Palaeontol., Abh.*, 79, (A): 192-257.
- Hofmann, H.J., Thurston, P.C. and Wallace, H., 1985. Archean stromatolites from Uchi greenstone belt, northwestern Ontario. In: L.D. Ayres et al. (Editors), *Evolution of Archean Supracrustal Sequences*. *Geol. Assoc. Can., Spec. Pap.*, 25: 125-132.
- Hofmann, H.J. and Schopf, J.W., 1983. Early Proterozoic microfossils. In: J.W. Schopf (Editor), *Earth's Earliest Biosphere, Its Origin and Evolution*. Princeton Univ. Press, Princeton, N.J., pp. 321-360.
- Holland, H.D., 1962. Model for the evolution of the Earth's atmosphere. In: A.E.J. Engel et al. (Editors), *Petrologic Studies: A Volume in Honor of A.F. Buddington*. *Geol. Soc. Am., Boulder, Colo.*, pp. 447-477.
- Holland, H.D., 1973. The oceans: a possible source of iron in iron-formations. *Econ. Geol.*, 68: 1169-1172.
- Holland, H.D., 1984. The chemical evolution of the atmosphere and oceans. Princeton Univ. Press, Princeton, N.J., 582 pp.
- Holland, H.D., in press. The Flin Flon paleosol and the composition of the atmosphere 1.8 b.y.b.p. *Am. J. Sci., Garrels Memorial Issue*.
- Holland, H.D., Lazar, B. and McCaffrey, M., 1986. Evolution of the atmosphere and oceans. *Nature*, 320: 27-33.
- Holland, H.D. and Malinin, S.D., 1979. The solubility and occurrence of non-ore minerals. In: *Geochemistry of Hydrothermal Solutions*, 2nd ed. H.L. Barnes (Editor), John Wiley, New York, N.Y., pp. 461-508.
- Holm, N.G., 1987. Biogenic influences on the geochemistry of certain ferruginous sediments of hydrothermal origin. *Chem. Geol.*, 63: 45-57.
- Horvath, F. and Berckhemer, H., 1982. Mediterranean back arc basins. In: H. Berckhemer and K. Hsu (Editors), *Alpine-Mediterranean Geodynamics*. Am. Geophys. Union., *Geodynamics Ser.*, 7: 141-173.
- Hough, J.L., 1958. Fresh-water environment of deposition of Precambrian banded iron formations. *J. Sediment. Petrol.*, 28: 414-430.
- Hovis, W.A. and Szajna, E.F., (Editors), undated. NIMBUS-7 CZCS coastal zone color scanner imagery for selected coastal regions. NASA Goddard level II photographic product, Walter A. Bohan Comp., 99 pp.
- Howard, A.S., 1985. Lithostratigraphy of the Staithes Sandstone and Cleveland Ironstone formations (Lower Jurassic) of northeast Yorkshire. *Proc. Yorkshire Geol. Soc.*, 45: 261-275.
- Hubbard, R.J., 1988. Age and significance of sequence boundaries on Jurassic and Early Cretaceous rifted continental margins. *Am. Assoc. Pet. Geol., Bull.*, 72: 49-72.
- Huber, N.K., 1959. Some aspects of the origin of the Ironwood Iron-formation of Michigan and Wisconsin. *Econ. Geol.*, 54: 83-118.
- Hunter, D.R., 1963. The Mozaan series in Swaziland. *Swaziland Geol. Surv., Bull.*, 3: 5-16.
- Hunter, R.E., 1970. Facies of iron sedimentation in the Clinton group. In: G.W. Fisher et al. (Editors), *Studies of Appalachian Geology, Central and Southern*. Wiley, New York, N.Y., pp. 102-121.
- Hurst, M.E., 1930. Pickle Lake-Crow River area, District of Kenora (Patricia Portion). *Ont. Dep. Mines, Annu. Rep.*, 34 (2): 1-35.
- Iijimia, A. and Matsumoto, R., 1982. Berthierine and chamosite in coal measures of Japan. *Clays Clay Miner.*, 30: 264-274.
- Ikonnikov, A.B., 1975. *Mineral resources of China*. *Geol. Soc. Am., Microform Publ.*, 2, 555 pp.
- Immega, I.P. and Klein, C. Jr., 1976. Mineralogy and petrology of some metamorphic Precambrian iron-formations in southwestern Montana. *Am. Mineral.*, 61: 1117-1144.
- Ingri, J. and Ponter, C., 1986. Iron and manganese layering in Recent sediments in the Gulf of Bothnia. *Chem. Geol.*, 56: 105-116.
- Ingri, J. and Ponter, C., 1987. Rare earth abundance patterns in ferromanganese concretions from the Gulf of Bothnia and the Barents Sea. *Geochim. Cosmochim. Acta*, 51: 155-161.
- Ireland, B.J., Curtis, C.D. and Whiteman, J.A., 1983. Compositional variation within some glauconites and illites and implications for their stability and origins. *Sedimentology*, 30: 769-786.
- Jackson, G.D., 1960. Belcher islands, Northwest Territories. *Geol. Surv. Can., Pap.* 60-20, 13 pp.
- Jackson, G.D., Iannelli, T.R., Narbonne, G.M. and Wallace, P.J., 1978. Upper Proterozoic sedimentary and volcanic rocks of northwestern Baffin island. *Geol. Surv. Can., Pap.* 78-14: 1-15.
- Jaff, R., Albrecht, P. and Oudin, J.L., 1988. Carboxylic acids as indicators of oil migration: II. Case of the Mahakam delta, Indonesia. *Geochim. Cosmochim. Acta*, 52: 2599-2607.
- Jam L., P. and Mendez Arocha, M., 1962. *Geología de las islas de Margarita, Coche, y Cubagua*. Soc. Cienc. Nat. La Salle, Venezuela, Mem., 22: 51-93.
- James, H.E. and Van Houten, F.B., 1979. Miocene goethitic and chamositic oolites, northeastern Colombia. *Sedimentology*, 26: 125-133.
- James, H.L., 1951. Iron formation and associated rocks in the Iron River district, Michigan. *Geol. Soc. Am. Bull.*, 62: 251-266.
- James, H.L., 1954. Sedimentary facies of iron-formation. *Econ. Geol.*, 49: 235-293.
- James, H.L., 1958. Stratigraphy of pre-Keweenawan rocks in parts of northern Michigan. *U.S. Geol. Surv., Prof. Pap.*, 314-C, 44 pp.
- James, H.L., 1966. Chemistry of the iron-rich sedimentary rocks. In: M. Fleischer (Editor), *Data of Geochemistry, Chapter W*. (6th ed.), U.S. Geol. Surv., Prof. Pap., 440-W, 61 pp.
- James, H.L., 1983. Distribution of banded iron-formation

- in space and time. In: A.F. Trendall and R.C. Morris (Editors), Iron-formation: Facts and Problems. Elsevier, Amsterdam, pp. 471-490.
- James, H.L., Clark, L.D., Lamey, C.A. and Pettijohn, F.J., 1961. Geology of central Dickinson County, Michigan. U.S. Geol. Surv., Prof. Pap., 310, 176 pp.
- James, H.L. and Sims, P.K., 1972. Precambrian iron-formations of the world, Introduction. Econ. Geol., 68: 913-914.
- Jenkins, W.J., Edmond, J.M. and Corliss, J.B., 1978. Excess ^3He and ^4He in Galapagos submarine hydrothermal waters. Nature, 272: 156-158.
- Jenkins, R.J.F., 1985. The enigmatic Ediacaran (late Precambrian) genus *Rangea* and related forms. Paleobiology, 11: 336-355.
- Jenkyns, H.C., 1988. The Early Toarcian (Jurassic) anoxic event: stratigraphic, sedimentary, and geochemical evidence. Am. J. Sci., 288: 101-151.
- Johnson, T.C., Halfman, J.D., Rosendahl, B.R. and Lister, G.S., 1987. Climatic and tectonic effects on sedimentation in a rift-valley lake: Evidence from high-resolution seismic profiles, Lake Turkana, Kenya. Geol. Soc. Am., Bull., 98: 439-447.
- Jones, H.A., 1955. The occurrence of oolitic ironstones in Nigeria: their origin, geologic history, and petrology. Unpubl. PhD. thesis, Oxford Univ., Oxford, , 206 pp.
- Jones, H.A., 1965. Ferruginous oolites and pisolithes. J. Sediment. Petrol., V (35): 838-845.
- Jones, W.J., Nagle, D.P. Jr. and Whitman, W.B., 1987. Methanogens and the diversity of Archaeabacteria. Microbiol. Rev., 51: 135-177.
- Jongsma, D., Fortuin, A.R.W., Huson, S.R., Troelstra, G.T., Klaver, T., Peters, J.M., van Harten, D., de Lange, G.J. and ten Haven, L., 1983. Discovery of an anoxic basin within the Strabo Trench, eastern Mediterranean. Nature, 305: 795-797.
- Jowett, E.C., Rydzewski, A. and Jowett, R., 1987. The Kupferschiefer Cu-Ag ore deposits in Poland: a re-appraisal of the evidence of their origin and presentation of a new genetic model. Can. J. Earth Sci., 24: 2016-2037.
- Juniper, S.K. and Fouquet, Y., 1988. Filamentous iron-silica deposits from modern and ancient hydrothermal sites. Can. Mineral., 26: 859-869.
- Kalugin, A.S., 1973. Geology and genesis of the Devonian banded iron-formation in Altai, western Siberia and eastern Kazakhstan. In: Genesis of Precambrian Iron and Manganese Deposits. Proc. Kiev Symp. (1970). UNESCO, Paris, pp. 159-165.
- Kasting, J.F., 1987. Theoretical constraints on oxygen and carbon dioxide concentrations in the Precambrian atmosphere. Precambrian Res., 34: 205-229.
- Karl, D.M.P., LaRock, P.A. and Shultz, D.J., 1977. Adenosine triphosphate and organic carbon in the Cariaco Trench. Deep-Sea Res., 24: 105-113.
- Kartsev, A.A., Vagin, S.B., Serebryakova, L.K. and Kon- drat'yev, I.A., 1981. Recognition of zones of oil-gas accumulation in the west Cis-Caucasus on a basis of paleohydrodynamic reconstructions. Pet. Geol. (U.S.S.R.), 19: 35-38.
- Kazmierczak, J., 1979. The eukaryotic nature of Eosphaera-like ferriferous structures from the Precambrian Gunflint iron formation, Canada: A comparative study. Precambrian Res., 9: 1-22.
- Keith, M.L., 1982. Violent volcanism, stagnant oceans and some inferences regarding petroleum, strata-bound ores and mass extinctions. Geochim. Cosmochim. Acta, 46: 2621-2637.
- Kelly, V.C., 1951. Oolitic iron deposits of New Mexico. Am. Assoc. Pet. Geol., Bull., 35: 2179-2228.
- Kempe, S. and Degens, E.T., 1985. An early soda ocean? Chem. Geol., 53: 95-108.
- Kerr, P.F., Drew, I.M. and Richardson, D.S., 1970. Mud volcano clay, Trinidad, West Indies. Am. Assoc. Pet. Geol., Bull., 54: 2101-2110.
- Kharaka, Y.K., Lico, M.S., Wright, V.A. and Carothers, W.W., 1980. Geochemistry of formation waters from Pleasant Bayou No. 2 well and adjacent areas in coastal Texas. Proc. Fourth Geopressurized-Geothermal Energy Conf., Austin, Tex., pp. 168-193.
- Kimberley, M.M., 1974. Origin of iron ore by diagenetic replacement of calcareous oolite. Unpubl. Ph.D. thesis, Princeton Univ., Princeton, New Jersey, N.J., Vol. 1, 345 pp., Vol. 2, 386 pp.
- Kimberley, M.M., 1978a. Paleoenvironmental classification of iron formations. Econ. Geol., 73: 215-229.
- Kimberley, M.M., 1978b. Origin of stratiform uranium deposits in sandstone, conglomerate, and pyroclastic rock. In: M.M. Kimberley (Editor), Uranium Deposits, their Mineralogy and Origin. Mineral. Assoc. Can.. Short-Course Vol. 3, pp. 339-381.
- Kimberley, M.M., 1979a. Origin of oolitic iron formations. J. Sediment. Petrol., 49: 111-132.
- Kimberley, M.M., 1979b. Geochemical distinctions among environmental types of iron formations. Chem. Geol., 25: 185-212.
- Kimberley, M.M., 1980. The Paz de Rio oolitic inland-sea iron formation. Econ. Geol., 75: 97-106.
- Kimberley, M.M., 1981a. Development of Precambrian chemical sedimentation: Control by the rate of biological or tectonomagmatic evolution? EOS, Am. Geophys. Union, Trans., 62: 419.
- Kimberley, M.M., 1981b. Oolitic iron formations. In: K.H. Wolf (Editor), Handbook of Strata-bound and Stratiform Ore Deposits, Vol. 9: 25-76.
- Kimberley, M.M., 1983a. Constraints on genetic modeling of Proterozoic iron formations. In: L.G. Medaris Jr. et al. (Editors), Proterozoic Geology: Selected Papers from an International Proterozoic Symposium. Geol. Soc. Am., Mem., 161: 227-235.
- Kimberley, M.M., 1983b. Ferriferous ooids. In: T.M. Peryt (Editor), Coated Grains. Springer., Berlin, pp. 100-108.

- Kimberley, M.M., 1986. Did weathering on land or sea floor produce ironstone? *Am. Assoc. Pet. Geol., Bull.*, 70: 606-607.
- Kimberley, M.M., 1988. Relationship of iron formations to paleosol. *Terra Cognita*, 8: 213.
- Kimberley, M.M. and Llano, M., in press. Structural lineaments in the Margarita-Araya region of Venezuela: Boundaries of ecologic environments. *Soc. Cienc. Nat. La Salle, Venezuela, Mem.*, 48.
- Kimberley, M.M., Niederreither, M.S. and Llano, M., in press. Effect of marine currents, tides, wind, and Pleistocene sea-level changes on sedimentation in the Margarita-Araya region of Venezuela. *Soc. Cienc. Nat. La Salle, Venezuela, Mem.*, 48.
- Kimberley, M.M. and Sorbara, J.P., 1976. Post-Archean weathering of Steep Rock Group iron formation. In: *Geotraverse Workshop 1976*, Univ. Toronto Press, Toronto, Ont., pp. 32-1-32-17.
- King, L.H., Fader, G.B.J., Jenkins, W.A.M. and King, E.L., 1986. Occurrence and regional setting of Paleozoic rocks on the Grand Banks of Newfoundland. *Can. J. Earth Sci.*, 23: 504-526.
- Kirkham, R.V., 1979. Copper in iron-formation. *Geol. Surv. Can., Pap.* 79-1B: 17-22.
- Klein, C., 1983. Diagenesis and metamorphism of Precambrian banded iron-formations. In: A.F. Trendall and R.C. Morris (Editors), *Iron-formation: Facts and Problems*. Elsevier, Amsterdam, pp. 417-469.
- Klein, C. and Bricker, O.P., 1978. Some aspects of the sedimentary and diagenetic environment of Proterozoic banded iron formations - a reply. *Econ. Geol.*, 73: 1371-1373.
- Klein, C. and Fink, R.P., 1976. Petrology of the Sokoman iron formation in the Howells River area, at the western edge of the Labrador trough. *Econ. Geol.*, 71: 453-387.
- Klemm, D.D., 1979. A biogenetic model of the formation of the banded iron formation in the Transvaal Supergroup/South Africa. *Miner. Deposita*, 14: 381-385.
- Knauss, J.A., 1978. Introduction to physical oceanography. Prentice-Hall, Englewood Cliffs, N.J., 338 pp.
- Knoll, A.H., 1987. Why did the Proterozoic Eon End? *Geol. Soc. Am., Abstr. Progr.*, 19: 730.
- Knoll, A.H. and Awramik, S.M., 1983. Ancient microbial ecosystems. In: W.E. Krumbein (Editor), *Microbial Geochemistry*. Blackwell Scientific Publ., Oxford, pp. 287-315.
- Kobe, H.W. and Pettinga, J.R., 1984. Red Island (NZ) and its submarine-exhalative Mn-Fe mineralization. In: A. Wauschkuhn, C. Kluth and R.A. Zimmermann (Editors), *Syngensis and Epigenesis in the Formation of Mineral Deposits*. Springer, Berlin, pp. 562-572.
- Kodama, H. and Schnitzer, M., 1977. Effect of fulvic acid on the crystallization of Fe(III) oxides. *Geoderma*, 19: 279-291.
- Kolbe, H., 1970. Zur Entstehung und Charakteristik mesozoischer marin-sedimentärer Eisenerze im östlichen Niedersachsen. *Clausthaler Hefte Lagerstättenkd. Geochim. Miner. Rohst.*, 9: 161-184.
- Kolbe, H. and Simon, P., 1969. Die Eisenerze im Mittleren und Oberen Korallenoolith des Gifhorner Troges. In: H. Bottke et al. (Editors), *Sammelwerk Deutsche Eisenerzlagerstätten*, II.1. Die marin-sedimentären Eisenerze des Jura in Nordwestdeutschland. *Beih. Geol. Jahrb.*, 79, pp. 256-338.
- Kolbe, R.K.H., 1972. Influence of salt tectonics on formation and conservation of sedimentary iron ores. In: G. Richter-Bernburg (Editor), *Geology of Saline Deposits*. UNESCO, (1972), Paris, pp. 243-245.
- Krinsley, D. Pye, K. and O'Hara, P., 1987. Glauconite pellets in Jurassic mudrocks from the southern North Sea. *Geol. Soc. Am., Abstr. Progr.*, 19: 733-734.
- Krishnan, M.S., 1973. Occurrence and origin of the iron ores of India. In: *Genesis of Precambrian Iron and Manganese Deposits*. UNESCO Earth Sci. 9: 69-76.
- Kunzendorf, H., Walter, P., Stoffers, P. and Gwozdz, R., 1984. Metal variations in divergent plate-boundary sediments from the Pacific. *Chem. Geol.*, 47: 113-133.
- Kwak, T.A.P., Brown, W.M., Abeysinghe, P.B. and Tan, T.H., 1986. Fe solubilities in very saline hydrothermal fluids: Their relation to zoning in some ore deposits. *Econ. Geol.*, 81: 447-465.
- Laajoki, K. and Saikkonen, R., 1977. On the geology and geochemistry of the Precambrian iron-formations in Vayrylankyla, south Puolanka area, Finland. *Geol. Surv. Finland, Bull.*, 292, 136 pp.
- LaBerge, G.L., 1973. Possible biological origin of Precambrian iron formations. *Econ. Geol.*, 68: 1098-1109.
- Lagonell, E., 1987. Se repetira terremoto de Caracas. *Elite (Venezuela)*, 61, 3219: 14-16.
- Lalou, C. and Brichet, E., 1987. On the isotopic chronology of submarine hydrothermal deposits. *Chem. Geol.*, 65: 197-207.
- Lambeck, K., 1986. Planetary evolution: Banded iron formations. *Nature*, 320: 574.
- Lambert, M.B., 1976. The Back River volcanic complex, District of Mackenzie. *Geol. Surv. Can., Pap.* 76-1, (A): 363-367.
- Lambert, M.B., 1978. The Back River volcanic complex - a cauldron subsidence structure of Archean age. *Geol. Surv. Can., Pap.* 78-1A: 153-157.
- Lambert-Aikhionbare, D.O., 1982. Relationship between diagenesis and pore fluid chemistry in Niger Delta oil-bearing sands. *J. Pet. Geol.*, 4: 287-298.
- Lamplugh, G.W., Wedd, C.B. and Pringle, J., 1920. Bedded ores of the Lias, Oolites, and later formations in England, In: *Iron Ores*, Vol. 12. G. B. Geol. Surv., Mem., 240 pp.
- Landergren, S., 1948. On the geochemistry of Swedish iron ores and associated rocks. *Sver. Geol. Unders., Ser. C*, 496, 182 pp.
- Landing, W.M. and Bruland, K.W., 1987. The contrasting biogeochemistry of iron and manganese in the Pacific

- Ocean. *Geochim. Cosmochim. Acta*, 51: 29-43.
- LaRock, P.A., Lauer, R.D., Schwarz, J.R., Watanabe, K.K. and Wiesenburg, D.A., 1979. Microbial biomass and activity distribution in an anoxic, hypersaline basin. *Appl. Environm. Microbiol.*, 37: 466-470.
- Larue, D.K., 1981a. The early Proterozoic pre-iron formation Menominee Group siliciclastic sediments of the southern Lake Superior region: Evidence for sedimentation in platformal settings on an early Proterozoic craton. *J. Sediment. Petrol.*, 51: 397-414.
- Larue, D.K., 1981b. The Chocolay Group, Lake Superior region, U.S.A.: Sedimentological evidence for deposition in basinal and platformal settings on an early Proterozoic craton. *Geol. Soc. Am., Bull.*, 92: 417-435.
- Larue, D.K. and Sloss, L.L., 1980. Early Proterozoic sedimentary basins of the Lake Superior region. *Geol. Soc. Am., Bull.*, 91 (2): 1836-1874.
- Latal, E., 1952. Die Eisenerzlagerstätten Jugoslaviens. In: *Symposium sur les gisements de fer du monde*, Vol. 2. 19th Int. Geol. Congr., Algiers, pp. 529-563.
- Lawrence, J.R. and Taviani, M., 1988. Extreme hydrogen, oxygen and carbon isotope anomalies in the pore waters and carbonates of the sediments and basalts from the Norwegian Sea: methane and hydrogen from the mantle? *Geochim. Cosmochim. Acta*, 52: 2077-2083.
- Le Huray, A.P., Caulfield, J.B.D., Rye, D.M. and Dixon, P.R., 1987. Basement controls on sediment-hosted Zn-Pb deposits: A Pb-isotope study of Carboniferous mineralization in central Ireland. *Econ. Geol.*, 82: 1695-1709.
- Lemoalle, J., 1974. Bilan des apports en fer au lac Tchad. O.R.S.T.O.M., Ser. Hydrobiol., 8(1): 35-40.
- Lemoalle, J. and Dupont, B., 1973. Iron-bearing oolites and the present conditions of iron sedimentation in Lake Chad (Africa). In: G.C. Amstutz and A.J. Bernard (Editors), *Ores in Sediments*. Springer, Berlin, pp. 167-178.
- Lepp, H., 1963. The relation of iron and manganese in sedimentary iron formations. *Econ. Geol.*, 58: 515-526.
- Lepp, H., 1972. Normative mineral composition of the Biwabik Formation: a first approach. In: B.R. Doe and D.K. Smith (Editors), *Studies in Mineralogy and Precambrian Geology*. *Geol. Soc. Am., Mem.*, 135: 265-278.
- Lepp, H. (Editor), 1975. *Geochemistry of Iron*. Halsted Press, 464 pp.
- Lepp, H. and Goldich, S.S., 1973. Origin of Precambrian iron formations. *Econ. Geol.*, 59: 1025-1060.
- Liao, S.-F., 1964. A study on the paleogeographic-lithologic facies and the metallogenesis of the Ninghsiang type of iron ores (in Chinese). *Acta Geol. Sin.*, 44: 68-80.
- Lippmann, F., 1973. *Sedimentary carbonate minerals*. Springer, Berlin, 238 pp.
- Lobato, L.M., Forman, J.M.A., Fazikawa, K., Fyfe, W.S. and Kerrich, R., 1983. Uranium in overthrust Archean basement, Bahia, Brazil. *Can. Miner.*, 21: 647-654.
- Logvinenko, N.V., 1982. Origin of glauconite in Recent bottom sediments of the ocean. *Sediment. Geol.*, 31: 43-48.
- Lougheed, M.S., 1983. Origin of Precambrian iron-formations in the Lake Superior region. *Geol. Soc. Am., Bull.*, 94: 325-340.
- Lougheed, M.S. and Mancuso, J.J., 1973. Hematite frambooids in the Negaunee iron formation, Michigan: Evidence for their biogenic origin. *Econ. Geol.*, 68: 202-209.
- Lovering, T.W., 1929. The Rawlins, Shirley, and Seminoe iron-ore deposits, Carbon County, Wyoming. *U.S. Geol. Surv., Bull.*, 811-D: 203-235.
- Lovley, D.R., 1987. Microbial transformations of iron minerals. In: *U.S. Geol. Surv. Circ.*, 995: 42.
- Lucotte, M. and d'Anglejan, B., 1988. Processes controlling phosphate adsorption by iron hydroxides in estuaries. *Chem. Geol.*, 67: 75-83.
- Lunar, R. and Amoros, J.L., 1979. Mineralogy of the oolitic iron deposits of the Ponferrada-Astorga zone, north-western Spain. *Econ. Geol.*, 74: 751-762.
- Lundberg, B. and Smellie, J.A.T., 1979. Painirova and Mertaineu iron ores: Two deposits of the Kiruna iron ore type in northern Sweden. *Econ. Geol.*, 74: 1131-1152.
- Lyons, W.B., Spencer, M.J., Hines, M.E. and Gaudette, H.E., 1988. The trace metal geochemistry of pore water brines from two hypersaline lakes. *Geochim. Cosmochim. Acta*, 52: 265-274.
- MacDonald, A.J., 1983. The iron formation - gold association. In: A.C. Colvine (Editor), *The Geology of Gold in Ontario*. *Ont. Geol. Surv., Misc. Pap.*, 110: 75-83.
- Macgregor, M., Lee, G.W. and Wilson, G.V., 1920. The iron ores of Scotland. In: *Iron Ores*, Vol. 11. G.B. Geol. Surv. Mem., 236 pp.
- Mach, D.L., Ramirez, A. and Holland, H.D., 1987. Organic phosphorus and carbon in marine sediments. *Am. J. Sci.*, 278: 429-441.
- Mackenzie, F.T. and Garrels, R.M., 1966. Chemical mass balance between rivers and oceans. *Am. J. Sci.*, 264: 507-525.
- Majumber, T. and Chakraborty, K.L., 1977. Primary sedimentary structures in the banded iron-formation of Orissa, India. *Sediment. Geol.*, 19: 287-300.
- Majumber, T. and Chakraborty, K.L., 1979. Petrography and petrology of the Precambrian banded iron-formation of Orissa, India and reformation of the bands. *Sediment. Geol.*, 22: 243-265.
- Maloney, N.J., 1971a. Surface sediment facies of the continental margin off eastern Venezuela. *UNESCO Symp. Investigations and Resources of the Caribbean Sea and Adjacent Regions (Paris)*, pp. 251-260.
- Maloney, N.J., 1971b. Continental margin off central Venezuela. *UNESCO Symp. Investigations and Resources of the Caribbean Sea and Adjacent Regions (Paris)*, pp. 261-266.
- Mancuso, J.J., 1966. Sequence of oxidation and related mineral changes, Negaunee iron formation, eastern Marquette range, Michigan. *The Compass of Sigma Gamma Epsilon*, 43: 227-236.
- Mancuso, J.J., Lougheed, M.S. and Wygant, T., 1971. Pos-

- sible biogenic structures from the Precambrian Negaunee (iron) Formation, Marquette Range, Michigan. *Am. J. Sci.*, 271: 181–186.
- Mancuso, J.J., Lougheed, M.S. and Shaw, R., 1975. Carbonate apatite in Precambrian cherty iron-formation, Baraga County, Michigan. *Econ. Geol.*, 70: 583–586.
- Manheim, F.T., Popenoe, P., Siapno, W. and Lane, C., 1982. Manganese-phosphorite deposits of the Blake Plateau. In: P. Halbach and P. Winter (Editors), *Marine Rohstoffe und Meerestechnik*, Vol. 6. *Marine Mineral Deposits*. Glueckauf, Essen, pp. 9–44.
- Mann, V.I., 1961. Iron formations in the southeastern United States. *Econ. Geol.*, 56: 997–1001.
- Mansfield, G.R., 1922. Potash in the greensands of New Jersey. *U.S. Geol. Surv. Bull.*, 727, 146 pp.
- Markland, G.D., 1966. Geology of the Moose Mountain mine and its application to mining and milling. *Trans. Can. Inst. Min. Metall.*, 69: 159–170.
- Markun, C.D. and Randazzo, A.F., 1980. Sedimentary structures in the Gunflint iron formation. *Precambrian Res.*, 12: 287–310.
- Martini, J.E.J., 1986. Stratiform gold mineralization in paleosol and ironstone of early Proterozoic age, Transvaal Sequence, South Africa. *Miner. Deposita*, 21: 306–312.
- Mascle, J.R., Bornhold, B.D. and Renard, V., 1973. Diapiric structures off Niger delta. *Am. Assoc. Pet. Geol. Bull.*, 57: 1672–1678.
- Matthews, A., 1976. Magnetite formation by the reduction of hematite under hydrothermal conditions. *Am. Mineral.*, 61: 927–932.
- Mattson, P.H., 1984. Caribbean structural breaks and plate movements. In: W.E. Bonini, R.B. Hargraves and R. Shagam (Editors), *The Caribbean-South American Plate Boundary and Regional Tectonics*. *Geol. Soc. Am. Mem.*, 162: 131–152.
- Matsuzawa, I., 1953. The Sinian System in the district of Pangchiapu, southern Chahar, north China, and consideration of the origin of its contained Hsuanlung type iron ore deposits (in Japanese). *J. Soc. Min. Geol. Jpn.*, 3: 220–235.
- Matti, S. and Laajoki, K., 1975. Whole rock Pb-Pb isochron age for the Paakkö iron formation in Väyryläkylä, South Puolanka area, Finland. *Bull. Geol. Soc. Finl.*, 47: 113–116.
- Maynard, J.B., 1983. *Geochemistry of Sedimentary Ore Deposits*. Springer, New York, N.Y., 305 pp.
- Maynard, J.B., 1986. Geochemistry of oolitic iron ores, an electron microprobe study. *Econ. Geol.*, 81: 1473–1483.
- McCaig, A.M., 1988. Deep fluid circulation in fault zones. *Geology*, 16: 867–870.
- McGhee, G.R. and Bayer, U., 1985. The local signature of sea-level changes. In: U. Bayer and A. Seilacher (Editors), *Lecture Notes in Earth Sciences*, Vol. 1. *Sedimentary and Evolutionary Cycles*. Springer, Berlin, pp. 98–112.
- McKelvey, V.E., 1986. Subsea mineral resources. *U.S. Geol. Surv. Bull.*, 1689-A, 106 pp.
- McKibben, M.A., Williams, A.E. and Okubo, S., 1988. Metamorphosed Plio-Pleistocene evaporites and the origins of hypersaline brines in the Salton Sea geothermal system, California: Fluid inclusion evidence. *Geochim. Cosmochim. Acta*, 52: 1047–1056.
- McLennan, S.M., 1976. Paleo-environment of iron rich sedimentary rocks: A discussion. *Geol. Rundsch.*, 65: 1126–1129.
- McRae, S.G., 1972. Glauconite. *Earth-Sci. Rev.*, 8: 397–440.
- Mellon, G.V., 1962. Petrology of Upper Cretaceous oolitic iron-rich rocks from northern Alberta. *Econ. Geol.*, 57: 921–940.
- Mel'nik, Yu.P., 1982. *Precambrian Banded Iron-formations, Physicochemical Conditions of Formation*. Elsevier, Amsterdam, 310 pp.
- Metz, H.L., 1964. Geology of the El Pilar fault zone, State of Sucre, Venezuela. Ph.D. Thesis, Princeton Univ., Princeton, N.J., 102 pp.
- Metz, S., Trefry, J.H. and Nelsen, T.A., 1988. History and geochemistry of a metalliferous sediment core from the Mid-Atlantic Ridge at 26° N. *Geochim. Cosmochim. Acta*, 52: 2369–2378.
- Michelson, J.E., 1976. Miocene deltaic oil habitat, Trinidad. *Am. Assoc. Pet. Geol. Bull.*, 60: 1502–1519.
- Miki, T. and Fukuoka, M., 1983. "Glauconites" from the Tertiary sedimentary rocks in northern Kyusku, Japan (in Japanese). *J. Jpn. Assoc. Pet. Technol.*, 48: 19–28.
- Miller, A.R., Densmore, C.D., Degens, E.T., Hathaway, J.C., Manheim, F.T., McFarlin, P.F., Docklington, R. and Jokela, A., 1966. Hot brines and recent iron deposits in deeps of the Red Sea. *Geochim. Cosmochim. Acta*, 30: 341–359.
- Miller, R.G. and O'Nions, R.K., 1985. Source of Precambrian chemical and clastic sediments. *Nature*, 314: 325–330.
- Millero, F.J., Sotolongo, S. and Izaguirre, M., 1987. The oxidation kinetics of Fe (II) in seawater. *Geochim. Cosmochim. Acta*, 51: 793–801.
- Miyano, T. and Beukes, N.J., 1987. Physiochemical environments for the formation of quartz-free manganese oxide ores from the Early Proterozoic Hotazel Formation, Kalahari manganese field, South Africa. *Econ. Geol.*, 82: 706–718.
- Moorhouse, W.W., 1970. A comparative atlas of textures of Archean and younger volcanic rocks. *Geol. Assoc. Can., Spec. Pap.*, 8, 20 plates.
- Moore, E.S., 1918. The iron-formation on Belcher Islands, Hudson Bay, with special reference to its origin and its associated algal limestones. *J. Geol.*, 26: 412–438.
- Moore, J.C., Mascle, A., Taylor, E., Andreieff, P., Alvarez, F. et al., 1988. Tectonics and hydrology of the northern Barbados Ridge: Results from Ocean Drilling Program Leg 110. *Geol. Soc. Am., Bull.*, 100: 1578–1593.
- Morey, G.B., 1983. Animikie basin, Lake Superior region, U.S.A. In: A.F. Trendall and R.C. Morris (Editors), *Iron-formation: Facts and Problems*. Elsevier, Amsterdam, pp. 13–67.

- Morris, R.C., 1980. A textural and mineralogical study of the relationship of iron ore to banded iron-formation in the Hamersley iron province of Western Australia. *Econ. Geol.*, 75: 184-209.
- Morris, R.C., 1985. Genesis of iron ore in banded iron-formation by supergene and supergene-metamorphic processes — a conceptual model. In: K.H. Wolf (Editor), *Handbook of Strata-bound and Stratiform Ore Deposits*, Vol. 13. Elsevier, Amsterdam, pp. 73-235.
- Morris, R.C. and Horwitz, R.C., 1983. The origin of the BIF-rich Hamersley Group — deposition on a platform. *Precambrian Res.*, 21: 273-297.
- Morton, R.L. and Nebel, M., 1983. Physical character of Archean felsic volcanism in the vicinity of the Helen iron mine, Wawa, Ontario, Canada. *Precambrian Res.*, 20: 39-62.
- Muehlenbachs, K., 1986. Alteration of the oceanic crust and the ^{18}O history of seawater. In: J.W. Valley, H.P. Taylor, Jr and J.R. O'Neil (Editors), *Reviews in Mineralogy*, Vol. 16. Stable isotopes in high temperature geological processes. *Mineral. Soc. Am.*, pp. 425-444.
- Muessig, K.W., 1984. Structure and Cenozoic tectonics of the Falcon Basin, Venezuela, and adjacent areas. p. 217-230 In: W.E. Bonini et al. (Editors), *The Caribbean-South American plate boundary and regional tectonics*. *Geol. Soc. Am., Mem.*, 162, 421 pp.
- Muller, G. and Forstner, U., 1973. Recent iron ore formation in Lake Malawi, Africa. *Mineral. Deposita*, 8: 278-290.
- Muller, J.E., 1977. Evolution of the Pacific margin, Vancouver island, and adjacent regions. *Can. J. Earth Sci.*, 14: 2062-2085.
- Muller-Karger, F.E. and McClain, C.R., 1987. Frontal structures in the Caribbean Sea as seen in a time series of CZCS images: Nov. 1978-Dec. 1982 (abstr.). *EOS Trans., American Geophys. Union*, 68: 336.
- Muller-Karger, F.E., McClain, C.R. and Richardson, P.L., 1988. The dispersal of the Amazon's water. *Nature*, 333: 56-59.
- Murray, J.W. and Mackintosh, E.E., 1968. Occurrence of interstratified glauconite-montmorillonoid pellets, Queen Charlotte Sound, British Columbia. *Can. J. Earth Sci.*, 5: 243-247.
- Muskatt, H.S., 1972. The Clinton group of east-central New York. N.Y. Geol. Assoc., Guidebook, 44th Annu. Meet., pp. A1-A37.
- Nakai, N. and Jensen, M.L., 1964. The kinetic isotope effect in the bacterial reduction and oxidation of sulfur. *Geochim. Cosmochim. Acta*, 28: 1893-1912.
- Nakhla, F.M. and Shehata, M.R.N., 1967. Contributions to the mineralogy and geochemistry of some iron-ore deposits in Egypt (U.A.R.). *Mineral. Deposita*, 2: 357-581.
- Nassim, G.L., 1950. The oolithic hematite deposits of Egypt. *Econ. Geol.*, 45: 578-581.
- Newland, D.H. and Hartnagel, C.A., 1908. Iron ores of the Clinton formation in New York State. N.Y. State Museum, Bull., 123, 76 pp.
- Nicolini, P., 1967. Remarques comparatives sur quelques éléments sedimentologiques et paleogeographiques liés aux gisements de fer oolithiques du Djebel Ank (Tunisie) et de Lorraine (France). *Mineral. Deposita*, 2: 95-101.
- North American Commission on Stratigraphic Nomenclature, 1983. North American stratigraphic code. *Am. Assoc. Pet. Geol., Bull.*, 67: 841-875.
- Novokhatsky, I.P., 1973. Precambrian ferruginous-siliceous formations of Kazakhstan. In: *Genesis of Precambrian Iron and Manganese Deposits*. UNESCO Earth Sci., 9: 153-157.
- Odin, G.S., 1985. Significance of green particles (glaucony, berthierine, chlorite) in arenites. In: G.G. Zuffa (Editor), *Provenance of Arenites*. NATO ASI Ser. C, 148: Reidel, Dordrecht, pp. 279-307.
- Odin, G.S. and Letolle, R., 1980. Glauconitization and phosphatization environments: A tentative comparison. In: Y.K. Bentor (Editor), *Marine Phosphorites Geochemistry, Occurrence, Genesis*. Soc. Econ. Paleontol. Mineral., Spec. Publ., 29: 227-237.
- Odin, G.S. and Matter, A., 1981. De glauconiarum origine. *Sedimentology*, 28: 611-641.
- Oehler, D.Z. and Smith, J.W., 1977. Isotopic composition of reduced and oxidized carbon in Early Archean rocks from Isua, Greenland. *Precambrian Res.*, 5: 221-228.
- Oftedahl, C., 1958. A theory of exhalative-sedimentary ores. *Geol. Foeren. Stockholm Foerh.*, 80: 1-19.
- Ohmoto, H., 1986. Stable isotope geochemistry of ore deposits. In: J.W. Valley, H.P. Taylor, Jr. and J.R. O'Neil (Editors), *Reviews in Mineralogy*, Vol. 16. Stable isotopes in high temperature geological processes. *Mineral. Soc. Am.*, pp. 491-559.
- Ohmoto, H. and Felder, R.P., 1987. Bacterial activity in the warmer, sulphate-bearing Archaean oceans. *Nature*, 328: 244-246.
- Ohmoto, H. and Lasaga, A.C., 1982. Kinetics of reactions between aqueous sulfates and sulfides in hydrothermal systems. *Geochim. Cosmochim. Acta*, 46: 1727-1745.
- Ojakangas, R.W., 1983. Tidal deposits in the Early Proterozoic basin of the Lake Superior region — The Palms and the Pokegama Formations: Evidence for subtidal-shelf deposition of Superior-type banded iron-formation. In: L.G. Medaris, Jr. (Editor), *Early Proterozoic Geology of the Great Lakes Region*. *Geol. Soc. Am., Mem.*, 160: 49-66.
- Okita, P.M., Maynard, J.B., Spiker, E.C. and Force, E.R., 1988. Isotopic evidence for organic matter oxidation by manganese reduction in the formation of stratiform manganese carbonate ore. *Geochim. Cosmochim. Acta*, 52: 2679-2685.
- Okita, P.M., Maynard, J.B. and Martinez Vera, A., 1986. Molango: Giant sedimentary manganese deposit in Mexico (abstr.). *Am. Assoc. Pet. Geol., Bull.*, 70: 627.

- Okita, P.M. and Shanks, W.C. III, 1987. Stable isotope study of the Molango managanese deposit, Hidalgo State Mexico. *Geol. Soc. Am., Abstr. Progr.*, 19: 793.
- Okuda, T., 1981. Water exchange and the balance of phosphate in the Gulf of Cariaco, Venezuela, In: F.A. Richards (Editor), *Coastal and Estuarine Sciences*, 1. *Coastal Upwelling*. Am. Geophys. Union, pp. 274-281.
- Okuda, T., Bonilla Ruiz, J. and Garcia, A.J., 1974. Algunas características bioquímicas en el agua de la Fosa de Cariaco. *Bol. Inst. Oceanograf.*, Univ. Oriente, Cumana, Venezuela, 13: 163-174.
- Ooi Jin Bee, 1982. *The Petroleum Resources of Indonesia*. Oxford Univ. Press, Oxford, 256 pp.
- O'Rourke, J.E., 1961. Paleozoic banded iron-formations. *Econ. Geol.*, 56: 331-361.
- O'Rourke, J.E., 1962. The stratigraphy of Himalayan iron ores. *Am. J. Sci.*, 260: 294-302.
- Oyarzun, R., Clemmey, H. and Collao, S., 1986. Geologic and metallogenic aspects concerning the Nahuelbuta mountains banded iron formation, Chile. *Mineral. Deposita*, 21: 244-250.
- Page, B.M., 1958. Chamositic iron ore deposits near Tajmiste, western Macedonia, Yugoslavia. *Econ. Geol.*, 53: 1-21.
- Palmquist, S., 1935. Geochemical studies on the iron-bearing Liassic series in southern Sweden. *Medd. Lunds Geol.-Mineral. Inst.*, 60, 204 pp.
- Parak, T., 1975. Kiruna iron ores are not "intrusive-magmatic ores of the Kiruna type". *Econ. Geol.*, 70: 1242-1258.
- Parak, T., 1985. Phosphorus in different types of ore, sulfides, in the iron deposits, and the type and origin of ores at Kiruna. *Econ. Geol.*, 80: 646-665.
- Patchett, P.J. and Arndt, N.T., 1986. Nd isotopes and tectonics of 1.9-1.7 Ga crustal genesis. *Earth Planet. Sci. Lett.*, 78: 329-338.
- Paull, C.K. and Neumann, A.C., 1987. Continental margin brine seeps: Their geological consequences. *Geology*, 15: 545-548.
- Perry, E.C. Jr., Tan, F.C. and Morey, G.B., 1973. Geology and stable isotope geochemistry of the Biwabik iron formation, northern Minnesota. *Econ. Geol.*, 68: 1110-1125.
- Perry, E.C. Jr., Ahmad, S.N. and Swulius, T.M., 1978. The oxygen isotope composition of 3800 m.y. old metamorphosed chert and iron formation from Isukasia, West Greenland. *J. Geol.*, 86: 223-239.
- Petranek, J., 1964. Ordovician sedimentary iron ores in Ejpovice (in Czechoslovakian). *Sb. Geol. Ved (Collection of Geological Sciences)*, 2: 39-153.
- Petranek, J., Duremberg, D. and Melka, K., 1988. Oolitic iron ore deposit at Chrustenice (Ordovician, Bohemia). *Lozisk. Geol., Mineral.* (Prague, Czechoslovakia), 28: 9-55.
- Petrush, W., 1977. Mineralogical characteristics of an oolitic iron deposit in the Peace River district, Alberta. *Can. Mineral.*, 15: 3-13.
- Pimentel-Klose, M.R. and Jacobsen, S.B., 1985. Depleted mantle evolution from Nd isotopes in Precambrian banded iron formations (abstr.). *EOS Trans. Am. Geophys. Union*, 66: 414-415.
- Pitman, W.C. III, 1978. Relationship between eustacy and stratigraphic sequences of passive margins. *Geol. Soc. Am. Bull.*, 89: 1389-1403.
- Plaksenko, N.A., Koval, I.K. and Shchogolev, I.N., 1973. Precambrian ferruginous-siliceous formations associated with the Kursk Magnetic Anomaly. In: *Genesis of Precambrian Iron and Manganese Deposits*, UNESCO Earth Sci., 9: 89-94.
- Pomerene, J.B., 1964. Geology and ore deposits of the Belo Horizonte, Ibirite, and Macacos quadrangles, Minas Gerais, Brazil. *U.S. Geol. Surv., Prof. Pap.*, 341-D, 84 pp.
- Por, F.D., 1985. Anchialine pools — comparative hydrobiology. In: G.M. Friedman and W.E. Krumbein (Editors), *Hypersaline Ecosystems*, The Gavish Sabkha. Springer, Berlin, pp. 136-144.
- Poreda, R.J., Jenden, P.D., Kaplan, I.R. and Craig, H., 1986. Mantle helium in Sacramento basin natural gas wells. *Geochim. Cosmochim. Acta*, 50: 2847-2853.
- Porrenga, D.H., 1967. Glauconite and chamosite as depth indicators in the marine environment. *Mar. Geol.*, 5: 495-501.
- Posey, H.H., Light, M.P.R., Kyle, J.R. and Price, P.E., 1986. Thermal model for salt dome cap rocks and mineral deposits (abstr.). *Am. Assoc. Pet. Geol.*, 70: 634.
- Postma, D., 1977. The occurrence and chemical composition of Recent Fe-rich mixed carbonates in a river bog. *J. Sediment. Petrol.*, 47: 1089-1098.
- Postma, D., 1981. Formation of siderite and vivianite and the pore-water composition of a Recent bog sediment in Denmark. *Chem. Geol.*, 31: 225-244.
- Postma, D., 1982. Pyrite and siderite formation in brackish and freshwater swamp sediments. *Am. J. Sci.*, 282: 1151-1183.
- Postma, D., 1985. Concentration of Mn and separation from Fe in sediments: 1. Kinetics and stoichiometry of the reaction between birnessite and dissolved Fe (II) at 10°C. *Geochim. Cosmochim. Acta*, 49: 1023-1033.
- Prescott, D.M., 1988. The geochemistry and palaeoenvironmental significance of iron pisoliths and ferromanganese crusts from the Jurassic of Mallorca, Spain. *Eclogae Geol. Helv.*, 81: 387-414.
- Pride, D.E. and Hagner, A.F., 1972. Geochemistry and origin of the Precambrian iron formation near Atlantic City, Fremont County, Wyoming. *Econ. Geol.*, 67: 329-338.
- Pulfrey, W., 1933. The iron-ore oolites and pisolithes of North Wales. *Geol. Soc. London, Q. J.*, 89: 401-430.
- Purucker, M.E., 1984. Oolitic ironstones and banded iron-formation: Controls on chemical sedimentation, Part 1. Ph.D. Diss., Princeton Univ., Princeton, N.J., 53 pp.
- Quade, H., 1970. Der Bildungsraum und die genetische

- Problematik der vulkansedimentaeren Eisenerze. Clausthaler Hefte Lagerstaettenkd. Geochem. Miner. Rohst., 9: 27-65.
- Quirke, T.T., 1961. Geology of the Temiscamie iron-formation, Lake Albanel iron range, Mistassini Territory, Quebec, Canada. Econ. Geol., 56: 299-320.
- Quirke, T.T., Jr., Goldich, S.S. and Krueger, H.W., 1960. Composition and age of the Temiscamie Iron-formation, Mistassini Territory, Quebec, Canada. Econ. Geol., 55: 311-326.
- Rai, K.L., Sarkar, S.N. and Paul, P.R., 1980. Primary depositional and diagenetic features in the banded iron formation and associated iron-ore deposits of Noamundi, Singhbhum district, Bihar, India. Mineral. Deposita, 15: 189-200.
- Ranger, M.J., Pickerill, R.K. and Fillion, D., 1984. Lithostratigraphy of the Cambrian ?-Lower Ordovician Bell Island and Wabana groups of Bell, Little Bell, and Kelys islands, Conception Bay, eastern Newfoundland. Can. J. Earth Sci., 21: 1245-1261.
- Rawson, P.F., Greensmith, J.T. and Shalaby, S.E., 1983. Coarsening-upward cycles in the uppermost Staithes and Cleveland ironstone formations (Lower Jurassic) of the Yorkshire coast; England. Proc. Geol. Assoc., 94: 91-93.
- Read, H.H. and Watson, J., 1968. Introduction to Geology. 2nd ed. Macmillan, London, 693 pp.
- Rechenberg, H.P., 1956. Die Eisenerzlagerstatte, "Vivaldi" bei Ponferrada, Leon, Spanien. Neues Jahrb. Mineral., Geol., Palaeontol., Abh., 89: 111-136.
- Reeves, R.G., 1966. Geology and mineral resources of the Monlevade and Rio Piracicaba quadrangles, Minas Gerais, Brazil. U.S. Geol. Surv., Prof. Pap., 341-e, 58 pp.
- Reimer, T.O., 1980. Archean sedimentary baryte deposits of the Swaziland Supergroup (Barberton Mountain Land, South Africa). Precambrian Res., 12: 393-410.
- Reimer, T.O., 1987. Weathering as a source of iron in iron-formations: The significance of alumina-enriched paleosols from the Proterozoic of Southern Africa. In: P.W.U. Appel and G.L. LaBerge (Editors), Precambrian Iron-Formations. Theophrastus Publ., Athens, pp. 601-619.
- Reyes-Vasquez, G., Ferraz-Reyes, E. and Vasquez, E., 1979. Toxic dinoflagellate blooms in northeastern Venezuela during 1977. In: D.L. Taylor and H.H. Seiger (Editors), Toxic Dinoflagellate Blooms. Elsevier, New York, N.Y., pp. 191-194.
- Reymer, A. and Schubert, G., 1986. Rapid growth of some major segments of continental crust. Geology, 14: 299-302.
- Rich, J.E., Johnson, G.L., Jones, J.E. and Campsie, J., 1986. A significant correlation between fluctuations in seafloor spreading rates and evolutionary pulsations. Paleoceanography, 1: 85-95.
- Richards, F.A., 1975. The Cariaco Basin (Trench). Oceanogr. Mar. Biol. Annu. Rev., 13: 11-67.
- Richards, S.M., 1966. The banded iron formations at Broken Hill, Australia, and their relationship to the lead-zinc ore bodies, Part 1: Econ. Geol., 61: 72-96; Part 2: Econ. Geol., 61: 257-274.
- Richter, D.K. and Fuchtbauer, H., 1978. Ferroan calcite replacement indicates former magnesian calcite skeletons. Sedimentology, 25: 843-860.
- Robbins, E.I., La Berge, G.L. and Schmidt, R.G., 1987. Evidence for iron-stripping and silica-stripping micro-organisms in Precambrian granular and banded iron formations. U.S.G.S. Circulat 995: 58-95.
- Roberts, D. and Gale, G.H., 1978. The Caledonian-Appalachian lapetus Ocean. In: D.H. Tarling (Editor), Evolution of the Earth's Crust. Academic Press, London, pp. 255-342.
- Robertson, A.H.F., 1976. Origins of ochres and umbers: evidence from Skouriotissa, Troodos Massif, Cyprus. Inst. Min. Metall., (London) Trans., Sect. B, 85: 245-251.
- Robertson, A.H.F. and Hudson, J.D., 1972. Cyprus umbers: chemical precipitates on a Tethyan ocean ridge. Earth Planet. Sci. Lett., 18: 93-101.
- Robin, P.-Y., 1979. Theory of metamorphic segregation and related processes. Geochim. Cosmochim. Acta, 43: 1587-1600.
- Rohrlich, V., Metzger, A. and Zohar, E., 1980. Potential iron ores in the Lower Cretaceous of Israel and their origin. Isr. J. Earth-Sci., 29: 73-80.
- Rohrlich, V., Price, N.B. and Calvert, S.E., 1969. Chamosite in the Recent sediments of Loch Etive, Scotland. J. Sediment. Petrol., 39: 624-631.
- Ronov, A.B., Khain, V.E., Balukhovsky, A.N. and Seslavinsky, K.B., 1980. Quantitative analysis of Phanerozoic sedimentation. Sediment. Geol., 25: 311-325.
- Roscoe, S.M., 1969. Huronian rocks and uraniferous conglomerates in the Canadian Shield. Geol. Surv. Can. Pap. 68-40, 205 pp.
- Rossignol-Strick, M., 1987a. Rainy periods and bottom water stagnation initiating brine accumulation and metal concentrations. 1. The late Quaternary. Paleoceanography, 2: 333-360.
- Rossignol-Strick, M., 1987b. Rainy periods and bottom water stagnation initiating brine accumulation and metal concentrations. 2. Precambrian gold-uranium ore beds and banded iron formations. Paleoceanography, 2: 379-394.
- Rowley, D.B. and Sahagian, D., 1986. Depth-dependent stretching: A different approach. Geology, 14: 32-35.
- Rozenson, I., Zak, I. and Spiro, B., 1980. The distribution and behavior of iron in sequences of dolomites, clays, and oxides. Chem. Geol., 31: 83-96.
- Ruckmick, J.C., 1962. The iron ores of Cerro Bolivar, Venezuela. Econ. Geol., 58: 218-236.
- Rusinova, O.V., Lobanov, A.S., Korennova, N.G., Zhukhlistov, A.P., rusinov, V.L., Troneva, N.V. and Boronikhin, V.A., 1985. Zinc-bearing berthierine from a lead-zinc deposit. Dokl. Akad. Nauk SSSR (Trans. U.S.S.R.

- Acad. Sci., Earth Sci. Sect.), 280: 733-738.
- Russell, M.J., 1975. Lithogeochemical environment of the Tynagh base-metal deposit, Ireland, and its bearing on ore deposition. Inst. Min. Metall. (London), Trans., Sect. B, 84: 128-133.
- Rutledge, J.J., 1910. The Clinton iron-ore deposits in Stone Valley, Huntingdon County, Pennsylvania. Am. Inst. Min. Eng. Trans., 40: 134-164.
- Sackett, W.M., Brooks, J.M., Bernard, B.B., Schwab, C.R., Chung, H. and Parker, R.A., 1979. A carbon inventory for Orca Basin brines and sediments. Earth Planet. Sci. Lett., 44: 73-81.
- Sage, R.P., 1979. No. 12 Wawa area, District of Algoma. In: V.G. Milne et al. (Editors), Summary of Field Work for 1979. Ont. Geol. Surv. Misc. Pap., 90: 48-53.
- Saif, Saiful-Islam, 1983. Petrographic and geochemical characteristics of iron-rich rocks and their significance in exploration for massive sulfide deposits, Bathurst, New Brunswick, Canada. J. Geochem. Expl., 19: 705-721.
- Sakamoto, T., 1950. The origin of the Pre-Cambrian banded iron ores. Am. J. Sci., 248: 449-474.
- Salvador, A., 1987. Late Triassic-Jurassic paleogeography and origin of Gulf of Mexico basin. Am. Assoc. Pet. Geol., Bull., 71: 419-451.
- Santamaría, F. and Schubert, C., 1974. Geochemistry and geochronology of the southern Caribbean-northern Venezuela plate boundary. Geol. Soc. Am., Bull., 7: 1085-1098.
- Scelzo, M.A. and Voglar, J.F., 1980. Ecological study of the *Artemia* populations in Boca Chica salt lake, Margarita Island, Venezuela. In: G. Persoone, P. Sorgeloos, O. Roels and E. Jaspers (Editors), The Brine Shrimp *Artemia*, Vol. 3. Universa Press, Wetteren, pp. 115-125.
- Schaub, H.P., 1955. Discussion: Physical limits of glauconite formation. Bull. Am. Assoc. Pet. Geol., 39: 1878-1882.
- Schellmann, W., 1969. Die Bildungsbedingungen sedimentärer Chamosit- und Hamatit-Eisenerze am Beispiel der Lagerstätte Echte. Neues Jahrb. Mineral. Geol. Palaeont., Abh., 111: 1-31.
- Scherban, I.P. and Shirokikh, I.N., 1971. Stability of silicasiderite and silica-ankerite mineral associations under hydrothermal conditions. Doklady Nauk U.S.S.R., 196: 139-140.
- Schiavon, N., 1988. Goethite ooids: growth mechanisms and sandwave transport in the Lower Greensand (Early Cretaceous, southern England). Geol. Mag., 125: 57-62.
- Schidlowski, M., 1988. A 3,800-million-year isotopic record of life from carbon in sedimentary rocks. Nature, 333: 313-318.
- Schidlowski, M., Eichmann, R. and Fiebiger, N., 1976. Isotope fractionation between organic carbon and carbonate carbon in Precambrian banded ironstone series from Brazil. Neues Jahrb. Mineral., Monatsh., 8: 344-353.
- Schmidt, R.G., 1963. Geology and ore deposits of the Cuyuna North Range, Minnesota. U.S. Geol. Surv., Prof. Pap., 407, 95 pp.
- Schoen, R., 1962. Petrology of iron-bearing rocks of the Clinton group in New York State. Unpubl. Ph.D. thesis, Harvard Univ., Cambridge, Mass., 151 pp.
- Schubert, C., 1979. El Pilar fault zone, northeastern Venezuela: Brief review. Tectonophysics, 52: 447-455.
- Schubert, C. and Sifontes, R.S., 1970. Bocono fault, Venezuelan Andes: Evidence of post-glacial movement. Science, 170: 66-69.
- Schubert, G. and Reymer, A.P.S., 1985. Continental volume and freeboard through geologic time. Nature, 316: 336-339.
- Schultz, R.W., 1966. Lower Carboniferous cherty iron-stone at Tynagh, Ireland. Econ. Geol., 61: 311-342.
- Schweigart, H., 1965. Genesis of the iron ores of the Pretoria Series, South Africa. Econ. Geol., 60: 269-298.
- Scott, S.D., 1987. Seafloor polymetallic sulfides: Scientific curiosities or mines of the future? In: P.G. Teleki, M.R. Dobson, J.R. Moore and U. Von Stackelberg (Editors), Marine Minerals. NATO ASI Ser. C, 194, Reidel, Dordrecht, pp. 277-300.
- Seiglie, G.A., Pannella, G. and Smith, A.L., 1979. Siderite spherulites of San Sebastian Formation (Oligocene), northern Puerto Rico. Am. Assoc. Pet. Geol., Bull., 63: 370-375.
- Seijas I., F.J., 1972. Geología de la región de Carúpano. In: Fourth Venezuelan Geological Congress, 1969, Caracas, Mem., 5 (3): 1887-1923.
- Sellards, E.H. and Baker, C.L., 1934. The Geology of Texas, Vol. 2, Structural and Economic Geology. Univ. Texas, Bull. 3401, 884 pp.
- Shanks, W.C. III and Bischoff, J.L., 1980. Geochemistry, sulfur isotope composition, and accumulation rates of Red Sea geothermal deposits. Econ. Geol., 75: 445-459.
- Shaulov, M.A., 1973. Problem of the existence of gas pools feeding mud volcanism in Taman. Pet. Geol. (U.S.S.R.), 11: 98-100.
- Shegelski, R.J., 1975. Geology and geochemistry of iron formations and their host rocks in the Savant Lake-Sturgeon Lake greenstone belts, a progress report. In: Geotraverse Workshop 1975, Univ. Toronto Press, Toronto, Ont., pp. 34-1-34-21.
- Shegelski, R.J., 1976. The geology and geochemistry of Archean iron formations and their relation to reconstructed terrains in the Sturgeon and Savant Lake greenstone belts. In: Geotraverse Workshop 1976, Univ. Toronto Press, Toronto, Ont., pp. 29-1-29-22.
- Shegelski, R.J., 1978. Stratigraphy and geochemistry of Archean iron formations in the Sturgeon Lake-Savant Lake greenstone terrain, northwestern Ontario. Ph.D. Dissert., Univ. Toronto, Toronto, Ont., 251 pp.
- Sheldon, R.P., 1970. Sedimentation of iron-rich rocks of Llandovery age (Lower Silurian) in the southern Appalachian basin. In: W.B.N. Berry and A.J. Boucot (Editors), Correlation of the North American Silurian Rocks. Geol. Soc. Am., Spec. Pap., 102: 107-112.
- Shepard, F.P., 1973. Sea floor off Magdalena delta and Santa

- Marta area, Colombia. *Geol. Soc. Am., Bull.*, 84: 1955-1972.
- Sheridan, R.E., 1983. Phenomena of pulsation tectonics related to the breakup of the eastern North American continental margin. *Tectonophysics*, 94: 169-185.
- Sheridan, R.E. and Enos, P., 1979. Stratigraphic evolution of the Blake Plateau after a decade of scientific drilling. In: M. Talwani, W. Hay and W.B.F. Ryan (Editors), Maurice Ewing Series 3. Am. Geophys. Union, Washington, D.C., pp. 109-122.
- Sheu, D.-D., 1987. Sulfur and organic carbon contents in sediment cores from the Tyro and Orca Basins. *Mar. Geol.*, 75: 157-164.
- Sheu, D.-D. and Presley, B.J., 1986a. Formation of hematite in the euxinic Orca Basin, northern Gulf of Mexico. *Mar. Geol.*, 69: 309-321.
- Sheu, D.-D. and Presley, B.J., 1986b. Variations of calcium carbonate, organic matter and iron sulfides in anoxic sediment from the Orca Basin, Gulf of Mexico. *Mar. Geol.*, 70: 103-118.
- Sheu, D.-D., Shakur, A., Pigott, J.D., Wiesenburg, D.A., Brooks, J.M. and Krouse, H.R., 1988. Sulfur and oxygen isotopic compositions of dissolved sulfate in the Orca basin: implications for origin of the high-salinity brine and oxidation of sulfides at the brine-seawater interface. *Mar. Geol.*, 78: 303-310.
- Shikazono, N., 1977. Composition of siderite and the environments of formation on vein-type deposits in Japan. *Econ. Geol.*, 72: 632-641.
- Shimoyama, T., 1984. Sulphur concentration in the Japanese Paleogene coal. In: R.A. Rahmani and R.M. Flores (Editors), *Sedimentology of Coal and Coal-bearing Sequences*. Int. Assoc. Sedimentol., Spec. Publ. 7: 361-371.
- Shklnka, R. and McIntosh, J.R., 1972. Geology of the Steep Rock Lake area, District of Rainy River: Ont. Dep. Miners, *Geol. Rep.*, 93, 114 pp.
- Shkolnik, E.L., 1973. Effusive jasper iron formation and iron ores of the Uda area. In: *Genesis of Precambrian iron and manganese deposits*: UNESCO Earth Sciences 9: 187-189.
- Shokes, R.F., Trabant, P.K., Presley, B.J. and Reid, D.F., 1977. Anoxic, hypersaline basin in the northern Gulf of Mexico. *Science*, 196: 1443-1446.
- Sholkovitz, E.R. and Copland, D., 1981. The coagulation solubility and adsorption properties of Fe, Mn, Cu, Ni, Cd, Co, and humic acids in a river water. *Geochim. Cosmochim. Acta*, 45: 181-190.
- Shtsherbak, V.M., Kryukov, A.S. and Tilepov, Z.T., 1973. On the issue of genesis and metamorphism of ferromanganese formations in Kazakhstan. In: *Genesis of Precambrian iron and manganese deposits*. UNESCO, Earth Sciences 9: 249-254.
- Siehl, A. and Thein, J., 1978. Geochemische Trends in der Minette (Jura, Luxemburg/Lothringen). *Geol. Rundsch.*, 67: 1052-1077.
- Siever, R., 1987. The silica cycle in the Precambrian. *Geol. Soc. Am., Abstr. Progr.*, 19: 844.
- Sifontes G., R.S. and Santamaría, F., 1972. Rocas intrusivas jóvenes en la región de Carupano. In: C. Petzall (Editor), *Sixth Caribbean Geological Congress, Margarita Island, Venezuela, Mem. Trans. Vol., CROMOTIP*, Caracas, pp. 121-125.
- Sigurdsson, H., 1977. Chemistry of the crater lake during the 1971-72 Soufrière eruption. *J. Volcanol. Geotherm. Res.*, 2: 165-186.
- Sigurdsson, H., 1987. Letal gas bursts from Cameroon crater lakes. *EOS, Am. Geophys. Union, Trans.*, 68: 570-573.
- Silver, E.A., Case, J.E. and MacGillavry, H.J., 1975. Geophysical study of the Venezuelan borderland. *Geol. Soc. Am., Bull.*, 86: 213-226.
- Simon, P., 1969. Die Lias-Eisenerze der Grube Friderike. In: H. Bottke et al. (Editors), *Sammelwerk Deutsche Eisenerzlagerstätten*, II-1. Beih. *Geol. Jahrb.*, Hannover, 79: 40-58.
- Simonson, B.M., 1984. High-energy shelf deposit. In: R.W. Tillman and C.T. Siemers (Editors), *Siliciclastic Shelf Sediments*. Soc. Econ. Paleontol. Mineral., Spec. Publ. 34: 251-268.
- Simonson, B.M., 1985. Sedimentological constraints on the origins of Precambrian iron-formations. *Geol. Soc. Am., Bull.*, 96: 244-252.
- Simonson, B.M., 1987. Early silica cementation and subsequent diagenesis in arenites from four Early Proterozoic iron formations of North America. *J. Sediment. Petrol.*, 57: 494-511.
- Sims, P.K., 1972. Banded iron-formations in Vermillion district. In: P.K. Sims and G.B. Morey (Editors), *Geology of Minnesota: a centennial volume*. Minnesota Geol. Surv., St. Paul, Minn., pp. 79-81.
- Sims, P.K. and James, H.L., 1984. Banded iron-formations of Late Proterozoic age in central Eastern Desert, Egypt: geology and tectonic history. *Econ. Geol.*, 79: 1777-1784.
- Simpson, T.A. and Gray, T.R., 1968. The Birmingham red-ore district, Alabama. In: J.D. Ridge (Editor), *Ore Deposits in the United States, 1933-1967*, Vol. 1. Am. Inst. Min. Metall. Pet. Eng., New York, N.Y., pp. 187-206.
- Singh, I.B., 1980. Precambrian sedimentary sequences of India: Their peculiarities and comparison with modern sediments. *Precambrian Res.*, 12: 411-436.
- Skerman, V.B.D., McGowan, V. and Sneath, P.H.A. (Editors), 1980. Approved lists of bacterial names. *Int. J. Syst. Bactiol.*, 30: 225-420.
- Skinner, B.J., 1969. *Earth Resources*. Prentice-Hall, Englewood Cliffs, N.J., 150 pp.
- Skinner, B.J. and Porter, S.C., 1987. *Physical Geology*, 3rd ed. Wiley, New York, N.Y., 768 pp.
- Skocek, V., 1963a. Oolitic iron ores from the regions of Raca and Bechlova (in Czechoslovakian). *Sb. Geol. Ved (Collection Geol. Sci.)* 1: 31-63.
- Skocek, V., 1963b. Petrographic composition and genesis of iron ore in the Brezina region (in Czechoslovakian): *Rozpr. Cesk. Akad. Ved (Proc. Czechoslovakian Acad. Sci.)*, 73(4), 109 pp.

- Skocek, V., Al-Qaraghuli, N. and Saadallah, A.A., 1971. Composition and sedimentary structures of iron ores from the Wadi Husainiya area, Iraq. *Econ. Geol.*, 66: 995-1004.
- Skyring, G.W. and Donelly, T.H., 1982. Precambrian sulfur isotopes and a possible role for sulfite in the evolution of biological sulfate reduction. *Precambrian Res.*, 17: 41-61.
- Sofer, Z., 1985. An unusual occurrence of light hydrocarbon gases in a well offshore northeast Palawan island, the Philippines. *Precambrian Res.*, 30: 179-188.
- Sokolova, E.I., 1964. Physicochemical investigations of sedimentary iron and manganese ores and associated rocks. *Istr. Prog. Sci. Transl.*, Jerusalem, 220 pp.
- Solignac, M., 1930. Les caractères mineralogiques du minerai de fer oolithique de djebel el Ank (Tunisie méridionale). *C. R. Acad. Sci., paris*, 191: 107-109.
- Solomon, M. and Walshe, J.L., 1979. The formation of massive sulfide deposits on the sea floor. *Econ. Geol.*, 74: 797-813.
- Sonnenfeld, P., 1984. Brines and Evaporites. Acad. Press, Orlando, Fla., 613 pp.
- Sonnenfeld, P., Hudec, P.P., Turek, A. and Boon, J.A., 1977. Base-metal concentration in a density-stratified evaporite pan. In: J.H. Fisher (Editors), *Reefs and Evaporites — Concepts and Depositional Models. Studies in Geology*, 5. Am. Assoc. Pet. Geol., 181-186.
- Sorby, H.C., 1857. On the origin of the Cleveland Hill iron-stone. *Proc. Geol. Polytech. Soc. West Riding Yorkshire*, 3: 457-461.
- Sorokin, V.I., Vlasov, V.V., Varfolomeeva, E.K. and Ursin, M.A., 1979. Effect of the medium on development of glauconite composition. *Lithology and Mineral Resources (U.S.S.R.)*, 14: 690-693.
- Soudry, D., Moshkovitz, S. and Ehrlich, A., 1981. Occurrence of siliceous microfossils (Diatoms, silicoflagellates and sponge spicules) in the Campanian Mishash Formation, southern Israel. *Eclogae Geol. Helv.*, 74: 97-107.
- Spencer, E. and Percival, F.G., 1952. The structure and origin of the banded hematite jaspers of Singhbhum, India. *Econ. Geol.*, 47: 365-383.
- Stanier, R.Y. and Cohen-Bazire, G., 1977. Phototrophic prokaryotes: the cyanobacteria. *Annu. Rev. Microbiol.*, 31: 225-274.
- Stanton, R.L., 1972a. Ore Petrology. McGraw-Hill, New York, N.Y., 713 pp.
- Stanton, R.L., 1972b. A preliminary account of chemical relationships between sulfide lode and "banded iron formation" at Broken Hill, New South Wales. *Econ. Geol.*, 67: 1128-1145.
- Steidinger, K.A. and Baden, D.G., 1984. Toxic marine dinoflagellates, p. 201-261 In: D.L. Spector (Editor), *Dinoflagellates*. Academic Press, 545 pp.
- Stanier, R.Y. and Cohen-Bazire, G., 1977. Phototrophic prokaryotes: The cyanobacteria. *Annu. Rev. Microbiol.*, 31: 225-274.
- Stanton, R.L., 1976. Petrochemical studies of the ore environment at Broken Hill, New South Wales. *Trans. and 118-141.*
- Starkey, J.A. Jr., 1962. The bog ore and bog iron industry of south New Jersey. *Bull. N.J. Acad. Sci.*, 7: 5-8.
- Stille, P. and Clauer, N., 1986. Sm-Nd isochron-age and provenance of the argillites of the Gunflint Iron Formation in Ontario, Canada. *Geochim. Cosmochim. Acta*, 50: 1141-1146.
- Stobernack, J., 1970. Metamorphose der Glimmerschiefer und Genese in der westlichen Bong Range/Liberia. *Clausthaler Hefte Lagerstättenkd. Geochem. Miner. rohst.*, 9: 85-107.
- Stoffers, P. and Kuehn, R., 1974. Red Sea evaporites: A petrographic and geochemical study, In: R.B. Whitmarsh, D.E. Weser, D.A. Ross et al. (Editors), *Initial Report of the Deep-Sea Drilling Project*, 23. U.S. Government Printing Office, Washington, pp. 821-847.
- Strakhov, N.M., 1969. Principles of lithogenesis, Vol. 2. S.I. Tomkeieff and J.E. Hemingway (Editors), Oliver and Boyd, Edinburgh, 609 pp.
- Strauss, H., 1986. Carbon and sulfur isotopes in Precambrian sediments from the Canadian Shield. *Geochim. Cosmochim. Acta*, 50: 2653-2662.
- Stumm, W. and Morgan, J.J., 1981. Aquatic chemistry, 2nd ed. Wiley-Interscience, New York, N.Y., 780 pp.
- Suess, E. and Von Huene, R., 1988. Ocean drilling program leg 112, Peru continental margin: Part 2, Sedimentary history and diagenesis in a coastal upwelling environment. *Geology*, 16: 939-943.
- Sverjensky, D.A., 1984. Oil field brines as ore-forming solutions. *Econ. Geol.*, 79: 23-37.
- Sverjensky, D.A., 1987. The role of migrating oil field brines in the formation of sediment-hosted Cu-rich deposits. *Econ. Geol.*, 82: 1130-1141.
- Svitalski, N., 1937. Krivoy rog and the iron ores of this district. In: N. Svitalski (Editor), *The Southern Excursion, the Ukrainian Soviet Socialist Republic*. 17th Int. Geol. Congr., Moscow, pp. 51-77.
- Sylvester, A.G., 1988. Strike-slip faults. *Geol. Soc. Am. Bull.*, 100: 1666-1703.
- Talbot, M.R., 1973. Major sedimentary cycles in the Corallian beds (Oxfordian) of southern England. *Paleontol., Palaeoclimatol., Palaeoecol.*, 14: 293-317.
- Talbot, M.R., 1974. Ironstones in the Upper Oxfordian of southern England. *Sedimentology*, 21: 433-450.
- Tarling, D.H. (Editor), 1978. *Evolution of the Earth's Crust*. Academic Press, London, 443 pp.
- Taylor, F.J.R., 1985. The taxonomy and relationships of red tide flagellates. In: D.M. Anderson, A.W. White and D.G. Baden (Editors), *Toxic Dinoflagellates*. Elsevier, New York, N.Y., pp. 11-26.
- Taylor, J.H., 1949. Petrology of the Northampton Sand Ironstone formation. *G.B. Geol. Surv. Mem.*, 111 pp.
- Taylor, J.H., 1951. Sedimentation problems of the Northampton Sand Ironstone. *Yorkshire Geol. Soc., Proc.*, 28: 74-85.

- Tegengren, F.R., 1921. The iron ores and iron industry of China, part 2. Geol. Surv. China, Mem., Peking, Ser. A (2), 180 pp.
- Teyssen, T.A.L., 1984. Sedimentology of the Minette oolitic ironstones of Luxembourg and Lorraine: a Jurassic subtidal sandwave complex. *Sedimentology*, 31: 195–211.
- Thode, H.G. and Goodwin, A.M., 1983. Further sulfur and carbon isotope studies of late Archean iron-formations of the Canadian Shield and the rise of sulfate-reducing bacteria. *Precambrian Res.*, 20: 337–356.
- Thompson, G., Humphris, S.E., Schroeder, B., Sulanowska, M. and Rona, P.A., 1988. Active vents and massive sulfides at 26°N (TAG) and 23°N (Snakepit) on the mid-Atlantic ridge. *Can. Mineral.*, 26: 697–711.
- Thwaites, F.T., 1914. Recent discoveries of "Clinton" iron ore in eastern Wisconsin. *U.S. Geol. Surv., Bull.*, 540: 338–342.
- Tiffin, D.L., Cameron, B.E.B. and Murray, J.W., 1972. Tectonics and depositional history of the continental margin off Vancouver Island, British Columbia. *Can. J. Earth Sci.*, 9: 280–296.
- Timofeeva, Z.V., 1966. Some features of lithology and geochemistry of iron-rich ore gangues and ores in the Bechayl Plateau (northern Caucasus) (in Russian). *Litol. Polezn. Iskop. (J. Lithol. Mineral.)* 1: 33–48.
- Timofeeva, Z.V. and Belashow, Yu. A., 1972. The distribution of rare earth elements in oolitic iron ores of the northern Caucasus (in Russian). *Litol. Polezn. Iskop. (J. Lithol. Mineral.)* 3: 128–135.
- Timofeyeva, Z.V., Kuznetsova, L.D. and Dontsova, Ye.I., 1976. Oxygen isotopes and siderite formation. *Geochem. Int.*, 10: 101–112.
- Tipping, E., 1981. The adsorption of aquatic humic substances by iron oxides. *Geochim. Cosmochim. Acta*, 45: 191–199.
- Tissot, B.P. and Welte, D.H., 1984. Petroleum formation and occurrence, 2nd ed. Springer, Berlin, 699 pp.
- Tolbert, G.E., Tremaine, J.W., Melcher, G.C. and Gornes, C.B., 1971. The recently discovered Serra dos Carajás iron deposits, northern Brazil. *Econ. Geol.*, 66: 985–994.
- Towe, K.M., 1983. Precambrian atmospheric oxygen and banded iron formations: A delayed ocean model. *Precambrian Res.*, 20: 161–170.
- Trefry, J.H., Presley, B.J., Keeney-Kennicutt, W.I. and Trocine, R.P., 1984. Distribution and chemistry of manganese, iron, and suspended particulates in Orca Basin. *Geo-Marine Lett.*, 4: 125–130.
- Trendall, A.F., 1968. Three great basins of Precambrian banded iron formation deposition. A systematic comparison. *Geol. Soc. Am., Bull.*, 79: 1527–1544.
- Trendall, A.F., 1973a. Time-distribution and type-distribution of Precambrian iron-formations in Australia. In: *Genesis of Precambrian Iron and Manganese Deposits*. UNESCO Earth Sci. 9: 49–57.
- Trendall, A.F., 1973b. Precambrian iron formations of Australia. *Econ. Geol.*, 68: 1023–1034.
- Trendall, A.F., 1973c. Varve cycles in the Weeli Wollie Formation of the Precambrian Hamersley Group, Western Australia. *Econ. Geol.*, 68: 1089–1097.
- Trendall, A.F., 1983a. Introduction. In: A.F. Trendall and R.C. Morris (Editors), *Iron-formation: Facts and Problems*. Elsevier, Amsterdam, pp. 1–12.
- Trendall, A.F., 1983b. The Hamersley basin. In: A.F. Trendall and R.C. Morris (Editors), *Iron-formation: Facts and Problems*. Elsevier, Amsterdam, pp. 69–129.
- Trendall, A.F. and Blockley, J.G., 1970. The iron formations of the Precambrian Hamersley Group, Western Australia, with special reference to the associated crocidolite. *West. Aust. Geol. Surv., Bull.*, 119, 336 pp.
- Triplehorn, D.M., 1966. Morphology, internal structure, and origin of glauconite pellets. *Sedimentology*, 6: 247–266.
- Trompette, R., 1981. Late Precambrian tillites of the Volta Basin and the Dahomeyides orogenic belt (Benin, Ghana, Niger, Togo and Upper-Volta). In: M.J. Hambrey and W.G. Harland (Editors), *Earth's Pre-Pleistocene Glacial Record*. Cambridge Univ. Press, Cambridge, pp. 135–139.
- Trythall, R.J.B., Eccles, C., Molyneaux, S.G. and Taylor, W.E.G., 1987. Age and controls of ironstone deposition (Ordovician) North Wales. *Geol. J.*, 22: 31–43.
- Turcotte, D.L. and Burke, K., 1978. Global sea-level changes and the thermal structure of the Earth. *Earth Planet. Sci. Lett.*, 41: 341–346.
- Tyler, S.A. and Twenhofel, W.H., 1952. Sedimentation and stratigraphy of the Huronian of Upper Michigan. *Am. J. Sci.*, 250: 1–27 and 118–151.
- Ulloa, M., Carlos, E., 1978. Hierro oolítico en el norte de Sur America. *Colomb. Minist. Minas Energia. Inst. Nac. Invest. Geol. Min.*, 24 pp.
- Umeorah, E.M., 1987. Depositional environment and facies relationship of the Cretaceous ironstone of the Agbaja Plateau, Nigeria. *J. Afr. Earth Sci.*, 6: 385–390.
- Upchurch, S.B., Strom, R.N. and Nuckles, M.G., 1980. Silicification of Miocene rocks from central Florida. In: T.M. Scott and S.B. Upchurch (Editors), *Miocene of the Southeastern United States*. Fla. Bur. Geol. Spec. Publ., 25: 251–284.
- Urban, H., 1966. Bildungsbedingungen und Faziesverhältnisse der marin-sedimentären Eisenerzlagerstätten am Kahlenberg bei Ringsheim/Baden. *Jahresh. Geol. Landesamtes Baden-Württemb.*, 8: 125–267.
- Usui, A., Yuasa, M., Yokota, S., Nohara, M., Nishimura, A. and Murakami, F., 1986. Submarine hydrothermal manganese deposits from the Ogasaware (Bonin) arc, off the Japanese islands. *Mar. Geol.*, 73: 311–322.
- Vail, P.R., Hardenbol, J. and Todd, R.G., 1984. Jurassic unconformities, chronostrata-chronostratigraphy and sea-level changes from seismic stratigraphy and biostrata-biostratigraphy. In: J.S. Schlee (Editor), *Interregional Unconformities and Hydrocarbon Exploration*. Am. Assoc. Pet. Geol., Mem., 36: 129–144.
- Vail, P.R. and Mitchum, R.M. Jr., 1979. Global cycles of

- relative changes of sea level from seismic stratigraphy. In: J.S. Watkins, L. Montadert and P.W. Dickerson (Editors), Geological and Geophysical Investigations of Continental Margins. Am. Assoc. Pet. Geol., Mem., 29: 469-472.
- Vail, P.R., Mitchum, R.M., Jr., Todd, R.G., Widmier, J.M., Thompson, S., III, Sangree, J.B., Bubb, J.N. and Hatlelid, W.G., 1977. Seismic stratigraphy and global changes in sea level. In: C.E. Payton (Editor), Seismic Stratigraphy — Applications to Hydrocarbon Exploration. Am. Assoc. Pet. Geol., Mem., 26: 49-212.
- Van der Westhuizen, W.A., Strydom, D., Schock, A.E., Tordiffe, E.A.W. and Beukes, G.J., 1986. Petrochemical evidence on the probable origin of ferriferous metasediments in Western Bushmanland. Mineral. Deposita, 21: 121-128.
- Van der Wood, T.B., 1977. Strontium isotope systematics in the Hamersley Range: theories of origin of banded iron formations and their significance to atmospheric history. Unpubl. M.S. Thesis, Florida State Univ. Tallahassee, Fla., 105 pp.
- Van Hise, R.B. and Leith, C.K., 1911. The geology of the Lake Superior region. U.S. Geol. Surv. Monogr., 52, 641 pp.
- Van Houten, F.B., 1967. Cenozoic oolitic iron ore, Paz de Rio, Boyaca, Colombia. Econ. Geol., 62: 992-999.
- Van Houten, F.B., 1985. Oolitic ironstones and contrasting Ordovician and Jurassic paleogeography. Geology, 13: 722-724.
- Van Houten, F.B. and Bhattacharyya, D.P., 1982. Phanerozoic oolitic ironstones — geologic record and facies model. Annu. Rev. Earth Planet. Sci., 10: 589-626.
- Van Houten, F.B. and Karasek, R.M., 1981. Sedimentologic framework of Late Devonian oolitic iron formation, Shatti Valley, westcentral Libya. J. Sediment. Petrol., 51: 415-427.
- Van Houten, F.B. and Purucker, M.E., 1984. glauconitic peloids and chamositic ooids — favorable factors, constraints, and problems. Earth-Sci. Rev., 20: 211-243.
- Veizer, J., 1983. Geologic evolution of the Archean-Early Proterozoic Earth. In: J.W. Schopf (Editor), Earth's Earliest Biosphere, Its Origin and Evolution. Princeton Univ. Press, Princeton, N.J., pp. 240-259.
- Velde, B., 1976. The chemical evolution of glauconite pellets as seen by microprobe determinations. Mineral. Mag., 40: 753-760.
- Velde, B., Raoult, J.-F. and Leikine, M., 1974. Metamorphosed berthierine pellets in Mid-Cretaceous rocks from north-eastern Algeria. J. Sediment. Petrol., 44: 1275-1280.
- Vierbuchen, R.C., 1984. The geology of the El Pilar fault zone and adjacent areas in northeastern Venezuela. In: W.E. Bonini, R.B. Hargraves and R. Shagam (Editors), The Caribbean-South American Plate Boundary and Regional Tectonics. Geol. Soc. Am., Mem., 162, pp. 189-212.
- Vignali, M., 1972. Excursion geologica al extremo occidental de Araya. In: C. Petzall (Editor), Sixth Caribbean Geology Conference, Margarita Island, Venezuela, Mem. Trans. Vol., CROMOTIP, Caracas, pp. 44-47.
- Voglar, J., Kingland, R. and Rodriguez, A., 1981. Contribution al estudio de la laguna de Boca Chica, Isla de Margarita, Venezuela: Thirty-first Natl. Conv. Venezuelan Assoc. Arts Sci., Univ. Zulia, Maracaibo, Venezuela, 13 pp.
- Vogt, P.R., Schneider, E.D. and Johnson, G.L., 1969. The crust and upper mantle beneath the sea. In: P.J. Hart (Editor), The Earth's Crust and Upper Mantle. Am. Geophys. Union, Geophys. Monogr., 13: 556-617.
- Voitov, G.I., Lebedev, V.I.S., Gureyev, I.E., Lebedev, V.I.S. and Cherevichnaya, L.F., 1975. Natural gases of the Yuzhno-Belozerskoye iron-ore deposit (Ukrainian crystalline shield). Acad. Sci., U.S.S.R., Dokl., Earth Sci. Sect., 1-6: 204-206.
- Von der Borch, C.C., Lock, D.E. and Schwebel, D., 1975. Ground-water formation of dolomite in the Coorong region of South Australia. Geology, 4: 283-285.
- Von Humboldt, A., 1881. Personal Narrative of Travels to the Equinoctial regions of America during the years 1799 to 1804, Vol. 1. George Bell, London.
- Verona, I.D., Kravchenko, V.M., Pervago, V.A. and Frumkin, I.M., 1973. Precambrian ferruginous formations of the Aldan Shield. In: Genesis of Precambrian iron and manganese deposits, UNESCO Earth Sci., 9: 243-247.
- Vorontsov, V.V., Gorbalenhove, M.V. and Dyufur, L.S., 1975. Visean iron ores of the southern Timan. Geol. Rudn. Mestorozh., 17: 65-75.
- Wagner, P.A., 1928. The iron deposits of the Union of South Africa. Geol. Surv. S. Afr., Mem., 26, 268 pp.
- Wakefield, S.J., 1980. Geochemical studies on the leaching of metalliferous sediments from the East Pacific. J. Geol. Soc. London, 137: 379-380.
- Walker, J.C.G., 1984. Suboxic diagenesis in banded iron formations. Nature, 309: 340-342.
- Walker, J.C.G. and Brimblecombe, P., 1985. Iron and sulfur in the pre-biologic ocean. Precambrian Res., 28: 205-222.
- Walker, J.C.G. and Zahnle, K.J., 1986. Lunar nodal tide and distance to the moon during the Precambrian. Nature, 320: 600-602.
- Walter, M.R., 1983. Archean stromatolites: Evidence of the Earth's earliest benthos. In: J.W. Schopf (Editor), Earth's Earliest Biosphere, Its Origin and Evolution. Princeton Univ. Press, Princeton, N.J., pp. 187-213.
- Walter, M.R. and Hofmann, H.J., 1983. The palaeontology and palaeoecology of Precambrian iron-formations. In: A.F. Trendall and R.C. Morris (Editors), Iron-formation: Facts and Problems. Elsevier, Amsterdam, pp. 373-400.
- Ward, B.B., 1986. Methane oxidation in the marine water column (abstr.). EOS Trans., Am. Geophys. Union, 67: 1066.

- Ward, W.C., Folk, R.L. and Wilson, J.L., 1970. Blackening of eolianite and caliche adjacent to saline lakes, Isla Mujeres, Quintana Roo, Mexico. *J. Sediment. Petrol.*, 40: 548-555.
- Watkins, D., 1972. Metamorphism of iron formations on the Melville Peninsula, Northwest Territories. Unpubl. M.Sc. Thesis, Carleton Univ., Ottawa, 103 pp.
- Weber, F., 1973. Genesis and supergene evolution of the Precambrian sedimentary manganese deposit at Moanda (Gabon). In: *Genesis of Precambrian iron and manganese deposits*, UNESCO Earth Sci., 9: 307-332.
- Weller, J.M., 1958. Stratigraphic facies differentiation and nomenclature. *Am. Assoc. Pet. Geol. Bull.*, 42: 609-639.
- White, D.A., 1954. The stratigraphy and structure of the Mesabi range, Minnesota. *Minn. Geol. Surv. Bull.*, 38, 92 pp.
- Whitehead, T.H., Anderson, W., Wilson, V., Wray, D.A. and Dunham, K.C., 1952. The Liassic ironstones. *G.B. Geol. Surv. Mem.*, 211 pp.
- Wiesenburg, D.A., Brooks, J.M. and Bernard, B.B., 1985. Biogenic hydrocarbon gases and sulfate reduction in the Orca Basin brine. *Geochim. Cosmochim. Acta*, 49: 2069-2080.
- Willden, R., 1960. Sedimentary iron-formation, Christmas quadrangle, Arizona. *U.S. Geol. Surv., Prof. Pap.*, 400-B: 21-23.
- Willden, R., 1961. Composition of the iron-formation of Devonian age in the Christmas quadrangle, Arizona. *U.S. Geol. Surv., prof. Pap.*, 424-D: 304-306.
- Williams, P.J., 1986. Petrology and origin of iron-rich silicate-magnetite-quartz rocks from Flowerdale near Gairloch, Wester Ross. *Scott. J. Geol.*, 22: 1-12.
- Williams, P.J. and Manby, G.M., 1987. Syngenetic sulfides and Fe-Mn metasediments in Middle to Upper Paleozoic sequences of Karnten, Southern Austria. *Econ. Geol.*, 82: 1070-1076.
- Wilson, I.D.H. and Underhill, D.H., 1971. The discovery and geology of major new iron deposits on Melville Peninsula, Eastern Arctic. *Can. Min. J.*, 92: 40-48.
- Wilson, I.G., 1966. Chamosite ooliths in the Raasay iron-stone. *Scott. J. Sci.*, 1(1): 47-57.
- Wilson, J.L., 1975. Carbonate Facies in Geologic History. Springer, Berlin, 471 pp.
- Winn, R.D., Jr. and Bailes, R.J., 1987. Stratiform lead-zinc sulfides, mudflows, turbidites: Devonian sedimentation along a submarine fault scarp of extensional origin, Jason deposit, Yukon Territory, Canada. *Geol. Soc. Am. Bull.*, 98: 528-539.
- Winters, G.V. and Buckley, D.E., 1986. The influence of dissolved $\text{FeSi}_3\text{O}_3(\text{OH})_6$ on chemical equilibria in pore waters from deep sea sediments. *Geochim. Cosmochim. Acta*, 50: 277-288.
- Winterhalter, B., 1966. Iron-manganese concretions from the Gulf of Bothnia and the Gulf of Finland. *Geotek. Julk.*, 69, 77 pp.
- Winterhalter, B. and Siivola, J., 1967. An electron micro-probe study of the distribution of iron, manganese and phosphorus in concretions from the Gulf of Bothnia, northern Baltic Sea. *C. R. Soc. Géol. Finland*, 39: 161-172.
- Witzke, B.J., 1980. Middle and Upper Ordovician paleogeography of the region bordering the transcontinental arch. In: T.D. Fouch and E.R. Magatham (Editors). *Paleozoic Paleogeography of the West-central United States*. Soc. Econ. Paleontol. Mineral., Rocky Mountain Sect., Proc. West Central U.S. Paleogeography Symp. 1, Denver, Colo., pp. 1-18.
- Wright, J.D., 1975. Iron deposits of Nova Scotia. *Nova Scotia Dep Mines, Econ. Geol. Ser.*, 75-1, 154 pp.
- Yakontova, L.K., Andreeva, N.Ya., Cipurskij, S.I. and Naumenko, P.I., 1985. New data on the mineralogy and formation conditions of the Kerch iron ore (in Russian). *Mineral. Zhurnal (Kiev Nauk Dumka)*, 7: 29-43.
- Yang, Decheng, Kaine, B.P. and Woese, C.R., 1985. The Phylogeny of Archaeabacteria: Systemics of Applied Microbiology, 6: 251-256.
- Yeo, G.M., 1984. The Rapitan Group: Relevance to the global association of Late Proterozoic glaciation and iron-formation. Ph.D. Diss., Univ. Western Ontario, London, Ont., 603 pp.
- Yeo, G.M. and Gross, G.A., 1987. A review of the evidence for a hydrothermal-exhalative origin for Precambrian banded iron-formation. *Geol. Soc. Am., Abstr. Progr.*, 19: 902.
- Yorath, C.J., 1980. The Apollo structure in Tofino Basin, Canadian Pacific continental shelf. *Can. J. Earth Sci.*, 17: 758-775.
- Young, F.G., 1972. Cretaceous stratigraphy between Blow and Fish rivers, Yukon Territory. *Geol. Surv. Canada, Pap.* 72-1 (A): 229-235.
- Young, F.G., 1977. The mid-Cretaceous flysch and phosphatic ironstone sequence, northern Richardson mountains, Yukon Territory. *Geol. Surv. Canada, Pap.* 77-1-C: 67-74.
- Young, F.G. and Robertson, B.T., 1984. The Rapid Creek Formation: An Albian flysch-related phosphatic iron formation in northern Yukon Territory. In: D.F. Smith and D.J. Glass (Editors), *The Mesozoic of Middle North America*. Can. Soc. Pet. Geol., Mem., pp. 361-372.
- Young, G.A., 1922. Iron-bearing rocks of Belcher islands. Hudson Bay. *Geol. Surv. Canada, Summ. Rep. for 1921, part E*, 61 pp.
- Young, G.M., 1973. Tillites and aluminous quartzites as possible time markers for Middle Precambrian (Aphelian) rocks of North America. p. 97-127 In: G.M. Young (Editor), *Huronian Stratigraphy and Sedimentation*. Geol. Assoc. Canada, Spec. Pap., 12, 271 pp.
- Young, G.M., 1976. Iron-formation and glaciogenic rocks of the Rapitan Group, Northwest Territories, Canada. *Precambrian Res.*, 3: 137-158.
- Young, G.M., 1982. The late Proterozoic Tindir Group, east-central Alaska: Evolution of a continental margin. *Geol. Soc. Am., Bull.*, 93: 759-783.

- Young, G.M., 1983. Tectono-sedimentary history of early Proterozoic rocks of the northern Great Lakes region. In: L.G. Medaris, Jr. (Editor), Early Proterozoic Geology of the Great Lakes Region. Geol. Soc. Am., Mem., 160, pp. 15-32.
- Young, G.M., 1988. Proterozoic plate tectonics, glaciation and iron-formations. *Sediment. Geol.*, 58: 127-144.
- Young, T.P., 1988. The lithostratigraphy of the upper Ordovician of central Portugal. *J. Geol. Soc.*, 145: 377-392.
- Zbinden, E.A. and Holland, H.D., 1987. A paleosol near Flin Flon, Manitoba, and its implications for atmospheric oxygen 1.8 b.y. B.P. *Geol. Soc. Am., Abstr. Progr.*, 19: 903.
- Zelenov, K.K., 1960. Transportation and accumulation of iron and aluminum in volcanic provinces in the Pacific. *Izv. Akad. Nauk (U.S.S.R.), Geol. Ser.*, 8: 47-59.
- Zitzmann, A., 1977. The iron ore deposits of the western U.S.S.R. In: A. Zitzmann (Editor), The Iron Ore Deposits of Europe and Adjacent Areas, Vol. 1. Bundesanst. Geowiss. Rohst., Hannover, pp. 325-391.
- Zumpe, H.H., 1971. Microstructures in Cenomanian glauconite from the Isle of Wright, England. *Mineral. Mag.*, 38: 215-224.